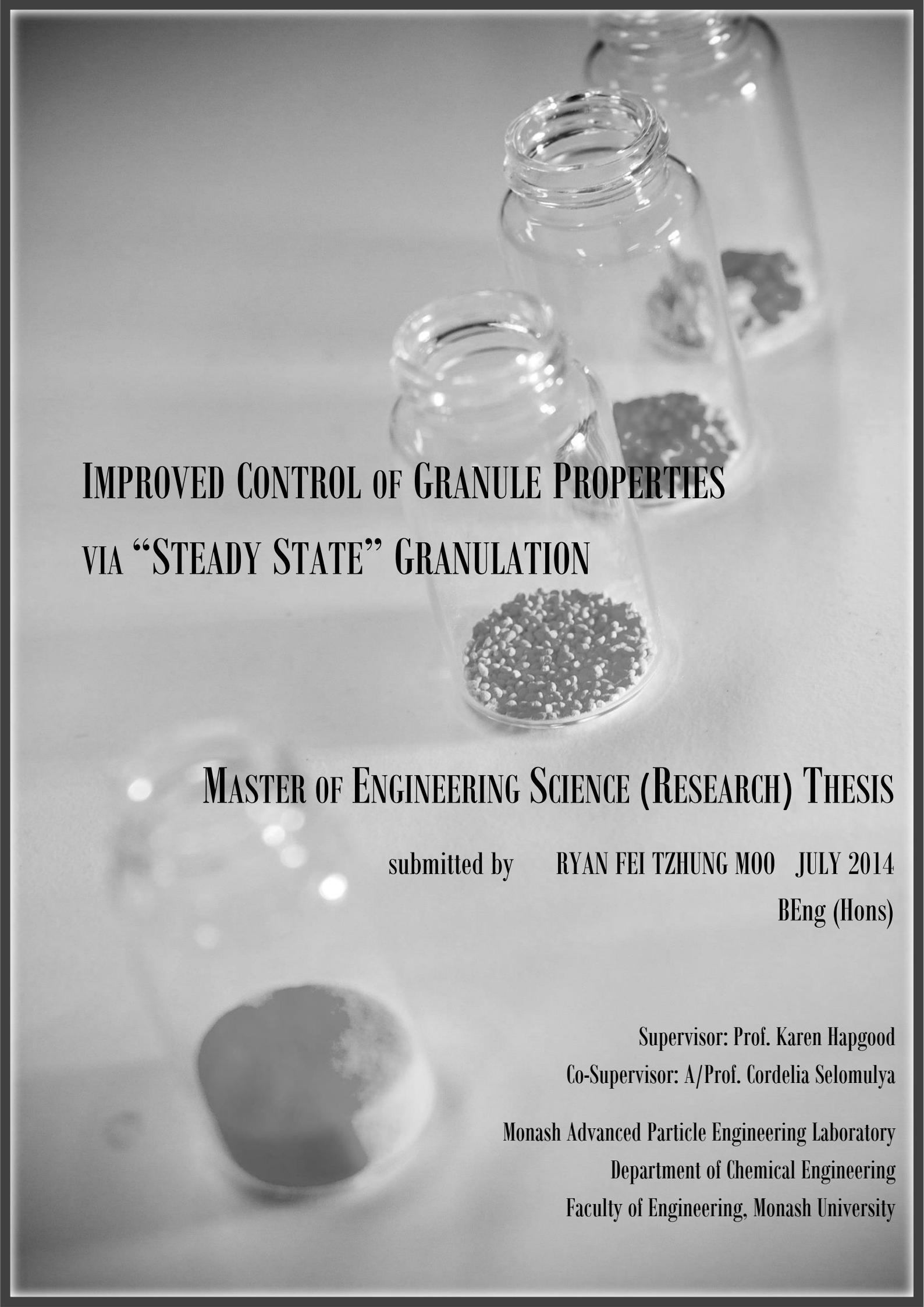

Improved Control of Granule Properties via "Steady State" Granulation

Master of Engineering Science (Research) Thesis

submitted by RYAN FEI TZHUNG MOO JULY 2014

BEng (Hons)

Supervisor: Prof. Karen Hapgood

Co-Supervisor: A/Prof. Cordelia Selomulya

Monash Advanced Particle Engineering Laboratory

Department of Chemical Engineering

Faculty of Engineering, Monash University

Copyright Notices

Notice 1

Notice 2

DECLARATION

In accordance with Monash University Doctorate Regulation 17.2 Doctor of Philosophy and Research Master's regulations the following declarations are made:

I hereby declare that this thesis contains no material which has been accepted for the award of any other degree or diploma at any university or equivalent institution and that, to the best of my knowledge and belief, this thesis contains no material previously published or written by another person, except where due reference is made in the text of the thesis.

The core theme of the thesis is the understanding and application of "steady state" granulation approach in wet granulation process to produce granule dosage form with improved control of attributes. The ideas, development and writing up of all the papers in the thesis were the principal responsibility of myself, the candidate, working within the Department of Chemical Engineering under the supervision of Prof. Karen Hapgood (main supervisor, 75%) and A/Prof. Cordelia Selomulya (co-supervisor, 25%).

I have not renumbered sections of submitted or published papers in order to generate a consistent presentation within the thesis.

Signed:

……

ACKNOWLEDGEMENT

A research project requires dedication of the candidate in constantly putting effort and time to achieve significant progresses but the credits should go to a group of people who have supported, assisted, supervised and contributed in terms of technical and analytical skills, guidance and background knowledge. First, I would like to express my sincere gratitude to two of my supervisors, Prof. Karen Hapgood and A/Prof. Cordelia Selomulya for their guidance throughout the whole course. It is a huge privilege to work with Karen who has such in-depth knowledge on granulation process and Cordelia who has been providing constructive ideas from her area of expertise. Their patience and encouragement are much appreciated especially when I faced problems either inside or outside of research. Under their supervision, research becomes more enjoyable and mind challenging. They have assisted me to become a responsible researcher by allowing me to take full charge of my own project.

Next, I would like to thank my research group mates, Thanh Nguyen and David Barling for their helps in training me on various equipment such as high shear mixer granulator, peristaltic pump, sieve shaker, Malvern Mastersizer etc. They also provided me with useful tips on running my granulation experiments. I also appreciate the company from my other research buddies, Fiona Low, Nazra Hameed, Shaun Rimos, Evone Tang and Bithi Roy who have been there for me to consult whenever I need to.

In the Department of Chemical Engineering, I would like to show my appreciation to Kim Phu, Chemical Store and Lab manager for her kindness and assistance on ordering items required for my experiments and training me on SEM, Mercury Intrusion Porosimeter, Helium Pycnometer etc. Furthermore, many thanks to Sally Sim, a research assistant from Monash Parkville campus who has trained and assisted me on the Malvern Morphologi G3 which is an important instrument for my research.

I also appreciate Nicola Buckingham's help from NUPLEX for her generosity in providing me with free sample packs of EXF grade hydroxypropyl cellulose (HPC). I would like to thank Monash University for granting me two scholarships, Monash International Postgraduate Research Scholarship (MIPRS) and Monash Graduate Scholarship (MGS) and providing the opportunity for me to complete my postgraduate studies.

Last but not least, I would like to dedicate my thesis to my family and two people who have been the biggest moral supports in this research path. The first person will be Thanh Nguyen who has been a big sister to me, assisting and accompanying me through highs and lows. Her patience and passion in research have allowed me to learn more about conducting good research. She is always happy and willing to give a free hand whenever she has the time and within her capabilities. The other person will be a best friend of mine who always encourages me to go forward and reassures me that I am capable of solving any problems and producing good work. I am very grateful to have both of them to keep pushing through, persist and make this research path fruitful.

SUMMARY

The project focuses on adopting a different granulating approach in aiming to achieve a "steady state" condition that is unachievable in conventional high shear wet granulation. Michaels *et al.* (2009) proposed that the liquid delivery rate and wet massing time are the two key aspects need to be adjusted in order to evenly distribute the granulating fluid across the powder system. Inhomogeneity in liquid distribution gives rise to a few major problems such as formation of lumps/balls, broad size distribution, inconsistency in granule properties from batch to batch etc. This often occurs due to short granulating time where wet agglomerates are being discharged to the next processing stage before equilibrium between granule growth and granule breakage is achieved, also called the "steady state" condition.

In wet granulation, powder particles are bound together via liquid bridges. As suggested, a lower liquid level was applied as opposed to 40% in industrial practices, which reduces the risk of overwetting the system. Reducing the liquid delivery rate to 2%/min (dry basis) ensures that the liquid has sufficient time to penetrate into the powder bed and prevent pooling which may lead to "lumps" formation. On the other hand, wet massing period was prolonged for more than 5 min to further enhance the liquid distribution and promote granule growth and granule breakage simultaneously to a point where granule properties show no significant changes with wet massing time. By reaching this "steady state", granule size will become relatively constant and a narrower size distribution can be produced.

A typical pharmaceutical formulation consists of 74 wt% lactose, 20 wt% microcrystalline cellulose (MCC), 3 wt% hydroxypropyl cellulose (HPC), 3 wt% croscarmellose sodium together with Rhodamine B as the model "drug" was used in this project. The powder was granulated in a 5 L high shear mixer granulator with impeller as the main means of agitation and dripping as the method of liquid delivery. The first part of the project was to test the feasibility of "steady state" granulation approach in a mixer granulator of different scale and within the operating conditions of interest. The effects of three major operating parameters: 1. wet massing time (0-30 min), 2. liquid level (24-30%) and 3. impeller speed (245-490 rpm) on the granule properties were investigated. The granules were characterized in terms of size distribution, morphology, circularity and bulk densities.

The target end product is a granule dosage form that is suitable for oral consumption, with desired attributes such as narrow size distribution, considerably spherical, smooth surfaces,

constant bulk densities and good dissolution performance. The key findings from this part of the work have confirmed earlier studies by Michaels *et al.* (2009). Wet massing has shown to be effective in narrowing granule size distribution and eliminating "lumps". Redistributing liquid evenly across the powder bed ensures larger agglomerates such as "lumps" to be broken down and smaller ones to coalescence, allowing them to grow to the same extent hence producing granules of similar sizes. Furthermore, granules that are wet massed for sufficiently long period of time exhibit positive structural change in terms of sphericity and surface smoothness.

A direct relationship between liquid level and size distribution was discovered where a gradual shift of size distribution towards the larger size range occurred when there was a fixed increment of liquid level. When a higher liquid level was used, rounder granules were formed as wet agglomerates are more plastically deformable and interparticle friction is reduced. Autohesion is used to explain the formation of spherical polymer matrix in terms of the mobility of MCC polymer chains under the presence of liquid and shear force. As a result, two main types of granules were observed: regular, spheroidal and irregular-shaped depending on the amount of liquid delivered.

Using a higher impeller speed was found to effectively reduce the amount of "lumps" formed compared to lower speeds. Since wet massing period is adequately long, impeller can break down these "lumps" without installing a chopper. With higher impeller speeds, spheronization of granules that possessed adequate liquid saturation to deform was promoted. Higher intensity of impeller speed also further consolidates granules with higher liquid content, producing dense granules.

"Steady state" conditions were achieved within the last 15 min of wet massing and this implies that wet massing period can be reduced to less than 30 min. Estimating the period of time when wet massing no longer have any significant effects on granule properties serves as an end-point determination of granulation process. "Steady state" or pseudo steady state is a suitable term to describe the approach as not all granule properties become constant at the end of the wet massing period.

Extending the research scope was to investigate the dissolution performance of "steady state" granules as a dosage form itself. They were found to dissolve via leaching where soluble components dissolve and create cavities that allow the penetration of dissolution medium into the internal structure and facilitate the dissolution of entrapped model "drug". Once all the

soluble components have been dissolved, a perforated and porous polymeric matrix is formed which does not disintegrate over the dissolution period. The dissolution rate of "steady state" granules was found to be dependent on the microstructure of granule. Although "steady state" granules appeared to be a dense solid mass, they dissolved fast especially regular, spheroidal ones. The phenomenon can be attributed to the high surface area available in the inner structure, created by the disappearance of soluble component and existing voids. On the other hand, irregular-shaped granules exhibited slower dissolution rate due to potential swelling that can cause pores to be blocked and diffusion path to be obstructed.

The aim of varying the compositions of soluble and insoluble components in the chosen pharmaceutical formulation to fine-tune the release rate of "steady state" granules has been achieved. The idea of altering the micro-structure of dosage form in order to control the release rate was performed by adjusting the formulation. Results showed that the dissolution rate is highly influenced by the penetration rate of dissolution medium which is determined by the amount of soluble component present in the matrix.

In the process of obtaining an optimal formulation to achieve the desired release rate, other granule properties are also affected due to the incorporation of more/less of soluble/insoluble components. Liquid level was found to be a crucial factor that affects the properties of granule with MCC as one of the main ingredients in the formulation. With "steady state" granulation approach, granule size distribution can be easily tuned to the desired range by just varying the liquid level. The studies have displayed the prospects of "steady state" granulation approach in producing granule dosage form with well-controlled properties as well as the potential of "steady state" granules as a drug carrier for immediate release formulations.

PUBLICATIONS AND AWARDS

Publications from research project:

Conference publication(s):

1. **R.F.T. Moo**, C. Selomulya and K. Hapgood (2013), "*Improved Control of Granule Properties via "Steady State" Granulation*", 6th International Granulation Workshop, 26th - 28th June, Sheffield, UK,
2. **R.F.T. Moo**, C. Selomulya and K. Hapgood (2013), "*Improved Control of Granule Properties via "Steady State" Granulation*", CHEMECA, 29th Sep - 2nd Oct, Brisbane, Australia.

Award(s):

3rd Prize in 'Best Poster' Award by TTC, 6th International Granulation Workshop, 26th -28th June, Sheffield, UK

Publications from other fields of research:

Journal publication(s):

1. N. Fu, M.W. Woo, **F.T. Moo**, X.D. Chen, "*Microcrystallization of lactose during droplet drying and its effect on the property of the dried particle*", Chemical Engineering Research and Design, Volume 90, Issue 1, January 2012, Pages 138-149

TABLE OF CONTENTS

Page Number

DECLARATION I

ACKNOWLEDGEMENT II

SUMMARY III

PUBLICATIONS AND AWARDS VI

TABLE OF CONTENTS VII

LIST OF FIGURES X

LIST OF TABLES XVI

1 INTRODUCTION 1

1.1 PHARMACEUTICAL DOSAGE FORMS 1

1.2 PAEDIATRIC MEDICINE 2

1.3 RESEARCH AIMS 4

1.4 THESIS OUTLINE 4

2 LITERATURE REVIEW 6

2.1 GRANULATION 6

2.2 WET GRANULATION 7

2.3 HIGH SHEAR WET GRANULATION 8

2.4 CONVENTIONAL HIGH SHEAR WET GRANULATION 9

2.5 COMPLEXITIES AND CHALLENGES 9

2.6 EFFECTS OF PARAMETERS ON GRANULATION BEHAVIOUR 10

2.6.1 AMOUNT OF LIQUID ADDED 11

2.6.2 METHOD OF LIQUID DELIVERY AND ADDITION RATE 13

2.6.3 IMPELLER SPEED AND ROLE OF CHOPPER 20

2.6.4 WET MASSING TIME 24

2.7 END POINT DETERMINATION OF GRANULATION PROCESS 26

2.8 "STEADY STATE" GRANULATION 28

2.9 DRUG RELEASE MECHANISMS 32

2.10 LITERATURE SUMMARY AND RESEARCH GAP 39

3 MATERIALS AND METHODOLOGY 42

3.1 FORMULATION 42

3.1.1 LACTOSE 42

3.1.2 MICROCRYSTALLINE CELLULOSE 43

3.1.2.1 USE OF MCC AS EXTRUSION AID IN WET GRANULATION 43

3.1.3 HYDROXYPROPYL CELLULOSE 46

3.1.4 CROSCARMELLOSE SODIUM 47

3.1.5 MANNITOL 47
3.1.6 RHODAMINE B 48
3.2 EXPERIMENTAL PROCEDURE 49
3.2.1 HIGH SHEAR WET GRANULATION 49
3.2.2 CHARACTERIZATION OF GRANULE PROPERTIES 52
3.2.2.1 GRANULE SIZE DISTRIBUTION 52
3.2.2.2 GRANULE MORPHOLOGY 53
3.2.2.3 GRANULE CIRCULARITY 54
3.2.2.4 GRANULE BULK POURED AND TAPPED DENSITIES 55
3.2.2.5 DISSOLUTION PERFOMANCE OF "STEADY STATE" GRANULES 56
3.2.2.5.1 BULK DISSOLUTION TEST 56
3.2.2.5.2 SINGLE GRANULE DISSOLUTION 57
3.2.2.5.3 GRANULE SIZE DISTRIBUTION DURING DISSOLUTION TESTING 58

4 FEASIBILITY OF "STEADY STATE" GRANULATION 59
4.1 INTRODUCTION 59
4.2 EXPERIMENTAL 59
4.3 RESULTS 61
4.3.1 CONVENTIONAL GRANULATION 61
4.3.2 "STEADY STATE" GRANULATION 62
4.3.2.1 EFFECTS OF WET MASSING TIME, LIQUID LEVEL AND IMPELLER SPEED ON GRANULE SIZE DISTRIBUTION 62
4.3.2.2 EFFECTS OF WET MASSING TIME, LIQUID LEVEL AND IMPELLER SPEED ON GRANULE MORPHOLOGY AND CIRCULARITY 68
4.3.2.3 EFFECTS OF WET MASSING TIME, LIQUID LEVEL AND IMPELLER SPEED ON GRANULE BULK DENSITIES 76
4.4 DISCUSSION 79
4.5 CONCLUSIONS 82

5 DISSOLUTION PERFORMANCE OF "STEADY STATE" GRANULES 84
5.1 INTRODUCTION 84
5.2 EXPERIMENTAL 85
5.3 RESULTS 86
5.4 DISCUSSION 91
5.5 CONCLUSIONS 96

6 EFFECT OF VARYING FORMULATION COMPOSITION ON GRANULE PROPERTIES AND DISSOLUTION PROFILE 97
6.1 INTRODUCTION 97
6.2 EXPERIMENTAL 98
6.3 RESULTS 99
6.3.1 GRANULE SIZE DISTRIBUTION AS A FUNCTION OF FORMULATION 99
6.3.2 GRANULE MORPHOLOGY, CIRCULARITY AND BULK DENSITIES AS A FUNCTION OF FORMULATION 101
6.3.3 EFFECT OF FORMULATION ON THE DISSOLUTION PERFORMANCE OF "STEADY STATE" GRANULES 105
6.3.4 CASE STUDY: MANNITOL-MCC FORMULATION 109
6.4 DISCUSSION 112

6.5 CONCLUSIONS **116**

7 CONCLUSIONS AND RECOMMENDATIONS **118**

7.1 CONCLUSIONS **118**

7.2 RECOMMENDATIONS **120**

NOMENCLATURE AND ABBREVIATIONS **123**

REFERENCES **125**

APPENDICES **132**

A. GRANULE SIZE DISTRIBUTION PLOTS AND RAW DATA 132
B. GRANULE CIRCULARITY RAW DATA 140
C. GRANULE BULK DENSITIES RAW DATA 143
D. DISSOLUTION TESTING RAW DATA 145
E. FOCUSED BEAM REFLECTANCE MEASUREMENT PLOTS 170

LIST OF FIGURES

Figure 2.1: Fine particles are agglomerated into larger entity called granule. 6

Figure 2.2: Modern approach of describing granulation process as a combination of three sets of rate processes. Adopted from Iveson et al. (2001). 7

Figure 2.3: Different states of saturation attained by liquid-bound granules. Adopted from Iveson et al. (2001). 8

Figure 2.4: Schematic diagram of a high shear mixer granulator.....9

Figure 2.5: Effect of amount of liquid on 50% particle diameter at an impeller rotation speed of 600 rpm and wet massing time of 6 min. Taken from Ohno *et al.* (2007). 12

Figure 2.6: Different methods of liquid delivery: a) Pouring, b) Dripping and c) Spraying. .13

Figure 2.7: Granule size distributions obtained using three different liquid delivery methods: a) Dry addition, b) Wet addition and c) Spray addition in high shear mixer. Taken from Osborne *et al.* (2011). 14

Figure 2.8: Effect of liquid delivery methods on granule size distribution. Taken from Rahmanian *et al.* (2011).....15

Figure 2.9: Two nucleation mechanisms proposed which take into account the effect of the size of binder droplet: a) Immersion distribution and b) Distribution mechanism. Adapted from Schaefer *et al.* (1996). 16

Figure 2.10: Schematic overview of the possible nucleation mechanisms in the high shear mixer granulator. Inset from Dries and Vromans (2004). 17

Figure 2.11: The five steps of nucleation: 1. Droplet formation, 2. Droplet impact on the powder and possible breakage, 3. Droplet coalescence at the powder surface, 4. Droplet penetration into the powder pores and 5. Mixing of the liquid and powder by mechanical dispersion. Inset from Litster *et al.* (2001) 18

Figure 2.12: Proposed nucleation regime map for liquid bound granules. Adopted from Hapgood *et al.* (2003). 19

Figure 2.13: Two types of flow regime observed in a high shear granulator: a) Bumping flow and b) Roping flow. Inset from Litster *et al.* (2002).....20

Figure 2.14: Morphology of granules of 1000-1400 µm produced after a) 25 min at 450 rpm, b) after 17 min at 800 rpm and c) after 4 min at 1500 rpm. Taken from Ohno *et al.* (2007). .21

Figure 2.15: Bimodal breakage: a) Many small particles and a few large particles and b) Many small particles and one large particle. Inset from Realpe and Velázquez (2008). 23

Figure 2.16: Effects of a) impeller rotation speed and b) wet massing time on pore size distribution. Taken from Ohno *et al.* (2007).....26

Figure 2.17: Different granulation stages divided up in a power consumption profile at increasing amount of granulating liquid. Taken from Leuenberger *et al.* (2009).....27

Figure 2.18: Pseudo steady state condition is achieved when the rate of coalescence and rate of breakage reach an equilibrium point. Inset from Michaels et al. (2009).....29

Figure 2.19: Chord-length distributions of wet granules produced by "steady state" granulation and "conventional" granulation at 2-L scale. Taken from Michaels *et al.* (2009). 31

Figure 2.20: The existence of "steady state" condition in HSWG where granule size distribution did not show significant changes towards the end of wet massing period. Taken from Michaels *et al.* (2009). 31

Figure 2.21: Granule morphology changes during wet massing period: a) 0 min WMT and b) 40 min WMT in "steady state" granulation. Taken from Michaels *et al.* (2009). 31

Figure 2.22: "Typical" immediate release dissolution profile, very fast initial release with a levelling off. Inset from am Ende 2011. 33

Figure 2.23: Dissolution comparison between different excipient (MCC, calcium dibasic phosphate and disintegrant SSG) ratios and a constant drug load. Inset from am Ende 2011.33

Figure 2.24: Schematic diagram illustrating the differences between the terms: a) "Drug dissolution" and b) "Drug release". Adapted from Siepmann *et al.* (2013). 34

Figure 2.25: Effect of process parameters: a-b) amount of water added, c-d) impeller rotation speed and e-f) kneading time on 50% pore diameter (left) and dissolution profiles of mefenamic acid in tablets (right). Inset from Ohno et al. (2007). 36

Figure 2.26: Dissolution profiles of tablets compressed from granules produced in "steady state" and "conventional" granulation. Taken from Michaels *et al.* (2009). 37

Figure 3.1: Lactose monohydrate 42

Figure 3.2: Microcrystalline cellulose 43

Figure 3.3: a) MCC (Avicel PH101) pellet, b) Surface details of pellet, c) Dissolved MCC (Avicel PH101) pellet and d) Surface details of dissolved pellet. Taken from Kleinebudde (1997). 45

Figure 3.4: Hydroxypropyl cellulose 46

Figure 3.5: Croscarmellose sodium 47

Figure 3.6: Mannitol 47

Figure 3.7: a) Experimental setup of "steady state" granulation b) Side view of high shear jacketed mixing bowl c) Impeller 3 blades mounted vertically in mixing bowl 49

Figure 3.8: Temperature profiles of powder bed throughout the 3 main stages in granulation process. Region A: Pre-mixing, Region B: Liquid addition and Region C: Wet massing 50

Figure 3.9: a) Liquid droplets that formed after exiting the delivery tube and b) Liquid droplets that fell on lactose powder bed in a petri dish. 51

Figure 3.10: Dried granules (at 27% LL, 245 rpm and 0 min WMT) were sieved into two size fractions: a) > 2 mm and b) < 2 mm before being analysed in Mastersizer. 53

Figure 3.11: "Steady state" granules in the dispersion unit were dispersed on the glass plate. 54

Figure 3.12: a) "Steady state" granules poured into a 5 ml graduated measuring cylinder through a funnel. b) Poured volume was determined by taking the average of V_{p1} and V_{p2} ... 55

Figure 3.13: Sampling procedure of dissolution test: Step 1. Withdrawal of solution, Step 2: Replenish of fresh deionized water, Step 3. Filter the solution through a syringe filter, Step 4: Pipette the filtered solution into microplate. 57

Figure 3.14: A single "steady state" granule dissolved in a petri dish and examined under optical microscope. 57

Figure 3.15: FBRM angled at 45° and faced the beaker wall to detect the particles in solution. 58

Figure 4.1: “Conventional” granulation: 40% liquid level and 30 s of wet massing. 61

Figure 4.2: Granule size distributions produced at a) 24% LL and 245 rpm and b) 30% LL and 490 rpm narrowed down after 30 min of wet massing. 63

Figure 4.3: Granule size distributions produced a) after 5 min of wet massing and b) at the end of wet massing period at 3 different impeller speeds. 66

Figure 4.4: Effects of liquid level and impeller speed on the formation and breakage of "lumps" over the wet massing period: a) 0 min WMT, b) 5 min WMT, c) 15 min WMT and d) 30 min WMT. 67

Figure 4.5: Steady state" granules of 180-355 µm produced after 30 min of wet massing.....69

Figure 4.6: "Steady state" granules of 355-500 µm produced after 30 min of wet massing. .70

Figure 4.7: Rounding and surface smoothing of "steady state" granules produced at 30% LL and 490 rpm were observed over the wet massing period: a) 0 min WMT, b) 5 min WMT, c) 15 min WMT and d) 30 min WMT. 71

Figure 4.8: Morphology of "steady state" granules produced at a) 24% LL and 245 rpm, b) 30% LL and 245 rpm, c) 24% LL and 490 rpm and d) 30% LL and 490 rpm. 72

Figure 4.9: Internal structure of "steady state" granules produced at 30% LL and 490 rpm. 73

Figure 4.10: Evolution of granule circularity profile during wet massing period at 24-30% LL and 245-490 rpm. 74

Figure 4.11: Effect of impeller speed on the granule circularity profile at 30% LL. 74

Figure 4.12: Effects of a) liquid level at different impeller speeds and b) impeller speed at different liquid levels on granule circularity after 30 min of wet massing. 75

Figure 4.13: "Steady state" granules of 355-500 µm formed at a) 24% LL and 245 rpm and b) 30% LL and 490 rpm. 76

Figure 4.14: Poured density of "steady state" granules over wet massing period. 77

Figure 4.15: Tapped density of "steady state" granules over wet massing period. 77

Figure 4.16: Effect of impeller speed on a) poured and b) tapped densities of "steady state" granules at different liquid level. 78

Figure 4.17: Effect of impeller speed on Hausner ratio at different liquid levels. 79

Figure 5.1: Two types of "steady state" granules tested: 1. Irregular-shaped granules – a) 24% LL and 245 rpm, c) 24% LL and 490 rpm and 2. Regular, spheroidal granules – b) 30% LL and 245 rpm, d) 30% LL and 490 rpm. 85

Figure 5.2: Dissolution profiles of "steady state" granules (180-355 µm) produced after 30 min of wet massing) obtained by monitoring the release of Rhodamine B over time.....87

Figure 5.3: Soluble components leached out from “steady state” granules (30% LL and 490 rpm), leaving a matrix of insoluble components. a) 0 min DT and b) 5 min DT 88

Figure 5.4: Morphology of "steady state" granules produced at a) 24% LL and 245 rpm, b) 30% LL and 245 rpm, c) 24% LL and 490 rpm and d) 30% LL and 490 rpm after 60 min of dissolution time.....89

Figure 5.5: Single particle dissolution: 1. Irregular-shaped granules produced at 24% LL and 245 rpm and 2. Regular, spheroidal granules produced at 30% LL and 490 rpm 89

Figure 5.6: FBRM used to detect the change in number of particle during dissolution testing. a) Irregular-shaped granules (24% LL and 245 rpm) and b) Regular, spheroidal granules (30% LL and 490 rpm) 91

Figure 5.7: Single granule dissolution performed on a granule produced at 30% LL, 490 rpm and after 30 min of wet massing. a) 1 min DT and b) 3 min DT.....93

Figure 5.8: a) Leaching mechanism occurs during dissolution of "steady state" granules b) Shrinking core model proposed to describe the leaching mechanism (where t3>t2>t1) 94

Figure 6.1: Potential effects of varying the composition of formulation on the dissolution rate of "steady state" granules.....98

Figure 6.2: Size distributions of "steady state" granules with increasing amount of MCC in formulation, produced at 30% LL and 490 rpm. 100

Figure 6.3: Adjustment of liquid level to achieve similar size distribution (74 wt% lactose and 20 wt% MCC). a) 69 wt% lactose and 25 wt% MCC and b) 64 wt% lactose and 30 wt% MCC.....100

Figure 6.4: a) Effect of formulation on the circularity of granules at 30% LL and 490 rpm. b) Effect of liquid level on the circularity of granules of different formulations.....101

Figure 6.5: Morphology of granules produced at 490 rpm and after 30 min WMT. a) 74 wt% Lactose 20 wt% MCC – 30.0% LL, b) 69 wt% Lactose 25 wt% MCC – 30.0% LL, c) 69 wt% Lactose 25 wt% MCC – 32.5% LL, d) 69 wt% Lactose 25 wt% MCC – 35.0% LL, e) 64 wt% Lactose 30 wt% MCC – 30.0% LL, f) 64 wt% Lactose 30 wt% MCC – 35.0% LL, g) 64 wt% Lactose 30 wt% MCC – 40.0% LL, h) 59 wt% Lactose 35 wt% MCC – 30.0% LL 102

Figure 6.6: a) Effect of formulation on the poured density and tapped density of granules at 30% LL and 490 rpm. b) Effect of liquid level on the poured density and tapped density of granules of different formulations. 103

Figure 6.7: a) Effect of formulation on the Hausner ratio at 30% LL and 490 rpm. b) Effect of liquid level on the Hausner ratio of granules of different formulations. 104

Figure 6.8: Dissolution profiles of "steady state" granules with increasing amount of MCC in formulation, produced at 30% LL and 490 rpm. 106

Figure 6.9: Morphology of "steady state" granules: a) 74 wt% lactose and 20 wt% MCC, b) 69 wt% lactose and 25 wt% MCC, c) 64 wt% lactose and 30 wt% MCC and d) 59 wt% lactose and 35 wt% MCC after 60 min of dissolution time. 106

Figure 6.10: Dissolution profiles of "steady state" granules with increasing amount of MCC in formulation and of similar size distributions by adjusting the liquid level. 107

Figure 6.11: Morphology of "steady state" granules: a) 74 wt% lactose and 20 wt% (30% LL) MCC, b) 69 wt% lactose and 25 wt% MCC (32.5% LL) and c) 64 wt% lactose and 30 wt% MCC (35% LL) after 60 min of dissolution time. 108

Figure 6.12: Dissolution profiles of "steady state" granules of different formulations: a) 69 wt% lactose and 25 wt% MCC and b) 64 wt% lactose and 30 wt% MCC.....108

Figure 6.13: Size distributions of mannitol-MCC formulated granules produced at 30% LL, 490 rpm and 0-30 min wet massing. 109

Figure 6.14: Granule size distributions produced using a lactose-MCC formulation and a mannitol-MCC formulation at 30% LL and 490 rpm. 110

Figure 6.15: Dissolution profiles of lactose-MCC formulated and mannitol-MCC formulated "steady state" granules. 111

Figure 6.16: Morphology of mannitol-MCC formulated granules a) before and b) after 60 min of dissolution testing. 111

Figure 6.17: Effect of matrix porosity (amount of soluble component) on the release of Rhodamine B within the first 10 min dissolution window. a) Varying composition of formulation (20-35 wt% MCC) with constant liquid level of 30% and b) Varying liquid level (30-35%) at different compositions of formulation (20-30 wt% MCC).....114

LIST OF TABLES

Table 1.1: Pharmaceutic ingredient and its function in solid dosage forms (Ansel et al. 1999) 2

Table 2.1: Summary of diffusion related theories and dissolution kinetic models.....38

Table 3.1: Summary of the properties of ingredient used in the formulation Refractive index taken from (Malvern 1997) and solubility data taken from Rowe *et al.* (2006).....48

Table 3.2: Experimental work done in "steady state" granulation project.....52

Table 4.1: Summary of "steady state" granulation operating conditions for granule characterization analysis 60

Table 4.2: Evolution of volume weighted mean diameter, D4,3 (μm) over wet massing period 64

Table 5.1: Summary of "steady state" granules used for dissolution studies 86

Table 6.1: Summary of formulations being tested and the corresponding liquid level being applied.....99

Table 6.2: Summary of granules properties at varying formulation compositions but similar size distributions 105

Table 6.3: Comparison of properties between mannitol-MCC formulated granules and lactose-MCC formulated granules produced at 30% LL, 490 rpm and 30 min WMT.....110

CHAPTER ONE

Introduction

1 INTRODUCTION

1.1 PHARMACEUTICAL DOSAGE FORMS

Drug substances are potent in nature and mostly administered in very low dosage of milligrams which is difficult to be measured by patients without any appropriate measuring devices. From a clinical standpoint, delivering an accurate drug dosage with the most convenient means of administration is of paramount importance. Pharmaceutical dosage forms are designed to carry the drug substances to be delivered into or applied on human bodies. A dosage form usually contains multiple non-medicinal agents mixed together with the active pharmaceutical ingredient (API). The choice of dosage form and route of administration depend on the nature of the illness, whether it is best treated systemically or locally. Common routes of administration practiced are oral, parenteral, intrarespiratory, intranasal, epicutaneous etc (Ansel 1981).

The oral route provides a natural, uncomplicated and safe way of administering drugs. Primary dosage forms that are widely applied through oral administration are available in either solids or liquids. The nature of the drugs such as stability, solubility and absorptivity, mode of drug release and effective drug absorption sites are taken into consideration when choosing the suitable form as the drug carrier (Ansel *et al.* 1999). In terms of patient compliance, the dosage form should be relatively easy to be recognized, dispensed and delivered without any complications and discomfort.

Tablets and capsules are typical solid dosage forms designed to pass the drugs through the mouth and down the gastrointestinal tract. Commercial tablets and capsules appear in different shapes and colours determined by the manufacturers, most importantly with appropriate sizes for ease in swallowing. Direct or roller compaction (dry method) and wet granulation (wet method) are two well-developed tablet making technologies. Powders used to produce the final solid dosage forms are mixture of pharmaceutic ingredients/excipients, each playing specialized pharmaceutical role listed in Table 1.1.

Table 1.1: Pharmaceutic ingredient and its function in solid dosage forms (Ansel et al. 1999)

Ingredient type	Pharmaceutical function	Examples
Diluent	• To create the bulk required for formulation • To improve flow and compression properties	Lactose, Mannitol, Microcrystalline cellulose
Binder	• To promote adhesion between drug substances and pharmaceutic ingredients in forming agglomerates	Hydroxypropyl cellulose, Methylcellulose
Disintegrant	• To cause dissociation of large entities into smaller particles, releasing encapsulated drug substances	Croscarmellose sodium, Starch
Sweetening agent	• To add a sweet taste into formulation, concealing the bitterness of drug substances	Mannitol, Sorbitol, Sucrose
Coating agent	• To protect drug substances from decomposing due to internal and external environment • To modify the release rate of drug substances	Methylcellulose, Sucrose
Colorant	• To make final products more appealing	Caramel, Ferric oxide (red)

1.2 PAEDIATRIC MEDICINE

Paediatric medicines have always received great attention as the targeted population is at a development stage where they are susceptible to sickness and need considerable amount of care. Paediatric population can be divided into sub-groups based on age (Walsh *et al.* 2011). Each age group may require the same medicine with different formulations, doses and forms. Clinical studies are actively performed to develop paediatric formulations that are age appropriate, dosage forms that are easy to be administered and administration devices that aid in delivery.

Delivering the correct dose is vital to achieve maximum therapeutic effect of drugs. Suitable dosage forms and proper use of administration devices will help in ensuring patients receive the required amount of medicine. Children are sensitive and tend to be repulsed by medicine. From a patient and carer perspective, the delivery method should not be intrusive or cause any discomfort while administering and be easy to carry out with clear instructions.

It has always been challenging to select and design an appropriate dosage form for children. Out of all practiced routes of administration, the oral route is the most common way of delivering medicinal products. Oral dosage forms should be easy to swallow and have acceptable palatability. Types of oral dosage form available are tablet, capsule, oral granules/sprinkles/powders, and oral solution/syrup/drops/suspension. When selecting an appropriate dosage form, the following three major factors are taken into account (Sam *et al.* 2012):

1. Efficacy of medication
2. Patient safety
3. Patient access to medication

Tablets or capsules are a common type of solid dosage form for adults but they may be difficult for children to swallow. Crushing or breaking of tablets for ease in administration may lead to inaccurate dosing hence imposing health risk on children. Solid dosage forms of smaller sizes such as granules, sprinkles and mini-tablets are designed to overcome the difficulty in swallowing. Potential advantages of these forms are good solid state stability, can be administered together with food or beverage and flexibility in dosing (Sam *et al.* 2012). On the other hand, they require the development of measuring system, verification of compatibility with food and beverage and taste masking (Sam *et al.* 2012).

Designing a dosage form can be complex and laborious. From early stages of characterizing drug substances and selecting suitable excipients to final stages of packaging and dispensing drug products to patients require an enormous effort from pharmacologist, toxicologist, researchers etc. One of the criteria in selecting an appropriate dosage form is accessibility of medication by patient. This criterion considers other factors related to ease of development, manufacturability, transport, storage and dispensing (Sam *et al.* 2012).

Manufacturability is defined as the extent to which a drug product of acceptable quality can be manufactured routinely at reasonable cost (Sam *et al.* 2012). Introducing new technology solely to produce a specific drug product for a small target population may not be time and cost effective. As a result, patients have to pay for expensive medicines. Therefore it is vital to develop a robust manufacturing process that can consistently produce a dosage form under stringent specifications.

"Steady state" granulation approach has been proposed and adopted in high shear wet granulation by Michaels *et al.* (2009). It has successfully produced considerable spherical granules with narrow size distributions and good dissolution performance (Michaels *et al.* 2009) without the need for milling to control granule size. Michaels *et al.* (2009) used the approach to produce tablets but the approach shows potential for producing a new oral solid dosage form i.e. "steady state" granules for direct use by the paediatric population. Paediatric granules produced will be much smaller than conventional tablets or capsules and easier to be administered. Accurate dosage can be delivered to children by adjusting the weight/volume of the granules given to the patient with proper measuring devices and instructions.

1.3 RESEARCH AIMS

The overall objective of this research project is to achieve an improved control of granule properties in high shear wet granulation using a different operating approach, called the "steady state" granulation approach. High shear wet granulation is usually used to produce granules which are later compressed into tablets. Industrial pharmaceutical processes adopt short granulation time with copious amount of liquid binder resulting in broad granule size distributions due to difficulties in controlling the transient process. The broad distributions are later milled to reach the appropriate size range. Adopting the "steady state" approach is expected to produce spherical granules (end product) with a narrow size distribution and other desired attributes such as constant bulk density and controlled release rate. Achieving these properties has huge implications on ensuring uniform distribution of drug substances across and within the dosage form. This will open up potential contributions in designing granule dosage form using high shear wet granulation. The project has the following specific research aims:

1. To investigate the effects of wet massing time, liquid level and impeller speed on the properties of "steady state" granules produced in a 5 L high shear mixer granulator
2. To define the "steady state" region through the study of the effects of selected operating parameters on granulation behaviour
3. To investigate the dissolution performance and identify the release mechanism of "steady state" granules
4. To control the rate of release of "steady state" granules by varying the composition of formulation
5. To investigate the effect of variation in composition of formulation on the properties of "steady state" granules

1.4 THESIS OUTLINE

This project has adopted the "steady state" granulation approach in high shear wet granulation process. The thesis is structured to provide an informative review on high shear wet granulation, explain the concept of "steady state" and discuss the key findings. The outline of the thesis is shown as followed:

CHAPTER 2: Literature review

Previous research on how operating conditions such as amount of liquid added, method of liquid delivery, impeller speed and wet massing time affect the granulation behaviour is

reviewed. The "steady state" concept introduced by Michaels *et al*. (2009) is also presented in this section.

CHAPTER 3: Material and methodology

Functionalities and properties of individual component in the pharmaceutical formulation used for the project are discussed. Experimental procedure of "steady state" granulation and characterization of granule properties are also elaborated.

CHAPTER 4: Feasibility of "steady state" granulation

The "steady state" granulation approach is applied using a 5 L high shear mixer granulator. Wet massing time, liquid level and impeller speed are the operating parameters selected to study their effect on the granulation behaviour. Granule properties are examined over a wet massing period to define the "steady state" region.

CHAPTER 5: Dissolution performance of "steady state" granules

Dissolution properties of "steady state" granules are determined by monitoring the release of Rhodamine B over time. The structure of "steady state" granules before and after dissolution is examined and compared using SEM to study the release mechanisms.

CHAPTER 6: Effect of varying formulation composition on granule properties and dissolution profile

The pharmaceutical formulation is adjusted by varying the composition of soluble and insoluble components to control the dissolution rate of "steady state" granules. The effect of increasing the composition of insoluble component on other granule properties is also studied.

CHAPTER 7: Conclusions and recommendations

The key findings of applying "steady state" granulation approach in the production of granules with narrow size distribution, considerably round shape and controlled release rate are summarised. Recommendations are made to suggest potential work to be carried out in future in order to gain a deeper understanding on the current findings.

CHAPTER TWO

LITERATURE REVIEW

2 LITERATURE REVIEW

Granulation has a long history in the pharmaceutical industry and given its importance in powder handling, a significant amount of research is still on-going in this field. The complexity of granulation processes has been the driving force for researchers to establish a deeper understanding of the process nature at different levels, from macroscopic to microscopic. Much has been done to describe the process in a simplistic manner such as developing regime map (Hapgood *et al.* 2003), implementing proper control (Hapgood *et al.* 2010) etc. This chapter discusses a general overview of granulation, narrowing down to high shear wet granulation and previous findings on parameters that affect granulation behaviour.

2.1 GRANULATION

Granulation is a particle size enlargement process where fine particles are agglomerated into a larger solid mass to achieve specific size and attributes (see Figure 2.1). This operation is widely employed in different industrial fields such as mining, food, agrochemicals and especially pharmaceutical products. The cohesive nature of fine powders causes them to flow poorly and difficult to handle. Hence pharmaceutical compounds are granulated to (Parikh 2007, Rhodes 2008):

- Enhance the flowability of material
- Improve the composition homogeneity of granules
- Increase the density of granules
- Improve the uniformity of drug distribution in final product
- Reduce dust exposure
- Improve tableting properties and appearance of products

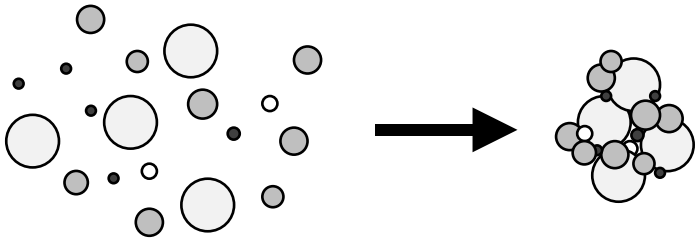

Figure 2.1: Fine particles are agglomerated into larger entity called granule.

Granulation can be conducted in two distinct methods: wet or dry (Parikh 2007). Batch wet granulation is most common in pharmaceutical industry where granulating fluid, also called a liquid binder is distributed over a powder bed to enhance the agglomeration of drug substances and other inert excipients. At completion of the process, larger entities called granules are formed. Granules are an intermediate product between the raw powders and the final solid dosage form such as tablet. It eliminates the disadvantage of direct usage of fine powders i.e. poor flowability and exhibits characteristics that favour tablet making such as higher stability, less likely to cake upon standing etc (Ansel *et al.* 1999).

2.2 WET GRANULATION

Wet granulation is governed by three rate processes (Iveson *et al.* 2001): 1. *wetting and nucleation* where liquid binder is poured, sprayed or dripped into mechanically agitated powder bed to initiate nucleation, 2. *coalescence and growth* where primary nuclei or agglomerates collide to form larger granules and layering of binder-coated granules by fine particles, 3. *attrition and breakage* where weak or less dense granules break due to impact or shear forces (see Figure 2.2).

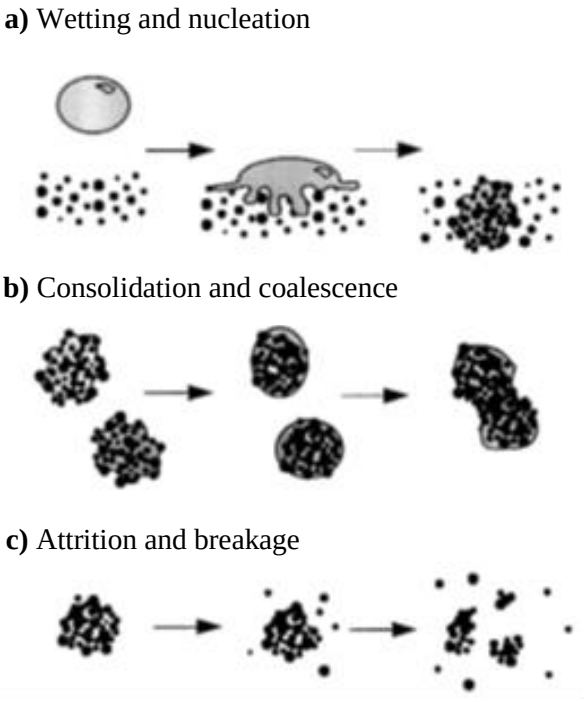

Figure 2.2: Modern approach of describing granulation process as a combination of three sets of rate processes. Adopted from Iveson et al. (2001).

When a mass of fine powder is agitated in the presence of liquid, particles collide and stick to each other. Liquid bridges hold the particles together and form granule nuclei. They then go through different states of liquid saturation in the growth process (see Figure 2.3). Daughter granules that are formed from the collision of granule nuclei will enlarge, densify, consolidate, deform and/or break. Wet granulation techniques that are frequently used are low shear and high shear granulation, spray drying, fluid bed granulation and extrusion/spheronization.

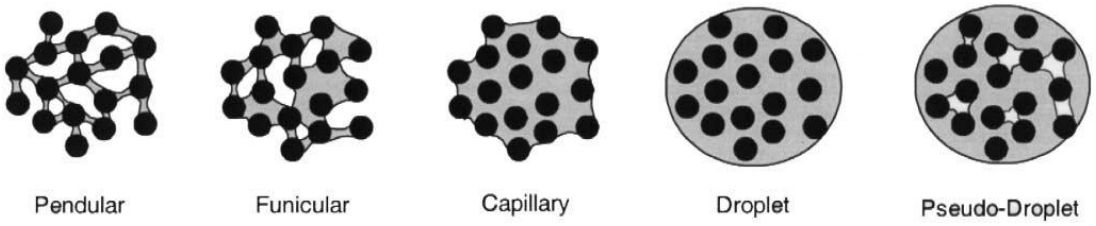

Figure 2.3: Different states of saturation attained by liquid-bound granules. Adopted from Iveson et al. (2001).

2.3 HIGH SHEAR WET GRANULATION

A high shear mixer granulator consists of a mixing bowl (which can be jacketed for temperature control), an impeller and an optional chopper. The impeller generates shearing and compaction forces that allow wetted powders to mix, agglomerate and densify. High shear granulation exhibits several advantages which gained its popularity such as short processing time, less consumption of liquid binder, greater densification of granules and reduction in segregation (Parikh 2007). High shear wet granulation (HSWG) can be divided into two main periods: liquid binder delivery and wet massing. Dry powders are usually pre-mixed before liquid introduction to improve homogeneity of ingredients in the mixing bowl. The liquid delivered can be a mixture of water and polymeric binder or purely water where the dry binder powder is mixed with other powdered ingredients in the mixer. The presence of impeller and chopper enhances the distribution of liquid binder within the powder bed. Wet massing is the subsequent stage in the granulation process where wet mass is continuously kneaded at high impeller speed after all the liquid binder has been added in order to distribute the liquid more uniformly across the powder bed.

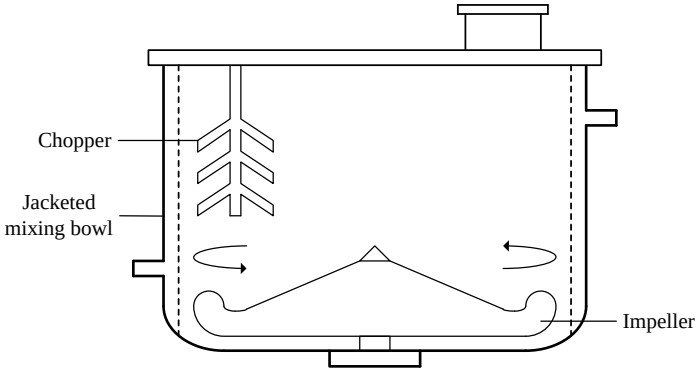

Figure 2.4: Schematic diagram of a high shear mixer granulator.

2.4 CONVENTIONAL HIGH SHEAR WET GRANULATION

In the production line of making pharmaceutical tablets out of fine powder, granulation is an intermediate stage. A typical process chain consists of blender, premix bin, granulator, wet mill, dryer, dry mill, blender, tableting press and other minor parts (Parikh 2007). In industrial manufacturing, conventional high shear wet granulation adopts larger amount of liquid than required and wet massing time is usually less than 5 min (Shi *et al.* 2011). An example of process design at manufacture scale consists of three stages: 1. Pre-blend (5 min), 2. Solution delivery (5-10 min), 3. Wet massing (1-3 min). The whole process takes 10-20 min to completion (Liu *et al.* 2009).

The downside of running granulation in such short period is the production of a broad granule size distribution. This is a major issue faced by the manufacturer in controlling such a transient process. Within a period of time, a wet granule can undergo multiple granulation mechanisms and attain different states (Iveson *et al.* 2001). It is difficult to track down and monitor a granule that is consistently changing its position with time. Wet and/or dry mills are placed downstream as sizing units to produce uniformly sized granules. However, size reduction may have some adverse effects on the final characteristics of a dosage form (Parikh 2007). The excessive heat generated when granules are compressed and pushed across a screen can cause degradation of drug or change in polymorphic form. In addition, the granules produced are generally irregular in shape and must later compressed into tablets of specific size (Ansel *et al.* 1999).

2.5 COMPLEXITIES AND CHALLENGES

Despite the advantages offered, the inherit complexity of granulation process restricts it from being a robust method with a straight forward scale-up procedure. This is because all

granulation rate processes are transient i.e. they occur simultaneously with other solid-liquid interactions such as dissolution of dry binder and dynamic adsorption of liquid onto excipients that can cause changes in binder viscosity, surface tension or contact angle. The complexities outlined above illustrate how conventional granulation process is sensitive to changes in many variables. For example, a batch of fine powder can be under-granulated, well-granulated or over-granulated depending on the amount of liquid added and the optimum amount of liquid required to achieve controlled granulation may vary for different formulations.

Moreover, process complications such as non-uniformity in liquid distribution, over-wetting that leads to uncontrolled granule growth or heat generated by the impeller that causes evaporation of binder solvent are common factors contributing to the difficulties in process control. In microscopic level, physical properties of materials are constantly changing throughout the process and hence affecting the degree of granulation. Granule temperature may increase due to particle-particle and/or particle-equipment friction. Shear forces imparted on granules vary from location to location where those situated towards the centre are exposed to less force.

The coupling of variables further complicates the monitoring procedure as the correlations are indirect and non-linear. Therefore, granulation processes are often considered as a "black box". After years of development, much has been studied to comprehend the dynamics of solid-liquid granular systems. However, to apply those learning on industrial practice is still difficult. Therefore granulation processes are in general empirically designed based on best practice and history at each individual company.

2.6 EFFECTS OF PARAMETERS ON GRANULATION BEHAVIOUR

The high dependency of granulation process on material properties and process variables provides the versatility of manipulating specific parameters to attain the desired outcome. Many studies have been performed to investigate the effects of physico-chemical properties of granulating materials and operating conditions on wet granulation kinetics. Key parameters in operating conditions are the amount of granulating fluid delivered, liquid binder addition method and addition rate, impeller speed, use of chopper, wet massing time and (occasionally) temperature control. Solid and liquid properties known to affect granulation process include the primary particle size and initial moisture content of the raw materials and the viscosity and wettability of liquid binder. It has been difficult to describe granulation

behaviour in a systemic way. By investigating how the variation of parameters affects the final granule properties, a better understanding of the evolution of a granule from primary particles can be achieved. Although the effects of physico-chemical properties are equally important, the literature review will focus mainly on the effects of operating parameters on granulation behaviour.

2.6.1 AMOUNT OF LIQUID ADDED

In high shear wet granulation, granulating fluid is the main aspect that acts to bind particles together and form granules. A suitable amount of liquid binder must be added as the liquid content in granules determines their structures during granulation process. A common issue in granulation is over-wetting due to excessive liquid which leads to lump formation or even caking. Therefore the liquid level of the wet mass has to be tightly controlled to meet stringent specifications.

When granulating fluid is added into the granulator, fine powders are wetted, binders are dissolved and liquid bridges are formed between primary particles at low saturations. Increasing the amount of liquid reduces the interparticle friction and increases the liquid saturation of agglomerates. Wet granules with higher liquid saturation are more deformable and granule growth by coalescence is enhanced. They also possess sufficient cohesive strength to resist being broken apart by shear forces due to increase in capillary and viscous forces (Mackaplow *et al.* 2000). Therefore the amount of liquid added is a crucial factor in the evolution of granule size. Realpe and Velázquez (2008) also proposed that there is a minimum amount of liquid required to form a liquid layer on the granule surface to increase the probability of coalescence between particles.

Before reaching the limit of over-wetting, granule size increases with increasing amount of liquid (Mackaplow *et al.* 2000, Ohno *et al.* 2007) (see Figure 2.5). In Mackaplow *et al.*'s work (2000), granule size was determined in two states, dry and wet. The amount of liquid added was found to have minimal effect on granule size in the wet state but increased the apparent dry granule size. They presumed that in drying stage, the size and number of recrystallized lactose bridges increased enabling the particles to be locked to each other. However, if too much liquid is added, large granule balls may form and retard the granulation process.

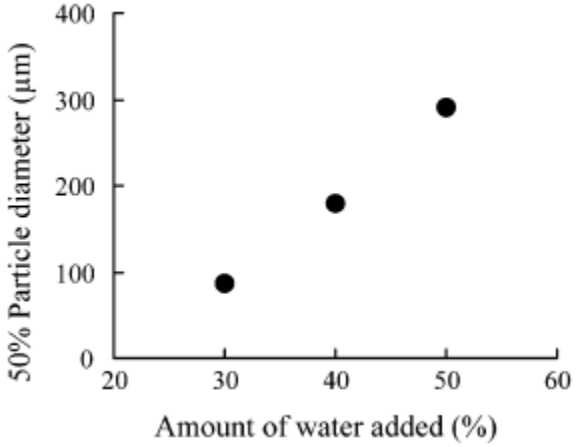

Figure 2.5: Effect of amount of liquid on 50% particle diameter at an impeller rotation speed of 600 rpm and wet massing time of 6 min. Taken from Ohno *et al.* (2007).

The amount of liquid added also affects the final granules in terms of bulk density, porosity, compressibility and strength. Bouwman *et al.* (2005) used microcrystalline cellulose and water as a model system to study the granulation mechanisms at different phases of granulation process. The densification process of wet granules was visualized using x-ray microtomography which allows investigation of any 3D region inside the granules. They found that densification of granules with higher water content was halted even after a long period of granulation. Therefore weaker and more deformable granules were produced as a result of increase in water availability and they did not survive the impact of impeller which led to granule breakage (Bouwman *et al.* 2005). However, this trend is not universal; granule porosity was found to decrease with an increase in the amount of liquid (Mackaplow *et al.* 2000, Ohno *et al.* 2007). Ohno *et al.* (2007) attributed the phenomenon to the dissolution of soluble components, lactose and HPC in the liquid added, allowing the two components to act as binder.

In summary, the amount of liquid delivered to granulation process influences the size distribution but also can affect granule densification, depending on the formulation used. However, there is no standard for determining the optimum liquid level required to achieve a target size range due to other physico-chemical factors such as primary particle size of granulating materials, type and concentration of binder used etc.

2.6.2 METHOD OF LIQUID DELIVERY AND ADDITION RATE

The liquid delivery method is crucial for achieving uniform liquid distribution across the powder bed. Common liquid delivery methods are pouring, dripping and spraying (see Figure 2.6). Knight *et al.* (1998) found that the spraying method produced a lower proportion of coarse granules compared to the pouring method, regardless of the primary particle size. Both methods produced bimodal size distributions which became narrower upon further wet massing. However, the spraying method was able to produce the narrowest size distribution. The finding was also supported by Scott *et al.*'s work (2000) where a bimodal size distribution of PEG granules was produced by the pouring method and eventually became unimodal at the end of the experiment.

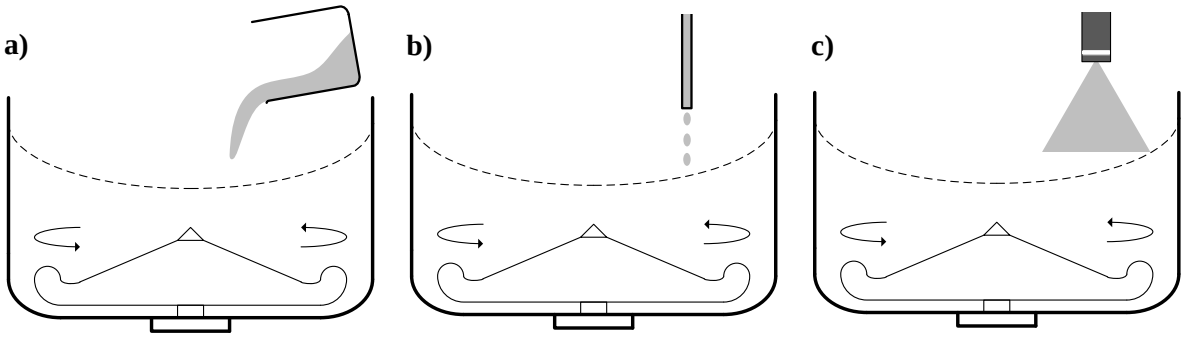

Figure 2.6: Different methods of liquid delivery: a) Pouring, b) Dripping and c) Spraying.

In contrast, other studies showed contradictory results where the choice of liquid delivery method had little influence on the granule size. Osborne *et al.* (2011) tested three types of addition method using HPMC as the binder: 1. Dry addition - HPMC was premixed with other powders and water was pumped into the mixer, 2. Wet addition - HPMC was mixed with water before pouring into the mixer and 3. Spray addition of HPMC binder solution. Both wet and spray addition methods produced similar size distributions while slightly larger granules were produced by applying the dry addition method (see Figure 2.7).

Osborne *et al.* (2011) also investigated the binder content of each granule size class by analysing the dye content in solutions of dissolved granules. Results showed that the binder content profiles for all three methods were very similar, showing high resemblance in terms of liquid distribution. This can be attributed to the constant shearing rate imposed by the high impeller speed that promotes similar granule growth and breakage rates. Rahmanian *et al.* (2011) also found that the liquid delivery methods adopted had no significant effect on the

granule size distributions (Refer to Figure 2.8). Mechanical agitation provided by the impeller and chopper was believed to be efficient enough in uniformly distributing all the liquid added to the same extent. These trials were all carried out at small scales but achieving uniform liquid distribution after scale-up is still a challenge (Ameye *et al.* 2002).

Liquid delivery method determines the nature of initial liquid distribution in powder bed. Under the same mechanical mixing conditions, a more uniform liquid distribution can be achieved with smaller initial liquid droplets produced by spraying method. Higher impeller and/or chopper speeds will be required to break down larger agglomerates or lumps that may be formed by pouring and dripping methods.

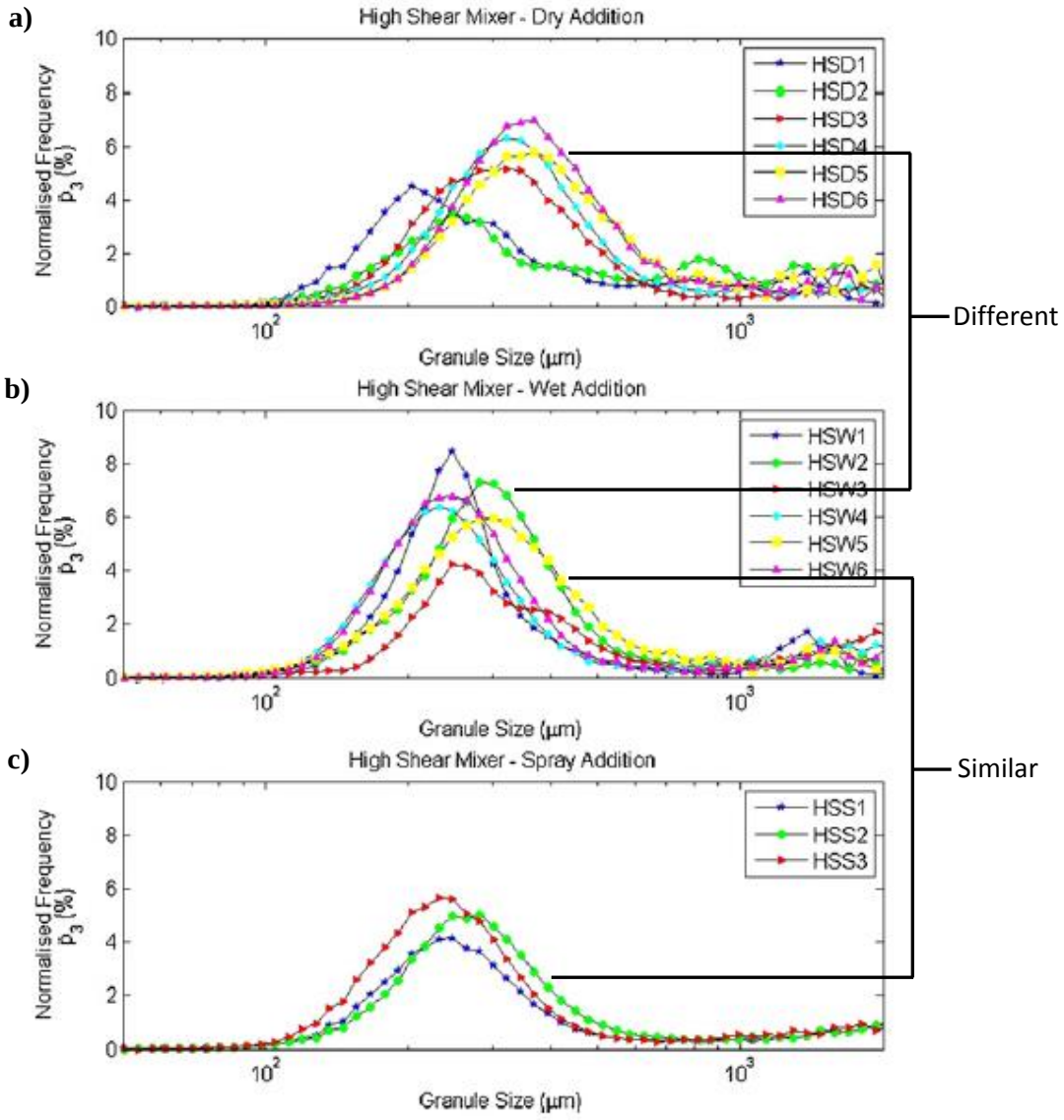

Figure 2.7: Granule size distributions obtained using three different liquid delivery methods: a) Dry addition, b) Wet addition and c) Spray addition in high shear mixer. Taken from Osborne *et al.* (2011).

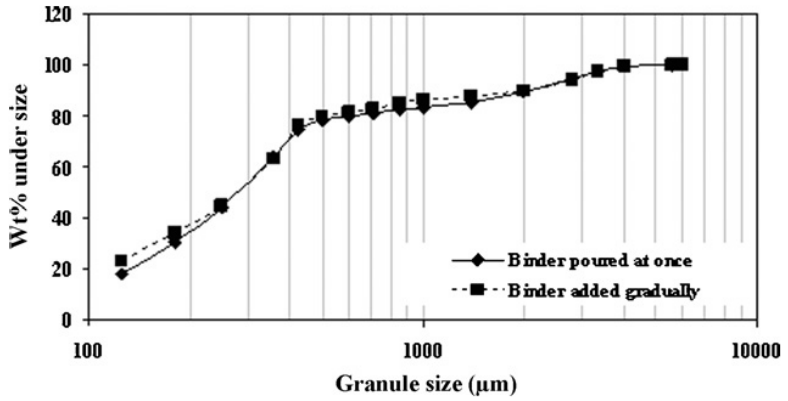

Figure 2.8: Effect of liquid delivery methods on granule size distribution. Taken from Rahmanian *et al.* (2011).

The nucleation mechanisms discussed below have been referred extensively to understand the formation of granules at microscopic level. Nucleation mechanisms are highly influenced by the size of the binder droplet produced by the method of delivery. To be more specific, the relative size of the binder droplet to primary powder particle is the most influential aspect. Schaefer and Mathiesen (1996) studied the effect of binder particle size on melt pelletization in a high shear mixer by using different grades of polyethylene glycol (PEG). They found that the size of molten binder influences the mechanisms of agglomerate formation. Two nucleation mechanisms were then proposed: 1. Immersion mechanism – Primary particles are immersed in droplets that are relatively larger in size and 2. Distribution mechanism – Primary particles are coated by droplets that are relatively smaller in size (Schaefer *et al.* 1996) (see Figure 2.9). In general, granule nuclei formed by immersion mechanism are denser with saturated pores while those by distribution mechanism may have air trapped inside (Scott *et al.* 2000). It was proposed that nucleation followed the immersion mechanism when pour-on method was used in the experiments conducted by Scott *et al.* (2000). No reported literature mentioned the type of mechanism that nucleation follows for dripping methods. However, it is also likely to be immersion nucleation, in contrast to finely atomised addition which is distribution nucleation.

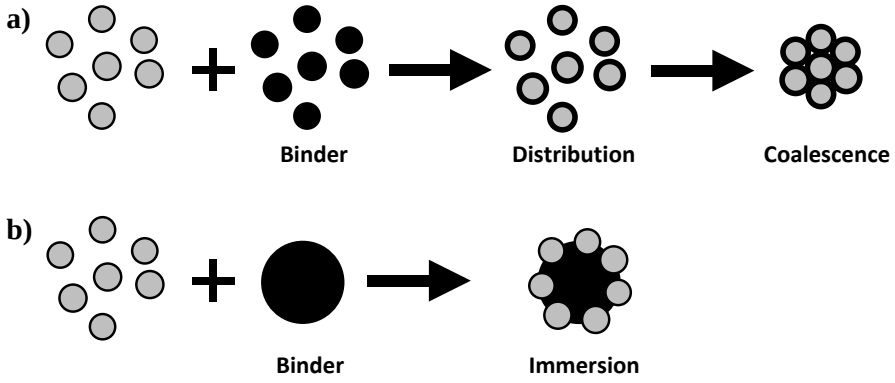

Figure 2.9: Two nucleation mechanisms proposed which take into account the effect of the size of binder droplet: a) Immersion distribution and b) Distribution mechanism. Adapted from Schaefer *et al.* (1996).

Following up the above findings, Dries and Vromans (2004) came out with a schematic overview of the possible nucleation mechanisms in high shear mixer granulators. The proposed mechanisms by Schaefer and Mathiesen (1996) were based on measurements at least 1 min after the start of liquid addition. This raised the question of what events may have occurred during the nucleation process in the very first minute of liquid addition. Hence Dries and Vromans (2004) initiated a study to investigate what was occurring at early seconds of the process that lead to granule inhomogeneity. They included the effect of granule breakage as it may occur to granule nuclei once formed in an intensively sheared mixer. The three different nucleation mechanisms suggested are: I. Penetration-involved nucleation and granule breakage, II. Penetration-involved nucleation and absence of granule breakage and III. Dispersion-only nucleation (van den Dries *et al.* 2003, van den Dries *et al.* 2004).

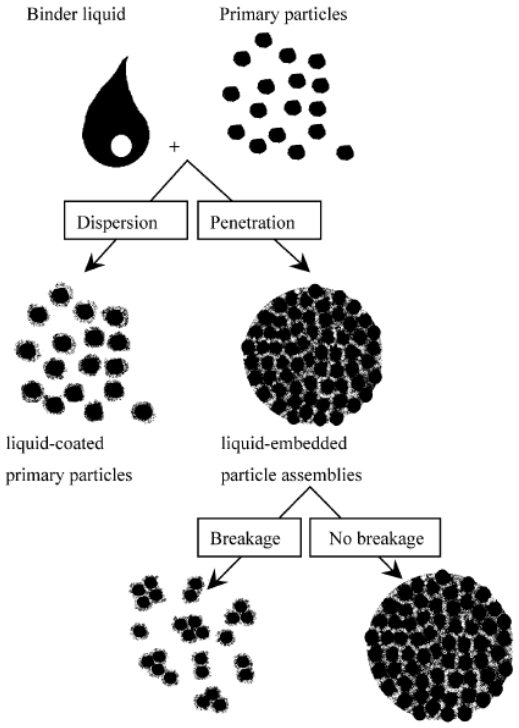

Figure 2.10: Schematic overview of the possible nucleation mechanisms in the high shear mixer granulator. Inset from Dries and Vromans (2004).

The effect of liquid addition rate on granulation behaviour cannot be neglected especially when dripping and spraying methods are applied. It is included in the dimensionless spray flux parameter, ψ_a (Eqn 2.1) which is a measure of the drop density in the spray zone, developed by Litster *et al.* (2001). They considered the process of nucleation in the spray zone of a granulator in five sequential steps (see Figure 2.11). It was suggested to keep ψ_a below 0.1 to ensure nucleation falls in the drop controlled regime where one drop of liquid forms one granule nucleus (Hapgood *et al.* 2003). In the nucleation regime map by Hapgood *et al.* (2003) (see Figure 2.12), nucleation in drop controlled regime is preferable to prevent pooling from occurring as highly saturated patches caused by local wetting will induce lump formation.

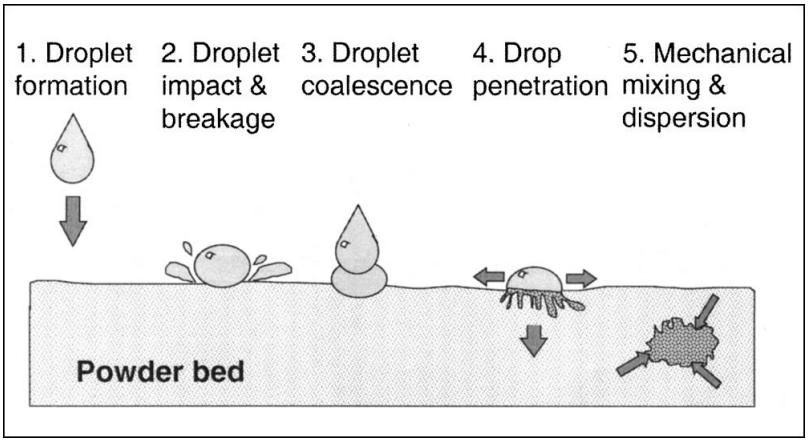

Figure 2.11: The five steps of nucleation: 1. Droplet formation, 2. Droplet impact on the powder and possible breakage, 3. Droplet coalescence at the powder surface, 4. Droplet penetration into the powder pores and 5. Mixing of the liquid and powder by mechanical dispersion. Inset from Litster *et al.* (2001)

$$\psi_a = \frac{3\dot{V}}{2\dot{A}d_d} \qquad \text{[Eqn. 2.1]}$$

$$\tau_p = \frac{t_p}{t_c} \qquad \text{[Eqn. 2.2]}$$

$$t_p = 1.35\frac{V_o^{2/3}}{\varepsilon^2 R_{pore}}\frac{\mu}{\gamma_{LV}\cos\theta_d} \qquad \text{[Eqn. 2.3]}$$

where:

$\dot{V}$ is the volumetric spray rate

$\dot{A}$ is the area flux of powder traversing the spray zone

d_d is the droplet diameter

τ_p is the dimensionless drop penetration time

t_p is the penetration time of the spray drops

t_c is the circulation time

V_o is the drop volume

ε is the powder bed porosity

R_{pore} is the radius of the pores

μ is the liquid viscosity

γ_{LV} is the liquid surface tension

θ_d is the dynamic contact angle of the liquid in the solid capillary

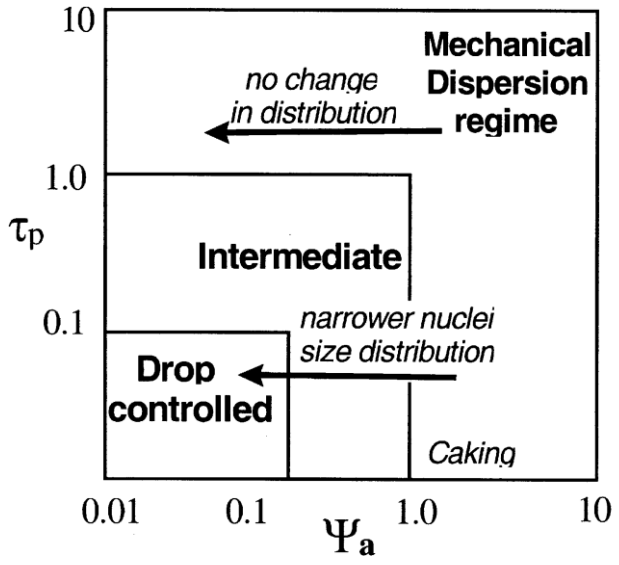

Figure 2.12: Proposed nucleation regime map for liquid bound granules. Adopted from Hapgood *et al.* (2003).

A case study was performed in attempt to improve the liquid distribution of an existing wet granulation process that has problem of "ball" formation. By reducing the dimensionless spray flux, the nucleation process can be shifted towards the drop controlled regime to achieve narrower size distribution. This was done by the implementation of a new nozzle which was expected to decrease "ball" formation but resulted in the opposite (Hapgood *et al.* 2010). Few possible reasons were given for the result: 1. "Ball" formation might due to rapid or induction growth of the granules instead of local wetting and 2. As the efficiency of liquid distribution increased, the total liquid required to achieve the same extent of granulation might be less.

Benali *et al.* (2009) investigated the effect of binder solution flow rate on granulation behaviour using microcrystalline cellulose powder. They found that the exhaustion of fine particles was faster at a higher flow rate and the extension of non-growth regime (wetting of primary fine particles) was reduced. Higher flow rate enhanced the formation of intermediate class granules (140-450 μm) and accelerated the overall granulation kinetics. However, the mean granule diameter profiles were not greatly influenced.

Although higher flow rate promotes faster granule growth, pooling may occur as a result of liquid binder overlapping on the surface before penetration and redistribution can take place. This will cause nucleation to fall in the mechanical dispersion regime as depicted in the nucleation regime map by Hapgood *et al.* (2003), resulting in caking of powders. Therefore, an optimum flow rate that ensures steady granule growth will be highly recommended.

2.6.3 IMPELLER SPEED AND ROLE OF CHOPPER

The shear forces created by both the impeller and the chopper are the main sources of agitation in high shear wet granulation. The impeller is the key feature in a high shear mixer granulator and it fulfils different roles in each stage of granulation process:

1. Pre-mixing – Promotes uniform blending of raw materials in mixing bowl
2. Liquid addition – Distributes liquid across powder bed and prevent localised wetting
3. Wet massing – Promotes consolidation, densification, deformation and/or breakage of granules

First, a high impeller speed is required to achieve "roping" flow pattern in the rotating powder bed (Litster *et al.* 2002). In the "roping" regime, a good vertical turnover is achieved, which is of paramount importance in the premixing and liquid addition stages. When powder bed is well mixed and undergoing roping flow, raw materials are homogenized and the liquid binder can be dispersed evenly throughout the powder bed. Poor liquid distribution occurs in the "bumping" regime as liquid accumulates on the same powder surface with the risk of pooling. In the pharmaceutical industry, the impeller speed range applied for vertical axis granulators less than 30 cm in diameter is 500 to 1500 rpm while for granulators larger than 1 m in diameter, 50 to 200 rpm is the range being applied (Rhodes 2008).

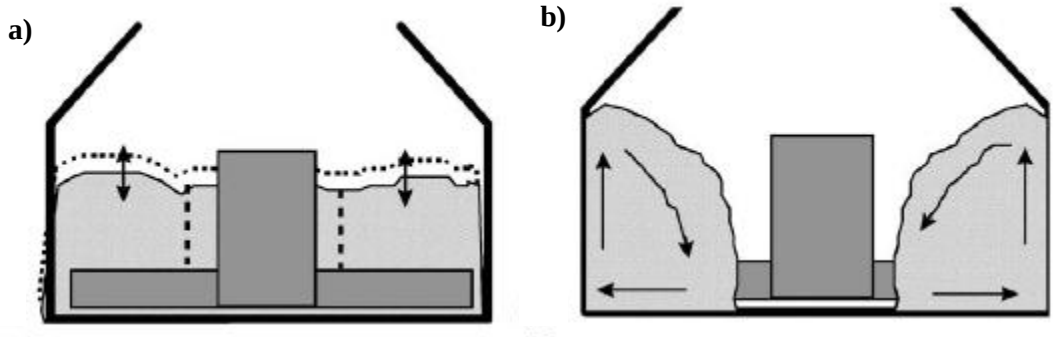

Figure 2.13: Two types of flow regime observed in a high shear granulator: a) Bumping flow and b) Roping flow. Inset from Litster *et al.* (2002).

The inherent complexity of granulation process is due to the constant movement of granules under the action of impeller which subjects granules to a wide range of stresses depending on the granule location. Granules experience compressive forces when being pushed ahead by the impeller blade and shearing forces when being lifted over and falling behind the blade (Knight 2004). Furthermore, granules closer to the blade are subjected to more intense forces compared to those situated a distance away. Thus, granules experience different states and rate processes occur concurrently. However, it is difficult to keep track and monitor the evolution of a single granule. Therefore, the effect of impeller speed on granulation kinetics and final granule properties has been investigated in depth.

Impeller speed can be distinguished into low, moderate and high depending on the intensity of agitation. The impeller speed was found to have pronounced effects on granule size distribution and surface morphology. Knight *et al.* (2000) investigated the effect of impeller speed on particle agglomeration by setting the impeller at three different speeds of 450, 800 and 1500 rpm. Granule size distribution produced at 800 rpm was the narrowest while granules formed at 450 rpm had the highest sphericity. At 1500 rpm, a rather broad size distribution was obtained and the granules were irregular shape (see Figure 2.14). It was deduced from the results that granule breakage became over-dominating and limiting granule growth at such high impeller speed. Equilibrium between the rate of growth and the rate of breakage was not achieved. The fragmented edges of granules also showed that they were subjected to intense shearing forces. Hence the impeller speed has an important role in breaking down larger granules. On the other hand, Ohno *et al.* (2007) adopted total revolution number (impeller rotation speed multiplied by granulation time) instead of impeller speed solely as the parameter to study the surface morphology of granules. SEM images showed that smoother and rounder granules were produced at higher total impeller revolutions.

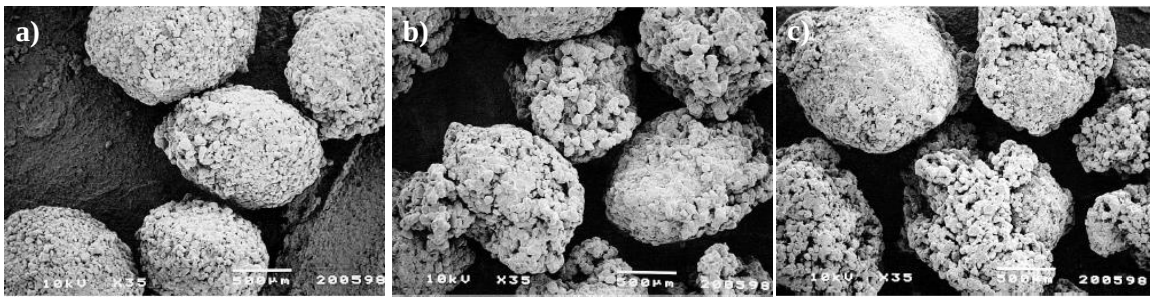

Figure 2.14: Morphology of granules of 1000-1400 µm produced after a) 25 min at 450 rpm, b) after 17 min at 800 rpm and c) after 4 min at 1500 rpm. Taken from Ohno *et al.* (2007).

Recent studies on the effect of impeller speed on granulation behaviour have shown similar trends. Firstly, a high impeller speed is necessary to achieve good control of granule growth as it can reduce preferential growth that may occur at highly saturated spots in the liquid addition stage (Benali *et al.* 2009). In terms of granule properties, increasing the agitation intensity (increased impeller speed) imparted more compaction on granules and enhanced the consolidation and densification mechanisms. Therefore less porous granules with high strength were formed at higher impeller speed which in turn reduced the granule compressibility and friability (Oulahna *et al.* 2003, Saleh *et al.* 2005, Benali *et al.* 2009). In addition, rounder and smoother granules were also produced by surface smoothing and spheronization driven at higher impeller speed (Michaels *et al.* 2009).

In Chitu *et al.*'s work (2011), more fine particles and lumps were observed when a low/moderate impeller speed was used and inhomogeneous products with broad size distribution were produced in the end of process. Running the granulation process at a sufficiently high impeller speed can reduce the amount of lumps effectively without the incorporation of chopper (Chitu *et al.* 2011). When wet mass is intensively agitated, granule breakage dominates over large agglomerates due to the increase in collision frequency between particles and between particles and wall of granulators.

It seems that higher impeller speed is favourable in producing granules with narrow size distribution (Mangwandi *et al.* 2010), spherical shape and smooth surfaces. However, there is a limit that if the impeller speed were set too high, adverse effects will occur. Granule breakage can be the dominating process where more fines are produced as a result of granules being crushed by the vigorous rotating blades (Oulahna *et al.* 2003). Not only do the granules lose their spherical shape, the homogeneity of the system will also be severely reduced. It was proposed that granule undergoes bimodal breakage that produces either many small particles and a few large particles or many small particles and one large particle (Realpe *et al.* 2008) (see Figure 2.15). When granules break down to fragments of various sizes, liquid bridges that hold the individual particle together will be released out and wet the surfaces of these fragments. This allows the adherence of fines that potentially resulted from excessive breakage on the wetted fragments.

The microscopic study of granulation mechanisms and their effect on granule properties conducted by Le *et al.* (2011) supported the occurrence of granule breakage. They found that purple coloured granules were formed when red and blue dyes were used simultaneously to

trace the granules. This suggested that when large wet agglomerates were broken down by intense shear forces, the liquid within were redistributed to the particles around and granule growth by coalescence between fragmented granules was enhanced.

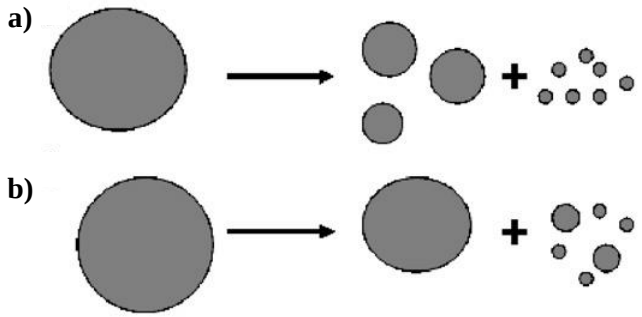

Figure 2.15: Bimodal breakage: a) Many small particles and a few large particles and b) Many small particles and one large particle. Inset from Realpe and Velázquez (2008).

Badawy *et al*. (2012) have proposed how the variations in amount of liquid and impeller speed can affect the granule size in high shear wet granulation. The amount of liquid added affects the liquid saturation of wet granules which in turn determines the mechanical properties of the wet granules. Wet granules with high liquid saturation are more plastically deformable while those with lower liquid saturation are considered brittle. At high impeller speed, the velocity of particle collisions increases and more pronounced granule deformation occurs on plastic granules, resulting higher probability of successful coalescence and rapid granule growth. Brittle granules undergo more attrition and even breakage at higher impeller speed, leading to reduction in granule size. Moreover, crushing of small brittle granules by large granules is also enhanced at high impeller speed. Crushing causes the liquid trapped within the small granules to be released (Mackaplow *et al.* 2000), promoting agglomeration of fragments and formation of irregular shaped granules.

The use of chopper depends on the operating conditions especially the impeller speed as past studies presented diverse findings on the effect of chopper on granulation behaviour. Chitu *et al.* (2011) showed that the formation of coarse granules was delayed due to the breakage action of the chopper at lower impeller speed while Knight *et al.* (1998) proved that the use of the chopper helped to narrow the granule size distribution. On the other hand, only a minor effect of the chopper was observed by Saleh *et al.* (2005). Michaels *et al.* (2009) also found that without a chopper installed, the granule size distribution was almost unaffected under the pseudo-steady state conditions.

In general, both the impeller and the chopper function to induce better mixing by evenly distributing liquid on powder particles. Different effects of impeller on granulation behaviour have been reported such as breaking larger agglomerates, spheronizing and densifying granules, narrowing size distributions etc. These effects are constantly interchanging over time or taking place simultaneously as the granules that come in contact with the impeller blade at any instant may have different characteristics (liquid saturation) from the ones after. Therefore, the choice of impeller speed will depend on the amount of liquid delivered, the delivery method and final granule properties.

2.6.4 WET MASSING TIME

Once liquid addition ends, the granulation process enters the final processing stage, wet massing by continuing to run the impeller and/or chopper. It is beneficial in terms of achieving more a homogeneous liquid distribution, enhancing granule densification and breaking down larger agglomerates. Wet massing in conventional granulation is usually kept below 5 min (Shi *et al.* 2011). To what extent wet massing should be carried out and how it affects the final granule properties is not yet fully understood.

Shi *et al.* (2011) conducted a study on the effect of wet massing in high shear wet granulation with microcrystalline cellulose as the only ingredient and water as the granulating fluid. Positive results were obtained in terms surface morphology and granule sphericity where almost all rough surface features were removed and the number of sphere-like granules increased after longer wet massing. These improved features increased the granule flowability. However, tabletability reduced as a result of intense densification at prolonged wet massing which formed denser and stronger granules. Plastic deformation or fragmentation is not highly favourable when granules with low porosity are being compressed into tablets. Strong inter-granular bonds are unable to be formed hence producing tablets with low tensile strength. This was in good agreement with the finding in Badawy *et al.*'s work (2000) where there was a reduction in maximum hardness of tablets compressed from granules produced at longer wet massing.

There is an indication of "steady state" conditions in Shi *et al.*'s work (2011) where granule properties such as granule porosity, flowability, specific surface area and tablet tensile strength showed no significant changes with increasing wet massing. However, no clear trend was presented between wet massing time and particle size. Other studies showed that granule size distribution tends to narrow as wet massing time increases (Knight *et al.* 1998) but not in

all cases (Knight *et al.* 2000, Scott *et al.* 2000). This phenomenon appeared to be dependent on the operating conditions i.e. liquid delivery method and impeller speed used. The granule size distributions obtained by Knight *et al.* (1998) using calcium carbonate powders narrowed as wet massing time increased regardless of the mean particle size, liquid to solid ratio and liquid delivery method. In Scott *et al.*'s work (2000), a narrow granule size distribution produced from PEG was achieved after 24 min of wet massing using the pour-on delivery method but not the melt-in method. Another study by Knight *et al.* (2000) to investigate the effect of impeller speed on agglomeration showed that the intensity of shearing forces by the impeller determined the extent of granule size distribution can be narrowed to at extended wet massing. The narrowest granule size distribution was obtained using an intermediate impeller speed of 800 rpm compared to the others at 450 and 1500 rpm. The granule size distributions appeared to be bimodal initially but became unimodal at longer wet massing time which has enhanced granule breakage.

Apart from promoting granule growth and granule breakage, granule consolidation and densification may also occur during wet massing. Studies showed that granule porosity was greatly reduced at extended wet massing (Ohno *et al.* 2007, Shi *et al.* 2011) and higher impeller speed also enhanced the densification process (Badawy *et al.* 2000). Ohno *et al.* (2007) applied 50% pore diameter as the parameter to monitor consolidation of granules (see Figure 2.16). They showed that wet massing time and impeller speed had pronounced effect on the reduction of granule porosity. Granule porosity affects some of the granule tableting properties such as compressibility (Badawy *et al.* 2000), strength (Rahmanian *et al.* 2011) and dissolution performance (Ohno *et al.* 2007). A decrease in granule porosity increased the granule strength but reduced granule compressibility and dissolution rate. Therefore, granule consolidation and densification have to be taken into consideration when deciding the length of wet massing period to prevent over-granulation. Excessive densification can lead to negative effects on product quality attributes.

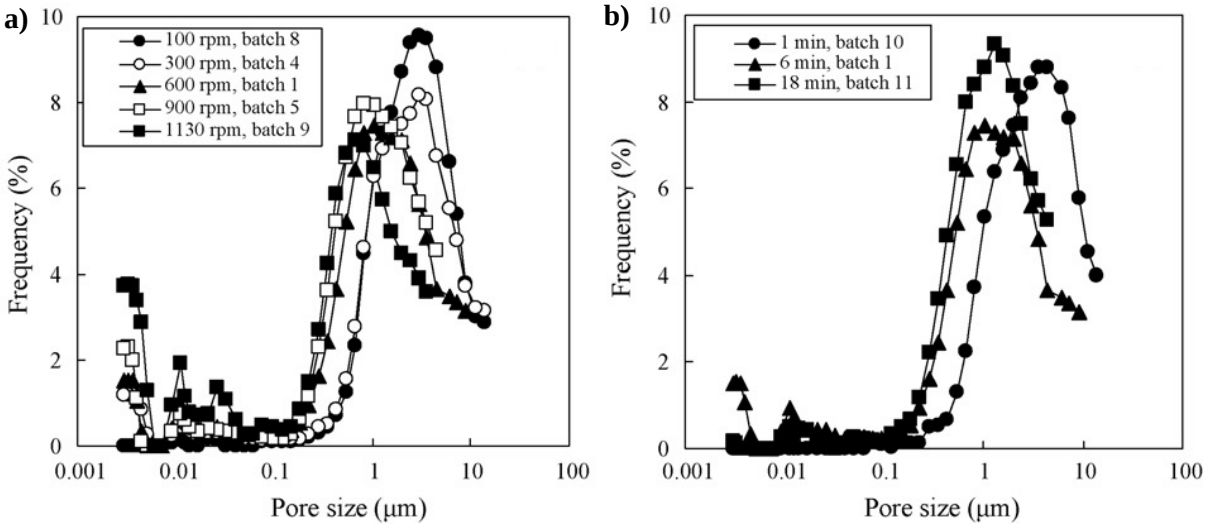

Figure 2.16: Effects of a) impeller rotation speed and b) wet massing time on pore size distribution. Taken from Ohno *et al.* (2007).

In conventional granulation, wet massing helps in further enhancing the liquid distribution but the aim is not necessarily to narrow the size distribution, as milling is placed downstream to size the granules down to the target size range. Furthermore, the adverse effects from wet massing such as over-densifying granules and increasing granule strength makes it less desirable to be extended for a longer period of time in tablet making process. However, it shows great potential in producing granule dosage forms. Not only can granule size distribution be narrowed down significantly, but also improve the granule morphology in terms of surface smoothness and sphericity.

2.7 END POINT DETERMINATION OF GRANULATION PROCESS

The most frequently asked question in granulation processing is "when to stop". Granules with desirable attributes and functionalities are aimed to be produced at the point of stopping the process. A popular way of determining the granulation end-point and still being practised in many conventional granulations is the hand squeeze test (Sakr *et al.* 2012) or also called the cohesion test (Liu *et al.* 2009). However, this method is highly subjective as it relies on operator judgement which depends on years of experience. Therefore, other means of determination have been developed to eliminate individual variation such as measurement of impeller torque or power consumption, use of an acoustic emission sensor or a refractive NIR moisture sensor (Liu *et al.* 2009).

Measurement of torque profile or power consumption profile has become a common feature that is now included in most mixers or granulators. The variation in power consumption during a moist agglomeration process is linked to the saturation level of granule which can then be related back to the granule size indirectly. A typical power consumption curve is shown in Figure 2.17 by Leuenberger *et al.* (2009) where the granulation process can be divided into various stages illustrating the different phases of liquid-solid interactions (liquid saturation of agglomerates) and growth regimes. Instead of saturation level, a parameter called wet mass consistency was later used to refine the previous relationship (Faure *et al.* 2001). Wet mass consistency describes the rheological properties of the wet mass which can be quantified using a mixer torque rheometer (MTR).

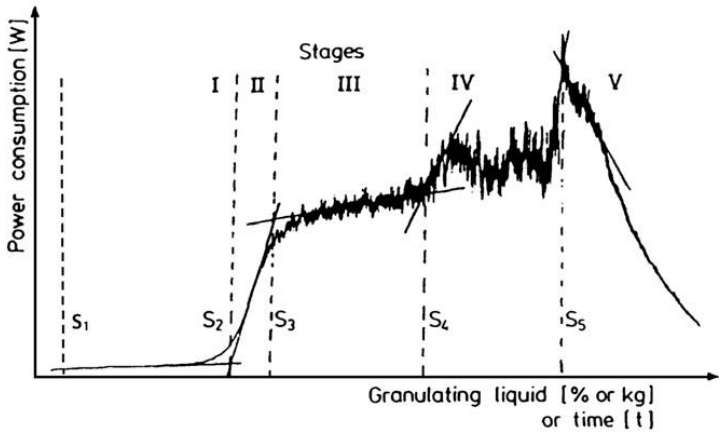

Figure 2.17: Different granulation stages divided up in a power consumption profile at increasing amount of granulating liquid. Taken from Leuenberger *et al.* (2009).

Mixer torque rheometer (MTR) has received much interest over the years as it can be used to characterize the powder binder interaction as liquid binder is constantly added into the agitated powder bed (Sakr *et al.* 2012). By monitoring the rheological changes of wet mass during granulation process, two values are measured: mean line torque and torque range. A torque curve is generated in terms of mean torque value which describes the mass resistance to mixing and corresponds to the increment in liquid to solid ratio during liquid addition. The rheological profile obtained allows the prediction of optimum liquid requirement for granulation which is represented by the maximum mean torque value (Oulahna *et al.* 2003). It also helps in predicting the stopping point in wet massing stage to achieve targeted water content in granules which has to be tightly controlled for desired properties. This approach has been proven to be more reliable compared to hand squeeze test (Sakr *et al.* 2012).

Several publications have applied the mixing torque approach as part of the preliminary characterization of the starting materials and investigation on the effects of selected variables on granulation process. Torque curves presented in the work by Mackaplow *et al.* (2000) showed that the duration of plateau region increased with the primary particle size and noise occurred as wall build-up became more serious with smaller particle size. Chitu *et al.* (2011) demonstrated that the liquid requirements varied with the type and concentration of binder used through torque curve analysis. Different types of binder such as PVP and HPMC in a range of concentrations were tested and growth rate was found to accelerate when more viscous binders were used (Chitu *et al.* 2011). They also found out that lactose required less binder to granulate than microcrystalline cellulose by comparing the rheological data of the two materials (Chitu *et al.* 2011).

Torque measurement can be useful in investigating the effects of variation in binder properties and granulating materials which have great influence on the liquid requirement. However, the torque curve cannot always distinguish whether the chopper is running or the design and impeller speed used in granulation process (Chitu *et al.* 2011). The relationship between impeller torque and granule properties is rather indirect.

2.8 "STEADY STATE" GRANULATION

Controlling the size and size distribution of granules has always been a challenge in granulation process. Recent work by Michaels *et al.* (2009) has achieved a breakthrough. The "steady state" approach adopted in their study successfully produced granules with uniform morphology, very narrow size distribution and excellent dissolution properties. They demonstrated experimentally the existence of steady state condition in granulation process using a commercial lactose-microcrystalline cellulose formulation. The suggested concept was "steady state" condition is reached when the number of breaking agglomerates approximately equals to the number of forming ones, inspired by Tardos *et al.*'s theoretical model (1997).

Stokes number is defined as the ratio of particle inertia to viscous drag (Khan 1997). This dimensionless number was adopted in the studies of stability of wet agglomerates in granular shear flows by Khan *et al.* (1997) and granule growth kinetics by Tardos *et al.* (1997). Based on the simple principles of energy dissipation, two Stokes numbers, St_{coal} and St_{def} were defined to describe the granule growth and deformation process (Tardos *et al.* 1997):

$$St_{coal} = \frac{initial\ kinetic\ energy}{dissipated\ energy\ in\ the\ bridge} = \frac{8\rho_p U_0 a}{9\mu} \qquad \text{[Eqn. 2.4]}$$

$$St_{def} = \frac{externally\ applied\ kinetic\ energy}{energy\ required\ for\ deformation} = \frac{m_p U_0^{\ 2}}{2V_p \tau(\dot{\gamma})} \qquad \text{[Eqn. 2.5]}$$

where:

ρ_p is the particle density

U_0 is the relative particle velocity

a is the particle radius

μ is the binder or granule surface viscosity

m_p is the mass of particle

V_p is the volume of particle

$\tau(\dot{\gamma})$ is some characteristic stress in the granule

It was proposed that when the deformation limit ($St_{def}^{\ *}$) overlaps with the coalescence limit ($St_{coal}^{\ *}$), granule growth is counterbalanced by granule breakage. Particles will grow by nucleation then coalescence until $a_{cr}^{\ coal}$ (critical particle size at growth limit) is reached while large granules which continue to grow beyond $a_{cr}^{\ def}$ (critical particle size at deformation limit) will become unstable, deform and break down. The rate of coalescence and rate of breakage will eventually come to an equilibrium point and "steady state" condition is achieved (see Figure 2.18). Following this, some computer simulations were performed to support and confirm the existence of $a_{cr}^{\ def}$ during granule formation in a constant shearing environment (Khan 1997, Talu *et al.* 2000).

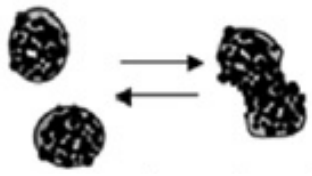

Figure 2.18: Pseudo steady state condition is achieved when the rate of coalescence and rate of breakage reach an equilibrium point. Inset from Michaels et al. (2009).

The conceptual idea behind "steady state" granulation is to produce granules with size distribution that is independent of time and scale at the end of the process. Two operating parameters, liquid delivery rate and wet massing time were selected to achieve the desired result. Liquid was added into a mass of fine powder at a slow rate (2% of dry mass per min) and the wet mass was continuously kneaded under constant shear rate at an extended period of time. The aim of prolonging the liquid addition stage was to significantly reduce and/or completely eliminate any inhomogeneity that can potentially occur during the course of liquid distribution (Michaels *et al.* 2009). This allows each droplet to have enough time to penetrate down into the powder bed before the next liquid drop arrives at the same spot.

Wet granules formed at the end of liquid addition have different sizes and properties, including a broad liquid saturation distribution across the different granule size classes. Extending the wet massing period provides a sufficiently long timeframe to narrow the liquid distribution given all granules will have to pass through regions of highest shear stress in the granulator. Regardless of the processing scale, "steady state" granules will grow and consolidate to the same extent. Most granules will contain approximately the same amount of liquid after being agitated long enough. Since granule size and porosity become independent of mixing time and liquid addition rate, the impeller speed is the only parameter that controls both granule growth and granule breakage. The intensity of the shear stress imposed by the impeller plays a role in breaking down coarse or larger granules. At the same time, granules will densify and liquid will migrate to the surface promoting granule growth by layering of fine particles. With adequate wet massing, all these processes will reach an equilibrium point where further mixing will no longer have an effect on the final "steady state" granules.

"Steady state" or pseudo steady state conditions were proven to be achievable in high shear wet granulation by Michaels *et al.* (2009). As shown in Figure 2.19, a significant difference was observed between the granule size distributions produced by "steady state" granulation and "conventional" granulation. The size distribution of "steady state" granules was narrow compared to the conventional broad distribution. In addition, the size distribution stabilized completely after approximately 20 min of wet massing and no significant change was observed with increasing the agitation time up to 40 min (see Figure 2.20). The sphericity of granules was also greatly improved at longer wet massing time. It was deduced that the shear forces and the "roping" motion of the particle helped in smoothing and rounding the granules (see Figure 2.21).

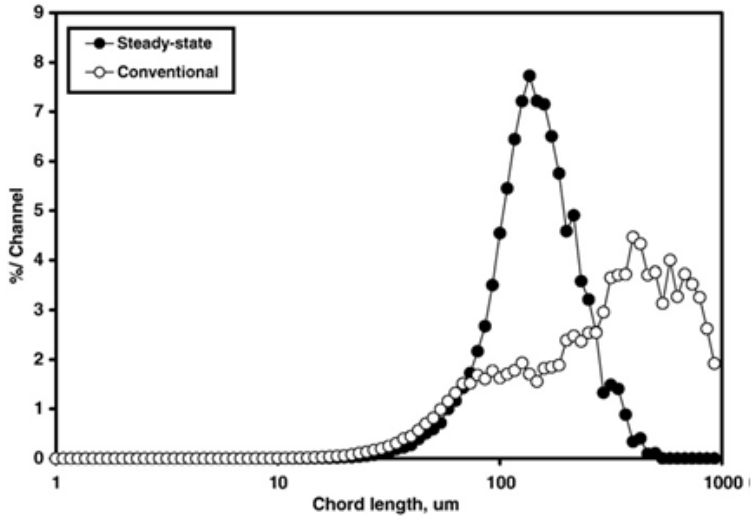

Figure 2.19: Chord-length distributions of wet granules produced by "steady state" granulation and "conventional" granulation at 2-L scale. Taken from Michaels *et al.* (2009).

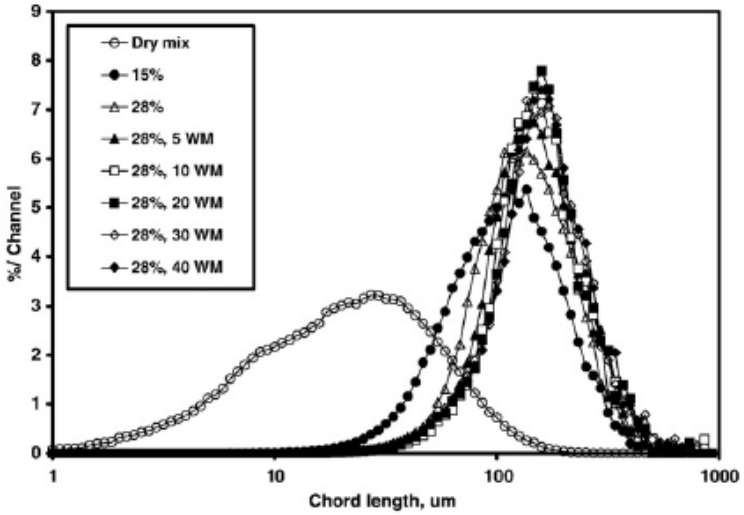

Figure 2.20: The existence of "steady state" condition in HSWG where granule size distribution did not show significant changes towards the end of wet massing period. Taken from Michaels *et al.* (2009).

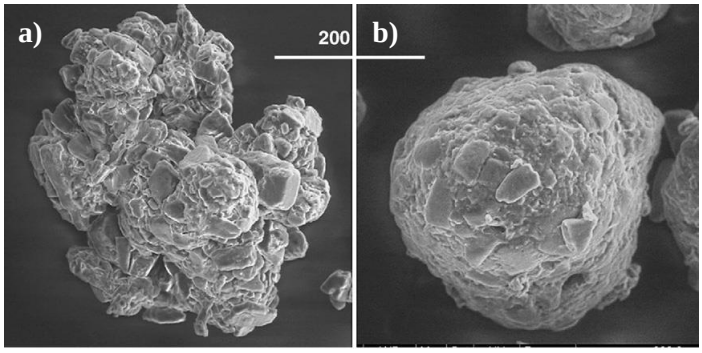

Figure 2.21: Granule morphology changes during wet massing period: a) 0 min WMT and b) 40 min WMT in "steady state" granulation. Taken from Michaels *et al.* (2009).

The "steady state" approach has been applied in Boerefijn *et al.*'s work (2009) using a simple gum powder and water as a two-component binder delivered by a two-phase nozzle. They managed to produce narrow granule size distribution and proved that the approach is workable on other granulating material. However, there have been no further follow up studies on "steady state" granulation published to date.

2.9 DRUG RELEASE MECHANISMS

Over the years, pharmaceutical industries have made huge advances in designing dosage forms that are age appropriate, illness specific and ease in administration. Oral solid dosage forms can be designed to attain different drug release profiles depending on the stability and solubility of drug, targeted absorption site and frequency in dosing. Drug release can be categorized into immediate-release and modified-release. Modified-release includes extended-release, delayed-release, repeat action and targeted release (Ansel *et al.* 1999).

Immediate-release (IR) dosage forms allow drugs to dissolve freely in gastrointestinal contents without any delay. A "typical" IR profile where full release is achieved after 60 min is shown in Figure 2.22. Common immediate-release solid dosage forms are tablets and capsules. When designing a solid dosage formulation, the ratio of excipients can be a key to achieve the desired release rate as illustrated in Figure 2.23. On the other hand, modified-release dosage forms offer therapeutic or convenience benefits of drug release over a period of hours that are unachievable by immediate-release forms. For example, conventional forms that require to be taken three to four times daily can be substituted with modified-release dosage forms. Design of this type of dosage forms is based on:

1. time – how long the therapeutic effect will last,
2. course – how many times a dosage form needs to be taken daily and/or
3. location – the targeted absorption site of drug

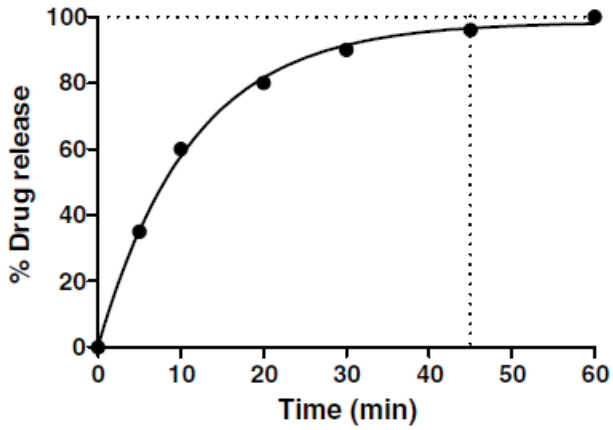

Figure 2.22: "Typical" immediate release dissolution profile, very fast initial release with a levelling off. Inset from am Ende 2011.

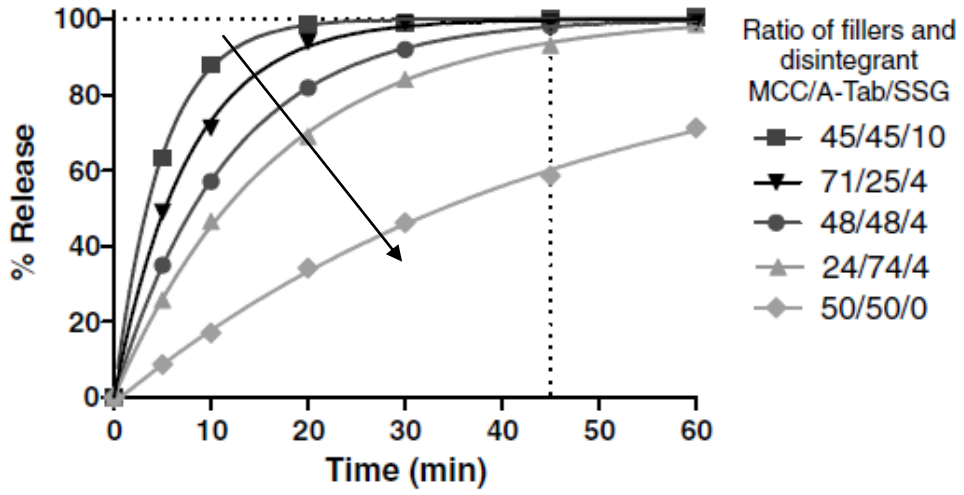

Figure 2.23: Dissolution comparison between different excipient (MCC, calcium dibasic phosphate and disintegrant SSG) ratios and a constant drug load. Inset from am Ende 2011.

The drug needs to be dissolved before it can be absorbed. The active pharmaceutical ingredient, formulation design and manufacturing process all influence how drug particles entrapped within a solid mass are being released i.e. the drug release mechanisms. Understanding the drug release behaviour is a crucial step and can be achieved through interpretation of dissolution data. Dissolution testing provides a means of measuring the extent and rate of drug release from a dosage form into an aqueous medium under a set of specified testing conditions (Long *et al.* 2009). It is also a key test to investigate *in vivo* performance of the dosage form (Long *et al.* 2009). Common oral solid delivery systems considered in dissolution studies are tablets, mini-tablets, coated pellets, oral strips etc which

can be categorized into four basic geometries: 1. Disc, 2. Cylinder, 3. Sphere and 4. Slab (am Ende 2011).

"Drug dissolution" and "drug release" are common terms adopted in the context of drug delivery but they have different definitions (see Figure 2.24). Drug dissolution involves five major physical phenomena, namely wetting of the particle's surface, breakdown of solid state bonds, solvation, diffusion through the liquid unstirred boundary layer surrounding the particle and convection in the surrounding bulk fluid (Siepmann *et al.* 2013). On the other hand, drug release is more complex with water diffusion into the system, polymer swelling, drug dissolution, polymer dissolution and/or degradation and diffusion of dissolved drug molecules though a polymeric network and/or water-filled pores. In a simplified manner, "drug dissolution" describes the dissolution of pure drug components in aqueous medium while dissolution of polymeric matrices that contain and release drug components into aqueous medium is best represented by "drug release" (Siepmann *et al.* 2013).

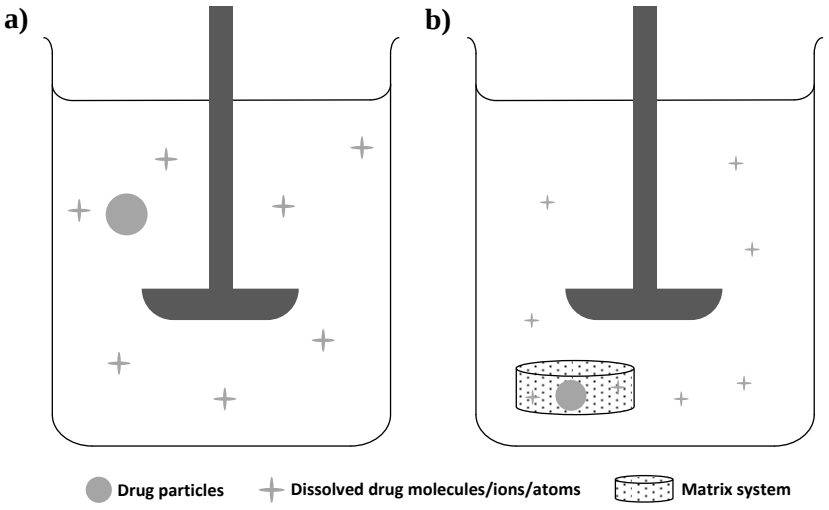

Figure 2.24: Schematic diagram illustrating the differences between the terms: a) "Drug dissolution" and b) "Drug release". Adapted from Siepmann *et al.* (2013).

Fundamentally, Wang and Flanagan (2009) explained dissolution as a process that involves two sequential steps: 1. Detachment of drug from solid into solution state and 2. Mass transport of solvated drug from a higher to lower concentration phase. The first step is governed by the solubility of drug and often regarded as the rate-limiting step. On the other hand, transport processes such as diffusion and convection control the second step. In general, the solubility of drug must be known in order to design the appropriate formulation and dosage form to aid in effective dissolution in the human body.

Dissolution and release of drug particles from a solid mass highly depends on the matrix porosity as it determines how fast dissolution medium can penetrate into the structure for solvation to occur. Mangwandi *et al.* (2010) investigated the effect of impeller speed on the dissolution properties of high shear granules produced from a low viscosity system i.e. distilled water as binder and a high viscosity system i.e. aqueous HPC as binder. HPC granules showed increasing mean dissolution time due to a decrease in porosity at increasing impeller speed but opposite results were obtained for water granules. HPC binder has a higher viscosity which resists consolidation. In contrast, water allows granules to consolidate at a greater extent under increasing impeller speeds. Studies by Le *et al*. (2011) supported the above result where dense, consolidated and non-porous granules require a longer time to dissolve than granules with high porosity. Therefore, the porosity of granules is a controlling factor in the dissolution and release of drug substances.

Tablet porosity often reflects the porosity of granules, with granule pore structure still being maintained after compression. Granules with smaller pore size often produce tablets of lower porosity. Ohno *et al.* (2007) studied and related the dissolution behaviour of mefenamic acid from tablets consisting of granules to the pore diameter of granules. The dissolution rate of mefenamic acid decreased with an increase in the amount of water added, impeller rotation speed and kneading time. They attributed the findings to the reduction of pore diameter as a result of consolidation (see Figure 2.25). A similar trend was also observed in Badawy *et al.*'s work (2012) where they concluded that smaller pores slow down the ingression of dissolution medium into the granules and subsequent granule disintegration.

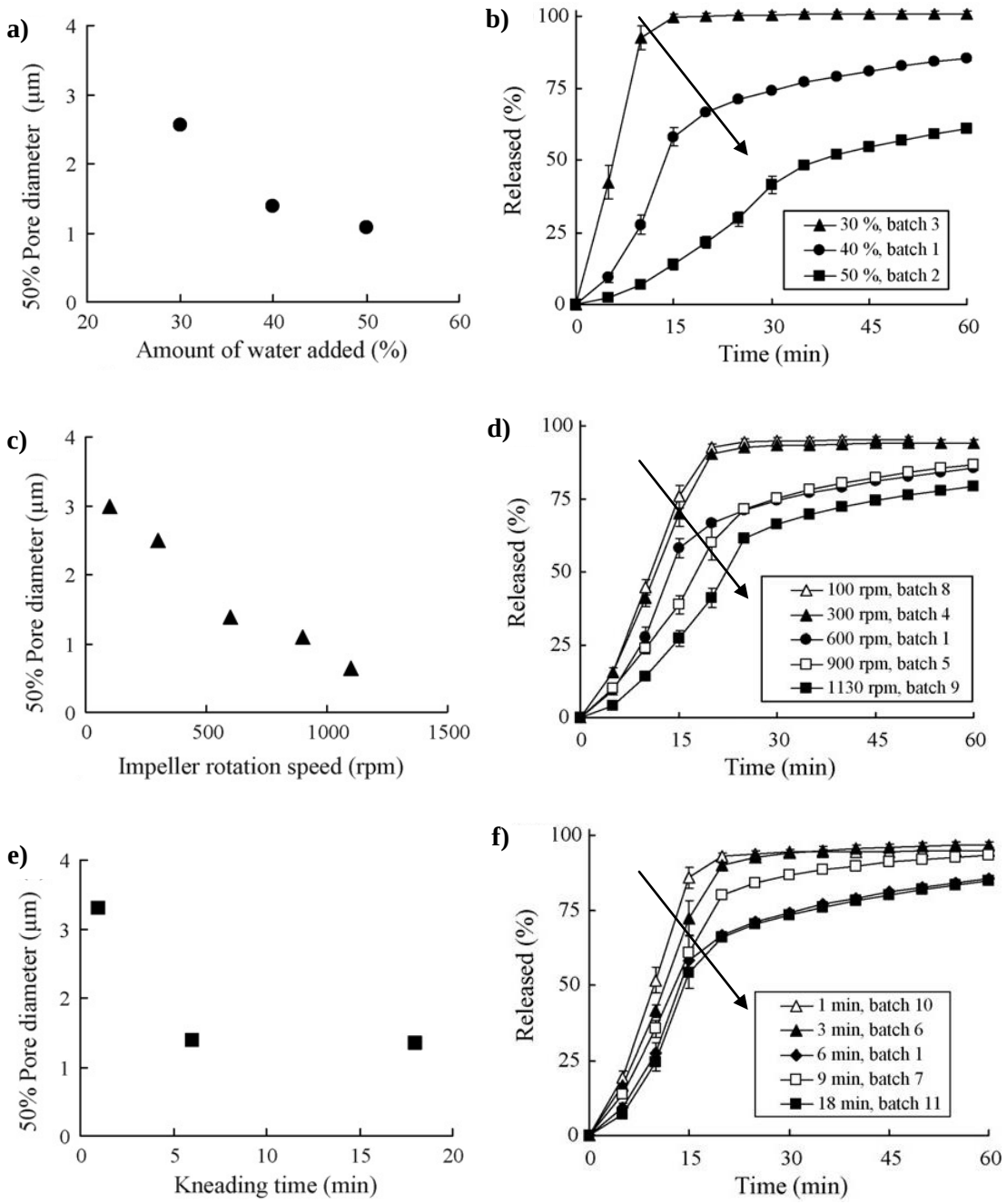

Figure 2.25: Effect of process parameters: a-b) amount of water added, c-d) impeller rotation speed and e-f) kneading time on 50% pore diameter (left) and dissolution profiles of mefenamic acid in tablets (right). Inset from Ohno et al. (2007).

Despite the general trend observed in previous dissolution studies, Michaels *et al.*'s work (2009) showed a conflicting result. The porosity of the "steady state" granules was found to be 16%, much lower compared to the "conventional" granules with porosity of 40-50% (Michaels *et al.* 2009). This result raised the concern of over-granulation, the cause of depressed dissolution which is not desirable for rapid release formulations. However, the

dissolution profiles of both tablets compressed from "steady state" and "conventional" granules were almost identical (see Figure 2.26). This was an unexpected result given the low porosity of "steady state" granules. Although pore size is slightly different to total porosity, they are assumed to be closely related.

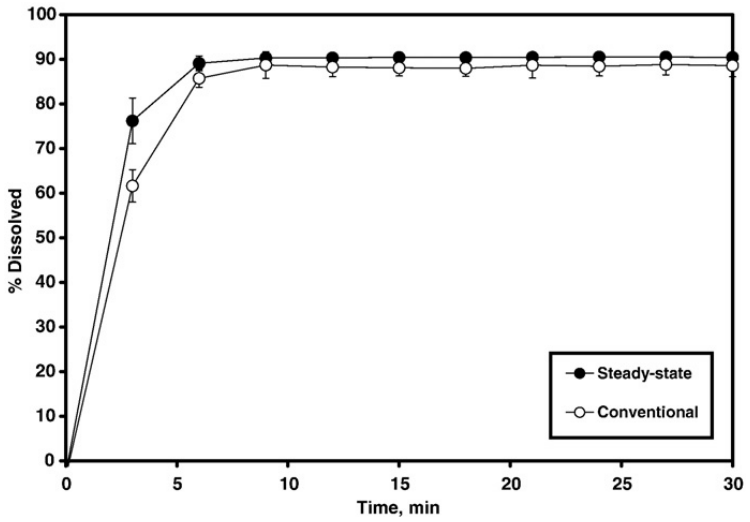

Figure 2.26: Dissolution profiles of tablets compressed from granules produced in "steady state" and "conventional" granulation. Taken from Michaels *et al.* (2009).

Mathematical theories and models have been proposed to quantify drug release from controlled release dosage forms. Verifying the actual release mechanism is usually done by comparing the experimental data obtained from dissolution testing with the solution of a theoretical model that deemed to best depict the dominant mechanism(s). Controlled release systems can be categorized into: 1. diffusion, 2. erosion/degradation, 3. ion exchange, 4. swelling and 5. osmotic pressure (am Ende 2011), although several mechanisms may take place simultaneously.

The diffusion theory has been applied greatly in the study of controlled release. Fick's first and second laws are the two basic equations in describing diffusion process. Noyes-Whitney equation and Nernst and Brunner equation were later developed to model the transport of solute molecules through a diffusion layer (Chen *et al.* 2009). In 1961, Higuchi introduced the famous square root equation relating the release rate of solid drugs from ointment bases and further expanded to other geometries with different release mechanisms (Higuchi 1963). Other empirical/semi-empirical models were then developed including zero order, first order, power law etc (Peppas *et al.* 1989).

Zero order, first order and square root of time are simplified models that commonly applied to fit release data. However, these models do not provide much insight into the actual release mechanism occurring on a dosage form, besides quantifying the rate of release. The square root of time equation by Higuchi (1961) was derived based on a planar system and many have misused it for other geometries such as disc and sphere in curve fitting (O'Connor *et al.* 1993, Eichie *et al.* 2008, Siepmann *et al.* 2011). Matrix geometry needs to be taken into consideration when developing and/or applying a model but using zero and first order models neglects this crucial factor. A semi-empirical model called the power law was then proposed which accounts for the matrix geometry and release mechanism (Fickian or non-Fickian) by varying the diffusion exponent, n (Korsmeyer *et al.* 1983, Peppas 1985, Ritger *et al.* 1987, Ritger *et al.* 1987, Peppas *et al.* 1989). The main drawback of the model is that it cannot fit the complete release curve (only first 60%) derived from Fick's second law as a short-time approximation was made in developing the model (Ritger *et al.* 1987).

Table 2.1: Summary of diffusion related theories and dissolution kinetic models

Law/Model	Equation	
Fick's First Law	$J = \frac{dQ}{Adt} = -D\frac{\partial C}{\partial x}$	Eqn. 2.6
Fick's Second Law	$\frac{\partial C}{\partial t} = \frac{-\partial J}{\partial x} = D\frac{\partial^2 C}{\partial x^2}$	Eqn. 2.7
Noyes and Whitney	$\frac{dQ}{dt} = k(C_s - C_b)$	Eqn. 2.8
Nernst and Brunner	$\frac{dQ}{dt} = DA\frac{(C_s - C_b)}{h}$	Eqn. 2.9
Zero Order	$Q = k_0 t$	Eqn. 2.10
First Order	$\ln(100 - Q) = \ln Q_0 - k_1 t$	Eqn. 2.11
Square Root of Time	$Q = k_H t^{1/2}$	Eqn. 2.12
Power Law	$\frac{M_t}{M_\infty} = kt^n$	Eqn. 2.13

where:

J is the flux (rate of diffusion)

dQ/dt is the rate of transfer of a diffusing substance

A is unit area

D is the diffusion coefficient

C is concentration

C_b is bulk solution concentration

C_s is solubility

$\partial C/\partial x$ is the concentration gradient

h is the diffusion layer thickness

Q is the percent of released component at time t

k , k_0 , k_1 and k_H are the coefficients (intercept) of equation

M_t/M_∞ is the fraction of released component at time t

n is the diffusion exponent indicative of the release mechanism

2.10 LITERATURE SUMMARY AND RESEARCH GAP

Wet granulation has the versatility of manipulating a wide range of parameters to achieve the desired outcome. In the liquid addition stage, the amount of liquid added, method of delivery and addition rate are the common process variables to be chosen. Liquid level determines whether a batch of powder is under-granulated or over-granulated. The amount of liquid added has to be tightly controlled to produce granules of desired sizes and prevent local wetting that can potentially lead to uncontrolled granule growth. The size of liquid droplet is often determined by the method of delivery and the relative size of liquid droplet to particle size affects the nucleation mechanisms undertaken in granulation process.

Impeller speed has a crucial role in achieving "roping" flow pattern in granulators, distributing liquid evenly across the powder bed and breaking down larger agglomerates. It has been proven that high impeller speed can significantly reduce the amount of lumps and produce spherical granules with narrow size distribution under a certain limit before granule breakage becomes over-dominating.

Wet massing shows to be effective in narrowing size distribution and "steady state" conditions do exist at prolonged wet massing where no significant changes were observed on granule properties. Prolonging wet massing allows every single wet granule to have the chance to experience approximately the same amount of forces and stresses resulted by the rotating impeller, independent of time and space. These granules will grow, consolidate, deform and/or break at similar rates and achieve comparable sizes.

The "steady state" granulation approach is useful in optimizing the granulation process from powdered raw material to granules. Better control is sought with longer process time compared to conventional ones. "Steady state" conditions are proposed to be achieved when

the rate of coalescence is approximately the same as the rate of breakage. However, quantification of both rates requires modelling hence "steady state" conditions are experimentally deduced to have achieved when granule properties show no significant changes with an increase in wet massing time.

Work by Michaels *et al.*'s (2009) has made further advancement in granulation process. The "steady state" approach has been adopted by Boerefijn *et al.* (2009) and successfully produced granules with narrow size distribution. Therefore it is of interest to demonstrate that the approach is workable beyond the chosen formulation and operating conditions implemented. Therefore independent replicate experiments and further investigation need to be carried out by varying the formulation and key parameters to obtain a reproducible and robust methodology.

The project will extend the study of "steady state" granulation by investigating process variables that have significant effects on the properties of "steady state" granules and implementing proper control to make reproducible granules with desired attributes. The "steady state" granulation will be replicated at a similar scale using a modified formulation based on the previous work by Michaels *et al.* (2009). The study looks into the following aspects: 1. Wet massing time, 2. Liquid level and 3. Impeller speed to confirm the "steady state" granulation behaviour presented in Michaels *et al.*'s work (2009). However, the main focus will be on producing controlled granules for direct use in paediatric products.

Dissolution performance of tablets compressed from "steady state" granules was investigated and found to be comparable with conventional tablets (Michaels *et al.* 2009). However, the dissolution performance of "steady state" granules as an oral solid dosage form directly is not known. "Steady state" granules can be regarded as solid spheres that contain multiple pharmaceutical excipients together with the drug substances to be delivered to patients. They are also much smaller in size compared to conventional mini-tablets and pellets hence suitable for oral administration in the paediatric population. Therefore, it is of interest to understand the release mechanism of "steady state" granules in order to achieve controlled release, which will be the focuses of the next stage of research:

1. ***To identify the release mechanisms of "steady state" granules*** – This can be achieved through quantitative analysis i.e. dissolution testing and qualitative analysis i.e. observation of change in granule morphology before and after dissolution.

Dissolution testing allows the determination of how fast drug substances are being released from dosage forms into aqueous medium. Final states of a dosage form including the shape and distribution of particles within the matrix have significant influence on the dissolution behaviour. Therefore observing the structural change in granules aids in predicting the possible physical phenomena occurred that lead to the resulting rate of release.

2. ***To control the rate of release by varying the composition of formulation*** – After understanding the release mechanisms of "steady state" granules, it is of interest to fine-tune the rate of release and achieve controlled release. Rate of release of a dosage form is highly dependent on the release mechanisms which determined by the design of formulation. A formulation usually contains both soluble and insoluble components to create the bulk required for a dosage form. The two main diluents incorporated in the formulation used in this project are lactose (soluble) and microcrystalline cellulose, MCC (insoluble). "Steady state" granules were discovered to be a spherical and dense solid mass consisting of lactose particles wrapped within a polymeric matrix (Michaels *et al.* 2009) as opposed to conventional granules that are irregular in shape. This interesting feature of "steady state" granules has raised the idea of varying the composition of lactose and MCC in attempt to control the rate of release. It is hypothesized that decreasing the amount of lactose will reduce the cavities created by dissolved lactose across the matrix. This will retard the penetration of dissolution medium into the granules and achieve a slower rate of release.

CHAPTER THREE

Materials and methodology

3 MATERIALS AND METHODOLOGY

To establish an understanding of "steady state" granulation behaviour, the proposed approach was applied and tested on a pharmaceutical formulation. This chapter discusses the characteristics and role of each ingredient incorporated in the formulation to provide better insights on how they interact with each other in forming the final dosage forms. The methodology developed for "steady state" granulation is elaborated including all the important features of the experimental work, main parameters to be investigated and characterization of the properties of end product. Granulation behaviour can then be studied in a systematic manner, from knowing the raw materials to analysing the final products.

3.1 FORMULATION

A lactose-microcrystalline cellulose formulation was used, consisting of five ingredients: approximately 59-74 wt% lactose monohydrate (Pharmatose® 200M, DFE Pharma), 20-35 wt% microcrystalline cellulose (Avicel PH101, FMC Biopolymer), 3 wt% hydroxypropyl cellulose (Klucel® EXF Pharm, Ashland), 3 wt% croscarmellose sodium (Dislocel) and 0.02 wt% Rhodamine B. This formulation was based on Merck's previous study on "steady state" granulation (Michaels *et al.* 2009) and modified slightly to fit the research aims of this project. The basis of each granulation run was 800 g of dry powder and the granulating fluid used was distilled water.

3.1.1 LACTOSE

Lactose is a common pharmaceutical excipient used in solid dosage forms such as tablets and capsules. It acts as filler or diluent that carries active pharmaceutical ingredients (API) to be delivered into patient's body. Lactose is a natural disaccharide present in mammal milk (Rowe *et al.* 2006). Solid state lactose appears in different isomeric forms depending on the crystallization and drying conditions. One of the common forms is α-lactose monohydrate which is prepared by crystallization from supersaturated solutions below 93.5°C (Rowe *et al.* 2006). Lactose monohydrate, also known as milk sugar

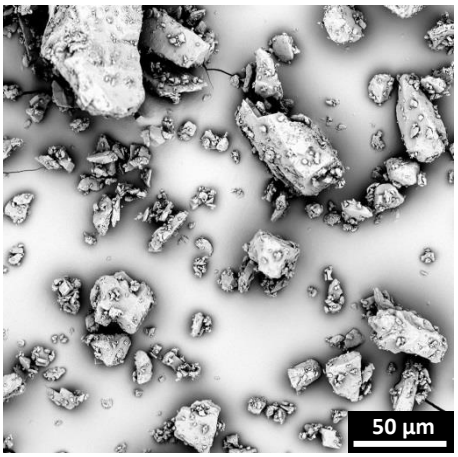

Figure 3.1: Lactose monohydrate

has a faint sweet taste and white colour in powder form. Pharmatose® 200M by DFE Pharma was used in this project. This α-lactose monohydrate is mechanically milled to different degrees of fineness as shown in Fig. 3.1. Milled lactose has poor flowability but high compactability which makes it suitable for wet granulation applications (O'Neil *et al.* 2006, Rowe *et al.* 2006, Pharma 2013).

3.1.2 MICROCRYSTALLINE CELLULOSE

Microcrystalline cellulose (MCC), a high molecular weight polymer ($[C_6H_{10}O_5]_n$ where $n \approx 220$) is a purified, depolymerized cellulose (Rowe *et al.* 2006). Porous MCC particles have great compression and binding properties that make it useful in providing a matrix or medium for API in oral pharmaceutical formulations. MCC is also stable and hygroscopic. Microscopically, MCC particles consist of both crystalline and amorphous regions. They swell and plasticize upon contact with aqueous forms, providing sufficient plasticity to wet mass in forming agglomerates.

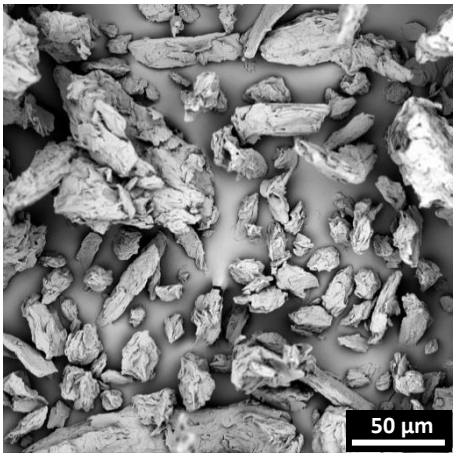

Figure 3.2: Microcrystalline cellulose

MCC is often incorporated as filler/diluent to create the desired bulk in the preparation of pharmaceutical solid dosage forms. Therefore it has become an essential pharmaceutical excipient in granulation especially wet extrusion/spheronization in making pellets and direct compaction in making tablets. Avicel PH101 by FMC Biopolymer, a white, odourless, tasteless and free-flowing powder (Rowe *et al.* 2006) was used in the experiments.

3.1.2.1 USE OF MCC AS EXTRUSION AID IN WET GRANULATION

Powdered MCC swell upon contact with aqueous solutions and become plastically mobile. This allows them to be moulded together with other particles into larger solid forms under the action of shearing/frictional/compaction forces. "Steady state" granules produced by Michaels *et al.* (2009) appeared to be a polymeric matrix wrapping up other ingredients within. MCC is believed to be the key ingredient in forming these spherical granules. Therefore it is of particular interest to understand the mechanism occurred during wet massing that shapes the wetted powder particles into the final form.

Past studies on the interaction between MCC and water under a sheared environment such as granulation and extrusion/spheronization have been carried out extensively with a few models being proposed. MCC was described as a "molecular sponge" due to its ability to physically retain large amount of water within the structure which is readily removed by evaporation as it is discovered to be "free" (Fielden *et al.* 1988). The amount of water can be absorbed by MCC was found to increase when the degree of crystallinity decreased (Suzuki *et al.* 1999). This property of MCC has shown to be important in determining the cohesiveness of the wetted particles. Addition of water brings out the plastic nature of MCC where it becomes highly deformable upon absorbing large quantity of water. A continuous liquid film, separating the particles may be formed when the amount of water added exceeds the maximum uptake of MCC hence resulting in a reduction in cohesiveness (Staniforth *et al.* 1988). Hence the effect of liquid on a MCC incorporated system cannot be overlooked.

Changes in the characteristics and structure of wetted MCC particles and granules under the presence of mechanical stress have been previously investigated. Wet granulation processes were found to decrease the crystallite size of cellulose with increasing granulation time and amount of water added (Suzuki *et al.* 2001) as well as reduce the porosity of MCC primary particles (Badawy *et al.* 2006). During the course of granulation, the size of the continuous solid region in MCC granules increased significantly suggesting that the MCC particles were forming a network (gel) (Suzuki *et al.* 2001). The gelling performance of MCC was interpreted using the crystallite-gel-model proposed by Kleinebudde (1997). MCC primary particles exist in the form of long fibrils which in the presence of water, will be broken down into smaller fragments with shorter chain lengths by the shearing forces exerted in wet granulation. These subunits are described as crystallites and they are able to form a solid matrix through crosslinking of hydrogen bonds at the amorphous ends (Kleinebudde 1997). Increasing the amount of liquid delivered increases the deformability of the crystallite-gel, allowing it to be shaped into a spherical structure.

Kleinebudde (1997) tested different types of MCC (70% w/w) together with lactose monohydrate (30% w/w) as the soluble filler to produce pellets by extrusion/spheronization. Results showed that pellets with smooth surfaces and no outer pores were produced. The initial appearance and structure of MCC particles completely disappeared. Based on the crystallite-gel-model, a delicate and coherent network should be formed by the crystallites at the end of wet processing. This was proven by the rough and porous structure left behind

after dissolving the pellets. The polymeric structure did not disintegrate and retained its original shape with lactose monohydrate being leached off (see Figure 3.3).

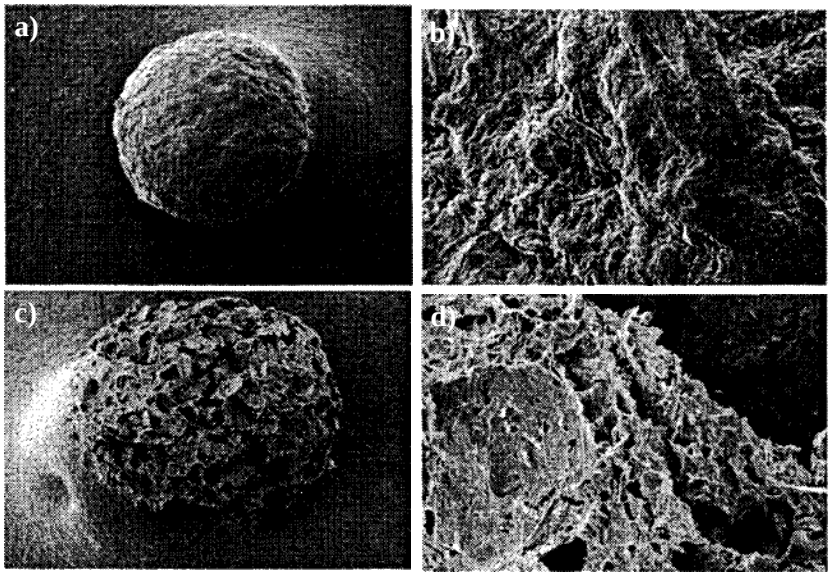

Figure 3.3: a) MCC (Avicel PH101) pellet, b) Surface details of pellet, c) Dissolved MCC (Avicel PH101) pellet and d) Surface details of dissolved pellet. Taken from Kleinebudde (1997).

At microscopic level, Millili *et al.* (1990) explained the interactions between high molecular weight polymers in pharmaceutical solids by a diffusion controlled mechanism called autohesion. It is defined as the mutual interdiffusion of free polymer chain ends across the particle-particle interface of high molecular weight polymers resulting in a strong stable link (Millili *et al.* 1990). This mechanism was originated in the rubber and plastics industries. Since pharmaceutical solid dosage forms incorporate high molecular weight polymers, the importance of understanding the interactions between polymer chains that result in the final state of a dosage form has increased.

Previous work showed processing factors such as time of contact, addition of solvent and pressure have significant effects on the degree of autohesion (Millili *et al.* 1990). The degree of autohesion was found to increase with time of contact as higher molecular weight polymers have sufficient time to diffuse further across the interface. Solvent plays an important role in the viscous flow of polymer chains. The driving force necessary for solid–solid diffusion to occur is produced by the surface tension and capillary pressure of solvent used. Addition of solvent decreases the viscosity of polymers hence increasing the mobility of polymer chain ends. This favours the diffusion of polymer chains resulting in higher degree of autohesion.

Furthermore, increasing pressure has shown to increase the surface contact of material which in turn enhances autohesion. This can be attributed to the plastic and/or elastic deformation of surface irregularities of particles allowing more contact between colliding particles. In granulation perspective, these factors can be translated to wet massing time, liquid level and impeller speed.

The autohesion process of MCC can be divided into few main steps: 1. Swelling and plasticisation of the polymeric material when in contact with water, 2. Deformation of material under the influence of processing environment which increases the interfacial contact area between particles, 3. Diffusion of polymeric chain ends across the particle-particle interface into swollen microcavities within the material, 4. Collapse of microcavities due to the evaporation of water upon drying and 5. Formation of strong stable link that creates the continuous solid region (Millili *et al.* 1990, Westermarck *et al.* 1999)

3.1.3 HYDROXYPROPYL CELLULOSE

Hydroxypropyl cellulose (HPC) is primarily used as a polymeric binder in oral products. HPC is described as a partially substituted poly(hydroxypropyl) ether of cellulose. It serves as a binding agent when a concentration of 2-6% w/w is added in oral pharmaceutical formulations. HPC powder is white in colour, odourless and tasteless. It is a stable and hygroscopic material which is commercially available in different grades. Klucel® Pharm HPC (EXF) is a finely ground type of HPC. It is thermoplastic, extremely flexible and water-soluble which allow it to be effective in tablet binding (Rowe *et al.* 2006).

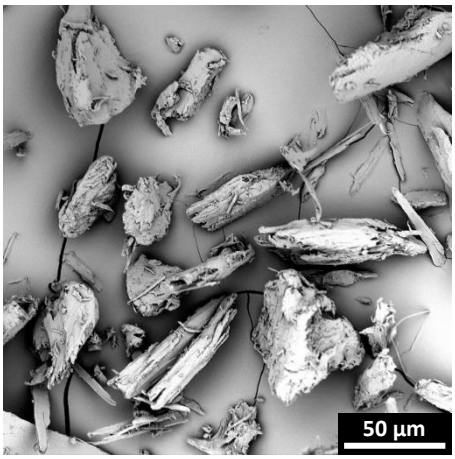

Figure 3.4: Hydroxypropyl cellulose

3.1.4 CROSCARMELLOSE SODIUM

Croscarmellose sodium (CCNa) is an internally crosslinked polymer of carboxymethylcellulose sodium. It is commonly used as a disintegrant for tablets, capsules and granules to facilitate the release of entrapped API. It is added at a concentration of 3% w/w in tablets prepared by wet granulation process. When croscarmellose sodium comes in contact with water, it will wick the water through capillary action and swell 4-8 times its original volume which allows tablets to disintegrate. Powder form of croscarmellose sodium is white in colour, odourless, stable and hygroscopic (Rowe *et al.* 2006).

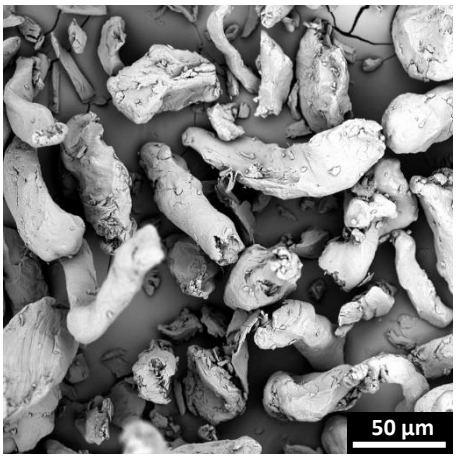

Figure 3.5: Croscarmellose sodium

3.1.5 MANNITOL

Mannitol is widely used as a diluent or sweetening agent in oral formulations especially chewable tablets for paediatric medicine. Mannitol is a naturally occurring sugar alcohol in plants and animals. It has approximately the same sweetness as glucose, good 'mouth feel' and cooling sensation. Mannitol appears in white, odourless and free flowing granules as seen in Fig. 3.6. It is stable in both dry state and aqueous solution (Rowe *et al.* 2006) and also suitable for use in paediatric formulations (unlike lactose). Pearlitol® 200SD by Roquette Pharma, a granulated mannitol was used to substitute lactose as the soluble component in formulation.

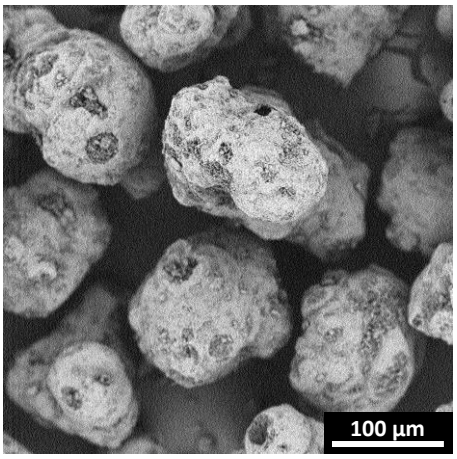

Figure 3.6: Mannitol

3.1.6 RHODAMINE B

Rhodamine B is a fluorescent dye used in this project as a model "drug" or tracer to simulate and monitor the release of a potential drug compound incorporated in "steady state" granules. It appears as faint green to very dark green powder which gives faint red to red or faint purple to purple depending on the amount dissolved in water. Rhodamine B fluoresces under ultraviolet light which makes it suitable to be analysed in UV spectrometer, mimicking drug release in dissolution test. It has been used as a drug substitute to investigate controlled-release dosage forms (Yang *et al.* 2012).

Table 3.1: Summary of the properties of ingredient used in the formulation Refractive index taken from Malvern (1997) and solubility data taken from Rowe *et al.* (2006).

No.	Raw material	d50 (µm)	Refractive index	Solubility (H_2O at 20°C)
1	Lactose monohydrate 200M[1]	46	1.347	1 in 5.24
2	Microcrystalline cellulose[2]	60	-	Insoluble
3	Hydroxypropyl cellulose[2]	42	-	1 in 2
4	Croscarmellose sodium[2]	25	-	Insoluble
5	Mannitol[1]	158	1.333	1 in 5.5
6	Rhodamine B	-	-	1 mg /ml

Note: d50 of raw material above was determined by 1. Malvern Mastersizer and 2. mechanical sieving.

3.2 EXPERIMENTAL PROCEDURE

3.2.1 HIGH SHEAR WET GRANULATION

High shear wet granulation provides a means of agglomerating primary powder into larger solid mass called granule. "Steady state" granulation approach was adopted in this project and its effect on the granulation behaviour was studied using a laboratory-scale mixer granulator. A schematic diagram of the experimental setup was shown in the figure below.

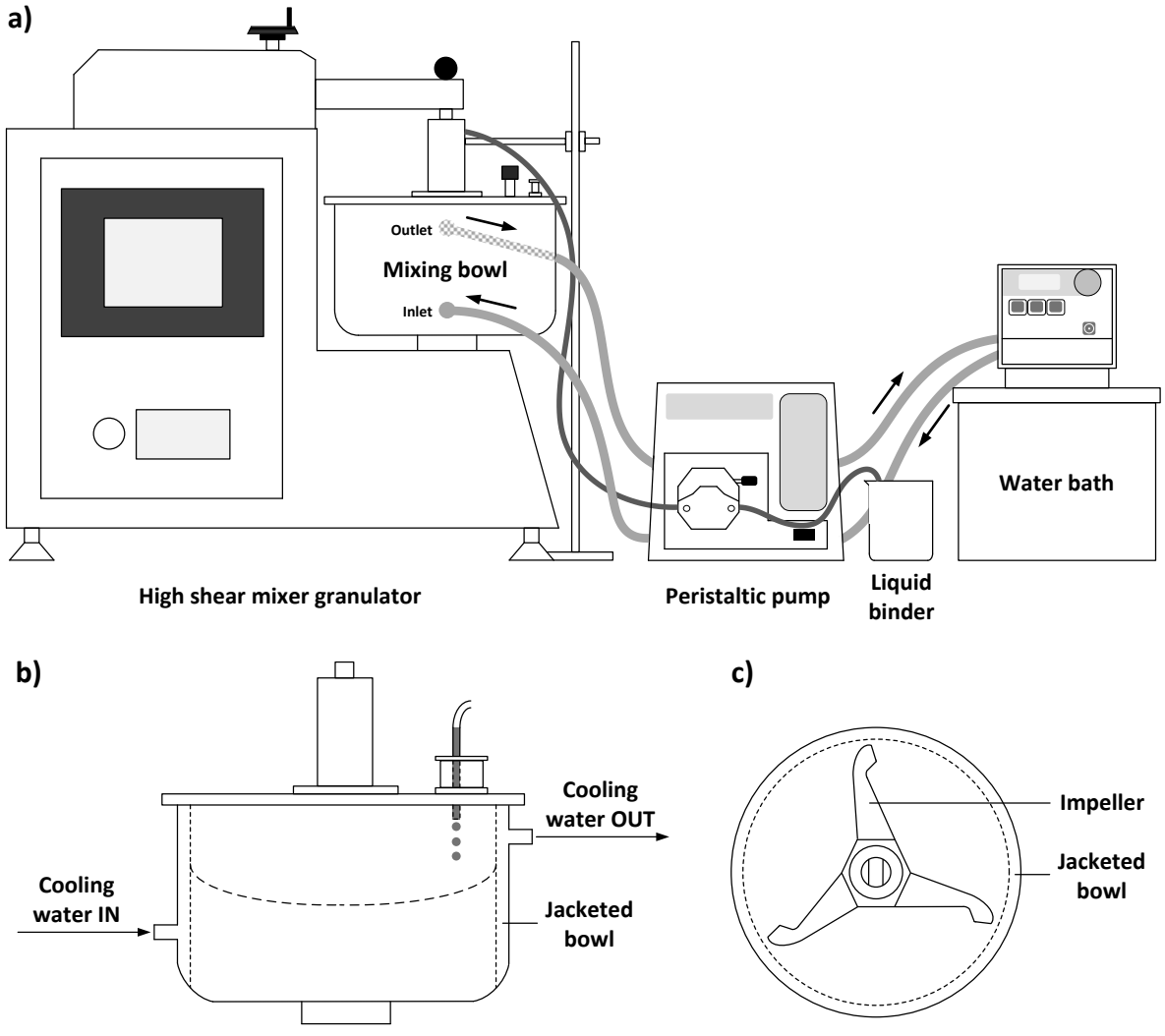

Figure 3.7: a) Experimental setup of "steady state" granulation b) Side view of high shear jacketed mixing bowl c) Impeller 3 blades mounted vertically in mixing bowl

Each powder batch was granulated in a 5 L high shear mixer granulator (KG5, International Key) with an impeller mounted in the vertical axis and no chopper installed. The impeller speed was adjusted to 245-490 rpm to achieve roping flow of dry ingredients in the mixing bowl where 245 rpm was found to be the onset of roping flow pattern. A jacketed bowl was

used to circulate water at 15 L/min and 22°C through the jacket to provide cooling. Ice packs were immersed in the water bath of the circulator (Polyscience) and constantly replaced to maintain the cooling water at 22°C. The temperature of the powder bed was monitored by taking measurements before pre-mixing, at each stage of the process and sampling points using an infrared thermometer (Digitech, QM7221).

The major difference between "steady state" granulation and conventional granulation is provision of cooling water throughout the "steady state" process. This allows the temperature of wet mass in the mixing bowl to be maintained at a constant low temperature without reaching higher temperature that may cause evaporation of liquid or deterioration of granule properties. Temperature profiles of "steady state" granulations with and without cooling were compared as shown in Figure 3.7. They were fairly similar during the pre-mixing and liquid addition stages. However, the temperature increased drastically over the wet massing stage and reached approximately 45°C when no cooling was provided. With a cooling jacket, the temperature was relatively constant at 26°C throughout the whole process. The final temperature difference between the two cases after 30 min of wet massing was approximately 20°C. "Steady state" granulation adopts extended wet massing where wet granules are continuously sheared for a sufficiently long period of time. Hence cooling is vital in this approach to control the temperature below 30°C and to exclude its effect on granulation behaviour.

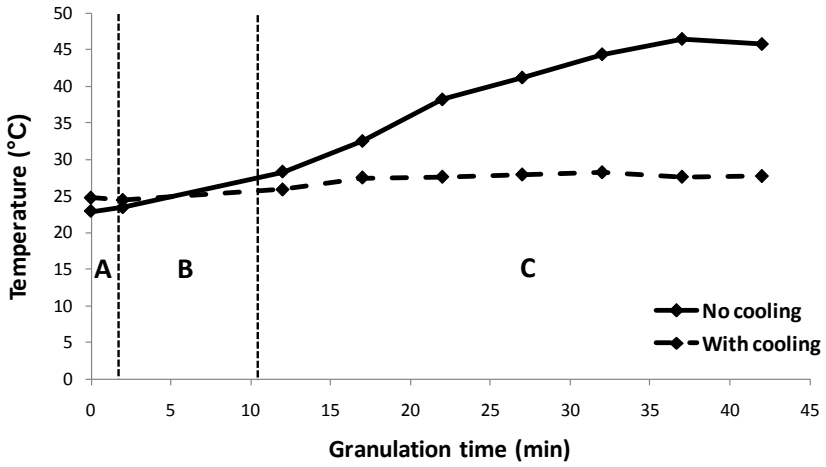

Figure 3.8: Temperature profiles of powder bed throughout the 3 main stages in granulation process. Region A: Pre-mixing, Region B: Liquid addition and Region C: Wet massing

Before liquid delivery, Rhodamine B was dissolved in distilled water using a magnetic stirrer for 5 minutes. A peristaltic pump (Masterflex® L/S®) with an attached delivery tube (Masterflex silicone tubing L/S® 16) with an inner diameter of 3.1 mm was used to deliver the liquid dye by dripping through the nozzle on the lid. The liquid delivery rate was set to be 2% per min (dry basis) (or 16 g/min). Dripping method delivers liquid droplet that is relatively larger than primary powder particles (see Figure 3.8), ensuring that nucleation of "steady state" granules follows the immersion mechanism.

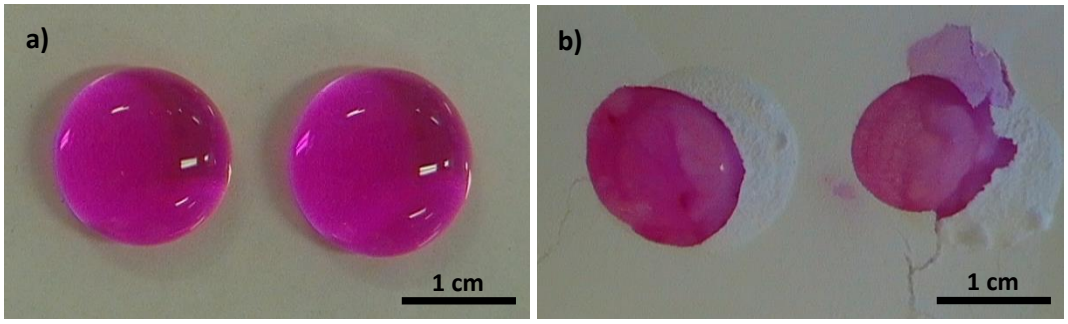

Figure 3.9: a) Liquid droplets that formed after exiting the delivery tube and b) Liquid droplets that fell on lactose powder bed in a petri dish.

The powder bed was pre-mixed for 2 min at 245-490 rpm to evenly distribute each ingredient in the mixing bowl. Liquid level (LL) of 24-30% (dry basis) was then delivered into the mixing bowl while the impeller continued rotating. After liquid addition, the wet mass was continuously mixed up to 30 minutes under the same impeller speed used in pre-mixing and liquid introduction stages. 50 g of granules (dry basis) were sampled at 0, 5, 15 and 30 min wet massing time (WMT) and dried in a convection oven at 60°C overnight.

The "steady state" granulation experiments were divided into two parts: 1. Variation in operating parameters (which ensures the replication of the original "steady state" work by Michaels *et al*. (2009)) and 2. Variation in composition of formulation. In Part One, liquid level and impeller speed were chosen to be investigated while compositions of lactose (soluble component) and MCC (insoluble component) were varied in the later part. The list of experiments carried out for this project is shown in the table below.

Table 3.2: Experimental work done in "steady state" granulation project

Experiment		Operating conditions		Composition (wt%)			
		Liquid level (%)	Impeller speed (rpm)	Lactose[1]	MCC	HPC	CCNa
Variation in operating parameters	A	***24***	***245***	74	20	3	3
	B	***27***	***245***	74	20	3	3
	C	***30***	***245***	74	20	3	3
	D	***30***	***490***	74	20	3	3
	E	***27***	***490***	74	20	3	3
	F	***24***	***490***	74	20	3	3
	G	***30***	***368***	74	20	3	3
	H	***27***	***368***	74	20	3	3
	I	***24***	***368***	74	20	3	3
Variation in formulation	J	30	490	***69***	***25***	3	3
	K	30	490	***64***	***30***	3	3
	L	30	490	***59***	***35***	3	3
	M	***35***	490	69	25	3	3
	N	***40***	490	64	30	3	3
	O	***32.5***	490	69	25	3	3
	P	***35***	490	64	30	3	3
	Q	30	490	***74***[2]	20	3	3

Note: 1. 0.02 wt% of the main excipient was substituted with Rhodamine B to be used as a model "drug".

2. Lactose was substituted with mannitol as the soluble pharmaceutical excipient.

3. Italic and bold text represents the variable that was varied.

3.2.2 CHARACTERIZATION OF GRANULE PROPERTIES

"Steady state" granules were characterized in terms of size distribution, morphology, circularity, bulk densities and dissolution properties. Malvern Mastersizer 2000 was used to determine the evolution of granule size distribution over wet massing period. Other granule properties were determined using a target granule size range of 180-355 µm which can be obtained by sieving. A vibrating sieve shaker (Retsch AS 200) together with a sieve set consisting of 8 test sieves: 1400 µm, 1000 µm, 710 µm, 500 µm, 355 µm, 180 µm, 63 µm and sieve pan was used. 15 g of sample was sieved for 5 min at an amplitude of 60 on the sieve shaker. Sieved samples were stored in amber glass jars wrapped in aluminium foil to reduce deterioration of the dye intensity of Rhodamine B to the minimum.

3.2.2.1 GRANULE SIZE DISTRIBUTION

Malvern Mastersizer 2000 uses laser diffraction technique which passes a laser light beam through a dispersed sample of particles. The intensity of light scattered created by the particles is measured and used to analyse the particle size (Instruments 2013). The

Mastersizer 2000 together with the dry powder dispersion unit, Scirocco 2000 was used to determine the granule size distribution in volume distribution.

Approximately 10-12 g of dried sample was first sieved using the sieve shaker to remove granules that were larger than 2 mm as the dry powder dispersion unit can only measure particle size up to 2000 µm (Instruments 2013). These granules that were larger than 2 mm can be regarded as "lumps" (see Figure 3.10). Therefore all the granule size distributions determined were normalized to account for the "lumps" that were excluded from the size analysis in Mastersizer i.e. the size fraction > 2 mm was manually added to the laser diffraction size data (refer to ***Appendix A*** for the normalization of size distribution).

A general tray was used to load the sieved sample in the dry dispersion unit. Obscuration levels were set from 0.5-6%. Vibration feed rate and dispersive air pressure were set at 25% and 0.4 bar respectively after a few trials to obtain consistent and reproducible triplicate measurements. An average of the triplicate measurements was calculated to represent the size distribution of each batch.

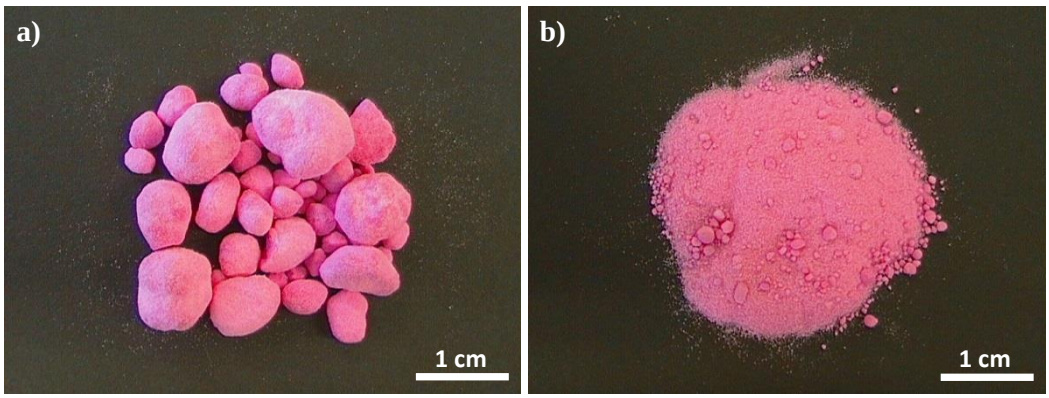

Figure 3.10: Dried granules (at 27% LL, 245 rpm and 0 min WMT) were sieved into two size fractions: a) > 2 mm and b) < 2 mm before being analysed in Mastersizer.

3.2.2.2 GRANULE MORPHOLOGY

Stereo zoom microscope (Motic SMZ-168) with Moticam 2300 was first used to observe the granule shape in bulk. A small amount of granules was placed on a black background in aid of a lamp. Scanning Electron Microscopy (SEM, Phenom^{TM}) was then used to examine the granule morphology including granule shape, structure and surface texture at high resolution. "Steady state" granules were placed on a specimen holder and sputter coated with a layer of

platinum for 15 s. The samples were examined under an accelerating voltage of 5kV. In addition, morphology of raw materials used in the formulation was also observed using SEM.

3.2.2.3 GRANULE CIRCULARITY

Malvern Morphologi G3 measures particle size and shape from 0.5 microns to several millimetres using a static image analysis technique. The Morphologi G3 was used to determine the circularity profile of "steady state" granules over wet massing period. The instrument measures HS (High Sensitivity) circularity of each particle in a bulk sample (refer to ***Appendix B*** for the definition of HS circularity).

Approximately 15 mg of granules were placed in the sample holder. The injection time and injection pressure were set as 20 ms and 1.2 bar. 80 s was allowed for the granules to settle on the glass plate after being injected into the dispersion chamber. Magnification of 5X was chosen to examine particles of 6.5-420 µm. Three scan areas of 8 mm in diameter were used to obtain optimal examination coverage of samples which allows more than a hundred granules to be characterized.

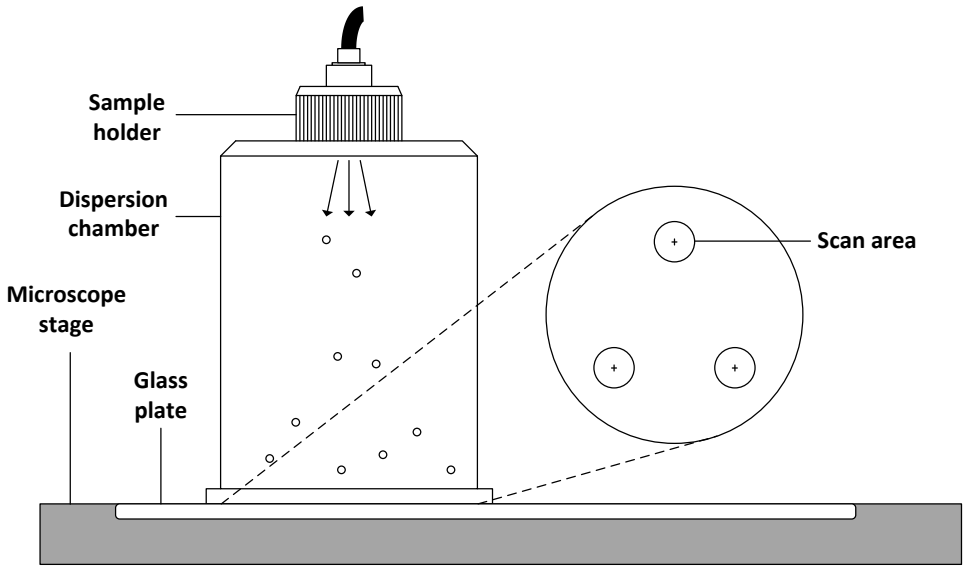

Figure 3.11: "Steady state" granules in the dispersion unit were dispersed on the glass plate.

3.2.2.4 GRANULE BULK POURED AND TAPPED DENSITIES

A 5 ml graduated measuring cylinder was used to determine the bulk poured and tapped densities of "steady state" granules. 1-2 g of granules was poured into the measuring cylinder using a funnel. Small sample size was used due to limited amount of granules (180-355 µm) produced at lower liquid level and 0 min WMT. Poured volume, V_p filled by granules was determined by taking the average of height of the sloped surface (see Figure 3.12). The measuring cylinder was then tapped until the tapped volume, V_t became constant. An average of triplicate measurements was determined to represent the bulk poured, tapped densities and Hausner ratio which were calculated as followed:

$$\text{Bulk poured density, } \rho_p = \frac{m}{V_p} \qquad \text{[Eqn 3.1]}$$

$$\text{Bulk tapped density, } \rho_T = \frac{m}{V_T} \qquad \text{[Eqn 3.2]}$$

$$\text{Hausner ratio, } H = \frac{\rho_T}{\rho_P} = \frac{V_P}{V_T} \qquad \text{[Eqn 3.3]}$$

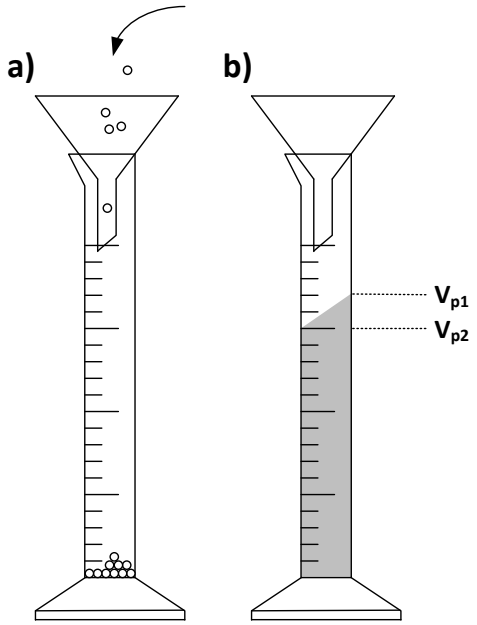

Figure 3.12: a) "Steady state" granules poured into a 5 ml graduated measuring cylinder through a funnel. b) Poured volume was determined by taking the average of V_{p1} and V_{p2}.

3.2.2.5 DISSOLUTION PERFOMANCE OF "STEADY STATE" GRANULES

3.2.2.5.1 BULK DISSOLUTION TEST

An in-house dissolution test was designed to determine the release profile of Rhodamine B contained in "steady state" granules. A 2 cm x 2 cm x 1.2 cm granule holder was made of an outer lining (Kartell, high-density polyethylene (HDPE) filtration disc) together with an inner lining of mesh. The granule holder was hung in the middle of a beaker to ensure the granules were fully immersed in the dissolution medium. Dissolution of granules was facilitated by using a magnetic stirrer rotating at 200 rpm.

500 mg of granules was dissolved in 50 ml of deionized water, providing a "sink" condition. Samples were taken at 5, 10, 15, 30 and 60 min dissolution times by withdrawing 2 ml of solution using a syringe. The same amount of fresh deionized water was added back to the beaker to replenish the level. The sample solution was passed through a syringe filter (Teflon, 30 mm in diameter, pore size of 0.45 μm) to remove any insoluble components. 200 μL of solution was pipetted into a 96 well standard microplate and this step was done repeated times. The microplate was then placed in a UV spectrometer (SpectraMax, M2) to measure the absorbance of the sample solution at a wavelength of 555 nm. Dissolution testing of granules produced at particular operating conditions was carried out in triplicate to obtain an average dissolution profile. The whole procedure is illustrated in Figure 3.13.

A calibration curve was constructed to calculate the amount of Rhodamine B released over time. Stock solution prepared for the calibration curve contained Rhodamine B and soluble components such as lactose and HPC (refer to ***Appendix D*** for the construction of calibration curve).

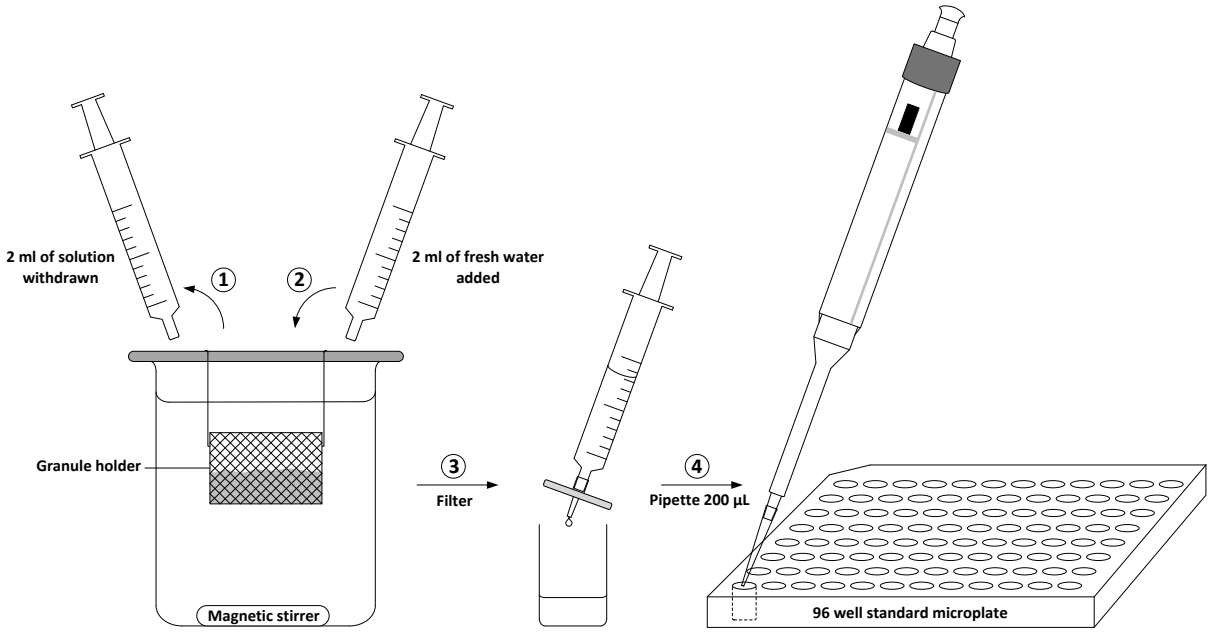

Figure 3.13: Sampling procedure of dissolution test: Step 1. Withdrawal of solution, Step 2: Replenish of fresh deionized water, Step 3. Filter the solution through a syringe filter, Step 4: Pipette the filtered solution into microplate.

3.2.2.5.2 SINGLE GRANULE DISSOLUTION

A single "steady state" granule was secured on carbon tape placed in a petri dish which was then filled with distilled water. Stereo zoom microscope (Motic SMZ-168) with Moticam 2300 was used to observe the change in morphology of the granule being dissolved over time. The dissolution time for a single granule is the same as bulk granule dissolution i.e. one hour.

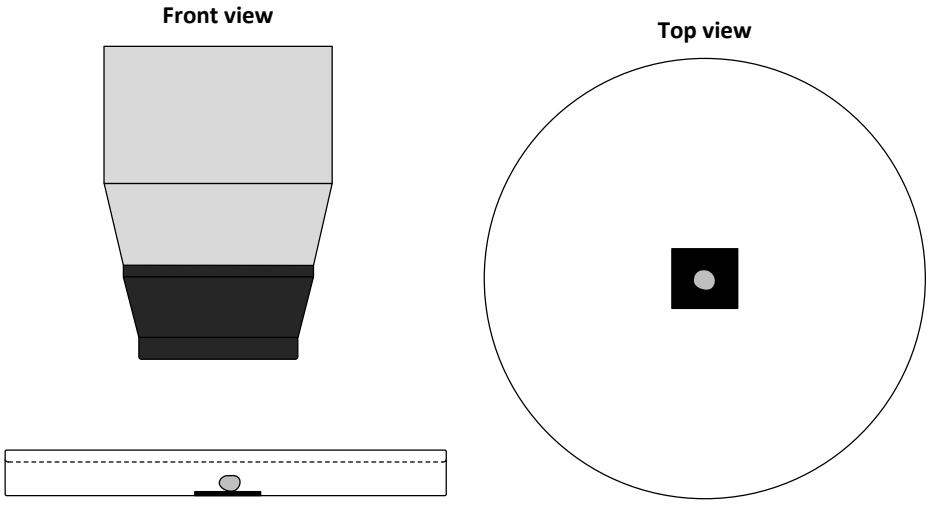

Figure 3.14: A single "steady state" granule dissolved in a petri dish and examined under optical microscope.

3.2.2.5.3 GRANULE SIZE DISTRIBUTION DURING DISSOLUTION TESTING

Focused Beam Reflectance Measurement (FBRM) was used to measure the number particles present in an agitated solution. 250 mg of "steady state" granules were added into 100 ml of distilled water agitated via a magnetic stirrer rotating at 200 rpm for an hour. The probe was positioned at an angle of 45° facing the beaker wall to avoid any signal due to the magnetic stirrer. The FBRM provides a real time measurement of the granule size distribution profile (as measured by the chord length distribution (Toledo)) during the dissolution test. 30 s was allowed to achieve a steady flow of granules within the dissolution bath after addition.

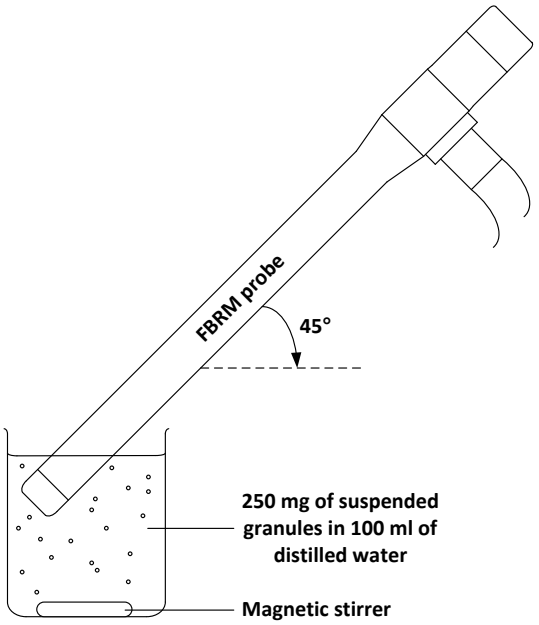

Figure 3.15: FBRM angled at 45° and faced the beaker wall to detect the particles in solution.

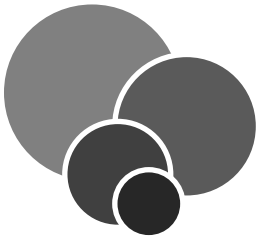

CHAPTER FOUR

FEASIBILITY OF "STEADY STATE" GRANULATION

4 FEASIBILITY OF "STEADY STATE" GRANULATION

4.1 INTRODUCTION

A better and comprehensive understanding of granulation is crucial in achieving the desired end product (granule) properties which in turn provides ease in downstream processes. Granulation time should be the main focus to improve this complex procedure that involves multiple mechanisms, causing granules to constantly shift through different saturation states within a limited timeframe (Iveson *et al.* 2001). Instead of trying to engineer granulation through stages of variable manipulation, the process should be allowed to keep running until everything comes to a state where no significant change is observed over time.

In general, steady state is defined as a stable condition that does not change over time. From a processing perspective, it is also an equilibrium state where a change in one direction is counterbalanced by another change in the opposite direction. A process goes through a transient state before reaching its steady state. Time is the key to reach this unchanging and continual condition.

"Steady state" granulation approach was originated from Michaels *et al.*'s (2009) work on high shear wet granulation. The term "steady state" or pseudo-steady state suggests that despite the inherent complexity of granulation, a state close to absolute steady state is achievable provided sufficient time is allowed. The two major processing periods, liquid addition and wet massing in high shear wet granulation are prolonged to allow the process to reach "steady state". This chapter replicates the approach by Michaels *et al.* (2009) using a similar formulation and a similar (but not identical) high shear mixer granulator to confirm the feasibility of "steady state" granulation in our equipment.

4.2 EXPERIMENTAL

To understand the granulation behaviour using "steady state" granulation approach, three operating parameters: 1. Wet massing time, 2. Liquid level and 3. Impeller speed were chosen to study their effects on the granules properties. Table 4.1 listed the range of each parameter to be investigated and the granule properties to be characterized.

Table 4.1: Summary of "steady state" granulation operating conditions for granule characterization analysis

Operating conditions			Granule properties			
Liquid level (%)	Impeller speed (rpm)	Wet massing time (min)	Size distribution	Morphology	Circularity	Bulk densities
24	245	0	✓	✓	✓	✓
		5	✓		✓	✓
		15	✓		✓	✓
		30	✓	✓	✓	✓
27	245	0	✓		✓	
		5	✓		✓	
		15	✓		✓	
		30	✓		✓	✓
30	245	0	✓	✓	✓	✓
		5	✓		✓	✓
		15	✓		✓	✓
		30	✓	✓	✓	✓
24	368	0	✓			
		5	✓			
		15	✓			
		30	✓		✓	✓
27	368	0	✓			
		5	✓			
		15	✓			
		30	✓		✓	✓
30	368	0	✓		✓	
		5	✓		✓	
		15	✓		✓	
		30	✓		✓	✓
24	490	0	✓	✓	✓	✓
		5	✓		✓	✓
		15	✓		✓	✓
		30	✓	✓	✓	✓
27	490	0	✓		✓	
		5	✓		✓	
		15	✓		✓	
		30	✓		✓	✓
30	490	0	✓	✓	✓	✓
		5	✓	✓	✓	✓
		15	✓	✓	✓	✓
		30	✓	✓	✓	✓

4.3 RESULTS

4.3.1 CONVENTIONAL GRANULATION

Industrial pharmaceutical high shear wet granulation processes commonly produce granules with broad and uncontrolled size distribution. This has been a recurring issue of granulating a mass of fine powders in a short period of processing time. Milling is often required downstream to reduce the particle size of the batch down to the desired size range.

In this study, a batch of "conventional" granules was produced based on the operating conditions adopted by Michaels *et al*. (2009) as a comparison to the "steady state" granules. The conventional granulation was replicated, using a liquid level of 40%, delivered by spraying method over 5 min with an additional of 30 s for wet massing. It represented the approach of short granulation time with copious amount of liquid generally adopted in the industry. As shown in Figure 4.1, the process produced a broad granule size distribution with possible over-wetting due to the addition of large amount of liquid. The mean particle size, d10, d50 and d90 were determined to be 1200 µm, 3180 µm and 5200 µm respectively. Hence "steady state" granulation approach was proposed to achieve a better control of granule size.

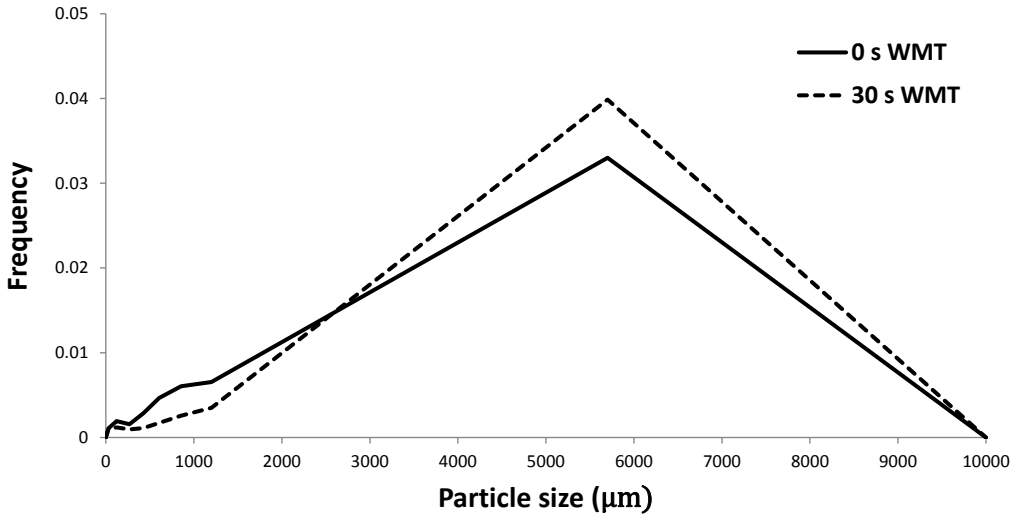

Figure 4.1: "Conventional" granulation: 40% liquid level and 30 s of wet massing.

4.3.2 "STEADY STATE" GRANULATION

4.3.2.1 EFFECTS OF WET MASSING TIME, LIQUID LEVEL AND IMPELLER SPEED ON GRANULE SIZE DISTRIBUTION

Controlling granule size within a certain range is crucial as the granule properties are highly dependent on the size. It is of high interest that high shear wet granulation process can be engineered to produce mono-sized spherical granules with tailored attributes. Hence the "steady state" granulation approach, which aims to achieve the above desired outcome with less liquid requirement and extended wet massing.

Extended wet massing has shown to be effective in narrowing down granule size distribution as portrayed in Figure 4.2. Granule size distributions became narrower as wet massing time increased from 0 min to 30 min. A similar trend was observed at all operating conditions (24-30% LL and 245-490 rpm) where the size distribution obtained after liquid addition appeared to be bimodal. As wet massing prolonged, the first population i.e. the smaller target size range became narrower and the second population i.e. amount of granules larger than 500 µm decreased. The trend observed closely matched with those in previous work (Knight *et al.* 1998, Knight *et al.* 2000, Scott *et al.* 2000) where the initial bimodal size distribution became unimodal after a sufficiently long period of wet massing.

A higher impeller speed was expected to be able to further reduce the amount of granules larger than 500 µm but that was not the case for 490 rpm. One plausible explanation was consolidation of wet granules was highly enhanced at higher impeller speed (Oulahna *et al.* 2003, Ohno *et al.* 2007) and transport of liquid from the inner matrix to granule surface occurred. Therefore fine particles were able to adhere on the wet surfaces and larger granules were formed by layering. Due to granule densification at higher impeller speed, strong and rigid granules were formed that could not be further broken down.

The formation of granules larger than 1000 µm was not observed in Michaels *et al.*'s study (2009). This discrepancy can be attributed to the use of chopper during granulation, the drop size used for the 2 L granulator and a different liquid delivery method i.e. spraying applied for the 25 L and 300 L granulator (Michaels *et al.* 2009). However, the amount of granules produced in this size range (600-2000 µm) was relatively low compared to the target size range in this project. They can be possibly eliminated by reducing the size of the initial liquid droplets delivered into the system.

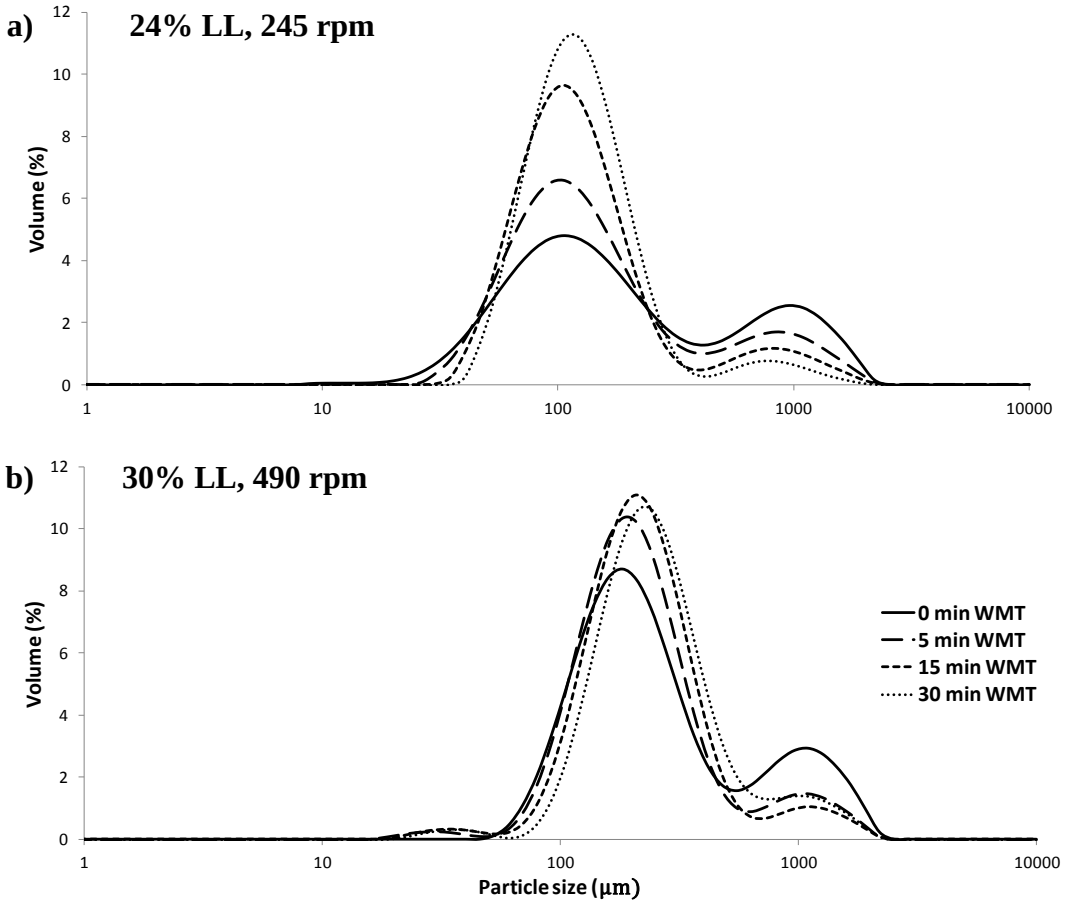

Figure 4.2: Granule size distributions produced at a) 24% LL and 245 rpm and b) 30% LL and 490 rpm narrowed down after 30 min of wet massing.

Span (relative width of size distribution, $\frac{d90-d10}{d50}$) and volume weighted mean diameter (D4,3) obtained by Mastersizer are quantitative data that can be applied to determine how narrow the size distribution becomes, apart from observing the change in size distribution curve. Volume weighted mean diameter (D4,3) is defined as the mean diameter of spheres with the same volume of analysed particles. At 0 min wet massing time, the initial span obtained for all granulation runs was relatively large i.e. 4.5-7.3. After 30 min of wet massing, the span was significantly reduced to 1.5-3.6 indicating that the size distributions became narrower. A decrease in standard deviation of D4,3 was also observed as wet massing prolonged (see Table 4.2). This implied that the granules produced were in a narrower size range.

Table 4.2: Evolution of volume weighted mean diameter, D4,3 (μm) over wet massing period

Impeller speed (rpm)	Liquid level (%)	Wet massing time (min)			
		0	5	15	30
245	24	337 ± 13	246 ± 17	184 ± 12	158 ± 5
	27	299 ± 13	272 ± 9	271 ± 9	251 ± 11
	30	320 ± 21	312 ± 8	279 ± 20	303 ± 23
368	24	304 ± 28	233 ± 33	219 ± 16	195 ± 13
	27	355 ± 27	258 ± 16	315 ± 3	239 ± 16
	30	382 ± 41	354 ± 26	378 ± 33	380 ± 36
490	24	252 ± 15	260 ± 18	230 ± 13	197 ± 6
	27	289 ± 45	246 ± 18	239 ± 8	224 ± 10
	30	371 ± 28	280 ± 23	267 ± 17	308 ± 8

The "steady state" granulation approach emphasizes on producing time-independent size distribution by promoting both granule growth and granule breakage to reach an equilibrium point. "Steady state" conditions were experimentally deduced to have achieved when no significant changes in granule properties were observed towards the end of the wet massing period. Granule size distributions produced at 245 rpm did not vary much between 15 min and 30 min WMT indicating "steady state" was achieved in that period. At higher impeller speeds of 368 rpm and 490 rpm, "steady state" condition was achieved at an earlier stage, between 5 min and 30 min WMT. This suggested that higher impeller speeds can drive granulation process to reach "steady state" faster.

The phenomenon could be explained due to increase in the probability of collision between granules and velocity of colliding granules at higher impeller speeds. Granule growth by coalescence of smaller agglomerates and granule breakage of larger agglomerates are favoured under these operating conditions. Therefore higher impeller speeds drive the two rate processes to reach an equilibrium point faster where granule size become relatively constant provided the wet massing period is sufficiently long. However, mathematical modelling will be required to prove the above claim, taking into account the impeller speed and granule size.

The granule size distributions produced by "steady state" granulation after 5 min of wet massing were broader compared to those produced after 30 min of wet massing (see Figure 4.3a). Granule growth and consolidation were still occurring whereas granule breakage was still mildly enhanced at this stage. Although the "steady state" approach uses less amount of liquid and a slower delivery rate to ensure the liquid is uniformly distributed, 5 min of wet massing was unable to narrow the size distributions significantly. "Steady state" condition

was not achieved in this short period of time. This proved that broad and uncontrolled size distributions produced by conventional granulation is inevitable as large amount of liquid is used and wet massing is usually less than 5 min.

A direct correlation between liquid level and granule size distribution was observed in "steady state" granulation (see Figure 4.3b). There was a gradual shift in the final size distribution towards the right (larger size range) as liquid level increased from 24% to 30%. Liquid level determines where the granule size distribution lies but not impeller speed. Regardless of the impeller speed used, the final size distributions produced at a specific liquid level overlapped with each other at approximately the same size range. Furthermore, the above trend was supported where the D4,3 increased with liquid level and the values were comparable for each liquid level at different impeller speeds. Both Mackaplow *et al.*'s (2000) and Ohno *et al.*'s (2007) studies showed similar trend where granule size increases gradually with the amount of liquid delivered.

Wet granules are constantly moving and colliding with each other and with equipment surfaces under the action of high impeller speed. This allows them to consolidate where particles migrate towards the centre and liquid binder being squeezed out to the surface. A viscous layer is formed around the granule which will aid wet collision. Liquid level used to granulate particles determines the liquid saturation of agglomerates hence the deformability. Wet granules with higher liquid content are more plastically deformable, allowing kinetic forces to be dissipated upon collision and leading to successful coalescence. In addition, the wet surfaces promote size enlargement by layering mechanism at the expense of fine particles. This explained why more granules of 180-500 μm were formed at increasing liquid level. On the other hand, 24% LL was not sufficient in producing granules of target sizes. It is suggested that granule size can be tuned to the desired range by varying the liquid level which becomes a huge advantage of using the "steady state" granulation approach (Michaels *et al.* 2009). Michaels *et al.* (2009) also discovered a sharp increase in granule size with increasing granulating fluid level at all impeller speeds.

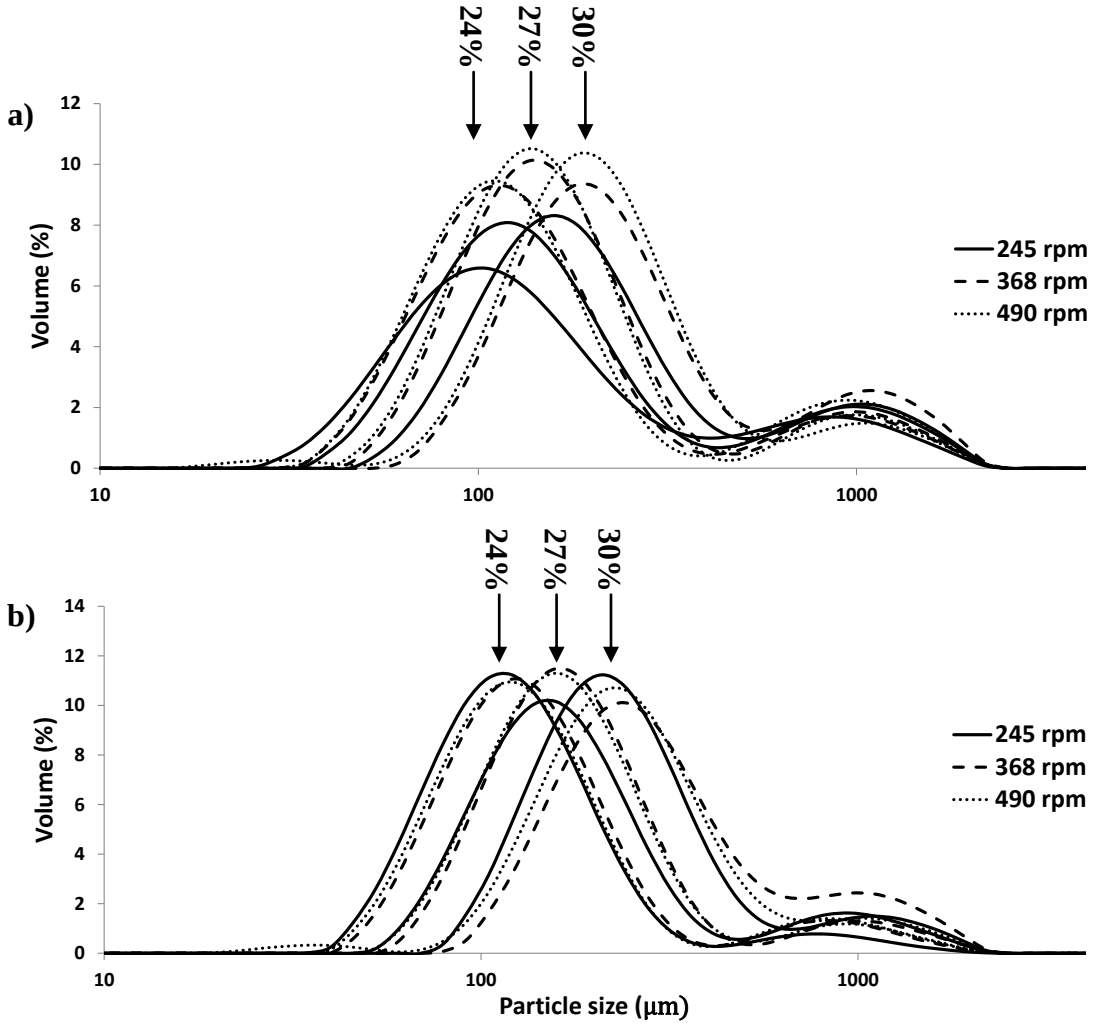

Figure 4.3: Granule size distributions produced a) after 5 min of wet massing and b) at the end of wet massing period at 3 different impeller speeds.

Furthermore, d10, d50 and d90 of granule size distribution produced at each operating condition were calculated to determine a specific granule size range to be focused on (refer to ***Appendix A***). An average of d10, d50 and d90 for this set of experiments were determined to be 93 µm, 168 µm and 472 µm respectively. Granules smaller than 168 µm were regarded as fines and/or non-agglomerated particles. 50-90% of the granules were in the size range of 168-472 µm. Available test sieves close to that size range are 180 µm and 500 µm hence 180-500 µm was set to be the target size range for the following granule characterization analysis.

The formation of "lumps" could be attributed to the immersion of primary powder particles in initial liquid droplets which needs to be broken down to achieve higher uniformity in liquid distribution. Wet massing shows a significant effect in breaking "lumps" over an extended period of time as seen in Figure 4.4. At 0 min WMT (end of liquid addition stage), "lumps"

were observed in each granulation batch. As wet massing time increased, the amount of "lumps" reduced, indicating that granule breakage was promoted by continuously kneading the wet mass. Majority of "lumps" were eliminated by the end of the wet massing period.

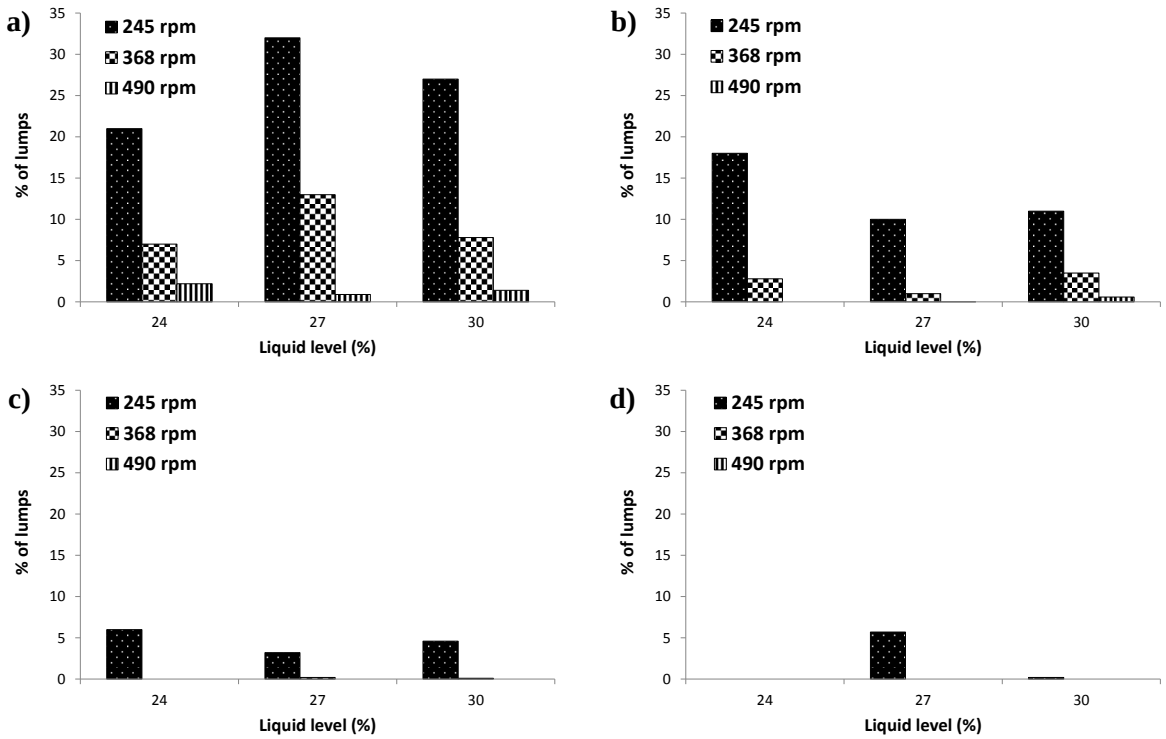

Figure 4.4: Effects of liquid level and impeller speed on the formation and breakage of "lumps" over the wet massing period: a) 0 min WMT, b) 5 min WMT, c) 15 min WMT and d) 30 min WMT.

The intensity of impeller speed was found to play a crucial role in promoting the breakage of "lumps". The amount of "lumps" formed at a particular liquid level reduced significantly when higher impeller speeds were used for the whole granulation process (see Figure 4.4a). At a lower impeller speed of 245 rpm, the amount of "lumps" was greater than 20% in mass of the sample batch at 0 min WMT. Increasing the impeller speed to twice the initial value i.e. 490 rpm reduced the amount to less than 3% only. Large wet agglomerates that formed from the initial liquid droplet exiting the delivery tube experienced greater shear forces imposed by the impeller blades and were broken down subsequently. Liquid within these agglomerates was then redistributed, achieving a higher uniformity in liquid distribution with higher impeller speeds. Moreover, running the granulation process at higher impeller speeds provides vigorous agitation that allows liquid droplets to penetrate into the powder bed faster and break down into finer droplets. Delivering liquid at a slow rate (2% of dry mass per min)

also helps in preventing pooling or any preferential growth that leads to uncontrolled size distribution by ensuring droplets do not overlap on powder surface.

A coupled effect of wet massing time and impeller speed on the breaking down of "lumps" was discovered. By comparing the effect of impeller speed at the same liquid level, the amount of wet massing time required to completely eliminate "lumps" at 24% LL was halved when the impeller speed was increased from 245 rpm to 368 rpm. Doubling the impeller speed to 490 rpm reduced the amount of wet massing time required by a factor of six. At higher liquid levels of 27% and 30%, doubling the impeller speed completely removed "lumps" after 15 min of wet massing. The results obtained matched with the findings in Benali *et al.*'s work (2009) and Chitu *et al.*'s (2011) study where the amount of lumps larger than 5 mm decreased with increasing impeller speed. Higher liquid level induces the formation of large agglomerates to increase. Therefore it requires either higher impeller speed or longer wet massing time if a lower impeller speed is used to break down these large agglomerates.

On the other hand, no direct relationship between the liquid level applied and the amount of "lumps" formed was observed. It was expected that the amount of "lumps" increases with liquid level. However, the amount of "lumps" produced at 27% LL was larger than that at 30% LL after liquid addition. This could be due to variation in sampling of granules. This part of the work aims to obtain an overview on how wet massing time and impeller speed affects the breakage of "lumps". Correlation between the liquid level applied and the amount of "lumps" formed may require more studies which are out of the project scope.

4.3.2.2 EFFECTS OF WET MASSING TIME, LIQUID LEVEL AND IMPELLER SPEED ON GRANULE MORPHOLOGY AND CIRCULARITY

In previous work conducted by Michaels *et al.* (2009), considerable changes in surface morphology and granule sphericity were observed at prolonged wet massing time where irregular shaped granules became rounder with smooth surfaces after 40 min of wet massing. The action of impeller has been found to have a pronounced effect on the spheronization of granules in high shear wet granulation (Knight *et al.* 2000, Chitu *et al.* 2011). It is one of the goals that this project adopted the "steady state" granulation approach: to produce granules that attain spherical shape.

Morphology of "steady state" granules were examined in two size classes: 180-355 µm and 355-500 µm. An optical microscope was used to obtain an overview of the granule shape in bulk as seen in Figure 4.5. At the lowest liquid level of 24% and lowest impeller speed of 245 rpm, the granules produced were irregular in shape, formed from a cluster of smaller granules. However, increasing the impeller speed from 245 rpm to 490 rpm did not enhance the spheronization of granules. In contrast, granules produced at 30% LL and 490 rpm appeared to be the roundest. In addition, more individual granules (as opposed to irregular-shaped granules that formed by smaller granules) were observed

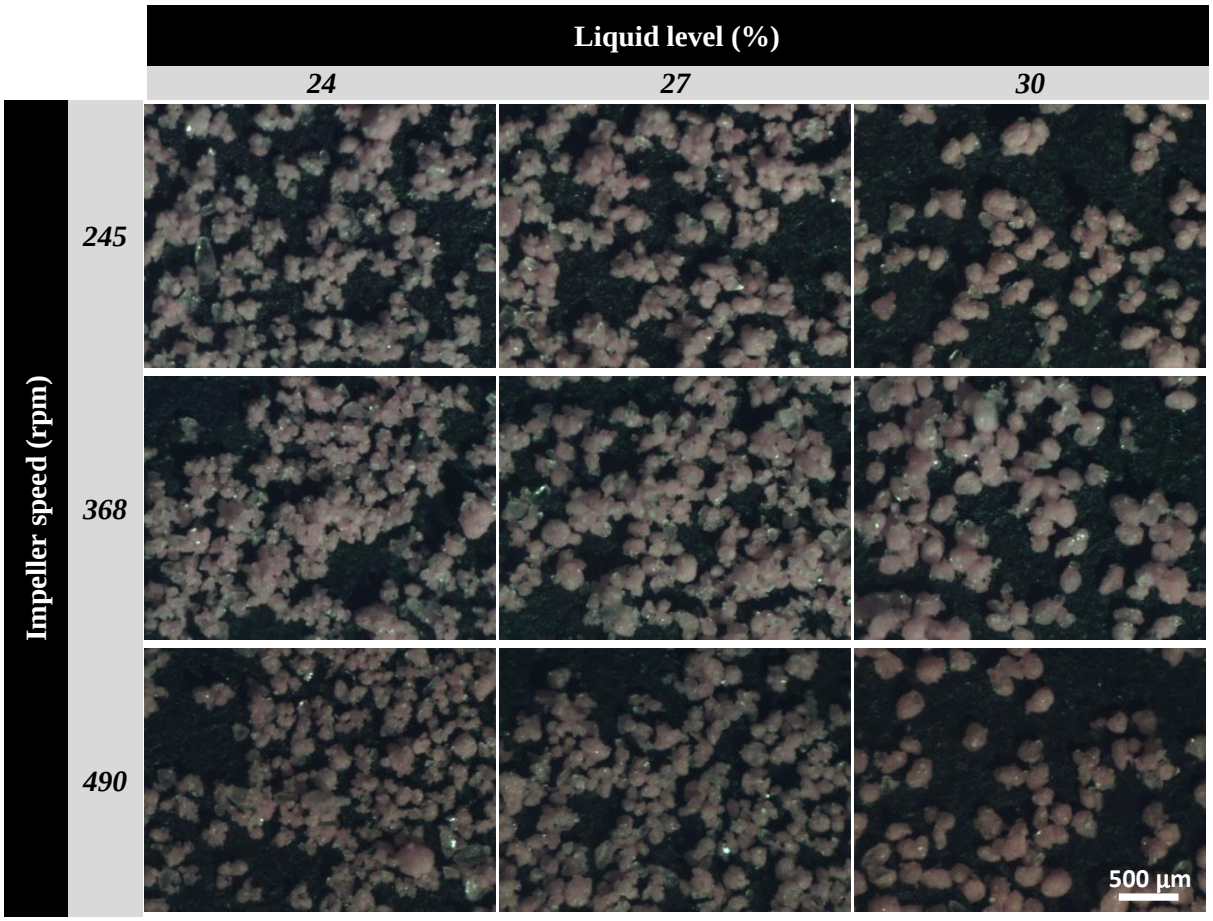

Figure 4.5: Steady state" granules of 180-355 µm produced after 30 min of wet massing.

Similar results were obtained for granules of 355-500 µm except at 30% LL and 245 rpm where more irregular shaped granules were produced as opposed to granules of 180-355 µm. However, smaller granules that formed these granules were not closely packed and could still be individually distinguished. As impeller speed increased from 245 rpm to 490 rpm, less irregular shaped granules were observed. In general, all the granules in this size range were quite spherical including smaller ones that formed the irregular shaped granules.

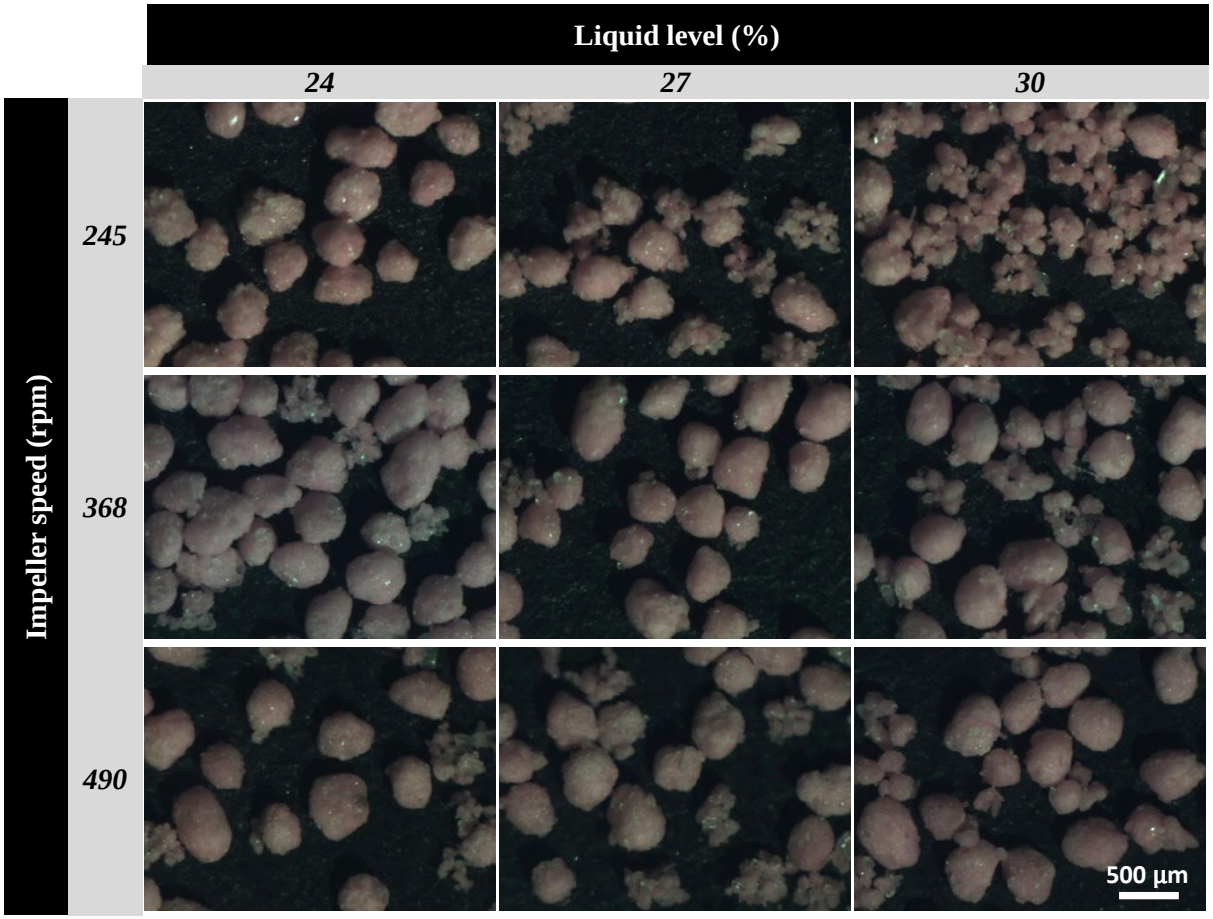

Figure 4.6: "Steady state" granules of 355-500 µm produced after 30 min of wet massing.

The morphology of "steady state" granules (180-355 µm) produced at the lowest and highest of liquid level and impeller speed were distinct hence they were selected to be examined using SEM (see Figure 4.5). High resolution images that illustrated the fine details of "steady state" granules were obtained. This allowed the identification of particles and/or small agglomerates that formed the irregular shaped granules. In addition, powder particles that adhered on granule surfaces contributing to the surface roughness could be identified.

"Steady state" granulation approach emphasizes the needs in extending wet massing period in order to achieve "steady state" condition. The approach not only has produced narrow granule size distribution but also allowed wet granules to spheronize. Increase in contact time promotes intermingling of MCC polymer chains hence increases the degree of autohesion (refer to ***Section 3.1.2.1*** in ***Chapter 3:*** *Material and Methodology* for the definition of autohesion). This can be observed in the structural change of granules produced at 30% LL and 490 rpm over the wet massing period (see Figure 4.7). Wet granules formed at 0 min WMT were generally irregular in shape where discrete lactose particles could be identified.

These granules later became rounder after 30 min of wet massing, showing high consistency with the observation in Michaels *et al.*'s work (2009) (refer to Figure 2.21 in ***Chapter 2:*** *Literature review*).

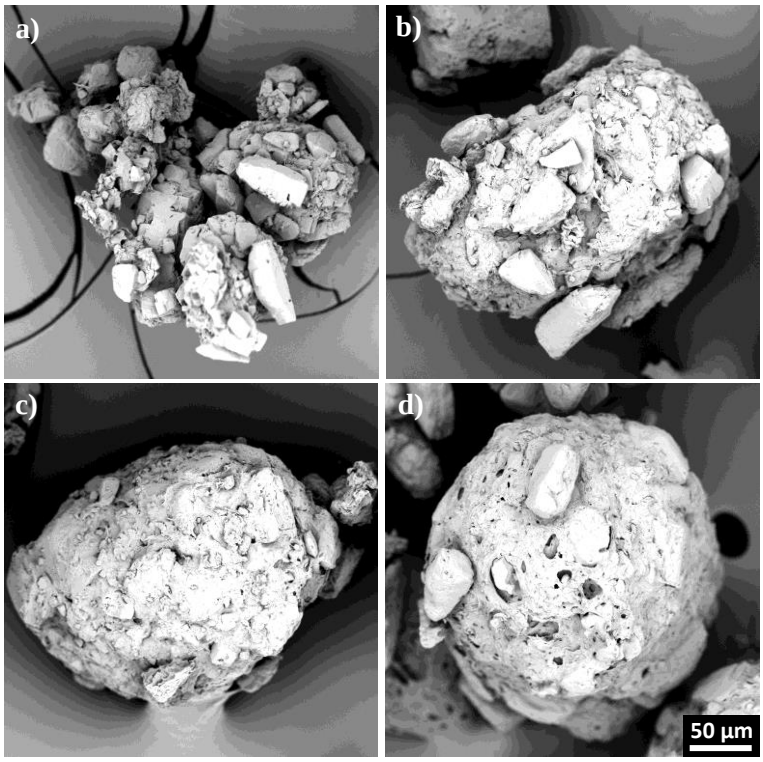

Figure 4.7: Rounding and surface smoothing of "steady state" granules produced at 30% LL and 490 rpm were observed over the wet massing period: a) 0 min WMT, b) 5 min WMT, c) 15 min WMT and d) 30 min WMT.

Apart from prolonged wet massing, the liquid level used is equally important in the rounding effect as it determines the liquid saturation of a wet granule hence the plastic deformability. Liquid addition decreases the polymer viscosity and increases the mobility of polymer chains. As liquid level increased from 24% to 30%, the smaller granules that formed the irregular-shaped granules appeared to be rounder and larger in size (see Figure 4.8a-b). However, increasing the impeller speed from 245 rpm to 490 rpm did not enhance the spheronization of granules at a lower liquid level of 24%. It suggested that autohesion of MCC polymer chains was restricted as they were less mobile when insufficient amount of liquid was delivered. Badawy *et al.* (2000) also commented that granules with lower liquid content tend to be brittle or less deformable hence they are unable to spheronize.

In contrast, rounder granules were produced at 30% LL and 490 rpm. More individual granules as opposed to irregular-shaped granules that formed by smaller granules were also

observed. Autohesion was greatly promoted when MCC polymer chains became more mobile at higher liquid level. Furthermore, it was known that impeller plays a crucial role in promoting good mixing and spheronization of granules (Michaels *et al.* 2009). Forces experienced by granules such as shear and pressure were expected to be more intense at a higher impeller speed. Therefore, diffusion of polymer chains across the interface of MCC particles was enhanced under these favourable operating conditions. At the same time, roping motion of deformable wet granules also helped in spheronization through the collision with each other and with the wall of mixing bowl. This phenomenon was identical to that in wet extrusion/spheronization where extrudates are subjected to frictional forces and shaped into spheres or pellets.

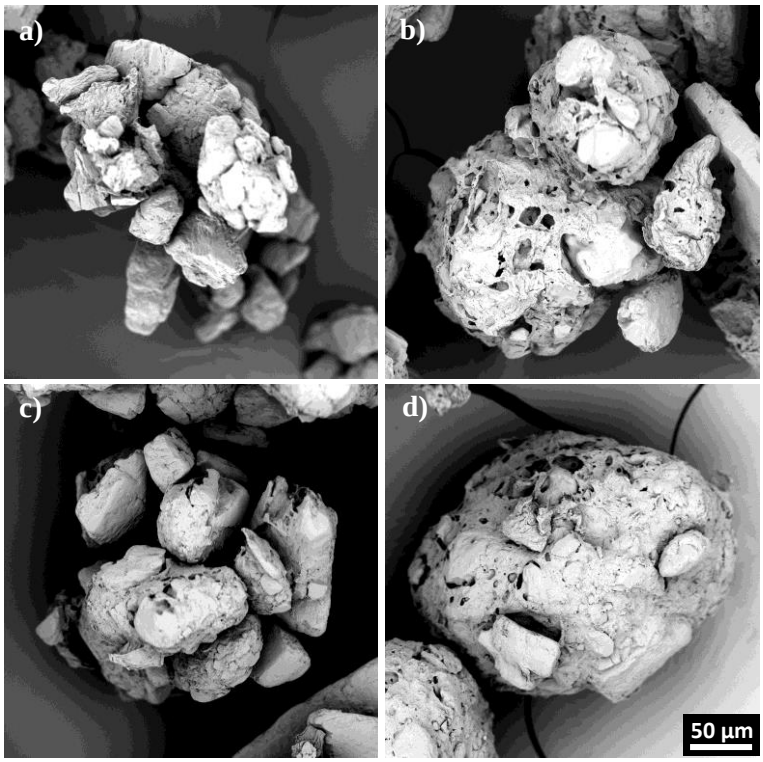

Figure 4.8: Morphology of "steady state" granules produced at a) 24% LL and 245 rpm, b) 30% LL and 245 rpm, c) 24% LL and 490 rpm and d) 30% LL and 490 rpm.

The internal structure of "steady state" granules produced at 30% LL and 490 rpm were examined to show the occurrence of autohesion in MCC polymer chains. An interconnected network was formed internally with lactose particles distributed across as seen in Figure 4.9. It is believed that MCC polymer strands inter-diffused from one surface to the other and wrapped any neighbouring lactose particles. The presence of high molecular weight polymeric binder, HPC also helped in increasing the degree of autohesion. It was also

observed that "steady state" granules possessed a porous structure despite the dense outer appearance. The formation of this polymeric matrix has a huge influence on the dissolution properties of "steady state" granules which will be discussed in ***Chapter 5:*** *Dissolution Performance of "Steady State" Granules*.

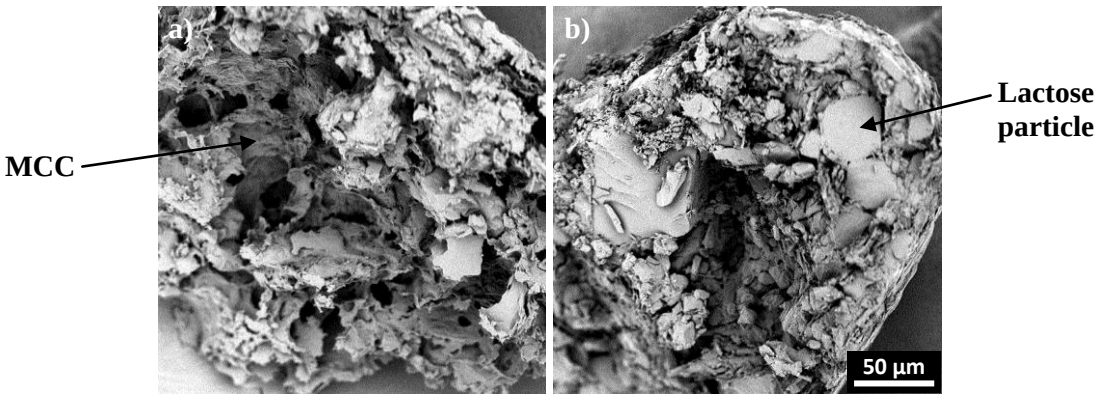

Figure 4.9: Internal structure of "steady state" granules produced at 30% LL and 490 rpm.

Qualitative data obtained using optical microscope and SEM was supported by determining the granule circularity profiles over wet massing period (see Figure 4.10). Granule circularity was found to increase linearly with wet massing time at 24-30% LL and 245 rpm. On the other hand, granules formed at 490 rpm also increased in circularity during the first 15 min of wet massing. However, attrition of granules might have occurred as a result of intense shearing at higher impeller speed which explained the decrease in circularity upon further wet massing.

Granules produced at 30% LL possessed higher circularity compared to those at lower liquid levels, showing that granules with higher liquid saturation are able to spheronize better. 368 rpm was found to be the optimum impeller speed to produce granules with the highest circularity after 30 min of wet massing (see Figure 4.11). Overall, extended wet massing helps in rounding of "steady state" granules produced at all operating conditions except 24% LL and 490 rpm.

It was observed that at 27% LL, granule circularity did not vary significantly at the end of wet massing period regardless of the impeller speed used. This indicated that "steady state" conditions have achieved in terms of granule circularity. During the last 15 min of wet massing, granule circularity did not change drastically at 24-27% LL with 245 rpm and 27-

30% LL with 490 rpm. Therefore a higher impeller speed is recommended when a higher liquid level is applied and vice versa in order to reach "steady state".

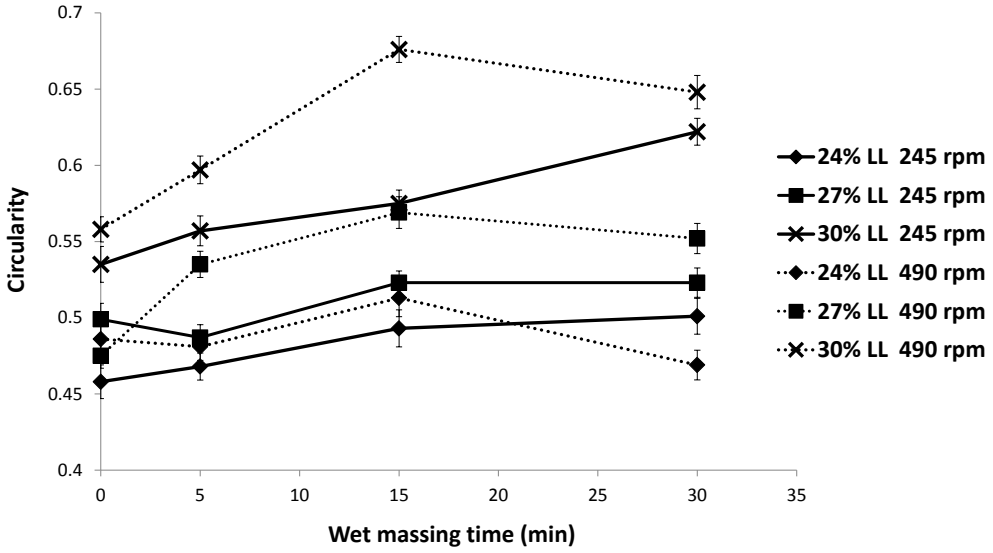

Figure 4.10: Evolution of granule circularity profile during wet massing period at 24-30% LL and 245-490 rpm.

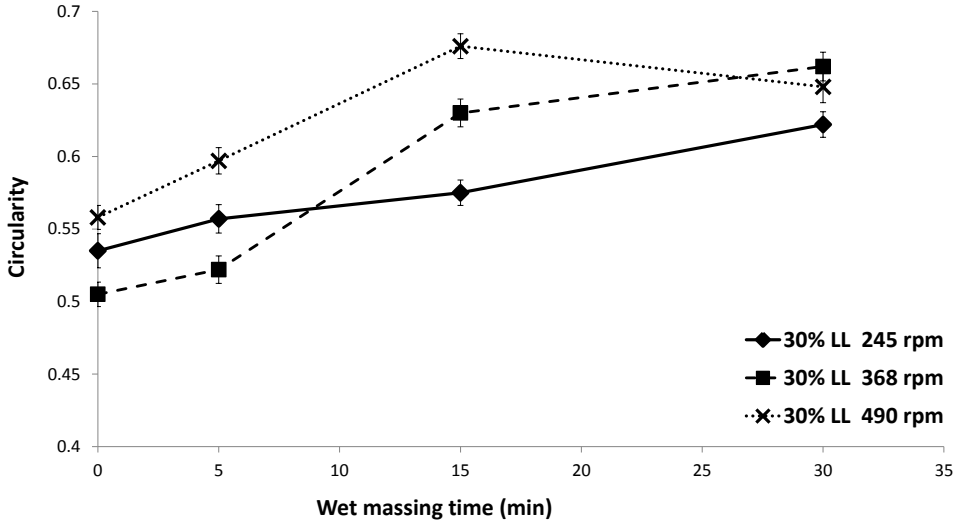

Figure 4.11: Effect of impeller speed on the granule circularity profile at 30% LL.

Circularity of "steady state" granules increased with liquid level at all impeller speeds as seen in Figure 4.12a. Granules formed at 30% LL and after 30 min of wet massing possessed the highest circularity compared to those at 24-27% LL. This proved that liquid level has a huge influence on the plastic deformability of wet granules, allowing them to be shaped into spherical solid mass under the action of impeller.

On the other hand, using higher impeller speed enhances the rounding of granules at higher liquid levels but not 24% LL. Circularity of granules produced at 24% LL decreased with increasing impeller speed. This can be explained by the brittle nature of wet granules with lower liquid content. Autohesion was also inhibited due to less mobile polymer chains. Increasing shear forces exerted by impeller causes these granules to undergo attrition and/or breakage and lose their spherical shape. The results obtained for 27-30% LL closely matched with Mangwandi *et al.*'s (2010) and Chitu *et al.*'s (2011) studies where they discovered that granule circularity/roundness increases with impeller speed to an optimal value beyond which granules decreased in circularity/roundness.

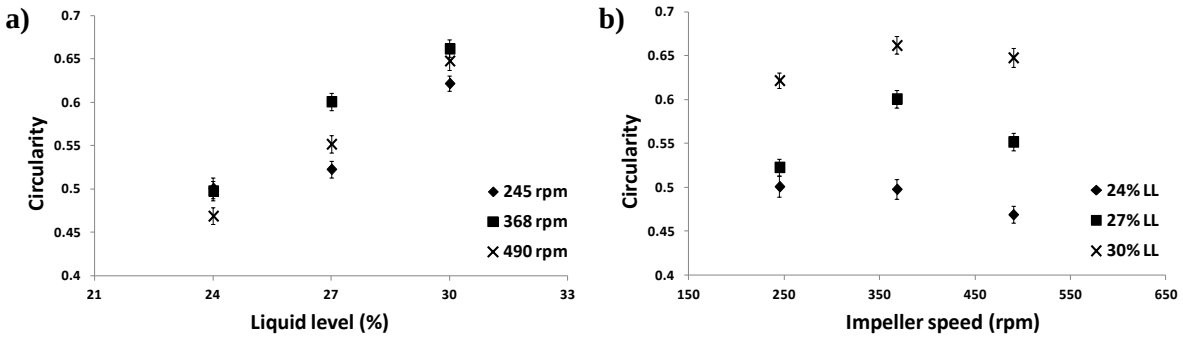

Figure 4.12: Effects of a) liquid level at different impeller speeds and b) impeller speed at different liquid levels on granule circularity after 30 min of wet massing.

"Steady state" granules of 355-500 µm produced at all operating conditions were observed to be spherical under optical micoscope. However, SEM images showed that there was a significant difference in terms of granule structure. Granules produced at 24% LL and 245 rpm appeared to be less compact and lactose particles were discretely attached within the granules (see Figure 4.13a). On the other hand, a distinct polymeric matrix with embedded lactose particles was observed at higher liquid level as illustrated in Figure 4.13b. This particular granule form was found to be similar to granules of 180-355 µm produced at 30% LL and 490 rpm. The degree of autohesion increased at a higher liquid level of 30% LL which allowed the formation of MCC matrix but not at 24% LL. In this project, an abundance of granules were formed in the size range of 180-355 µm. This size range was chosen for later characterization of granule properties such as bulk densities and dissolution performance.

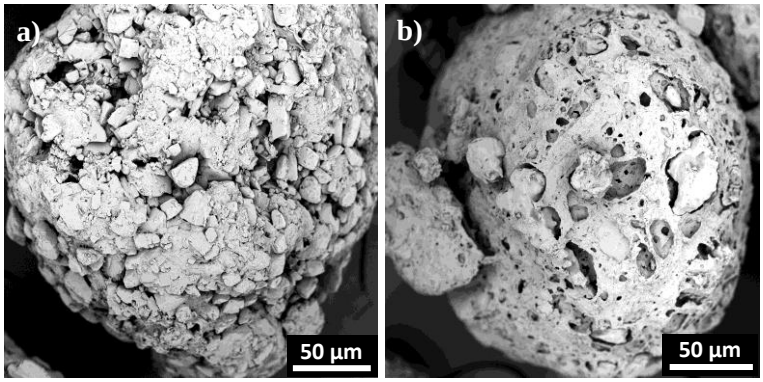

Figure 4.13: "Steady state" granules of 355-500 µm formed at a) 24% LL and 245 rpm and b) 30% LL and 490 rpm.

4.3.2.3 EFFECTS OF WET MASSING TIME, LIQUID LEVEL AND IMPELLER SPEED ON GRANULE BULK DENSITIES

Granules produced by high shear wet granulation are generally dense or less porous due to great shearing force imposed by the impeller that enhances the consolidation and densification of granules. "Steady state" granules produced by Michaels *et al.* (2009) were particularly dense with a porosity of 16% while conventional granules exhibited 40-50% in porosity. This is due to the effect of extended wet massing where wet granules are constantly sheared, allowing them to consolidate into compact solid mass. Consolidation occurs when particles start migrating to the centre of a wet granule and become closely packed.

Bulk density of a powder is referred as the mass of powder that can be packed into a specific volume which includes the voids exist between and within the particles themselves (Abdullah *et al.* 1999). Bulk density is found to be dependent on the particle size, shape, surface roughness and consolidating stress which can be transferred as the intensity of impeller speed. Bulk densities of "steady state" granules are examined in terms of "poured" (random loose packing) density and "tapped" (random dense packing) density which can be used to convey the changes in consolidation state of granules (Santomaso *et al.* 2003, Vasilenko *et al.* 2013).

Wet massing was found to have a significant effect on the densification of "steady state" granules. Both poured and tapped densities increased with wet massing time as illustrated in Figure 4.14 and 4.15. The measurements were highly reproducible as shown by the error bars up to ± 0.00794. The amount of shear force imposed on wet granules increases with time, causing them to densify gradually. However, each granule may consolidate to a different

extent depending on its location in the mixing bowl where higher intensity of force is exerted near the blade tip. Extending wet massing period has allowed granules to have the opportunity to experience relatively the same amount of force and achieve same degree of consolidation. No significant change in poured density was observed between 15 min and 30 min of wet massing but not for the case of tapped density. The fact that tapped density was still increasing towards the end of the wet massing period showed two possible reasons: 1. Narrowing of granule size distribution or 2. Change in granule circularity where rounder granules were able to achieve better packing. As a result, "steady state" condition in term of bulk density was not achieved where consolidation continues to occur with increasing wet massing time. Studies done by Badawy *et al.* (2000) and Badawy *et al.* (2012) also demonstrated similar trend.

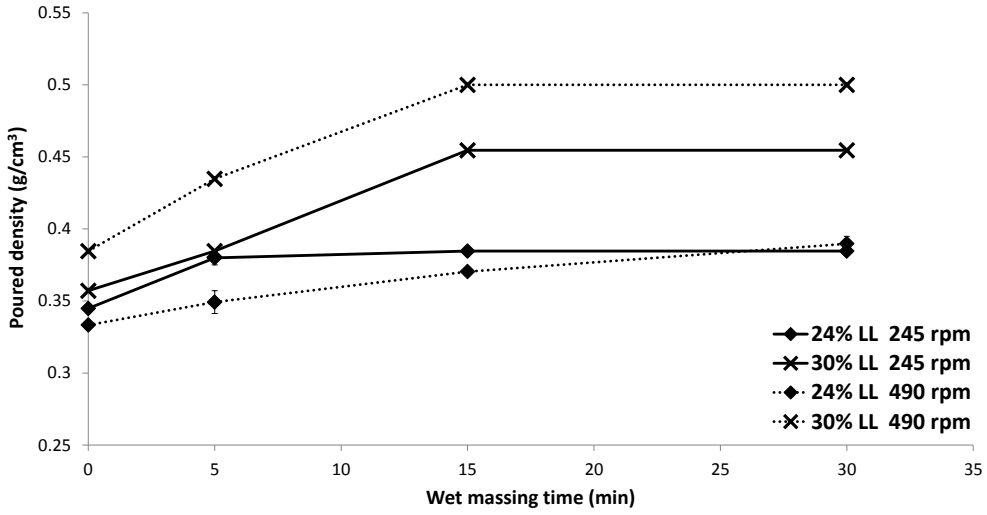

Figure 4.14: Poured density of "steady state" granules over wet massing period.

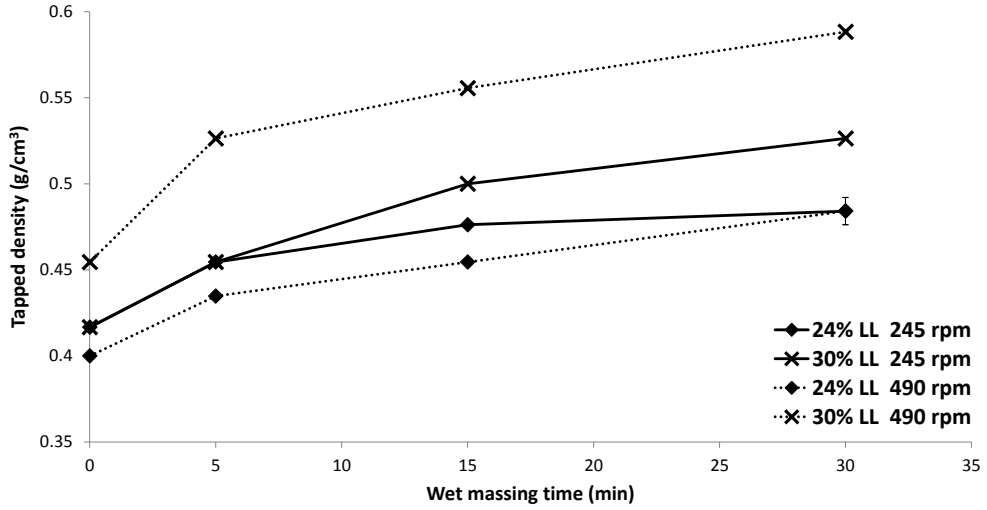

Figure 4.15: Tapped density of "steady state" granules over wet massing period.

Both poured and tapped densities of granules produced at 30% LL were found to increase linearly with impeller speed (see Figure 4.16). Notable increase in bulk densities with liquid level was also observed. The results were comparable to that in Badawy *et*'s *al.* (2000) and Badawy *et al.*'s (2012) work. Increasing liquid level produces granules with higher bulk densities. Friction between particles reduces and mobility of polymer chains increases when liquid content of granules increases. They become more deformable and able to consolidate further compared to those produced at lower liquid level. In contrast, increasing the impeller speed did not show a significant effect on the bulk densities of granules produced at 24-27% LL as illustrated by the rather flat profiles, indicating that the extent of densification was limited by the liquid saturation of granules.

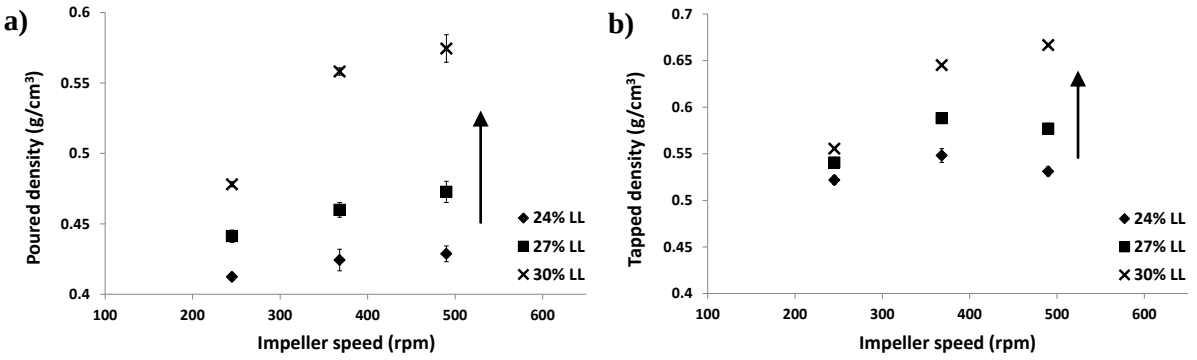

Figure 4.16: Effect of impeller speed on a) poured and b) tapped densities of "steady state" granules at different liquid level.

Hausner ratio is a dimensionless number used as an indication of the flowability of a powder or granular material. It provides a simple way of measuring the propensity of free flowing material by determining the ratio of tapped density to poured density. Powder or granular material with a Haunser ratio less than 1.25 belongs to group A powders – free flowing and easy to fluidize (Abdullah *et al.* 1999).

As seen in Figure 4.17, increasing liquid level decreased the Hausner ratio to less than 1.25, indicating that flowability of "steady state" granules improved. This can be attributed to the increase in granule circularity at higher liquid level. It can be further explained by referring to the image analysis of "steady state" granules by SEM (see Figure 4.8). Granules produced at 24% LL were found to be irregular in shape with rough surfaces hence flowability of these granules would be poorer than that of rounder granules with smooth surfaces formed at 30% LL. Zou and Yu (2009) also discovered that Hausner ratio decreased with an increase in

sphericity. In contrast, impeller speed did not affect Hausner ratio significantly. Hausner ratio was determined to provide an overview of how well "steady state" granules flow. It is recommended that more precise data on the flowability of material can be obtained using Flodex or FT4 powder rheometer.

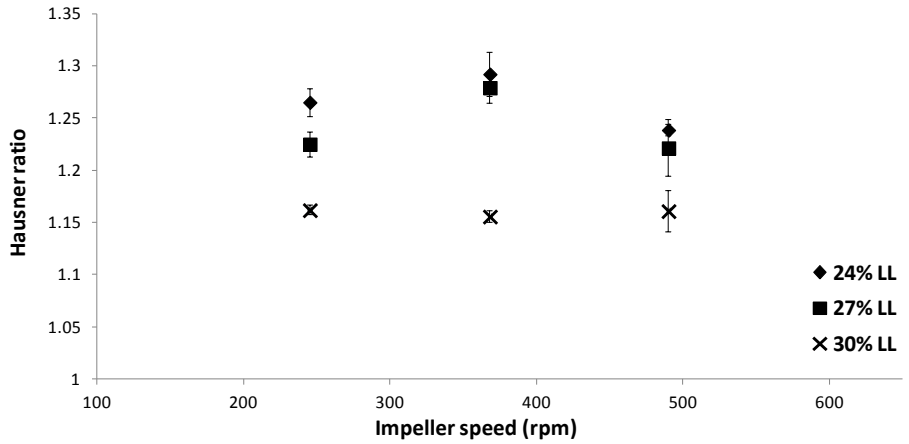

Figure 4.17: Effect of impeller speed on Hausner ratio at different liquid levels.

4.4 DISCUSSION

"Steady state" granulation has proven to be able to reproduce at a similar scale, mixer granulator and formulation. The granulation trends observed in this project corresponded well with those in Michaels *et al*'s work (2009). Final granule properties are discovered to be highly dependent on the pre-determined processing conditions. As opposed to conventional granulation, liquid addition rate has been adjusted to be slower i.e. 2 %/min (dry basis) and wet massing has been extended in "steady state" granulation (Michaels *et al.* 2009).

The extent of liquid dispersion can never be neglected at the initial stage of granulation process as it affects the nucleation of wetted powder particles which in turn determines the final size distribution. Many ways of achieving effective liquid dispersion have been proposed such as reducing the liquid delivery rate and providing vigorous mixing. Liquid droplets are more likely to overlap with each other on the powder surface when the liquid delivery rate is higher than the powder flux rate. This will cause drop coalescence and result in a broader size distribution (Iveson *et al.* 2001). Therefore using a slow delivery rate in "steady state" granulation ensures that each liquid droplet lands separately and forms one nucleus at a time.

High impeller speed is used to achieve roping flow of powder and good mixing. Increasing the impeller speed increases the powder flux through the nucleation zone. Nuclei that formed from initial droplets are carried away from the wetting zone and replaced with fresh powder which reduces the likelihood of drop coalescence. As less time and less binder volume are available for agglomeration, granule size can be reduced significantly (Iveson *et al.* 2001). Furthermore, intensive shearing by the impeller crushes the initial agglomerates and redistributes the liquid binder to neighbouring powder particles. This explained the decrease in "lumps" formation at the end of liquid addition stage when higher impeller speeds were used.

The phenomenon can be further explained using the nucleation regime map proposed by Hapgood *et al.* (2003) (refer to Figure 2.12 in ***Chapter 2***). Although dripping was used as the delivery method, the dimensionless spray flux that describes the spray pattern can be adopted to discuss the drop behaviour. Decreasing the delivery rate and increasing the droplet diameter will decrease the dimensionless spray flux. On the other hand, running granulation process at high impeller speed increases the powder bed porosity. In terms of binder fluid properties, distilled water has higher surface tension and lower viscosity compared to other polymeric binders (Hapgood *et al.* 2003). The three factors will decrease the dimensionless drop penetration time. Therefore, nucleation in "steady state" granulation will be shifted to the drop controlled regime, achieving better control of size distribution.

After liquid addition stage, broad granule size distribution was produced due to poor uniformity of liquid distribution throughout the powder bed (see Figure 4.3a). In wet massing stage, mechanical mixing and agitation by the impeller are the main means of further distributing liquid binder. Wet granules will be constantly colliding with each other and with equipment surfaces which allow them to consolidate. During this process, granule size and porosity reduce as entrapped air and liquid binder may be squeezed out. Granules with high porosity are generally weak and easy to be broken. Released liquid binder from broken granules wets neighbouring granules together with surface wetted granules after consolidation aid coalescence, resulting in potential granule growth. When granules achieve their optimum liquid saturation over a period of sufficient wet massing, granule size will become relatively constant. The theoretical concept of achieving equilibrium between rate of granule growth and granule breakage to produce narrow size distribution has been supported by the results obtained.

The intricate network formed in "steady state" granules as illustrated in Figure 4.9 can be further elucidated by Kleinebudde's crystallite-gel-model (1997) discussed in ***Chapter 3***. MCC, considered as a spongy material temporarily stores the absorbed liquid within itself. The shear force produced by the rotating impeller breaks down these wet MCC into smaller subunits called crystallites. When experiencing mechanical pressure, MCC partially releases the contained water which will act as a lubricant, inducing better mobility of powder and as a binder, agglomerating neighbouring particles such as lactose. The crystallites will then crosslink and form the gel-like structure that enwraps all the other ingredients together. Increasing the amount of liquid delivered decreases the deformability of the agglomerates, allowing them to be shaped into a spherical matrix through the collision with others and with equipment surfaces. This was validated by the structural change of "steady state" granules from an irregular to a rounder shape when the liquid level was increased from 24% to 30% (see Figure 4.8).

During the course of granulation, the original structure of MCC was completely destroyed and reassembled into a meshed network with discrete lactose particles distributed across. The enclosed structure was discovered to possess large internal voids, making it to be quite porous despite the concern of over-consolidating the granules (see Figure 4.9a). This feature of "steady state" granules will be particularly important when investigating the dissolution behaviour of these granules which will be discussed in ***Chapter 5***.

A high resemblance in the physical appearance between "steady state" granules produced at 30% LL (see Figure 4.8d) and pellets formed by extrusion/spheronization in Kleinebudde's study (1997) (see Figure 3.3a in ***Chapter 3***) was observed. Both matrices were spherical and dense except lactose particles were visible on the outer surface of "steady state" granules. When the wet agglomerates were being dried, permanent bonds will be formed between the intermingled polymer chain ends through autohesion, resulting in a stable solid matrix that will not disintegrate when comes in contact with water again (Kleinebudde 1997). It will be interesting to find out whether "steady state" granules behave the same way as the pellets that were dissolved in Kleinebudde's work (1997).

4.5 CONCLUSIONS

Granulation behaviour using "steady state" granulation approach has been studied extensively by investigating the effects of wet massing time, liquid level and impeller speed on granule properties such as size distribution, morphology and densities. Better understanding on how extended wet massing resulted in narrower granule size distribution, rounder and smoother surfaced granules was achieved. The idea of "steady state" approach was initiated by Michaels *et al*. (2009) and adopted in this project to produce a granule dosage form suitable for oral consumption. Key findings of this chapter that confirmed earlier studies by Michaels *et al.* (2009) are listed as followed:

1. Wet massing has shown to be effective in narrowing granule size distribution. The amount of "lumps" formed after liquid addition was reduced significantly and eliminated completely at the end of wet massing period. Bimodal size distribution became unimodal as a result of increased wet massing time. These proved that wet massing helps in redistributing liquid evenly across the powder bed where larger agglomerates such as "lumps" can be broken down and smaller ones can coalescence and grow. Achieving uniform liquid distribution will allow granules to grow to the same extent hence producing granules of similar sizes. Furthermore, granules that are wet massed for sufficiently long period of time exhibit structural change in terms of sphericity and surface smoothness. Granules with higher liquid content became rounder with smooth surfaces. Bulk densities of granules were found to increase with wet massing time as a result of enhanced consolidation over time.

2. Liquid level was found to be an important factor in determining granule size distribution. A direct relationship between liquid level and size distribution was discovered where a gradual shift of size distribution towards the larger size range occurred when there was a fixed increment of liquid level. Regardless of the impeller speed used, reproducible granule size distributions were observed at all liquid levels. Apart from that, liquid level also affects the granule sphericity significantly where rounder granules were formed as liquid level increased. Wet granules are more deformable at higher liquid level given interparticle friction is reduced and polymer chains are more mobile. Autohesion is used to explain the formation of spherical polymer matrix of "steady state" granules that encapsulates other ingredients. Increasing liquid level also increases the bulk densities and flowability of granules.

3. Impeller functions to provide good mixing and ensure uniform distribution of liquid within the powder bed. Using a higher impeller speed was found to effectively reduce the amount of "lumps" formed compared to lower speeds. Since wet massing period is adequately long, impeller can break down these "lumps" without installing a chopper. "Steady state" condition in term of size distribution was achieved faster at a higher impeller speed. Impeller was known to promote spheronization of granules due to the shear force exerted on wet granules that allows them to deform and shape. Higher intensity of impeller speed enhances the consolidation of granules with higher liquid content, producing dense granules.

4. In "steady state" granulation, wet massing period was extended up to 30 min as opposed to 5 min adopted in conventional granulation. "Steady state" conditions were achieved when no significant changes were observed in granule size distribution and circularity within the last 15 min of wet massing. This implies that wet massing period can be reduced to less than 30 min. Estimating the period of time when wet massing no longer have any significant effects on granule properties serves as an end-point determination of granulation process. However, bulk densities of granules continued to increase as wet massing prolonged. Therefore, "steady state" or pseudo steady state is a suitable term to describe the approach as not all granule properties become constant at the end of the wet massing period.

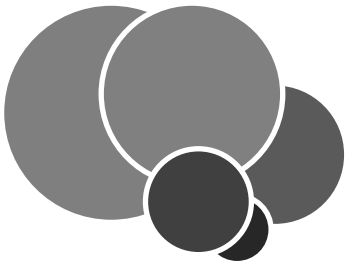

CHAPTER FIVE

DISSOLUTION PERFORMANCE OF "STEADY STATE" GRANULES

5 DISSOLUTION PERFORMANCE OF "STEADY STATE" GRANULES

5.1 INTRODUCTION

Each dosage form acts as a vehicle in transporting drug substances into the human body. When designing a solid dosage form, how the entrapped drug substances are released is of huge interest. Excellent dissolution performance is vital in solid dosage forms to achieve desirable controlled drug release, as only dissolved drug particles are able to diffuse through an aqueous medium into absorption sites in the body.

Oral solid dosage forms are designed for patients to administer through the mouth and down the gastrointestinal tract. They come in various forms and sizes, mainly tablets and capsules. Depending on the characteristics of API and formulation design, one dosage form may adopt a different release mechanism from the others. Therefore, identifying the release mechanism and quantifying the release rate are essential steps to be routinely carried out for the optimization of formulation design and the development of *in vivo* dissolution performance of a dosage form.

In ***Chapter 4:*** *Feasibility of "Steady State" Granulation*, two main types of granules: smooth and irregular were observed. They were typically formed at a liquid level of 24-30% and impeller speed of 245-490 rpm. In this chapter, the dissolution behaviour of these two types of "steady state" granule will be looked into. All granulation batches contained 0.02 wt% Rhodamine B as a model "drug". The chapter first discusses the release data obtained from the dissolution testing of "steady state" granules. Images analysis of "steady state" granules before and after dissolution was performed to examine the structural change of the dosage form. It allows the release mechanism of "steady state" granules to be observed and dissolution results to be interpreted.

5.2 EXPERIMENTAL

Dissolution performance of "steady state" granules (180-355 μm) was performed on two types of granules (see Figure 5.1):

1. Smooth, regular, spheroidal granules (formed at 30% LL) and
2. Irregular-shaped granules (formed at 24% LL)

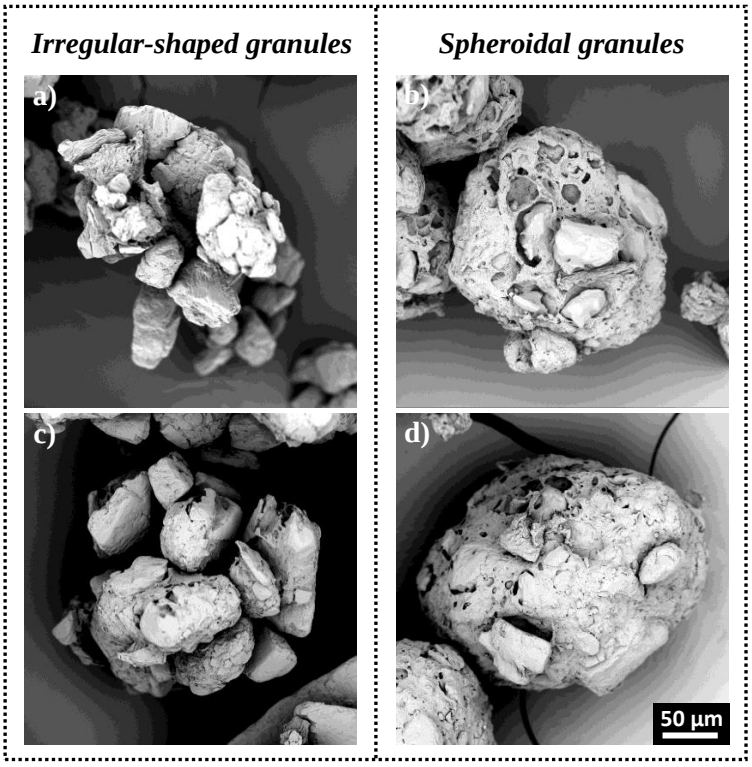

Figure 5.1: Two types of "steady state" granules tested: 1. Irregular-shaped granules – a) 24% LL and 245 rpm, c) 24% LL and 490 rpm and 2. Regular, spheroidal granules – b) 30% LL and 245 rpm, d) 30% LL and 490 rpm.

For each sample, the following characterization methods were used:

1. Dissolution testing – to obtain the release profile,
2. SEM image analysis – to observe the structural change of granule after dissolution,
3. Single particle (granule) dissolution – to examine the dissolution behaviour of a single granule in real time and
4. Focused Beam Reflectance Measurement (FBRM) – particle size analysis during dissolution.

Details of each method are provided in ***Chapter 3:*** *Material and Methodology* (***Sections 3.2.2.5.1 – 3.2.2.5.3***).

Table 5.1: Summary of "steady state" granules used for dissolution studies

Operating conditions			Dissolution properties			
Liquid level (%)	Impeller speed (rpm)	Wet massing time (min)	Dissolution testing	SEM	Single granule dissolution	FBRM
24	245	30	✓	✓	✓	✓
30	245	30	✓	✓		
24	490	30	✓	✓		
30	490	30	✓	✓	✓	✓

5.3 RESULTS

Dissolution rate of "steady state" granules was assessed quantitatively through dissolution testing. As illustrated in Figure 5.2, regular, spheroidal granules produced at higher liquid level of 30% possessed faster dissolution rate compared to irregular-shaped granules that formed from a cluster of smaller granules. Regular, spheroidal granules showed a burst release of Rhodamine B within the first 10 min of dissolution which later levelled off. More than 90% of Rhodamine B was released just after 15 min of dissolution time (DT). On the other hand, a slower and more gradual release was observed with irregular-shaped granules.

Both samples of regular, spheroidal granules that were produced at 30% LL but at different impeller speeds (245 rpm and 490 rpm) had comparable dissolution profiles. A slightly faster dissolution rate was shown by granules produced at 24% LL and higher impeller speed of 490 rpm compared to those at 245 rpm. The dissolution results differed from those reported by Ohno *et al.*'s (2007) where they found that the dissolution rate of tablets decreased as pore diameter of granules decreased with increasing liquid level and impeller speed. In this case, increasing liquid level and impeller speed have hastened the dissolution rate of "steady state" granules. Although the porosity of "steady state" granules was not characterized, they were expected to be less porous than conventional granules (Michaels *et al.* 2009) hence slower dissolution rate. However, the "steady state" granules have shown unexpectedly fast dissolution properties in this study and also in Michaels *et al.*'s work (2009) that raised our interest in understanding the behaviour of granules when interacting with a dissolution medium.

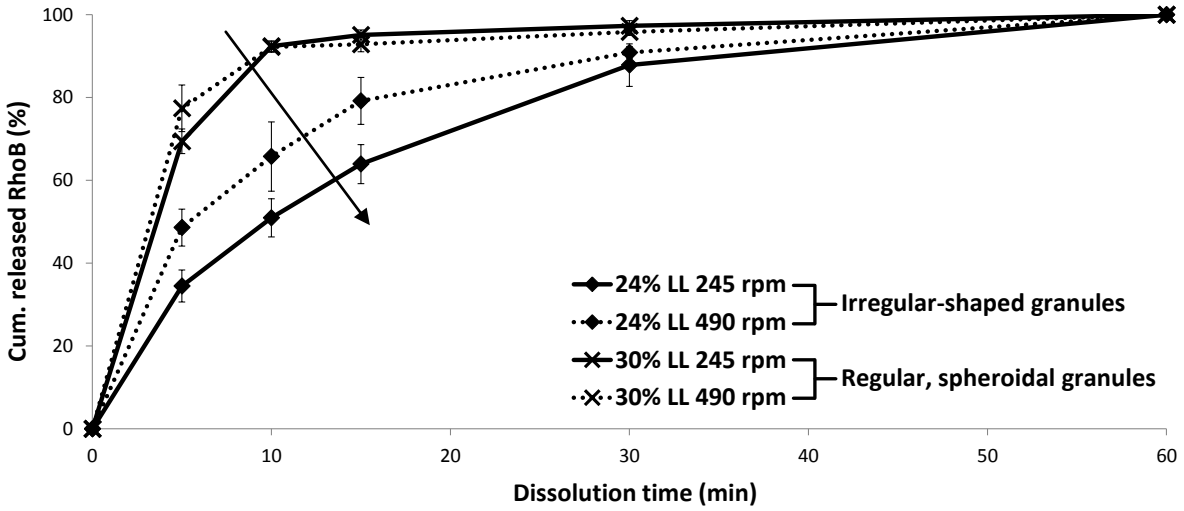

Figure 5.2: Dissolution profiles of "steady state" granules (180-355 µm) produced after 30 min of wet massing) obtained by monitoring the release of Rhodamine B over time.

It can be inferred from the dissolution testing that the microstructure attained by granules plays a major part in affecting the dissolution rate. The structural changes of "steady state" granules before and after dissolution were examined using SEM. "Steady state" granules appeared to be a polymeric matrix wrapping up all the other ingredients where embedded lactose particles were identified on the granule surface (see Figure 5.3a). Dissolution of "steady state" granules was discovered to occur by leaching where soluble components such as lactose and HPC, together with Rhodamine B leached out from the granules. As seen in Figure 5.3b, attached and/or embedded lactose particles on the granule surface would first dissolve and diffuse into the bulk dissolution medium. Cavities were formed by these dissolving components which allowed the penetration of dissolution medium into the inner structure of granule and facilitated the dissolution of entrapped model "drug" i.e. Rhodamine B. In a well-agitated dissolution bath, dissolved particles were carried away from the dissolution front through diffusion and convection.

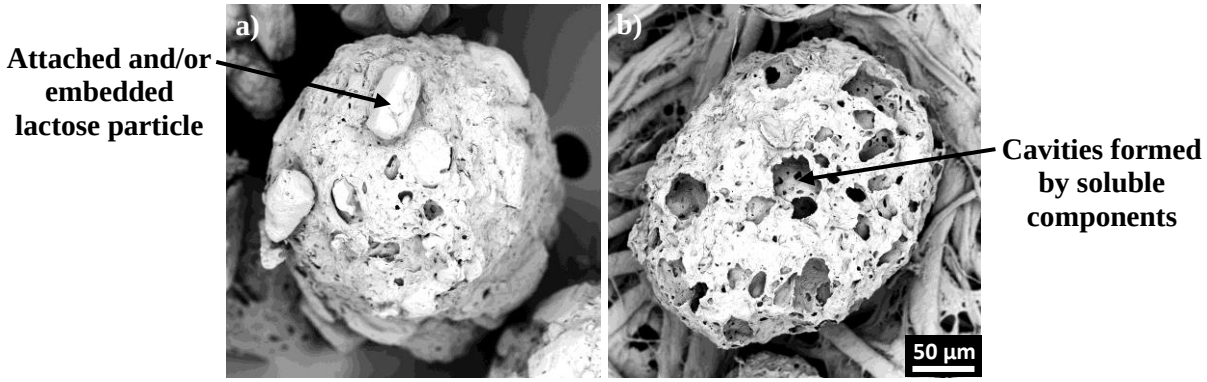

Figure 5.3: Soluble components leached out from "steady state" granules (30% LL and 490 rpm), leaving a matrix of insoluble components. a) 0 min DT and b) 5 min DT

As dissolution medium imbibed towards the core of granule, more Rhodamine B molecules were being released until the granule was completely saturated with dissolution medium. At the end of dissolution testing, a perforated and porous polymeric matrix of insoluble components was left behind (see Figure 5.4). The insoluble matrix remained intact and did not disintegrate throughout the dissolution testing. Hence it was discovered that "steady state" granules behaved similarly to the pellets produced by Kleinebudde (1997) when being dissolved (refer to Figure 3.3 in ***Chapter 3***). This rigid matrix was possibly formed as a result of autohesion of MCC polymer chains (Millili *et al.* 1990). Both regular, spheroidal and irregular-shaped granules had similar external structure after dissolution but irregular-shaped granules showed slower dissolution rate compared to regular, spheroidal ones.

To further investigate the difference in dissolution performance between regular, spheroidal and irregular-shaped granules, single particle dissolution was then carried out by immersing a granule in the dissolution bath to observe the dissolution behaviour in real time. This idea was adopted from a previous work where the dissolution kinetics of powders was studied using a single particle approach (Marabi *et al.* 2008). It was found that irregular-shaped granules first dissociated into smaller granules before leaching started whereas regular, spheroidal granules retained their structure and size throughout the dissolution testing (see Figure 5.5). Irregular-shaped granules were made up of a cluster of smaller granules that were loosely bonded to each other. Upon contact with aqueous form, these smaller granules would detach from each other. It would be expected that these granules show no sign of disintegration as the regular, spheroidal granules. On the other hand, no significant swelling or erosion was observed by regular, spheroidal granules given the long period of time immersed in dissolution medium.

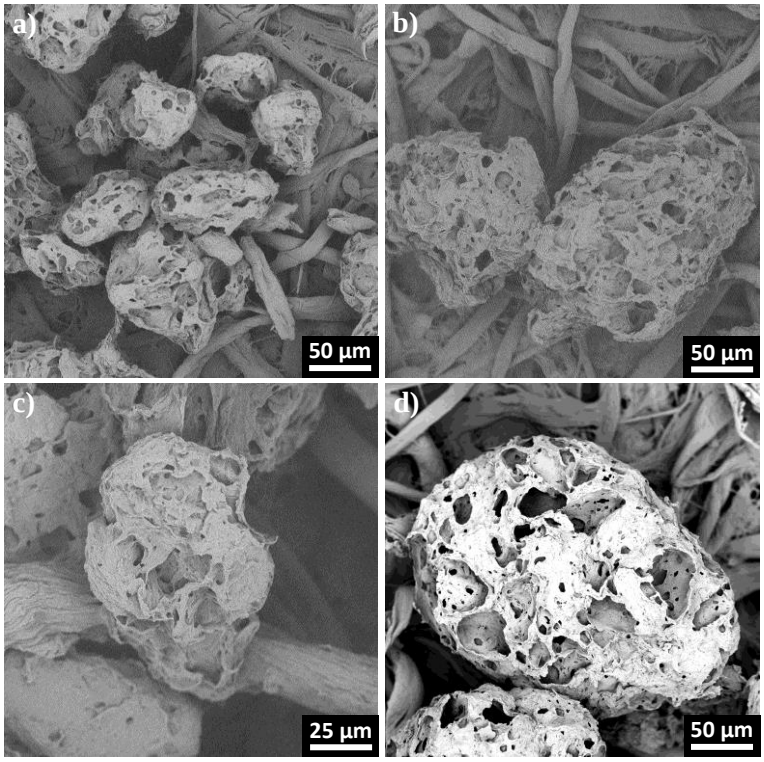

Figure 5.4: Morphology of "steady state" granules produced at a) 24% LL and 245 rpm, b) 30% LL and 245 rpm, c) 24% LL and 490 rpm and d) 30% LL and 490 rpm after 60 min of dissolution time.

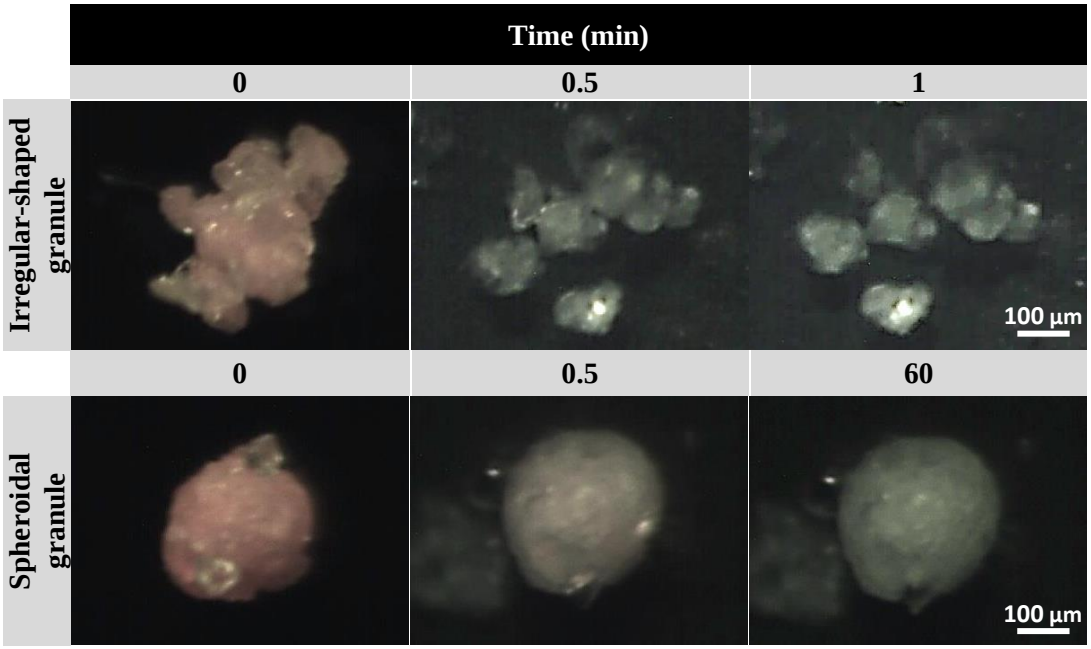

Figure 5.5: Single particle dissolution: 1. Irregular-shaped granules produced at 24% LL and 245 rpm and 2. Regular, spheroidal granules produced at 30% LL and 490 rpm

In order to verify the finding obtained from single particle dissolution, FBRM was used to detect the change in number of granule particle and size during dissolution testing. During the analysis, "steady state" granules were allowed to flow freely in a well-stirred dissolution bath rather than being placed in a granule holder. It is also worth mentioning that the chord length size distributions obtained by FBRM may not correspond directly to the granule size class (180-355 μm, obtained by mechanical sieving) used for the analysis.

Size distributions of the particles released during dissolution testing were distinctly different for regular, spheroidal granules and irregular-shaped granules as illustrated in Figure 5.6. Although data was collected continuously, only size distributions obtained at the start and end of testing are shown for clarity. Most of the irregular-shaped granules appeared at the smaller size range (< 300 μm) compared to that of regular, spheroidal granules. Given the same initial granule size distribution used for the analysis, this proved that irregular-shaped granules were made up of smaller granules adhering with each other and they underwent dissociation upon being immersed in dissolution medium. Furthermore, the dissolved granule size distribution did not vary significantly throughout the dissolution testing, indicating that the smaller granules did not disintegrate as well.

On the other hand, the initial size distribution of regular, spheroidal granules was at a larger size range (300 – 500 μm), consistent with the SEM images and granule size distributions in ***Chapter 4***. After 60 min DT, particles and/or fines of smaller sizes were detected, this could be possibly formed by collisions between flowing granules and surfaces that caused attrition. However, the larger granules were still present, showing that they did not undergo complete disintegration. The results have correlated well with the findings in single granule dissolution which showed that irregular-shaped granules dissociated into smaller granules upon contact with water while regular, spheroidal granules retained their structure after dissolution.

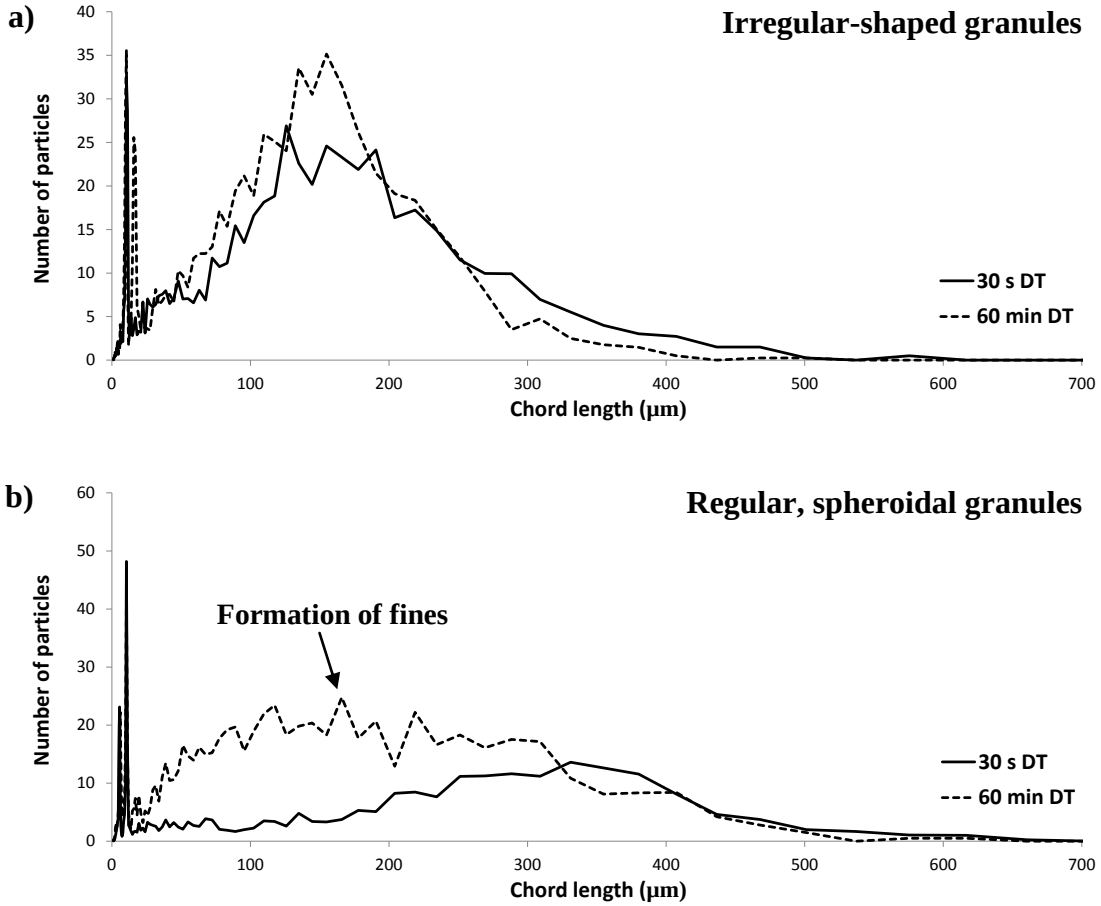

Figure 5.6: FBRM used to detect the change in number of particle during dissolution testing. a) Irregular-shaped granules (24% LL and 245 rpm) and b) Regular, spheroidal granules (30% LL and 490 rpm)

5.4 DISCUSSION

The main concern in adopting "steady state" granulation approach is over-consolidating granules in an extended period of time. This typically could cause depressed dissolution due to the less porous structure which is not desirable for rapid release formulations. Interestingly, "steady state" granules as a dosage form have presented good dissolution performance, comparable with the tablets compressed from "steady state" granules produced by Michaels *et al*. (2009) (see Figure 2.26 in ***Chapter 2:*** *Literature Review*).

Previous work on MCC-based pellets produced by extrusion/spheronization also found no signs of complete disintegration (Tho *et al.* 2003, Dukić-Ott *et al.* 2009, Wlosnewski *et al.* 2010). This is consistent with the conclusion drawn with granules from "steady state" granulation. Disintegration is an important aspect in breaking down a solid dosage form to

expose and release the entrapped drug. Although croscarmellose sodium (3 wt%) was incorporated in the formulation, its role in inducing disintegration was not fully demonstrated. This may be attributed to the loss of swelling potential of the disintegrant due to partial swelling during the liquid addition stage. In addition, the pressure exerted from the swelling of disintegrant becomes less effective against cavities created by the dissolving soluble components (Wlosnewski *et al.* 2010). This study used a freely soluble model "drug", Rhodamine B to study the dissolution performance of "steady state" granules. The lack of disintegration in these granules can be less desirable when a poorly soluble drug is to be delivered. The "burst" release shown by regular, spheroidal granules (see Figure 5.2) may compensate for this and achieve the same effect as disintegrating dosage form.

Leaching is the main release mechanism exhibited by "steady state" granules, in agreement with Kleinebudde's pellets (1997). Leaching is a heterogeneous reaction that occurs at a solid-liquid or solid-gas interface. It is common in hydrometallurgy processes and in the treatment and disposal of hazardous waste where solutes/metal ions are extracted from solid material (Baker *et al.* 1997, Safari *et al.* 2009). Physical factors that are found to influence leaching include particle size, homogeneity and porosity of solid matrix, flow rate of leachant etc. It is proposed that leaching of "steady state" granules can be generalized as diffusional release of a dissolved drug from a carrier matrix which takes place in several elementary steps (Baker *et al.* 1997):

i. Diffusion of dissolution medium to the solid-liquid interface
ii. Diffusion of dissolution medium into the solid matrices through the porous extracted region
iii. Adsorption of dissolution medium on the outer and inner surfaces of granules
iv. Solvation of soluble components
v. Desorption of solvated components from granules
vi. Diffusion of dissolved components through porous solid matrices to the interface then to the volume of dissolution medium

Regular, spheroidal granules and smaller granules that formed the irregular-shaped granules do not disintegrate when being dissolved in aqueous medium. It is suggested that the dissolution medium penetrates into the centre of granules as soluble components dissolve and diffuse away. Microscopic observation showed that the pink contour decreased in size over time, indicating a receding dissolution front (see Figure 5.7). For this phenomenon to occur, it

can be assumed that the soluble components were evenly distributed throughout the insoluble matrix and the dissolution occurred in the radial direction. A single granule from the size class of 355-500 µm was dissolved to obtain a clearer illustration of the recession. The granule highly resembled the regular, spheroidal granules of 180-355 µm which do not disintegrate throughout the dissolution process.

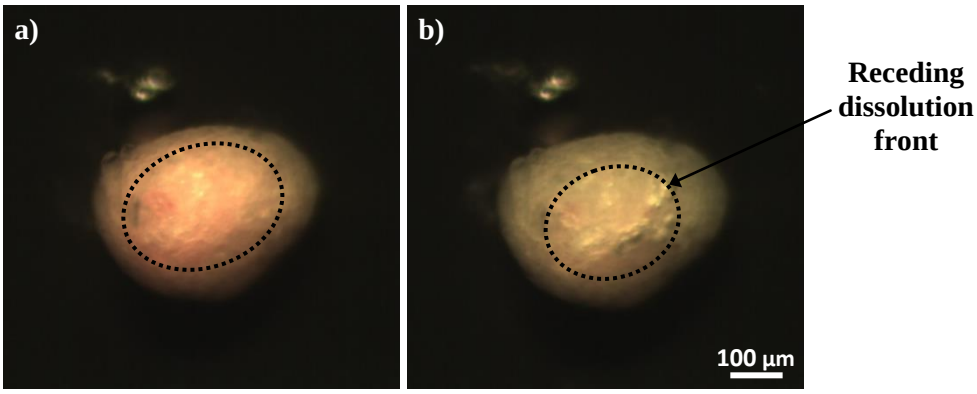

Figure 5.7: Single granule dissolution performed on a granule produced at 30% LL, 490 rpm and after 30 min of wet massing. a) 1 min DT and b) 3 min DT

Although "steady state" granules are relatively dense, they are still considered to be porous matrix structures. As soluble components dissolve, matrix porosity increases, affecting the rate of drug release to a large extent. Therefore, the rate of penetration of dissolution medium is highly dependent on the formation of cavities which is determined by the amount of soluble components i.e. lactose used in the formulation. Once the soluble components dissolve and start to diffuse, more surface contact and passages are created where the dissolution medium can penetrate further into the core.

The leaching mechanism of "steady state" granules can be best described by the shrinking core model where the core of a particle shrinks while the particle size remains constant due to the insoluble matrix of MCC. The unaffected core and extracted region is separated by a moving dissolution front which moves towards the unaffected core, creating more extracted region due to continuous drug dissolution and release (see Figure 5.6).

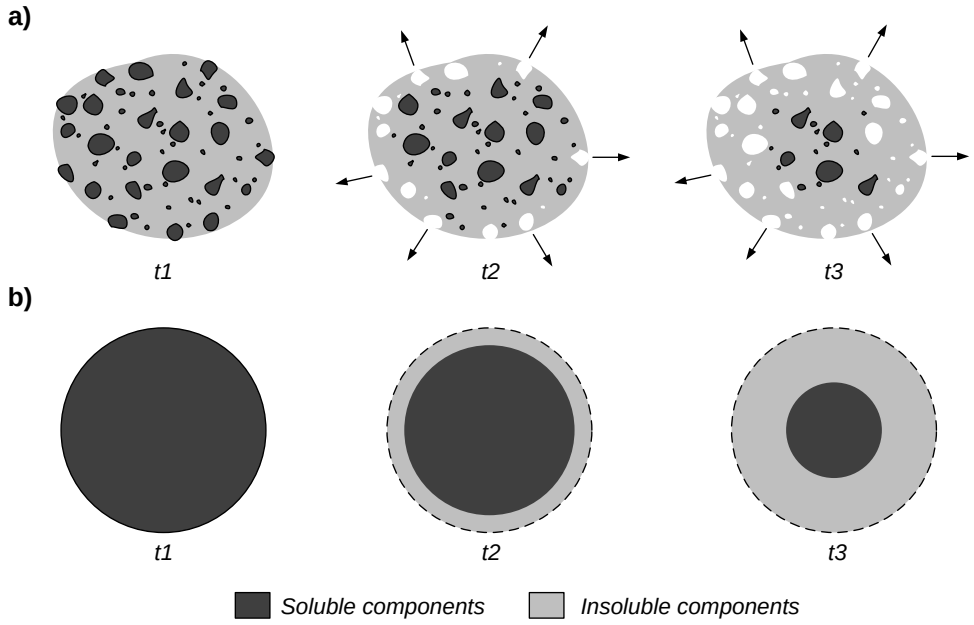

Figure 5.8: a) Leaching mechanism occurs during dissolution of "steady state" granules b) Shrinking core model proposed to describe the leaching mechanism (where t3>t2>t1)

The smaller granules that formed the irregular-shaped granules dissolved much more slowly than the regular, spheroidal granules, which raises questions. Usually, smaller particles have higher surface area which is expected to enhance dissolution. The roles that other ingredients i.e. lactose and croscarmellose sodium play in contributing to the dissolution behaviour of "steady state" granules are known but provide no insight as to why the above-mentioned phenomenon occurred. Therefore it all comes down to the microstructure of the insoluble MCC matrix. As discussed in ***Chapter 4***, MCC has exhibited extraordinary transformations in terms of shape and structure which reflect directly to the operating conditions being employed at time.

It was reported that the pore volume of MCC primary particles decreased after wet granulation (Badawy *et al.* 2006). The reduction in space between the cellulose fibres can be attributed to the shrinking phenomenon occurs during drying. MCC-based pellets have shown significant shrinkage when being dried in an oven, which causes them to reduce in size and densify (Kleinebudde 1994, Wlosnewski *et al.* 2010). The shrinking process was found to be well-explained by the mechanisms involved in autohesion (refer to ***Section 3.1.2.1*** in ***Chapter 3***). The evaporation of liquid binder from the swollen microcavities creates a capillary pressure that allows the intermingling polymer chains to collapse hence the smooth

surfaces seen on "steady state" granules. As a result, the existing pores within primary MCC particles that are available for diffusion of dissolved particles may be disappeared.

Kleinebudde (1997) concluded that the shrinking phenomenon was not completely reversible after observing the swelling of oven-dried pellets upon contact with water again. Microscopic observation showed that swelling was not observed on "steady state" granules or the amount of MCC used was insufficient to cause a significant increase in size. However, even swelling at a micro-scale can affect both the surface and internal structures, which ultimately controls the dissolution rate. Swelling of polymeric material helps in generating more surface contact with dissolution medium in solid dosage forms. Furthermore, an increase in pore size due to swelling was also observed in cellulose beads made of MCC (Ek *et al.* 1995). Although the actual dissolution performance of these beads was not investigated, it would be expected that this resulting effect of swelling will facilitate the penetration rate of dissolution medium.

The degree of swelling by MCC particles was expected to be lower when a lower liquid level i.e. 24% was delivered. Microcavities that were formed through the expansion of cellulose fibres were less and the degree of autohesion was not highly enhanced, which was reflected on the irregular-shape of granules. When these granules come in contact with water again, the MCC matrix may still have the capacity to swell. As previously proposed that the dissolution of "steady state" granules highly follows the shrinking core model, the unaffected region would recede towards the core over time. When the dissolution medium reaches a fresh layer, swelling of MCC or croscarmellose sodium can retard the medium from penetrating further as pores may be blocked and diffusion path becomes longer. Although internal swelling could not be observed in this case, it might be the main reason why granules produced at 24% LL showed a slower dissolution rate. At the same liquid level, a higher impeller speed would significantly enhance the intermingling of polymer chains due to increase in compaction force, resulting in a more compacted structure that might lose the swelling potential. Therefore, granules produced at 24% LL and 490 rpm dissolved faster than that at 245 rpm (see Figure 5.1).

On the other hand, MCC particles granulated with 30% LL would swell to a larger extent compared to those at 24% LL during the liquid addition stage. After wet granulation and being dried, the polymeric matrix that created by the establishment of strong stable links might possess very little swelling capacity which would avoid potential blockage of pores and obstruction to diffusion. Hence the dissolution rate became dependent on the cavities

formed by dissolved lactose particles. In addition, the internal structure of regular, spheroidal granules has high surface area that facilitates the solvation of Rhodamine B (see Figure 4.9 in ***Chapter 4***).

The formation of cavities by dissolved lactose particles was found to be a crucial factor in the dissolution performance of regular, spheroidal granules. It is proposed that the dissolution rate can be controlled by varying the composition of soluble component (lactose) and insoluble component (MCC), which will be discussed in ***Chapter 6***: *Effect of Varying Formulation Composition on Granule Properties and Dissolution Profile.*

5.5 CONCLUSIONS

Investigations into the dissolution performance of "steady state" granules have shown that the release mechanism attained by these granules is leaching where soluble components dissolve and create cavities that allow the penetration of dissolution medium into the internal structure and facilitate the dissolution of entrapped model "drug". Once all the soluble components have been dissolved, a perforated and porous polymeric matrix is formed which does not disintegrate over the dissolution period.

Dissolution rate of "steady state" granules was found to be dependent on the microstructure of the granule itself. Although regular, spheroidal granules appear to be a dense solid mass, they showed relatively faster dissolution rate compared to irregular-shaped granules. The phenomenon can be attributed to the high surface area available in the inner structure, created by the disappearance of soluble component and existing voids. On the other hand, irregular-shaped granules exhibited slower dissolution rate due to potential swelling that can cause pores to be blocked and diffusion path to be obstructed. The mechanical properties of wet agglomerates were believed to have changed to a certain extent due to long exposure of shearing and compaction.

In conclusion, granule dosage form produced using the "steady state" granulation approach has shown good dissolution performance despite the less porous structure produced by extended wet massing. This important characteristic allows "steady state" granules to be applied as a drug carrier for immediate release.

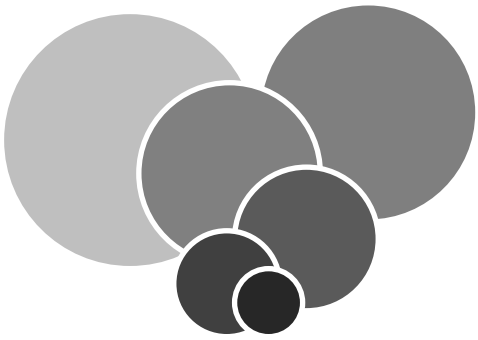

CHAPTER SIX

EFFECT OF VARYYING FORMULATION COMPOSITION ON GRANULE PROPERTIES AND DISSOLUTION PROFILE

6 EFFECT OF VARYING FORMULATION COMPOSITION ON GRANULE PROPERTIES AND DISSOLUTION PROFILE

6.1 INTRODUCTION

It has been determined in ***Chapter 5:*** *Dissolution Performance of "Steady State" Granules* that the geometrical shape and microstructure of "steady state" granules is highly dependent on the operating parameters and is the main factor affecting the dissolution performance. The dissolution profile of "steady state" granules can be regarded as immediate release as illustrated in Figure 5.1, comparing to Figure 2.22 in ***Chapter 2:*** *Literature Review*. The goal of the following chapter is to fine-tune and manipulate the rate of release by varying the formulation composition.

The release rate of a dosage form is influenced by the mechanisms that are determined by the design of formulation. The two main ingredients in the formulation used in this project are lactose (soluble) and microcrystalline cellulose, MCC (insoluble). Granulating these excipients using the "steady state" granulation approach creates a granule dosage form where leaching is the main release mechanism. MCC forms an insoluble polymeric matrix with a porous network that carries the drug whereas the lactose dissolves to create cavities for the penetration of dissolution medium and also interfacial solid/liquid area for solvation of drug.

It is a common practice to obtain the optimal excipients ratio by investigating how the formulation composition affect the dissolution rate (am Ende 2011). The interesting dissolution properties of "steady state" granules have raised the idea of varying the composition of lactose and MCC in attempt to control the rate of release. It is hypothesized that decreasing the amount of lactose will reduce the number of cavities created by the dissolved lactose across the matrix. This will retard the penetration of dissolution medium into "steady state" granules and achieve a slower rate of release (see Figure 6.1).

Apart from the dissolution performance, varying the composition of formulation will also affect other granule properties such as size distribution, morphology, circularity and bulk densities which will also be examined. Finally, a granulation batch where lactose is replaced with mannitol will be produced and investigated, as part of the long term goal of using "steady state" granules for paediatric formulations.

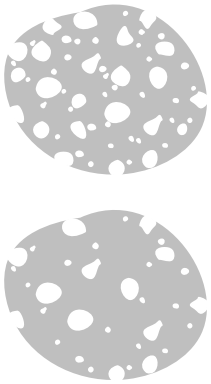

↓ Amount of lactose
↓ Formation of cavities
↓ Internal surface area for dissolution
↓ Penetration rate of dissolution medium
→ ***Slower dissolution rate***

Figure 6.1: Potential effects of varying the composition of formulation on the dissolution rate of "steady state" granules.

6.2 EXPERIMENTAL

To investigate the effect of formulation on the properties of "steady state" granule dosage form, the compositions of lactose (x wt%) and MCC (y wt%) were varied where $x + y = 94\ wt\%$ and the compositions of other ingredients, HPC (3 wt%) and croscarmellose sodium (3 wt%) remained constant. "Steady state" granules (74 wt% lactose and 30 wt% MCC) produced at 30% LL, 490 rpm and after 30 min of wet massing were chosen to be the reference as these granules appeared to attain the desirable properties: narrow size distribution, most spherical, smooth surfaces and possessed the fastest dissolution rate. It is of interest to control the dissolution rate of these regular, spheroidal granules by varying the ratio of lactose to MCC in the formulation and at the same time, maintaining the other positive attributes.

The experiments were further divided into two parts: 1. Varying composition of formulation with constant liquid level and 2. Varying liquid level at different compositions of formulation to maintain a constant particle size (refer to Table 6.1). Since MCC has higher affinity for water, reducing the ratio of lactose to MCC with the same liquid level will affect the liquid saturation in the system. The variation in formulation will reflect on the final granules. In this case, an increase in the amount of MCC will require higher liquid level to achieve the same granule size and the same degree of autohesion and produce granules that are comparable with the reference granules mentioned before in all aspects but with fine-tuned dissolution rate. These granules were analysed for the five main properties (size distribution,

morphology, circularity, bulk densities and dissolution performance). Full details of each characterization method can be found in ***Chapter 3:*** *Material and Methodology.*

In the final part of the project, a case study was carried out to produce a granule dosage form using a paediatric formulation. The soluble component i.e. lactose was substituted with mannitol. Lactose and mannitol have distinct physical characteristics and pharmaceutical functions (refer to ***Chapter 3***). Lactose is a common pharmaceutical excipient which used as filler in solid dosage forms. Incorporation of lactose in paediatric formulation raises the concern of lactose intolerance in some children. Hence mannitol is used instead to provide a sweet taste, good 'mouth feel' and cooling sensation.

Only one composition of the mannitol-MCC formulation was tested to investigate the effect of material on the microstructure of granule hence the dissolution performance. It is of interest to find out whether the porous MCC structure after dissolution, observed in ***Chapter 5*** will be formed when a different soluble component is used. The dissolution testing method was described in detail in ***Section 3.2.2.5*** in ***Chapter 3***.

Table 6.1: Summary of formulations being tested and the corresponding liquid level being applied.

Formulation composition	Lactose (wt %)	MCC (wt %)	Mannitol (wt %)	Liquid level (%)
1	74	20	-	30.0
2	69	25	-	30.0
	69	25	-	32.5
	69	25	-	35.0
3	64	30	-	30.0
	64	30	-	35.0
	64	30	-	40.0
4	59	35	-	30.0
5	-	20	74	30.0

6.3 RESULTS

6.3.1 GRANULE SIZE DISTRIBUTION AS A FUNCTION OF FORMULATION

As the amount of MCC in the formulation increased while the liquid level was maintained at 30% LL, a gradual shift in the granule size distribution towards the smaller size range occurred (see Figure 6.2). In order to ensure that the dissolution rate is independent of the granule size and shape but solely dependent on the variation of formulation, the liquid level

was adjusted to match the initial target size range of granules with 74 wt% lactose and 20 wt% MCC. Initial attempts of increasing the liquid level to 35% for formulation with 25 wt% MCC and 40% for formulation with 30 wt% MCC produced granules of larger sizes. These two liquid levels became the upper limits of the amount of liquid required for both the formulations. The desired liquid level was then predicted by simply comparing the size distributions with the target range (shown in red solid line, see Figure 6.3) and granules of different formulations were successfully tuned to have similar size distributions. This proved that the "steady state" granulation approach could offer a good control over granule sizes. Furthermore, varying the formulation composition did not affect the establishment of "steady state" condition towards the end of the wet massing period (refer to ***Appendix A***).

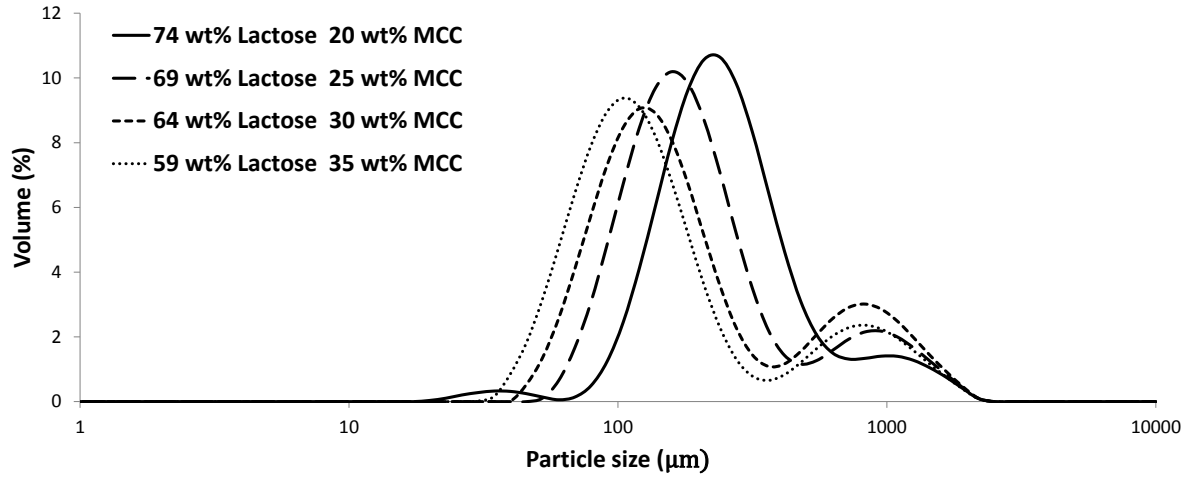

Figure 6.2: Size distributions of "steady state" granules with increasing amount of MCC in formulation, produced at 30% LL and 490 rpm.

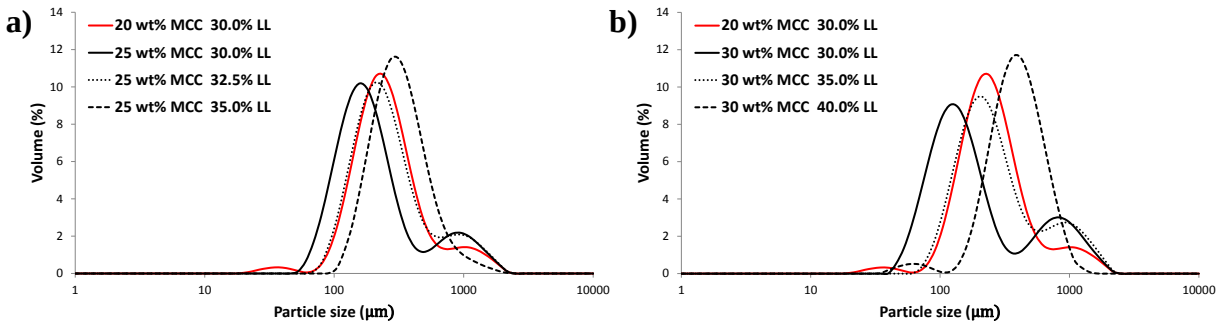

Figure 6.3: Adjustment of liquid level to achieve similar size distribution (74 wt% lactose and 20 wt% MCC). a) 69 wt% lactose and 25 wt% MCC and b) 64 wt% lactose and 30 wt% MCC

6.3.2 GRANULE MORPHOLOGY, CIRCULARITY AND BULK DENSITIES AS A FUNCTION OF FORMULATION

Apart from the size distribution of "steady state" granules, the effect of formulation on other granule properties such as morphology, circularity and bulk densities were also investigated. When the amount of MCC increased from 20 wt% to 35 wt% but maintaining the same liquid level of 30%, the circularity of "steady state" granules decreased gradually from 0.648 ± 0.151 to 0.510 ± 0.148 (see Figure 6.4a). The liquid level was no longer sufficient to promote autohesion in granules with higher MCC content (25-35 wt%) to the same extent as granules with 20 wt% MCC. An increase in granule circularity was observed when the liquid level was increased for both the formulations (see Figure 6.4b). With higher amount of MCC in the formulation, a larger amount of liquid was required to achieve the same extent of deformability and produce spherical granules. All the granules of different formulation compositions appeared to be considerably round and smooth (see Figure 6.5).

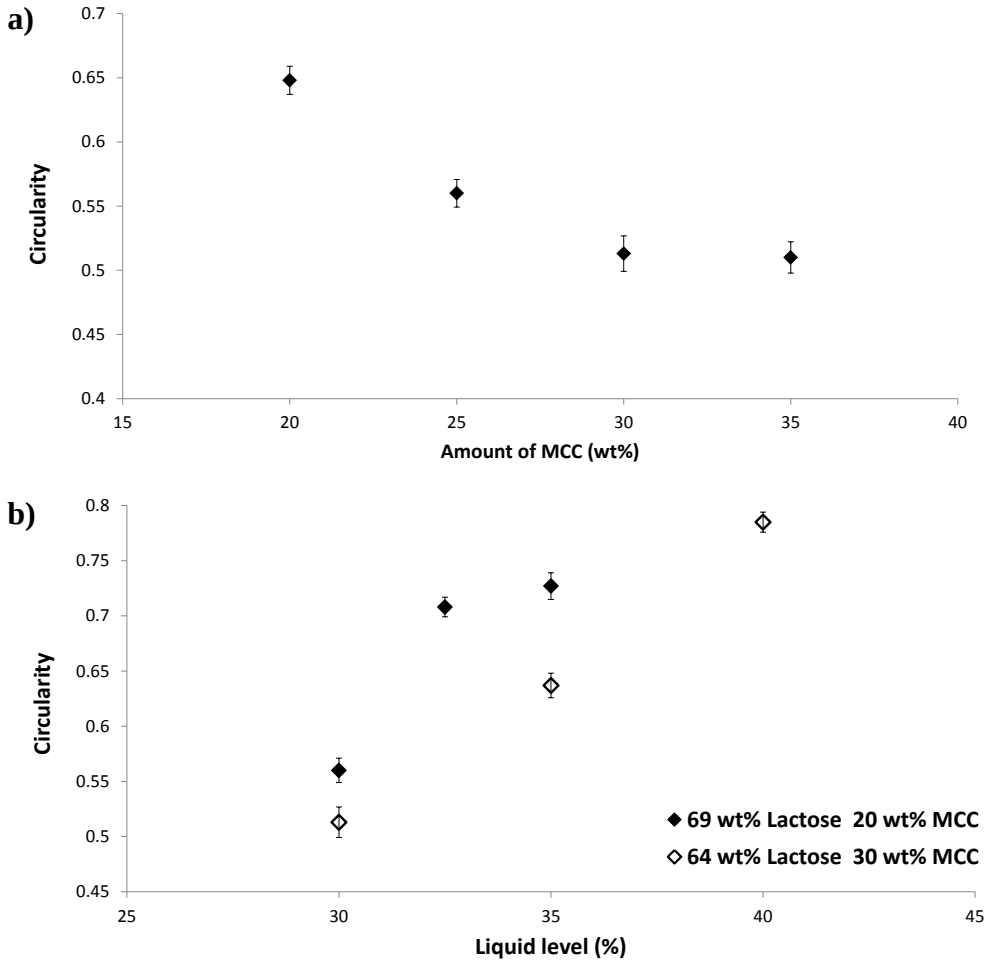

Figure 6.4: a) Effect of formulation on the circularity of granules at 30% LL and 490 rpm. b) Effect of liquid level on the circularity of granules of different formulations.

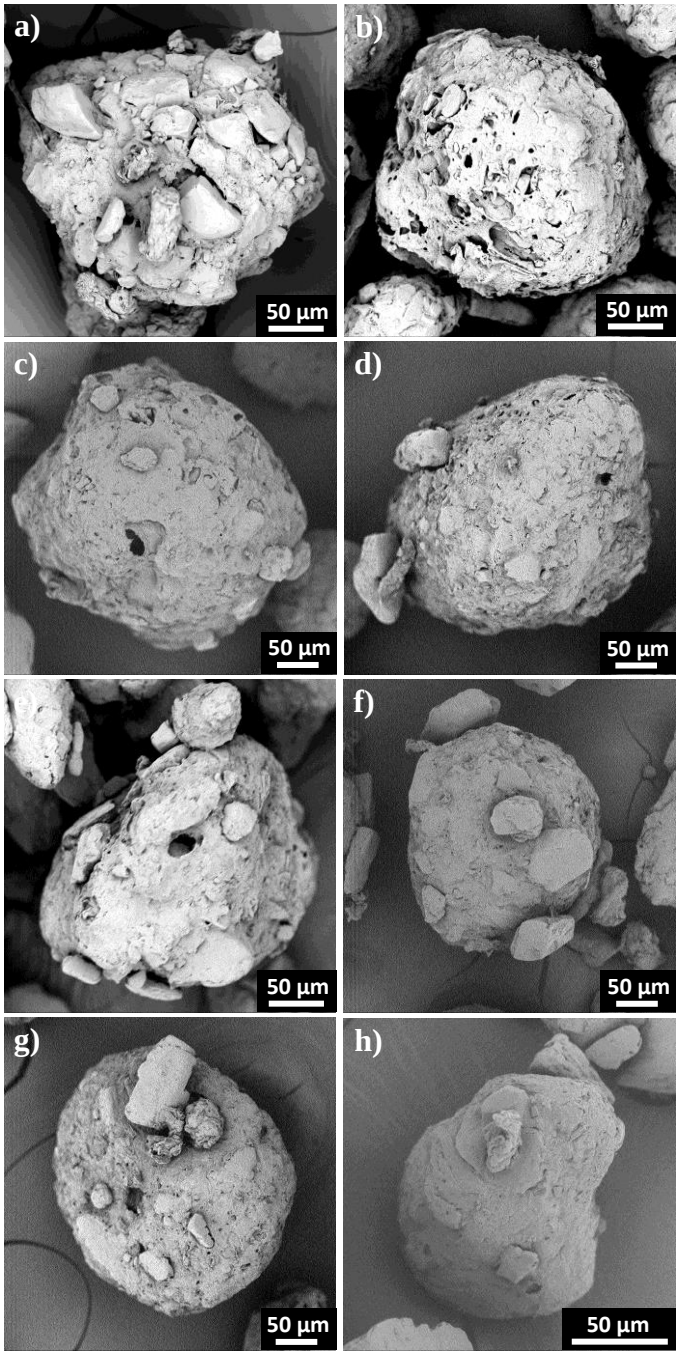

Figure 6.5: Morphology of granules produced at 490 rpm and after 30 min WMT. a) 74 wt% Lactose 20 wt% MCC – 30.0% LL, b) 69 wt% Lactose 25 wt% MCC – 30.0% LL, c) 69 wt% Lactose 25 wt% MCC – 32.5% LL, d) 69 wt% Lactose 25 wt% MCC – 35.0% LL, e) 64 wt% Lactose 30 wt% MCC – 30.0% LL, f) 64 wt% Lactose 30 wt% MCC – 35.0% LL, g) 64 wt% Lactose 30 wt% MCC – 40.0% LL, h) 59 wt% Lactose 35 wt% MCC – 30.0% LL

Increasing the amount of MCC also decreased both the poured and tapped densities of "steady state" granules when the same amount of liquid was used (see Figure 6.5a). Consolidation of granules was not enhanced when more MCC was incorporated in the formulation. A possible explanation is that MCC absorbed the water molecules upon liquid delivery and swelled, leaving a lower amount of liquid binder available for the formation of granules. This would decrease the liquid saturation of agglomerates, leading to less effective consolidation. On the other hand, increasing the liquid level increased both the poured and tapped densities of granules with higher MCC content.

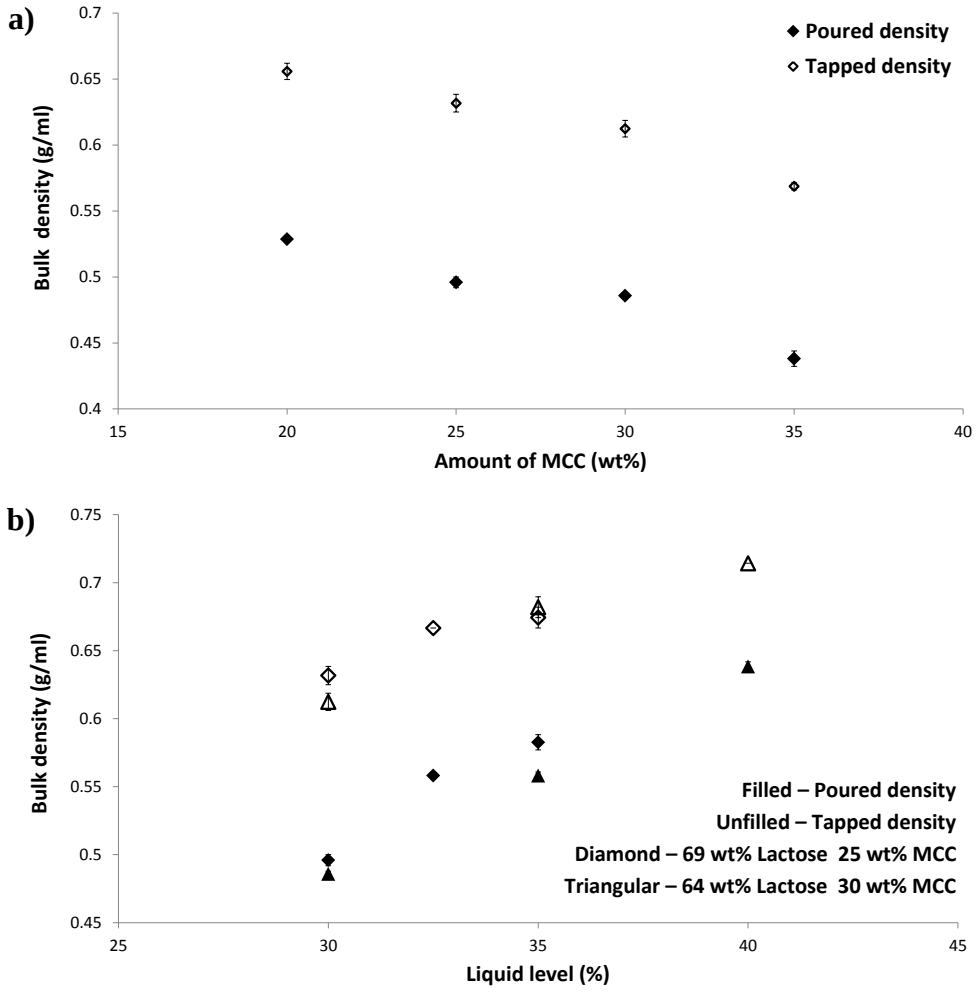

Figure 6.6: a) Effect of formulation on the poured density and tapped density of granules at 30% LL and 490 rpm. b) Effect of liquid level on the poured density and tapped density of granules of different formulations.

The effect of formulation on Hausner ratio of "steady state" granules showed the same trends as those observed in circularity and bulk density. At the same liquid level, the Hausner ratio increased when the composition of MCC increased, indicating a decrease in the flowability of granules which also supported by the result of granule circularity. A decrease in granule circularity will cause the flowability of granule to decrease as well. As liquid level increased, the Hausner ratio of granules with 25-30 wt% MCC reduced significantly where flowability of granule had improved. Results obtained in the characterization of granule circularity and bulk densities were in good agreement. Furthermore, the granules produced from different formulation compositions but with similar size distribution appeared to have comparable circularity, bulk densities and Hausner ratio (refer to Table 6.2). This also showed that with "steady state" granulation, the granule properties can be tailored easily according to the composition given by just varying the liquid level.

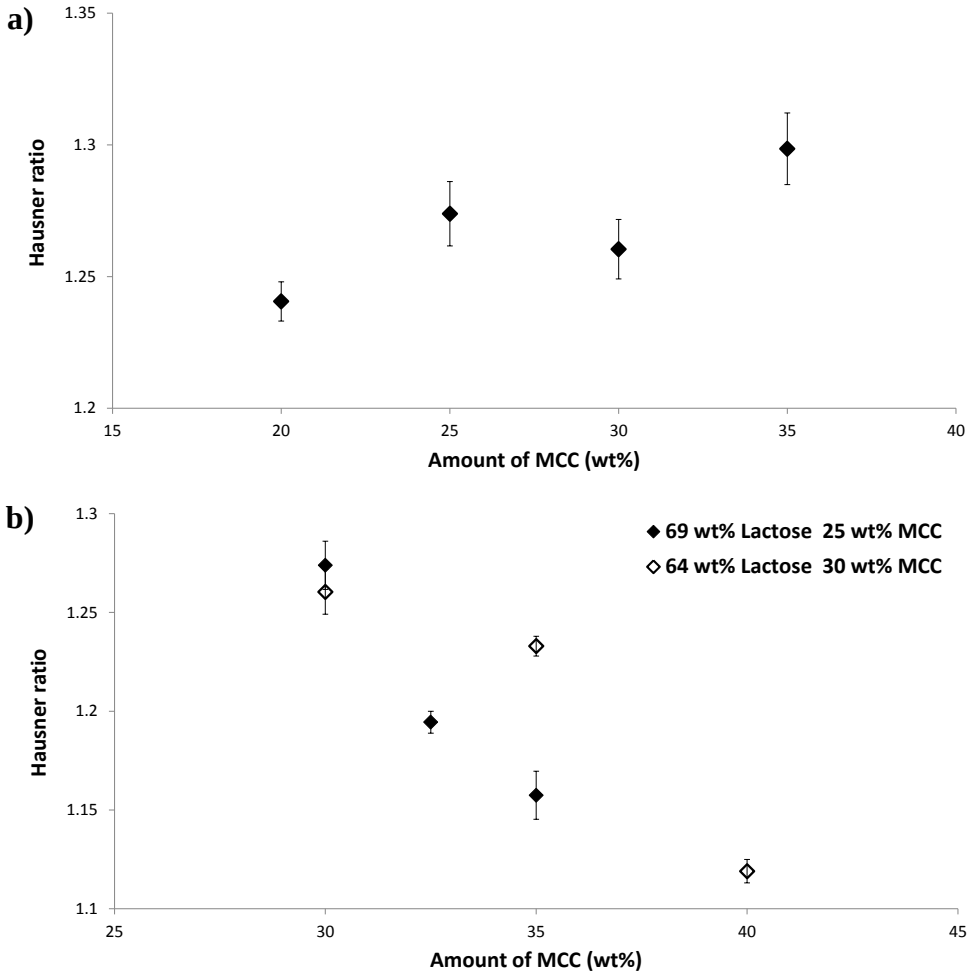

Figure 6.7: a) Effect of formulation on the Hausner ratio at 30% LL and 490 rpm. b) Effect of liquid level on the Hausner ratio of granules of different formulations.

Table 6.2: Summary of granules properties at varying formulation compositions but similar size distributions

Lactose (wt %)	MCC (wt %)	LL (%)	Circularity (-)	Poured density (g/ml)	Tapped density (g/ml)	Hausner ratio (-)
74	20	30.0	0.648 ± 0.151	0.529 ± 0.004	0.656 ± 0.011	1.240 ± 0.013
69	25	32.5	0.708 ± 0.125	0.558 ± 0.005	0.667 ± 0.000	1.194 ± 0.010
64	30	35.0	0.637 ± 0.162	0.553 ± 0.012	0.682 ± 0.013	1.233 ± 0.009

6.3.3 EFFECT OF FORMULATION ON THE DISSOLUTION PERFORMANCE OF "STEADY STATE" GRANULES

Dissolution rate of "steady state" granules has been successfully fine-tuned by varying the compositions of lactose and MCC as shown in Figure 6.7. As the amount of lactose incorporated in the formulation decreased from 74 wt% to 59 wt%, the dissolution rate slowed down significantly where the amount of Rhodamine B released in the first five min of dissolution time reduced from 77% to 44%. Approximately 95% of the Rhodamine B entrapped in the granules was released after 30 min of dissolution time for all four formulations. Varying the compositions of the two main ingredients successfully adjusted the release rate of the dosage form within the first 30 min window. This phenomenon can be attributed to the reduction in the cavities available throughout the granule for the penetration of dissolution medium and/or the decrease in dissolution area available in the polymeric matrix for the solvation of Rhodamine B.

SEM images of "steady state" granules after dissolution testing showed that the formation of cavities was reduced significantly and the non-disintegrating polymeric matrix appeared to be less porous when the amount of lactose was decreased (see Figure 6.8). A denser and less crinkly structure was observed as more MCC was used, possibly due to an increase in the layering of polymer chains.

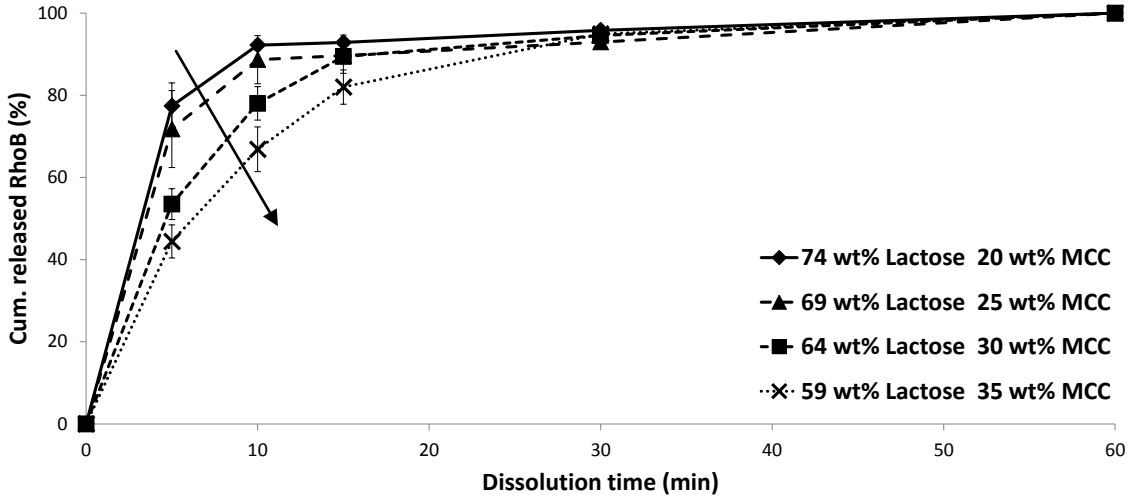

Figure 6.8: Dissolution profiles of "steady state" granules with increasing amount of MCC in formulation, produced at 30% LL and 490 rpm.

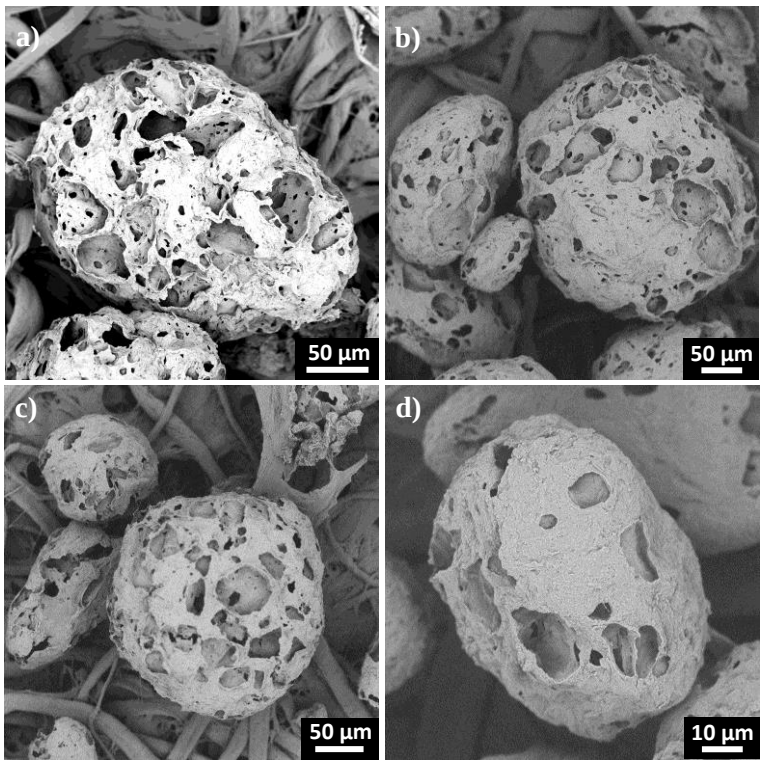

Figure 6.9: Morphology of "steady state" granules: a) 74 wt% lactose and 20 wt% MCC, b) 69 wt% lactose and 25 wt% MCC, c) 64 wt% lactose and 30 wt% MCC and d) 59 wt% lactose and 35 wt% MCC after 60 min of dissolution time.

Dissolution profiles of specifically formulated "steady state" granules (64-74 wt% lactose and 20-30 wt% MCC) with similar size distributions were compared. As illustrated in Figure 6.9, decreasing the amount of lactose in the formulation slowed down the dissolution rate of the dosage form. The result supported the hypothesis of varying the composition of formulation to achieve controlled release of "steady state" granules. Given two batches of granule dosage form of the same size, the batch with lower MCC content is expected to achieve a faster release rate compared to the other with higher MCC content. Increasing the MCC content actually increases the tortuosity of the granule which will prolong the diffusion process as dissolved molecules have to diffuse through a longer path across the porous layer.

Comparing the dissolution profiles of "steady state" granules (25-30 wt% MCC) in Figure 6.9 with those in Figure 6.7, the profiles appeared to be reproducible, indicating that the main factor determining the release rate is the compositions of the formulation. SEM images of granules after dissolution testing as illustrated in Figure 6.10 also showed a decrease in the formation of cavities on the granule surface as less lactose particles were present.

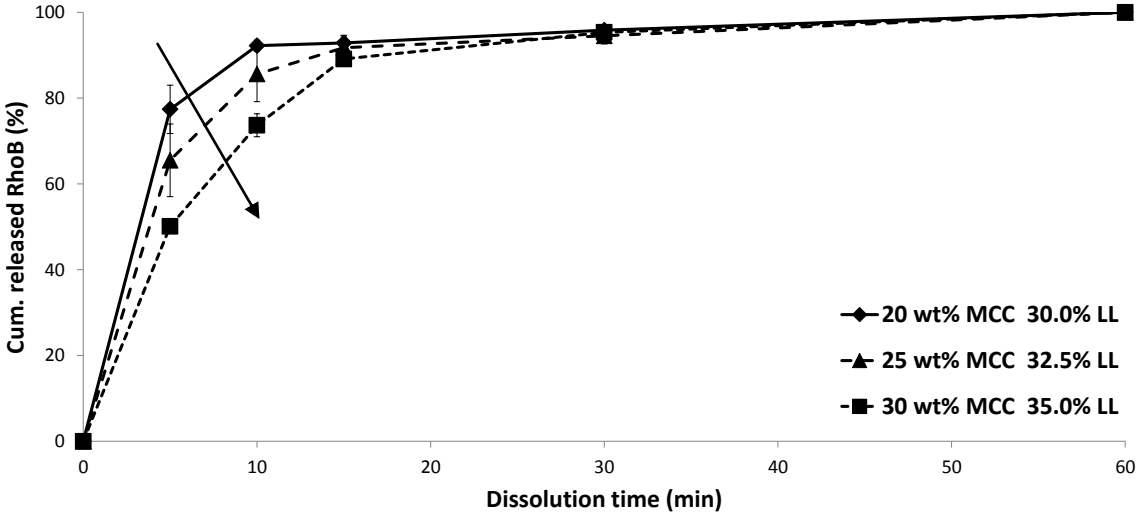

Figure 6.10: Dissolution profiles of "steady state" granules with increasing amount of MCC in formulation and of similar size distributions by adjusting the liquid level.

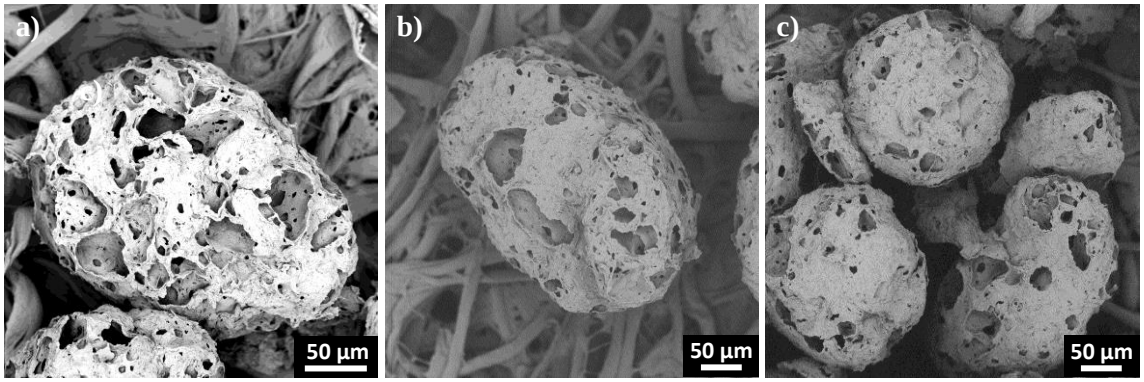

Figure 6.11: Morphology of "steady state" granules: a) 74 wt% lactose and 20 wt% (30% LL) MCC, b) 69 wt% lactose and 25 wt% MCC (32.5% LL) and c) 64 wt% lactose and 30 wt% MCC (35% LL) after 60 min of dissolution time.

Furthermore, the effect of liquid level on the dissolution rate of "steady state" granules with increasing MCC content was investigated (see Figure 6.11). There was a slight increase in the dissolution rate of granules that contained 25 wt% MCC in the first five min of dissolution testing when the liquid level applied increased. However, the dissolution profiles were highly comparable, suggesting that these granules attain similar microstructure regardless of the liquid level as the formulation used was the same. On the other hand, granules that contained 30 wt% MCC and produced at 40% LL showed a faster dissolution rate compared to those at lower liquid levels. A possible explanation is that larger granules formed at such high liquid level contain more lactose particles hence more voids will be created upon dissolution.

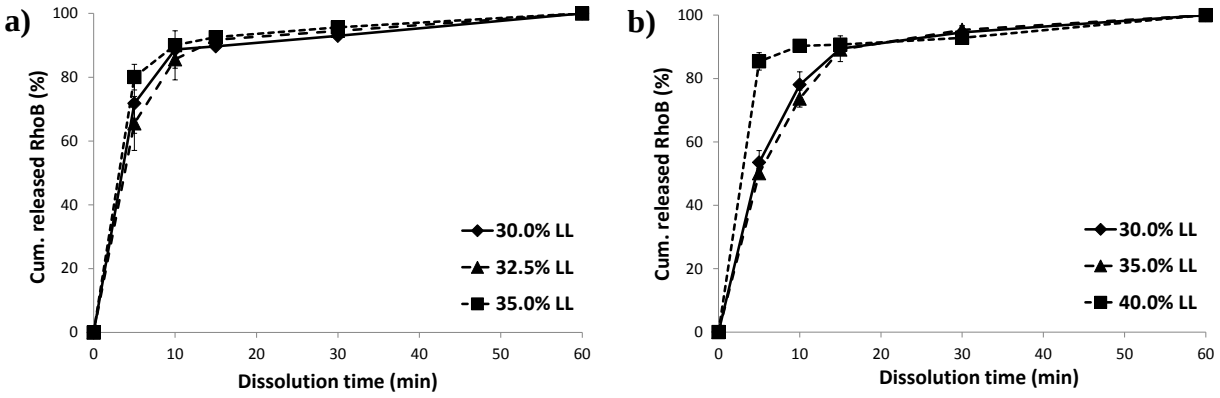

Figure 6.12: Dissolution profiles of "steady state" granules of different formulations: a) 69 wt% lactose and 25 wt% MCC and b) 64 wt% lactose and 30 wt% MCC

6.3.4 CASE STUDY: MANNITOL-MCC FORMULATION

A granulation batch with 74 wt% mannitol and 20 wt% MCC was produced at 30% LL and 490 rpm to study the potential of "steady state" granulation in creating paediatric granules. At 0 min WMT, the granule size distribution appeared to be bimodal which later became unimodal (see Figure 6.13). Granules produced from both mannitol-MCC formulation and lactose-MCC formulation showed comparable size distributions at the same operating conditions. Although "steady state" condition was achieved in the end of wet massing period, a broader size distribution was observed with mannitol-MCC formulation compared to that of lactose-MCC formulation (see Figure 6.14).

Although mannitol and lactose possess similar solubility, mannitol was reported to be non-hygroscopic and electrically charged (Juppo *et al.* 1992). Due to the poorer wettability, wet agglomerates containing crystalline form mannitol might not exhibit sufficient plastic deformability. This explained why more fines were formed towards the end of wet massing period, possibly due to the excessive breakage of these brittle-natured granules induced by intense shearing. On the other hand, granule growth would also be restricted hence the less narrow size distribution, Juppo *et al.* (1992) also observed a similar trend.

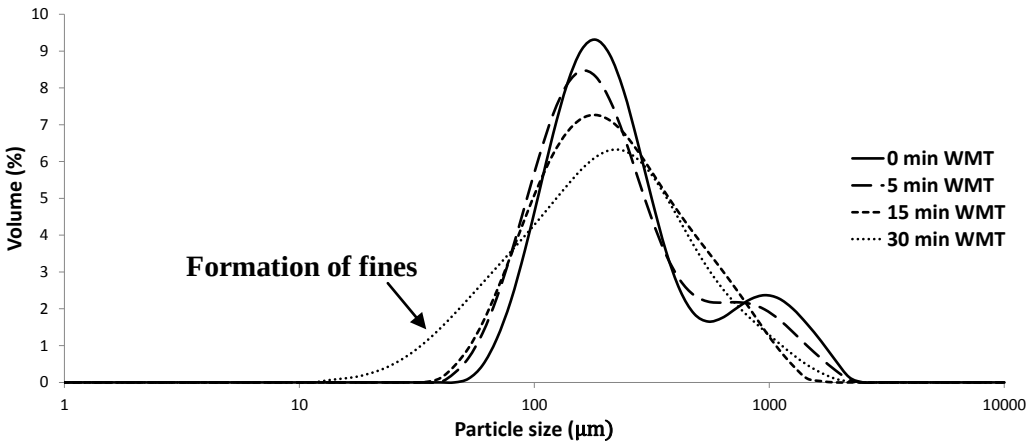

42290Figure 6.13: Size distributions of mannitol-MCC formulated granules produced at 30% LL, 490 rpm and 0-30 min wet massing.

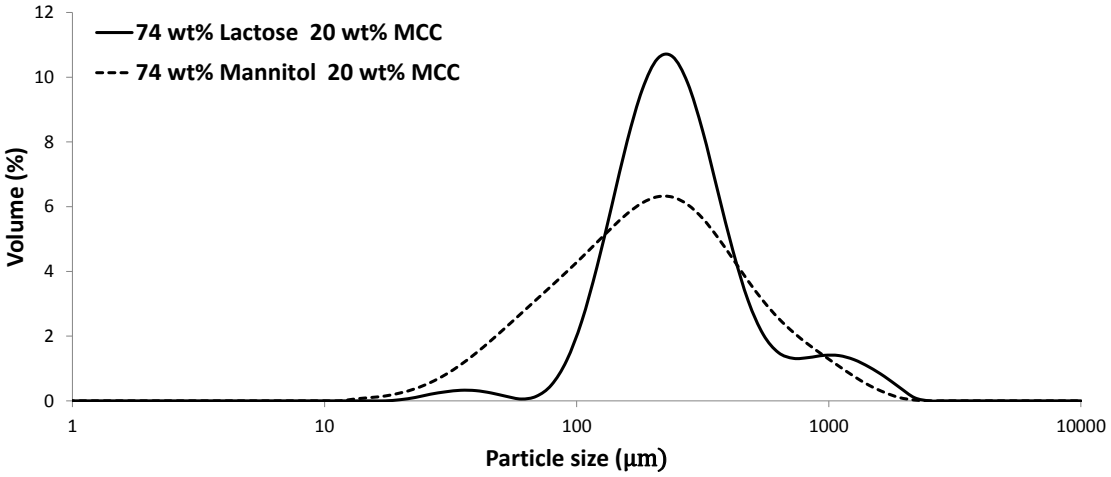

Figure 6.14: Granule size distributions produced using a lactose-MCC formulation and a mannitol-MCC formulation at 30% LL and 490 rpm.

In terms of other properties, mannitol-MCC formulated granules appeared to be more spherical and denser than lactose-MCC formulated granules (see Table 6.3). Unlike lactose-MCC formulated granules with discrete lactose particles attached on the surfaces, mannitol-MCC formulated granules showed considerably flat smooth surfaces (see Figure 4.8d in ***Chapter 4:*** *Feasibility of "Steady State" Granulation* and Figure 6.16a). The lactose particles act as "bumps" which will hinder lactose-MCC formulated granules to flow well. Therefore, mannitol-MCC formulated granules possessed better flowability.

Table 6.3: Comparison of properties between mannitol-MCC formulated granules and lactose-MCC formulated granules produced at 30% LL, 490 rpm and 30 min WMT

Properties / Granules	Mannitol-MCC formulated	Lactose-MCC formulated
D4,3 (µm)	262 ± 11	308 ± 8
Circularity (-)	0.865 ± 0.079	0.648 ± 0.151
Poured density (g/ml)	0.580 ± 0.005	0.529 ± 0.004
Tapped density (g/ml)	0.667 ± 0.000	0.656 ± 0.011
Hausner ratio (-)	1.150 ± 0.010	1.240 ± 0.013

Despite the similarities to the lactose-MCC formulated granules from the previous chapters, the dissolution performance of mannitol-MCC formulated granules was much slower compared to lactose-MCC formulated granules (see Figure 6.13). Mannitol-MCC formulated granules showed a gradual release rate rather than a "burst" release by lactose-MCC formulated granules. The morphology of mannitol-MCC formulated granules after dissolution testing was found to be distinct from lactose-MCC formulated granules. The

porous matrix that lactose-MCC formulated granules leave after dissolution was not observed instead a rough and wrinkled structure with no cavitities was formed (see Figure 6.14b). This might contribute to the slow release rate of the granules as the penetration of dissolution medium was limited by the absence of openings formed by lactose particles in lactose-MCC formulated granules. Hence it can be deduced that mannitol-MCC formulated granules do not dissolve via leaching from a continuous matrix, instead undergo a different release mechanism.

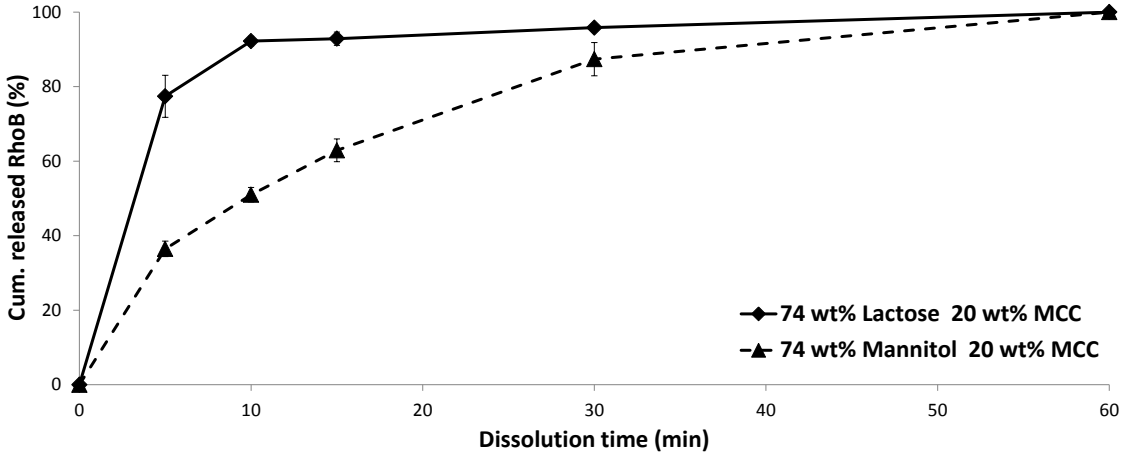

Figure 6.15: Dissolution profiles of lactose-MCC formulated and mannitol-MCC formulated "steady state" granules.

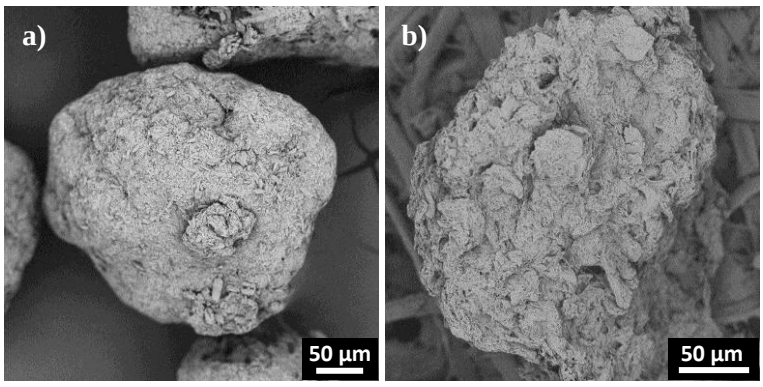

Figure 6.16: Morphology of mannitol-MCC formulated granules a) before and b) after 60 min of dissolution testing.

6.4 DISCUSSION

It is desirable to fine-tune the dissolution rate of solid dosage form to accommodate active pharmaceutical ingredient of different solubilities. The dissolution rate of "steady state" granules was found to be adjustable by varying the compositions of lactose and MCC in the formulation. Increasing the amount of insoluble component (MCC) is expected to create a polymeric matrix that possesses less internal voids upon dissolution of soluble component. Furthermore, the formation of cavities on granule surface will be reduced significantly leading to slower penetration of dissolution medium into the core of matrix.

As soluble components dissolve and diffuse away, the porosity of the insoluble MCC matrix increases, creating more channels for dissolution medium to penetrate into the unaffected region. The leaching mechanism of "steady state" granules is considered to be diffusion-controlled and can be described using Fick's First Law (Eqn. 2.6 in ***Chapter 2***) with an effective diffusion coefficient, D_{eff}. The effects of porosity and tortuosity are taken into account in defining the coefficient when dealing with porous matrices. Hence the effective diffusion coefficient, D_{eff} is defined as $\varepsilon D/\tau$ (Frenning 2011).

As solvated components are unable to diffuse through the solid phase of a matrix, the cross sectional area available for diffusion decreases, reducing the effective diffusion coefficient by a factor of ε. In this case, reducing the amount of lactose in the formulation decreases the porosity of the fully extracted matrix which gives a smaller effective diffusion coefficient, resulting in a slower dissolution rate. On the other hand, dissolved particles need to diffuse a longer distance across the porous layer since pore channels tend not to be straight. It takes longer time for the diffusion of particles/molecules in and out of the polymeric matrix through the micropores of the insoluble components as opposed to the wider openings created by dissolved lactose particles. Hence the effect of tortuosity, τ cannot be foreseen in the dissolution of "steady state" granules given the complex internal network of the insoluble polymeric matrix formed by MCC. Tortuosity of the matrix increases when more MCC is used in the formulation which may contribute to the slowing down of the dissolution rate.

The total matrix porosity (ε_{total}) available for the penetration of dissolution medium is the sum of existing internal voids (ε_{voids}) and cavities created by dissolved soluble components ($\varepsilon_{cavities}$). It is expected that decreasing the amount of lactose in granules will reduce the

cavities available for dissolution medium to penetrate into the insoluble MCC matrix. These cavities ($\varepsilon_{cavities}$) can be quantified by measuring the porosity of granules before (ε_{before}) and after (ε_{after}) dissolution testing, using mercury intrusion porosimetry. Although the porosity of "steady state" granules before dissolution was not characterized in this study, it could be assumed to be quite low and contribute a small fraction of the total matrix porosity. Therefore, Eqn 6.1 can be simplified where the total matrix porosity is estimated as the volume percentage of soluble component incorporated in the formulation, assuming lactose completely dissolves.

$$\varepsilon_{total} = \varepsilon_{voids} + \varepsilon_{cavities} \qquad \text{[Eqn 6.1]}$$

$$\varepsilon_{total} = \cancelto{0}{\varepsilon_{voids}} + \varepsilon_{cavities} = \varepsilon_{cavities} = \varepsilon_{after\ dissolution} = \%\ Vol_{\ soluble\ component} \qquad \text{[Eqn 6.2]}$$

Figure 6.17 described the effect of increasing the amount of lactose on the release of Rhodamine B with the assumption of cavities created by lactose particles being the only factor affecting the matrix porosity (see ***Appendix D*** for detailed calculations). A steady increase in the percentage released of Rhodamine B was observed when the amount of lactose increased from 59 wt% to 74 wt%, corresponding to a matrix porosity of 0.47 to 0.64 (see Figure 6.17a). Similar trend was noticed with granules of similar size distributions but different formulation compositions in Figure 6.17b. This showed that varying the formulation composition is the main means of fine-tuning the release rate of "steady state" granules, given the outstanding features of these granules: 1. Leaching as the release mechanism 2. Insoluble MCC matrix that does not disintegrate and 3. Formation of cavities/passages by soluble component.

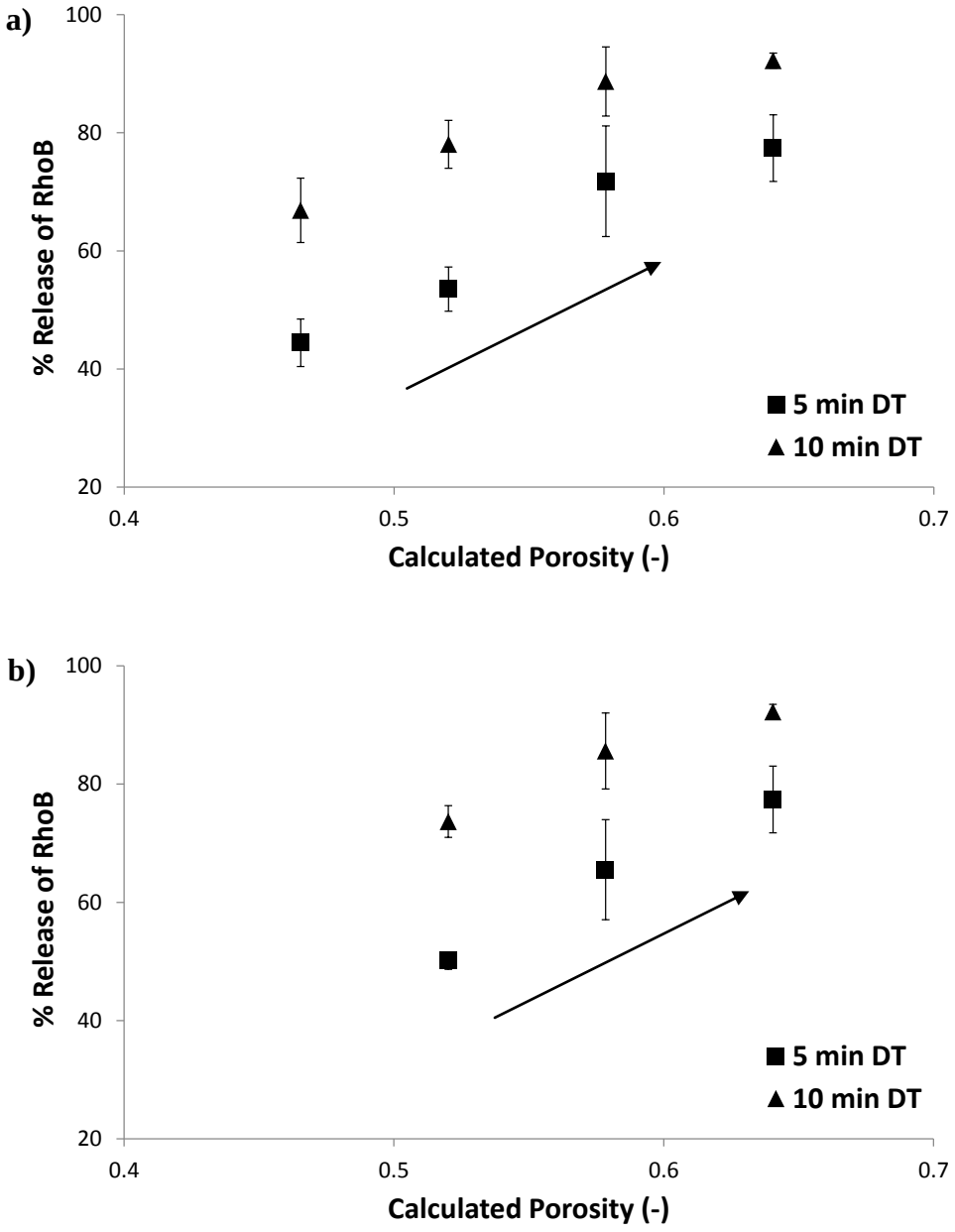

Figure 6.17: Effect of matrix porosity (amount of soluble component) on the release of Rhodamine B within the first 10 min dissolution window. a) Varying composition of formulation (20-35 wt% MCC) with constant liquid level of 30% and b) Varying liquid level (30-35%) at different compositions of formulation (20-30 wt% MCC)

It is worth mentioning that the decrease in the dissolution rates of granules with increasing amount of MCC but produced at the same liquid level could be possibly due to a combination of less formation of cavities and also swelling of MCC (see Figure 6.8). Since the same amount of liquid was delivered for the four formulation compositions, some MCC primary particles might be partially swollen. When these granules were being dissolved, the MCC

would have exhibited the retained swelling potential, caused blockage of pores and/or increased the tortousity of polymeric matrix. On the other hand, the dissolution profiles shown in Figure 6.10 were solely dependent on the amount of lactose incorporated in the formulation as all three batches of granules possessed very similar attributes. This has provided a fair judgement on the fine-tuned dissolution rate based on the variation in formulation composition.

"Steady state" granules as drug carriers show the potential of delivering drug substances that range from low to high solubilities upon successful fine-tuning of the dissolution rate. Depending on the course of drug action, the release rate of a dosage form needs to be adjusted. Rhodamine B as the model "drug" represents highly soluble drugs that present as dispersed solute in a matrix. Higher rate of imbibition of dissolution medium may be desirable when a poorly soluble drug is delivered and this can be achieved by increasing the amount of soluble component in the formulation.

When the formulation composition is varied, other granule properties such as size distribution, morphology, circularity and bulk densities are affected as well. A significant reduction was observed in these properties when the amount of MCC in the formulation was increased from 20 wt% to 35 wt% as the liquid level was deemed to be insufficient to promote autohesion of MCC polymer chains. MCC being described as a "molecular sponge", is able to retain large amount of water within its open porous structure where the bulk of the absorbed water is present as free water, able to evaporate readily (Fielden *et al.* 1988). In a well-distributed solid-liquid system, less water will be absorbed by individual MCC particles when the amount of MCC increases. This caused the cohesiveness of MCC to reduce and less extent of plastic deformation (Staniforth *et al.* 1988) which ultimately restricts granule growth by coalescence.

Furthermore, MCC polymer chains became less mobile and unable to enhance the spheronization of granules. Consolidation of wet granules was inhibited as well due to lower liquid saturation of wet granules, indicated by the decrease in the bulk densities. These adverse effects of increasing MCC can be reversed by increasing the liquid level delivered. Results have also proven that granule size of different formulations can be easily tuned via the "steady state" granulation approach by manipulating one variable i.e. liquid level since the size distribution becomes time independent after a sufficiently long period of wet massing.

Dissolution performance of lactose-MCC formulated and mannitol-MCC formulated granules were discovered to be vastly different. Mannitol-MCC formulated granules appeared to be much denser which explained the slow dissolution rate of these granules. Unlike lactose-MCC formulated granules, individual mannitol particle could not be identified on the granule surface. The size of mannitol primary particles used was about three times larger than that of MCC primary particles which would make them difficult to be enwrapped. Furthermore, the initial structure disappeared after wet granulation which could be attributed to recrystallization after drying. Based on SEM image analysis, it was speculated that dissolution of mannitol-MCC formulated granules involves erosion of matrix and diffusion of molecules (see Figure 6.14). However, the morphological change of mannitol particles being intensely sheared in a wet system is not fully understood yet. This showed that the release mechanism of a dosage form is highly dependent on the selection of ingredients.

6.5 CONCLUSIONS

The aim of varying the compositions of soluble and insoluble components in the chosen pharmaceutical formulation to fine-tune the release rate of "steady state" granules has been achieved. "Steady state" granules appear to be a polymeric matrix that is made of insoluble components with soluble components distributed across the matrix. This interesting finding raised the idea of altering the microstructure of the dosage form in order to control the release rate which could potentially be achieved by adjusting the formulation composition. Results showed that the dissolution rate is highly influenced by the penetration rate of dissolution medium which in turn is determined by the amount of soluble component present in the matrix.

Increasing the amount of insoluble component (MCC) or decreasing the amount of soluble component (lactose) decreases the formation of cavities on the granule surface available for the penetration of dissolution medium and also the formation of voids within the matrix hence less interfacial solid-liquid area for the dissolution of drug. Furthermore, diffusion of dissolved particles out from the matrix will be also inhibited, resulting in a slower release rate. It can be concluded that the porosity of the full extracted matrix corresponds to the amount of soluble component used plus existing voids. Mercury intrusion porosimetry will be useful in taking into account the overall effect of both internal voids and cavities created by soluble component on the dissolution rate of "steady state" granules.

In the process of obtaining an optimal formulation to achieve the desired release rate, other granule properties are also affected due to the incorporation of more/less of soluble/insoluble components. Liquid level was found to be a crucial factor that affects the properties of granule with MCC as one of the main ingredients in the formulation. With "steady state" granulation approach, granule size distribution can be easily tuned to the desired range by just varying the liquid level.

Mannitol-MCC formulated granules were found to be significantly different from lactose-MCC formulated granules in terms of the morphology and dissolution performance. In this study, mannitol-MCC formulated granules did not dissolve via the leaching mechanism and showed a slower dissolution rate. It is recommended to repeat the experiment with a finer grade of mannitol to investigate whether similar microstructure to that of lactose-MCC formulated granules can be reproduced, leading to comparable dissolution profiles.

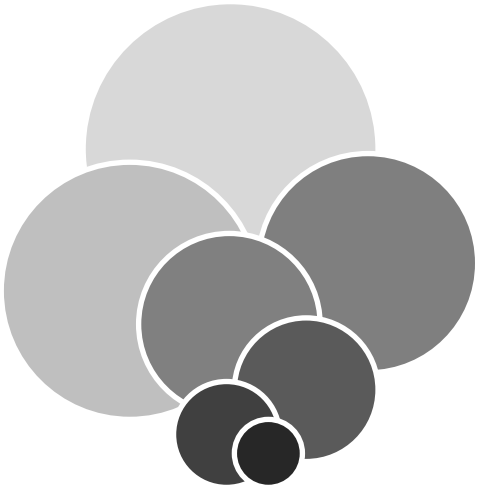

CHAPTER SEVEN

CONCLUSIONS AND RECOMMENDATIONS

7 CONCLUSIONS AND RECOMMENDATIONS

7.1 CONCLUSIONS

The main motivation of this project is to produce an oral solid dosage form i.e. granules by adopting the "steady state" granulation approach proposed by Michaels *et al*. (2009) in a high shear mixer granulator. The granule dosage form is set to possess the following desired attributes: narrow size distribution, spherical, constant bulk density, good dissolution performance and controlled release.

"Steady state" granulation approach has proved to be effective in resolving a recurring granulation issue in conventional industrial practice i.e. uncontrolled granule growth leading to a broad size distribution. The key idea is to achieve a very efficient liquid distribution by reducing the liquid delivery rate and prolonging the wet massing period. The findings in this project were in good agreement with those in Michaels *et al.*'s work (2009). "Steady state" conditions were achievable within the range of liquid level investigated, where significant narrowing of size distribution was observed after a sufficiently long period of wet massing. Each granule is assumed to have reached its optimal liquid saturation given the relatively constant granule size. Furthermore, preferential growth that causes the formation of lumps or the "balling" effect due to pooling can be significantly reduced.

Rounding of granules was discovered to be more pronounced at higher liquid level and impeller speed. Microcrystalline cellulose (MCC), a common pharmaceutical ingredient used as an extrusion aid in extrusion/spheronization process has exhibited similar granulation behaviour through the formation of spherical high shear granules. Autohesion, a self-diffusion mechanism was adopted to describe the interaction between MCC and water in a high sheared environment. Mobility of polymer chains is highly enhanced when an abundance of liquid is present. Under the exertion of intense shear force by the impeller, MCC polymer chains start to diffuse and form a continuum polymeric matrix that wraps up other ingredients. The final product appeared to be a spherical solid mass with discrete embedded and/or attached lactose particles on a smooth granule surface.

Extended wet massing shows the potential of producing over-granulated and dense granules as a result of excessive consolidation. The bulk density of granules was found to continuously increase over the wet massing period, which raised the concern of poor dissolution

performance by the granules but results from dissolution testing showed the contrary. No sign of supressed dissolution was observed as a full release was achieved within an hour of testing. "Steady state" granules demonstrated leaching as the main release mechanism where soluble component dissolved and diffused away from a porous and non-disintegrating matrix. The incorporation of lactose as the soluble component has facilitated the dissolution of entrapped model "drug" by creating cavities that enhance the penetration of dissolution medium. An interconnected network was believed to form inside the dense appearing structure, allowing dissolution medium to percolate through.

A relationship between formulation, operating parameters, microstructure of product and end-use properties in a particular dissolution mode was established from this work. Regular, spheroidal granules were found to show faster dissolution rate compared to irregular-shaped ones. However, a thorough understanding as to why this occurred requires extensive study on the internal structure of granules. Nevertheless, a strong influence of granule microstructure on the dissolution performance has led to the idea of manipulating the formulation to control the leaching/dissolution rate of the model "drug" and achieve controlled release. Adjusting the compositions of soluble and insoluble components proved to be feasible in fine-tuning the dissolution rate. The rate-determining step in the dissolution process would be the internal diffusion of dissolved components across the porous layer, which determined by the intragranular porosity and internal voids created by dissolved soluble components. Hence a controlled release by "steady state" granules is achievable by varying the formulation composition.

Varying the composition of formulation has significant effects on other granule properties particularly the size distribution. The liquid level required to produce granules of the same size distribution increases with the amount of MCC used. Since granule size becomes time independent with "steady state" granulation, the tuning of size distribution is more straightforward by just adjusting a single variable. A case study was also performed where lactose was substituted with mannitol as the soluble component to investigate the application of "steady state" granules with paediatric formulation. The expected dissolution performance was not observed with mannitol-MCC formulated granules and the microstructure of these granules was dissimilar to that of lactose-MCC formulated granules. The results suggested that coarser grade of mannitol might not be efficacious in forming the insoluble matrix of MCC which gives rise to the leaching effect.

The granulating condition reached after an extended period of wet massing is well accounted by the term "steady state" or pseudo steady state as the only granule property that becomes relatively constant is the size distribution. Although "steady state" granulation approach has shown great advantage in narrowing granule size distribution, the amount of time for the whole process to complete is significantly increased and cooling is vital in this case. From the efficiency and industrial costing perspectives, it may not be the optimum approach. However, it is possible that downstream processes such as wet and/or dry milling be eliminated from the production line given the well-controlled granule size formed and the elimination of lumps with the approach. In conclusion, "steady state" granulation has shown to be a robust granulating process for the production of granule dosage form.

7.2 RECOMMENDATIONS

In Michaels *et al.*'s work (2009), the effect of temperature on the establishment of steady state conditions was investigated by maintaining the temperature of powder mix at 45°C instead of the pre-set temperature of 22°C. They discovered that a higher temperature can speed up the process as the size distribution achieved after liquid addition showed no significant changes upon further wet massing. Moreover, the effect of temperature on granule properties is scarcely known as it was not extensively studied in previous work. It will be important to study the effect of temperature on "steady state" granule properties. This can be achieved by adjusting the temperature of powder bed using a circulator that circulates heating water through the jacketed bowl.

The uniformity in liquid distribution is highly desirable in granulation processes as it has a huge impact on granule size distribution which later can cause various downstream processing problems. Previous work showed that larger granules had relatively higher binder content compared to smaller granules (Osborne *et al.* 2011). Non-uniformity in liquid distribution can create a wide range of granules with multiple sizes where moisture content varies across the different size classes. This would require a longer time to dry the larger granules as they may appear to have dry surfaces but with a wet core at the end of the drying stage. Assuming liquid distribution is uniform and narrow size distribution has been achieved by "steady state" granulation approach, the amount of time required to dry a batch of granules will be significantly reduced. Drying time of granules that have relatively the same moisture content can then be investigated and modelled.

The analysis of granule porosity, specific surface area and internal structure can be helpful to further support the findings in the investigation of dissolution performance of "steady state" granules. Internal voids created by dissolved lactose particles can be determined quantitatively by measuring the granule porosity before and after dissolution testing using Mercury Intrusion Porosimeter. Hence the volume of voids available for the imbibition of dissolution medium can be related to the amount of soluble component used. The surface area available for dissolution can be measured by nitrogen adsorption to study the effect of disappearance of soluble components on the area exposed to dissolution medium. X-ray tomography, a technology that allows the production of virtual slices and reconstruction of a three-dimensional image of a scanned object can be used to enhance the visualisation of the internal structure of "steady state" granules. Not only the distribution of lactose particles within the matrix can be illustrated, but also the leaching mechanism of "steady state" granules can be validated.

Upon successful fine-tuning the rate of release by varying the composition of formulation, a release kinetic model i.e. shrinking core can be developed to quantify the rate of release of "steady state" granules. The model will allow one to either predict the rate of release based on specific sizes and composition of formulation or formulate a granule dosage form that can achieve a desired rate of release. The proposed release kinetic model can then be applied to estimate the amount of soluble components that contributes to the available cavities for dissolution medium to penetrate resulting in the desired rate of release.

Mathematical modelling of dissolution behaviour as a function of size and composition of formulation will provide a useful framework for others when adopting similar approach and formulation to engineer and produce granule dosage forms of certain size range and desired release rate.

More work is required to be undertaken to further investigate the effect of mannitol as the soluble component on the granulation behaviour specifically the microstructure and dissolution performance of granules by using a finer grade of particles. The "steady state" granulation approach will be adapted including the adjustment of operating conditions for paediatric formulations. It would also be ideal to incorporate API in the formulation to study the efficacy of "steady state" granules as an oral solid dosage form especially for the paediatric populations.

This research project has demonstrated the understanding on how “steady state” granulation approach can produce a granule dosage form that fulfils the end-use requirements of having narrow size distribution, spherical and excellent dissolution performance. It opens up potential avenues in creating a dosage form suitable for paediatric application given the smaller size class and uniformity in shape compared to the conventional granules that will be used for tableting.

NOMENCLATURE AND ABBREVIATIONS

Symbol	Definition	Dimensions
a	Particle radius	[m]
a_{cr}^{coal}	Critical particle size at growth limit	[m]
a_{cr}^{def}	Critical particle size at deformation limit	[m]
A	Unit area	[m^2]
$\dot{A}$	Area flux of powder traversing the spray zone	[m^2]
d_d	Droplet diameter	[µm]
C_b	Bulk solution concentration	[g/cm^3]
C_s	Solubility	[g/cm^3]
C	Concentration	[g/cm^3]
D	Diffusion coefficient	[m^2/s]
h	Diffusion layer thickness	[m]
H	Hausner ratio	[-]
J	Flux (rate of diffusion)	[$g/m^2 \cdot s$]
k	Drug release rate constant	[s^{-n}]
k_0	Zero-order release constant	[$units/m^2 \cdot s$]
k_1	First-order release constant	[$units/m^2 \cdot s$]
k_H	Higuchi dissolution constant	[$units/m^2 \cdot s^{1/2}$]
m	Mass of granule sample	[g]
m_p	Mass of particle	[g]
M_t	Amount of drug released at time *t*	[g]
M_∞	Amount of drug released at infinity	[g]
n	Diffusional exponent	[-]
Q	Amount released at time *t* per unit area exposure	[$units/m^2$]
R_{pore}	Radius of the pores	[µm]
St_{coal}	Stokes coalescence number	[-]
St_{coal}^*	Coalescence limit	[-]
St_{def}	Stokes deformation number	[-]
St_{def}^*	Deformation limit	[-]
t	Time	[s]
t_c	Circulation time	[ms]
t_p	Penetration time of the spray drops	[ms]
U_0	Relative particle velocity	[m/s]
V_o	Drop volume	[m^3]
$\dot{V}$	Volumetric spray rate	[m^3/s]

V_p	Volume of particle	[m^3]
V_p	Poured volume of granule	[cm^3]
V_T	Tapped volume of granule	[cm^3]

Greek Symbols

ε	Powder bed porosity	[-]
ε_{after}	Granule porosity after dissolution	[-]
ε_{before}	Granule porosity before dissolution	[-]
$\varepsilon_{cavities}$	Cavities created by soluble component	[-]
ε_{total}	Total matrix (granule) porosity	[-]
ε_{voids}	Internal voids in granule	[-]
γ_{LV}	Liquid surface tension	[J/m^2]
τ_p	Dimensionless drop penetration time	[-]
$\tau(\dot{\gamma})$	Some characteristic stress in the granule	[N/m^2]
μ	Liquid viscosity	[mPa·s]
μ	Binder or granule surface viscosity	[mPa·s]
θ_d	Dynamic contact angle of the liquid in the solid capillary	[degress,°]
ρ_p	Particle density	[g/m^3]
ρ_p	Bulk poured density	[g/m^3]
ρ_T	Bulk poured density	[g/m^3]
ψ_a	Dimensionless spray flux parameter	[-]

Abbreviations

API	Active Pharmaceutical Ingredient
coal	Coalescence
CCNa	Croscarmellose Sofium
def	Deformation
DT	Dissolution Time
FBRM	Focused Beam Reflectance Measurement
HPC	Hydroxypropyl Cellulose
HSWG	High Shear Wet Granulation
IR	Immediate Release
LL	Liquid Level
MCC	Microcrystalline Cellulose
PEG	Polyethylene Glycol
rpm	Revolutions per minute
RhoB	Rhodamine B
SEM	Scanning Electron Microscopy
WMT	Wet Massing Time

REFERENCES

Abdullah, E. C. and D. Geldart (1999). "The use of bulk density measurements as flowability indicators." Powder Technology **102**(2): 151-165.

am Ende, D. J. (2011). Chemical Engineering in the Pharmaceutical Industry: R&D to Manufacturing, WILEY.

Ameye, D., E. Keleb, C. Vervaet, J. P. Remon, E. Adams and D. L. Massart (2002). "Scaling-up of a lactose wet granulation process in Mi-Pro high shear mixers." European Journal of Pharmaceutical Sciences **17**(4–5): 247-251.

Ansel, H. C. (1981). Introduction to Pharmaceutical Dosage Forms, Lea & Febiger Philadelphia.

Ansel, H. C., L. V. Allen and N. G. Popovich (1999). Pharmaceutical Dosage Forms and Drug Delivery Systems, Lippincott Williams & Wilkins.

Badawy, S. F., D. Gray and M. Hussain (2006). "A Study on the Effect of Wet Granulation on Microcrystalline Cellulose Particle Structure and Performance." Pharmaceutical Research **23**(3): 634-640.

Badawy, S. I. F., M. M. Menning, M. A. Gorko and D. L. Gilbert (2000). "Effect of process parameters on compressibility of granulation manufactured in a high-shear mixer." International Journal of Pharmaceutics **198**(1): 51-61.

Baker, P. G. and P. L. Bishop (1997). "Prediction of metal leaching rates from solidified/stabilized wastes using the shrinking unreacted core leaching procedure." Journal of Hazardous Materials **52**(2–3): 311-333.

Benali, M., V. Gerbaud and M. Hemati (2009). "Effect of operating conditions and physico–chemical properties on the wet granulation kinetics in high shear mixer." Powder Technology **190**(1–2): 160-169.

Bouwman, A. M., M. J. Henstra, D. Westerman, J. T. Chung, Z. Zhang, A. Ingram, J. P. K. Seville and H. W. Frijlink (2005). "The effect of the amount of binder liquid on the granulation mechanisms and structure of microcrystalline cellulose granules prepared by high shear granulation." International Journal of Pharmaceutics **290**(1–2): 129-136.

Chen, Y. and D. Flanagan (2009). Chapter 7 - Theory of Diffusion and Pharmaceutical Applications. Developing Solid Oral Dosage Forms. Y. Qiu, Y. Chen, G. G. Z. Zhang, L. Liu and W. R. Porter. San Diego, Academic Press**:** 147-162.

Chitu, T. M., D. Oulahna and M. Hemati (2011). "Rheology, granule growth and granule strength: Application to the wet granulation of lactose–MCC mixtures." Powder Technology **208**(2): 441-453.

Chitu, T. M., D. Oulahna and M. Hemati (2011). "Wet granulation in laboratory-scale high shear mixers: Effect of chopper presence, design and impeller speed." Powder Technology **206**(1–2): 34-43.

Chitu, T. M., D. Oulahna and M. Hemati (2011). "Wet granulation in laboratory scale high shear mixers: Effect of binder properties." Powder Technology **206**(1–2): 25-33.

Dukić-Ott, A., M. Thommes, J. P. Remon, P. Kleinebudde and C. Vervaet (2009). "Production of pellets via extrusion–spheronisation without the incorporation of microcrystalline cellulose: A critical review." European Journal of Pharmaceutics and Biopharmaceutics **71**(1): 38-46.

Eichie, F. E., R. S. Okor and O. Esi (2008). "Matrix release from tablets prepared with aqueous dispersion of an acrylate methacrylate (a water-insoluble) copolymer as binder." International Journal of Health Research **1**(4): 235-240.

Ek, R., H. Lennholm, R. Davidson, C. Nyström and G. Ragnarsson (1995). "Pore swelling in beads made of cellulose fibres and fibre fragments." International Journal of Pharmaceutics **122**(1–2): 49-56.

Faure, A., P. York and R. C. Rowe (2001). "Process control and scale-up of pharmaceutical wet granulation processes: a review." European Journal of Pharmaceutics and Biopharmaceutics **52**(3): 269-277.

Fielden, K. E., J. M. Newton, P. O'Brien and R. C. Rowe (1988). "Thermal Studies on the Interaction of Water and Microcrystalline Cellulose." Journal of Pharmacy and Pharmacology **40**(10): 674-678.

Frenning, G. (2011). "Modelling drug release from inert matrix systems: From moving-boundary to continuous-field descriptions." International Journal of Pharmaceutics **418**(1): 88-99.

Hapgood, K. P., R. Amelia, M. B. Zaman, B. K. Merrett and P. Leslie (2010). "Improving liquid distribution by reducing dimensionless spray flux in wet granulation—A pharmaceutical manufacturing case study." Chemical Engineering Journal **164**(2–3): 340-349.

Hapgood, K. P., J. D. Litster and R. Smith (2003). "Nucleation regime map for liquid bound granules." AIChE Journal **49**(2): 350-361.

Higuchi, T. (1963). "Mechanism of sustained-action medication. Theoretical analysis of rate of release of solid drugs dispersed in solid matrices." Journal of Pharmaceutical Sciences **52**(12): 1145-1149.

Instruments, M. (2013). "Mastersizer 2000." Retrieved 26 February, 2013, from http://www.malvern.com/labeng/products/mastersizer/ms2000/mastersizer2000.htm.

Irfan Khan, M., and G.I. Tardos (1997). "Stability of wet agglomerates in granular shear flows." J. Fluid. Mech **347**: 347-368.

Iveson, S. M., J. D. Litster, K. Hapgood and B. J. Ennis (2001). "Nucleation, growth and breakage phenomena in agitated wet granulation processes: a review." Powder Technology **117**(1–2): 3-39.

Juppo, A. M., J. Yliruusi, L. Kervinen and P. Ström (1992). "Determination of size distribution of lactose, glucose and mannitol granules by sieve analysis and laser diffractometry." International Journal of Pharmaceutics **88**(1–3): 141-149.

Kleinebudde, P. (1994). "Shrinking and swelling properties of pellets containing microcrystalline cellulose and low substituted hydroxypropylcellulose: I. Shrinking properties." International Journal of Pharmaceutics **109**(3): 209-219.

Kleinebudde, P. (1997). "The Crystallite-Gel-Model for Microcrystalline Cellulose in Wet-Granulation, Extrusion, and Spheronization." Pharmaceutical Research **14**(6): 804-809.

Knight, P. (2004). "Challenges in granulation technology." Powder Technology **140**(3): 156-162.

Knight, P. C., T. Instone, J. M. K. Pearson and M. J. Hounslow (1998). "An investigation into the kinetics of liquid distribution and growth in high shear mixer agglomeration." Powder Technology **97**(3): 246-257.

Knight, P. C., A. Johansen, H. G. Kristensen, T. Schæfer and J. P. K. Seville (2000). "An investigation of the effects on agglomeration of changing the speed of a mechanical mixer." Powder Technology **110**(3): 204-209.

Korsmeyer, R. W., R. Gurny, E. Doelker, P. Buri and N. A. Peppas (1983). "Mechanisms of solute release from porous hydrophilic polymers." International Journal of Pharmaceutics **15**(1): 25-35.

Litster, J. D., K. P. Hapgood, J. N. Michaels, A. Sims, M. Roberts and S. K. Kameneni (2002). "Scale-up of mixer granulators for effective liquid distribution." Powder Technology **124**(3): 272-280.

Liu, L., M. Levin and P. Sheskey (2009). Chapter 29 - Process Development and Scale-up of Wet Granulation by the High Shear Process. Developing Solid Oral Dosage Forms. Q. Yihong, C. Yisheng, G. Z. Z. Geoff et al. San Diego, Academic Press**:** 667-699.

Long, M. and Y. Chen (2009). Dissolution Testing of Solid Products-Chapter 14, Elsevier Inc.

Mackaplow, M. B., L. A. Rosen and J. N. Michaels (2000). "Effect of primary particle size on granule growth and endpoint determination in high-shear wet granulation." Powder Technology **108**(1): 32-45.

Malvern (1997). Sample dispersion and refractive index guide, Malvern Instuments Ltd.

Malvern (2010). Morphologi G3 User Manual Malvern Instruments Ltd.

REFERENCES

Mangwandi, C., M. J. Adams, M. J. Hounslow and A. D. Salman (2010). "Effect of impeller speed on mechanical and dissolution properties of high-shear granules." Chemical Engineering Journal **164**(2–3): 305-315.

Marabi, A., G. Mayor, A. Burbidge, R. Wallach and I. S. Saguy (2008). "Assessing dissolution kinetics of powders by a single particle approach." Chemical Engineering Journal **139**(1): 118-127.

Michaels, J. N., L. Farber, G. S. Wong, K. Hapgood, S. J. Heidel, J. Farabaugh, J.-H. Chou and G. I. Tardos (2009). "Steady states in granulation of pharmaceutical powders with application to scale-up." Powder Technology **189**(2): 295-303.

Millili, G. P., R. J. Wigent and J. B. Schwartz (1990). "Autohesion in Pharmaceutical Solids." Drug Development and Industrial Pharmacy **16**(16): 2383-2407.

O'Connor, R. E. and J. B. Schwartz (1993). "Drug release mechanism from a microcrystalline cellulose pellet system." Pharmaceutical Research **10**(3): 356-361.

O'Neil, M. J., P. E. Heckelman, C. B. Koch and K. J. Roman (2006). An encyclopedia of chemicals, drugs and biologicals. The Merck Index. NJ, Merck Research Laboratories.

Ohno, I., S. Hasegawa, S. Yada, A. Kusai, K. Moribe and K. Yamamoto (2007). "Importance of evaluating the consolidation of granules manufactured by high shear mixer." International Journal of Pharmaceutics **338**(1–2): 79-86.

Osborne, J. D., R. P. J. Sochon, J. J. Cartwright, D. G. Doughty, M. J. Hounslow and A. D. Salman (2011). "Binder addition methods and binder distribution in high shear and fluidised bed granulation." Chemical Engineering Research and Design **89**(5): 553-559.

Oulahna, D., F. Cordier, L. Galet and J. A. Dodds (2003). "Wet granulation: the effect of shear on granule properties." Powder Technology **130**(1–3): 238-246.

Parikh, D. M. (2007). Handbook of pharmaceutical granulation technology. New York, N.Y., Informa Healthcare

Peppas, N. A. (1985). "Analysis of Fickian and non-Fickian drug release from polymers." Pharmaceutica Acta Helvetiae **60**(4): 110-111.

Peppas, N. A. and J. J. Sahlin (1989). "A simple equation for the description of solute release. III. Coupling of diffusion and relaxation." International Journal of Pharmaceutics **57**(2): 169-172.

Pharma, D. (2013). "Pharmatose® 200M." Retrieved 25 November, 2013, from http://www.dfepharma.com/en/excipients/lactose/milled/pharmatose-200m.aspx.

Rahmanian, N., A. Naji and M. Ghadiri (2011). "Effects of process parameters on granules properties produced in a high shear granulator." Chemical Engineering Research and Design **89**(5): 512-518.

Realpe, A. and C. Velázquez (2008). "Growth kinetics and mechanism of wet granulation in a laboratory-scale high shear mixer: Effect of initial polydispersity of particle size." Chemical Engineering Science **63**(6): 1602-1611.

Rhodes, M. (2008). Introduction to Particle Technology. Australia, John Wiley & Sons.

Ritger, P. L. and N. A. Peppas (1987). "A simple equation for description of solute release I. Fickian and non-fickian release from non-swellable devices in the form of slabs, spheres, cylinders or discs." Journal of Controlled Release **5**(1): 23-36.

Ritger, P. L. and N. A. Peppas (1987). "A simple equation for description of solute release II. Fickian and anomalous release from swellable devices." Journal of Controlled Release **5**(1): 37-42.

Rowe, R. C., P. J. Sheskey and S. C. Owen (2006). Handbook of Pharmaceutical Excipients. London, Pharmaceutical Press.

Safari, V., G. Arzpeyma, F. Rashchi and N. Mostoufi (2009). "A shrinking particle—shrinking core model for leaching of a zinc ore containing silica." International Journal of Mineral Processing **93**(1): 79-83.

Sakr, W. F., M. A. Ibrahim, F. K. Alanazi and A. A. Sakr (2012). "Upgrading wet granulation monitoring from hand squeeze test to mixing torque rheometry." Saudi Pharmaceutical Journal **20**(1): 9-19.

Saleh, K., L. Vialatte and P. Guigon (2005). "Wet granulation in a batch high shear mixer." Chemical Engineering Science **60**(14): 3763-3775.

Sam, T., T. B. Ernest, J. Walsh and J. L. Williams (2012). "A benefit/risk approach towards selecting appropriate pharmaceutical dosage forms – An application for paediatric dosage form selection." International Journal of Pharmaceutics **435**(2): 115-123.

Santomaso, A., P. Lazzaro and P. Canu (2003). "Powder flowability and density ratios: the impact of granules packing." Chemical Engineering Science **58**(13): 2857-2874.

Schaefer, T. and C. Mathiesen (1996). "Melt pelletization in a high shear mixer .9. Effects of binder particle size." Int. J. Pharm. **139**(1-2): 139-148.

Scott, A. C., M. J. Hounslow and T. Instone (2000). "Direct evidence of heterogeneity during high-shear granulation." Powder Technology **113**(1–2): 205-213.

Shi, L., Y. Feng and C. C. Sun (2011). "Massing in high shear wet granulation can simultaneously improve powder flow and deteriorate powder compaction: A double-edged sword." European Journal of Pharmaceutical Sciences **43**(1–2): 50-56.

Siepmann, J. and N. A. Peppas (2011). "Higuchi equation: Derivation, applications, use and misuse." International Journal of Pharmaceutics **418**(1): 6-12.

Siepmann, J. and F. Siepmann (2013). "Mathematical modeling of drug dissolution." International Journal of Pharmaceutics **453**(1): 12-24.

Staniforth, J. N., A. R. Baichwal, J. P. Hart and P. W. S. Heng (1988). "Effect of addition of water on the rheological and mechanical properties of microcrystalline celluloses." International Journal of Pharmaceutics **41**(3): 231-236.

Suzuki, T., H. Kikuchi, S. Yamamura, K. Terada and K. Yamamoto (2001). "The change in characteristics of microcrystalline cellulose during wet granulation using a high-shear mixer." Journal of Pharmacy and Pharmacology **53**(5): 609-616.

Suzuki, T. and H. Nakagami (1999). "Effect of crystallinity of microcrystalline cellulose on the compactability and dissolution of tablets." European Journal of Pharmaceutics and Biopharmaceutics **47**(3): 225-230.

Talu, I., G. I. Tardos and M. I. Khan (2000). "Computer simulation of wet granulation." Powder Technology **110**(1–2): 59-75.

Tardos, G. I., M. I. Khan and P. R. Mort (1997). "Critical parameters and limiting conditions in binder granulation of fine powders." Powder Technology **94**(3): 245-258.

Tho, I., S. Arne Sande and P. Kleinebudde (2003). "Disintegrating pellets from a water-insoluble pectin derivative produced by extrusion/spheronisation." European Journal of Pharmaceutics and Biopharmaceutics **56**(3): 371-380.

Toledo, M. "FBRM (Focused Beam Reflectance Measurement) Technology." Retrieved 14 February, 2014, from http://au.mt.com/au/en/home/supportive_content/specials/Lasentec-FBRM-Method-of-Measurement.html.

van den Dries, K., O. M. de Vegt, V. Girard and H. Vromans (2003). "Granule breakage phenomena in a high shear mixer; influence of process and formulation variables and consequences on granule homogeneity." Powder Technology **133**(1–3): 228-236.

van den Dries, K. and H. Vromans (2004). "Qualitative proof of liquid dispersion and penetration-involved granule formation in a high shear mixer." European Journal of Pharmaceutics and Biopharmaceutics **58**(3): 551-559.

Vasilenko, A., S. Koynov, B. J. Glasser and F. J. Muzzio (2013). "Role of consolidation state in the measurement of bulk density and cohesion." Powder Technology **239**(0): 366-373.

Walsh, J., D. Bickmann, J. Breitkreutz and M. Chariot-Goulet (2011). "Delivery devices for the administration of paediatric formulations: Overview of current practice, challenges and recent developments." International Journal of Pharmaceutics **415**(1–2): 221-231.

Westermarck, S., A. M. Juppo, L. Kervinen and J. Yliruusi (1999). "Microcrystalline cellulose and its microstructure in pharmaceutical processing." European Journal of Pharmaceutics and Biopharmaceutics **48**(3): 199-206.

Wlosnewski, J. C., M. Kumpugdee-Vollrath and P. Sriamornsak (2010). "Effect of drying technique and disintegrant on physical properties and drug release behavior of microcrystalline cellulose-based pellets prepared by extrusion/spheronization." Chemical Engineering Research and Design **88**(1): 100-108.

Yang, R., T. Vo T. N, A. V. Gorelov, F. Aldabbagh, W. M. Carroll, M. G. Meere and Y. Rochev (2012). "A mathematical model for pulsatile release: Controlled release of rhodamine B from UV-crosslinked thermoresponsive thin films." International Journal of Pharmaceutics **427**(2): 320-327.

APPENDICES

A. GRANULE SIZE DISTRIBUTION PLOTS AND RAW DATA

Normalization of granule size distribution obtained by Mastersizer was carried out to take into account granules that were larger than 2 mm. Approximately 10-12 g of sample was sieved to determine the amount of granules larger than 2 mm, x g. The initial size distribution was normalized by multiplying the volume percentage obtained for each particle size with $[1 - x/samplesize]$ i.e. the mass percentage of granules that were smaller than 2 mm in the sample batch. A sample of normalization was shown in Figure A.1.

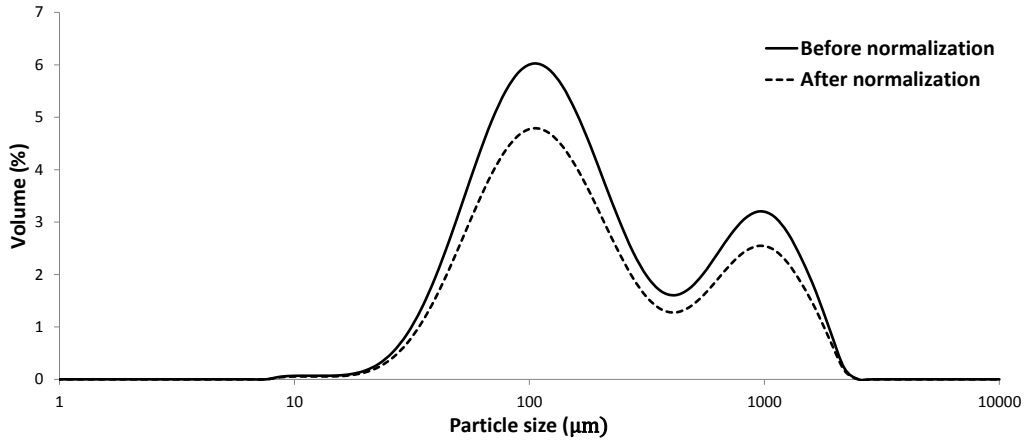

Figure A.1: Normalization of granule size distribution obtained at 24% LL, 245 rpm and 0 min WMT.

Size distribution profiles from Chapter 4: Feasibility of "Steady state" Granulation

Formulation used for the following results was 74 wt% lactose, 20 wt% MCC, 3% HPC and 3% croscarmellose sodium and operating conditions were 24-30% LL and 245-490 rpm.

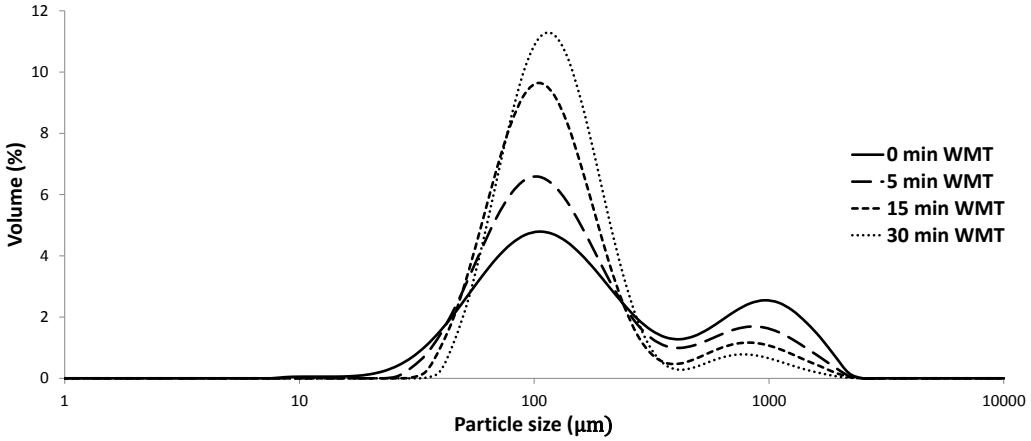

Figure A.2: Granule size distributions produced at 24% LL, 245 rpm and 0-30 min WMT.

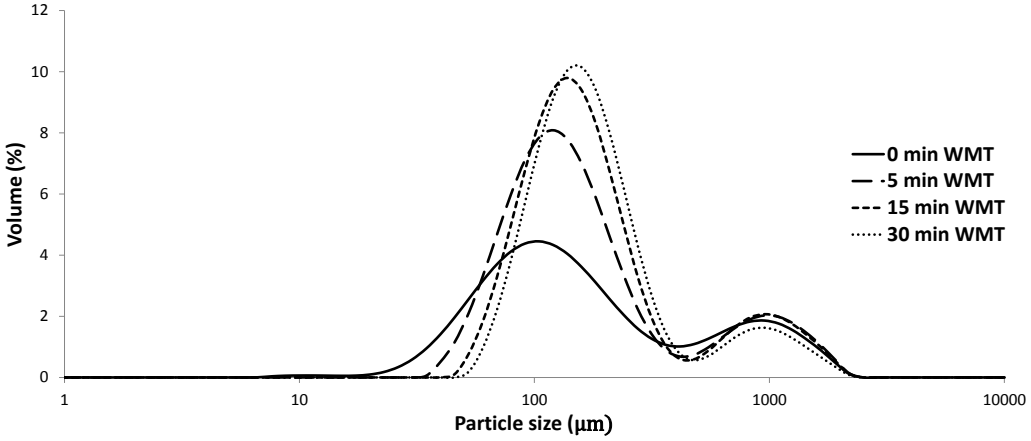

Figure A.3: Granule size distributions produced at 27% LL, 245 rpm and 0-30 min WMT.

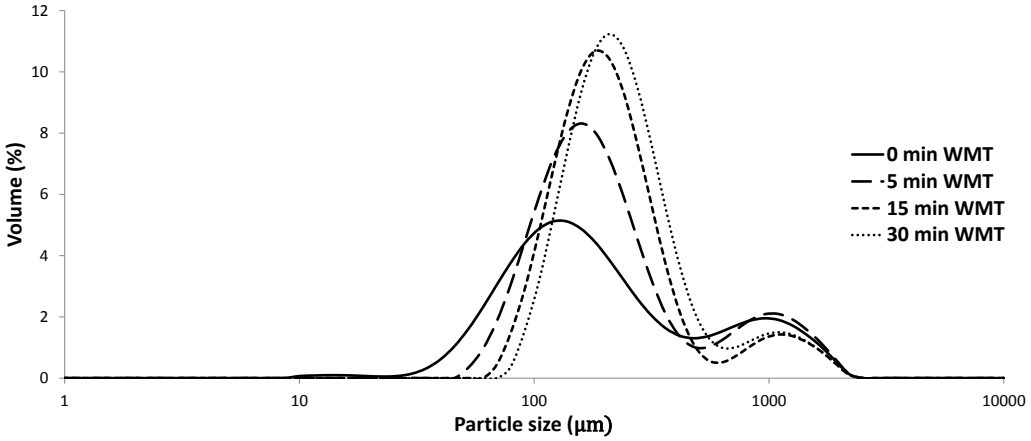

Figure A.4: Granule size distributions produced at 30% LL, 245 rpm and 0-30 min WMT.

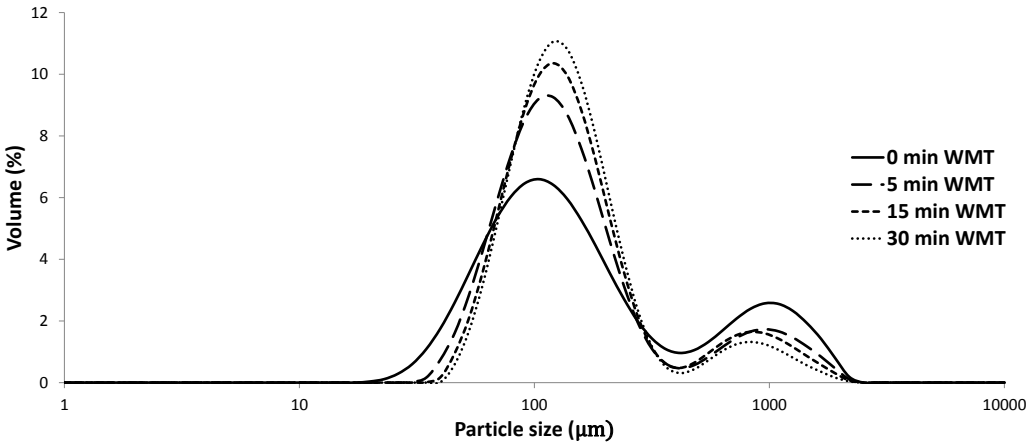

Figure A.5: Granule size distributions produced at 24% LL, 368 rpm and 0-30 min WMT.

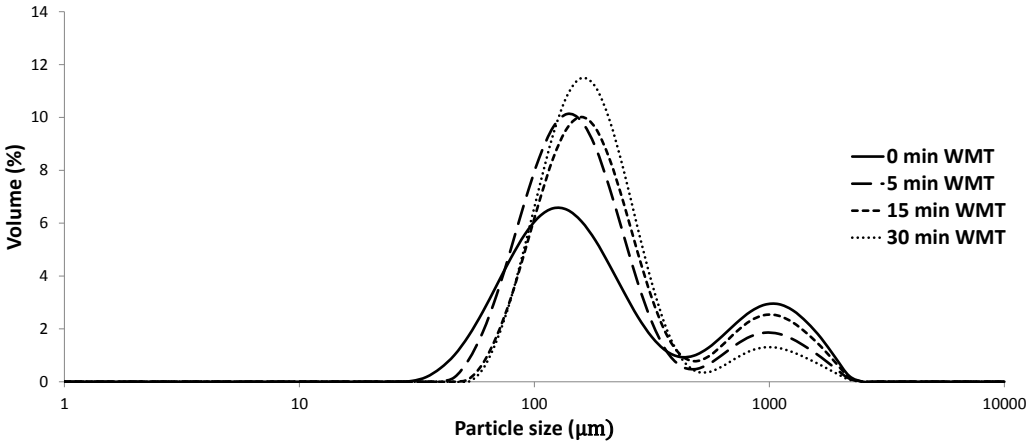

Figure A.6: Granule size distributions produced at 27% LL, 368 rpm and 0-30 min WMT.

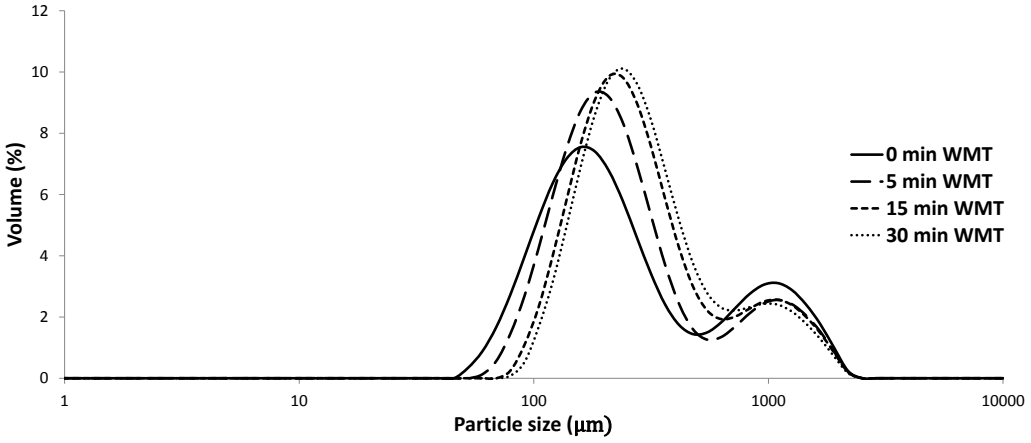

Figure A.7: Granule size distributions produced at 30% LL, 368 rpm and 0-30 min WMT.

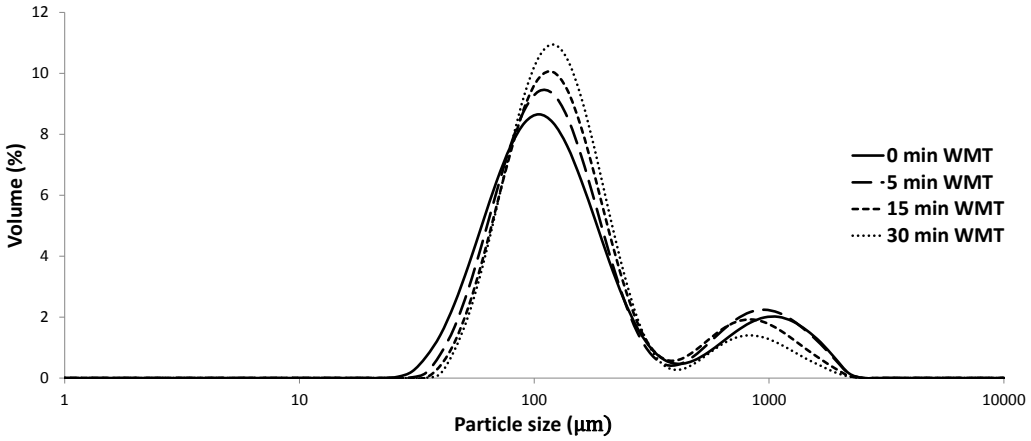

Figure A.8: Granule size distributions produced at 24% LL, 490 rpm and 0-30 min WMT.

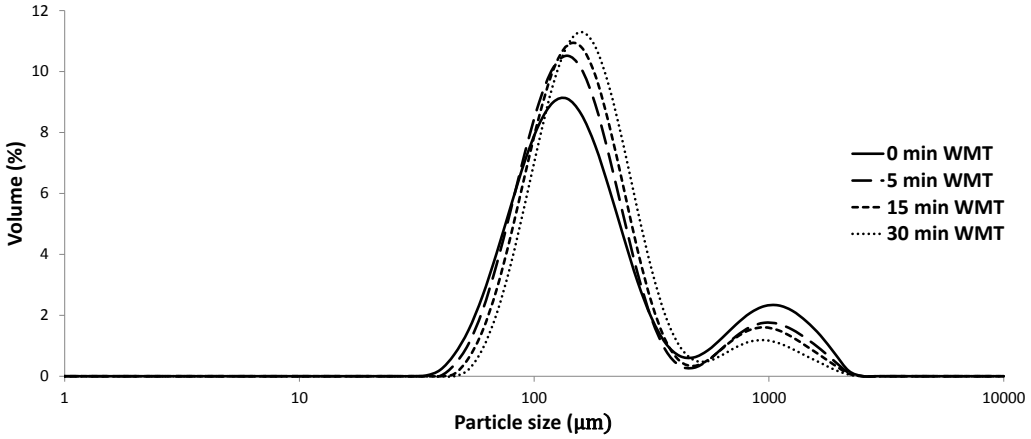

Figure A.9: Granule size distributions produced at 27% LL, 490 rpm and 0-30 min WMT.

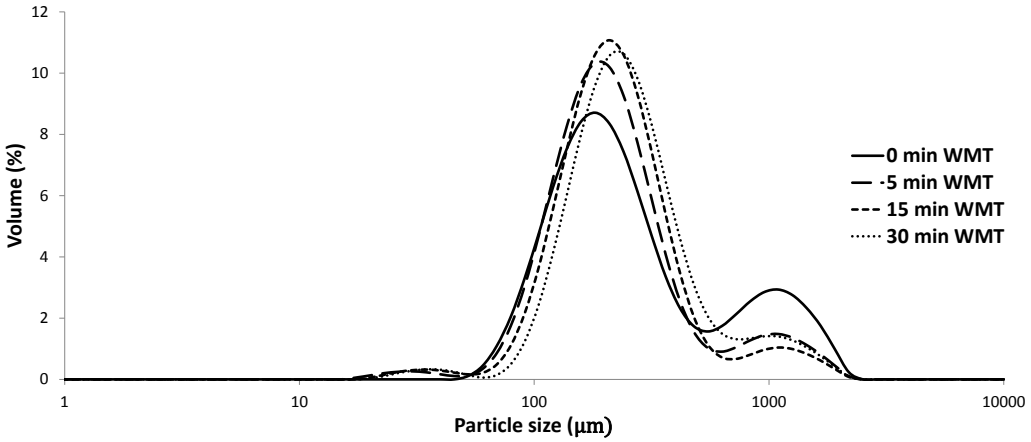

Figure A.10: Granule size distributions produced at 30% LL, 490 rpm and 0-30 min WMT.

Size distribution profiles from Chapter 6: Effect of Varying Formulation Composition on Granule Properties and Dissolution Profile

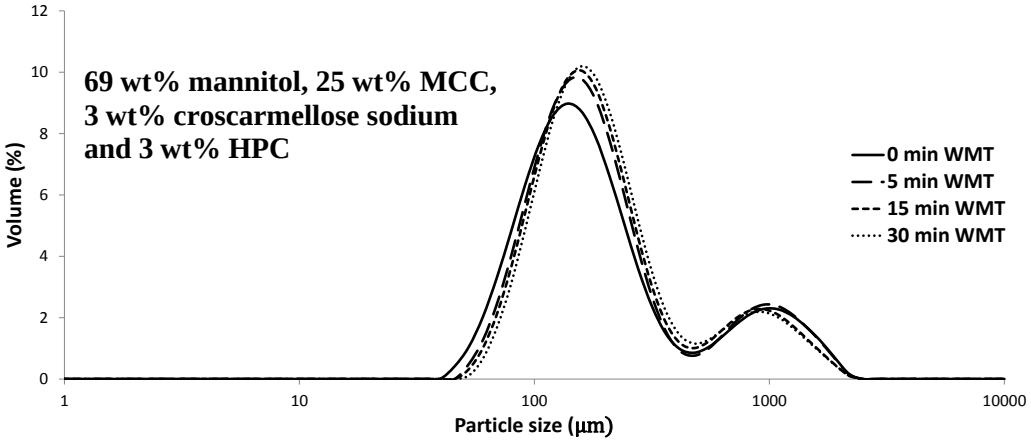

Figure A.11: Granule size distributions produced at 30% LL, 490 rpm and 0-30 min WMT.

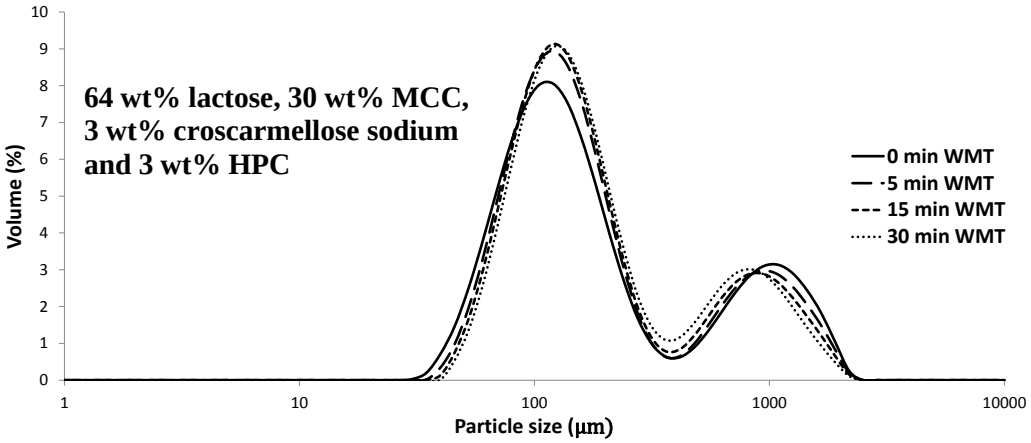

Figure A.12: Granule size distributions produced at 30% LL, 490 rpm and 0-30 min WMT.

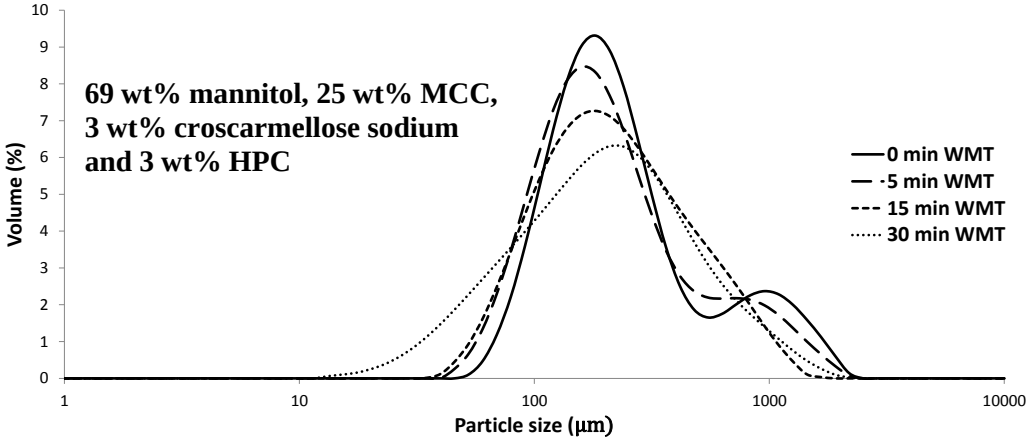

Figure A.13: Granule size distributions produced at 30% LL, 490 rpm and 0-30 min WMT.

d10, d50 and d90 of granule size distributions produced at 24-30% LL, 245-490 rpm and 30 min wet massing.

Impeller speed (rpm)	Liquid level (%)	d10	d50	d90
245	**24**	62.5 ± 0.6	111.8 ± 1.3	227.3 ± 7.7
	27	84.4 ± 0.4	152.8 ± 1.6	622.1 ± 79.2
	30	119.5 ± 2.0	211.7 ± 6.3	574.4 ± 168.2
368	**24**	68.4 ± 0.4	123.2 ± 2.1	347.2 ± 123.0
	27	90.5 ± 1.0	159.8 ± 2.5	416.6 ± 139.5
	30	137.1 ± 4.9	255.7 ± 15.8	863.4 ± 110.5
490	**24**	65.6 ± 0.3	119.0 ± 0.7	368.1 ± 70.5
	27	86.5 ± 2.5	155.1 ± 4.5	353.2 ± 58.0
	30	119.7 ± 0.7	244.5 ± 1.8	578.1 ± 51.1

Raw data for the amount of granules larger than 2 mm from mechanical sieving

Liquid level: 24% Impeller speed: 245 rpm

Wet massing time (min)	Sample weight (g)	Size class / Weight (g)	
		> 2mm	< 2mm
0	9.20	1.89	7.31
5	10.77	1.91	8.86
15	10.76	0.64	10.12
30	10.81	-	10.81

Liquid level: 27% Impeller speed: 245 rpm

Wet massing time (min)	Sample weight (g)	Size class / Weight (g)	
		> 2mm	< 2mm
0	10.64	3.39	7.25
5	10.75	1.05	9.70
15	11.11	0.36	10.75
30	10.98	0.63	10.35

Liquid level: 30% Impeller speed: 245 rpm

Wet massing time (min)	Sample weight (g)	Size class / Weight (g)	
		> 2mm	< 2mm
0	16.32	4.33	11.99
5	15.91	1.80	14.11
15	16.37	0.76	15.61
30	16.10	0.03	16.07

Liquid level: 24% Impeller speed: 368 rpm

Wet massing time (min)	Sample weight (g)	Size class / Weight (g)	
		> 2mm	< 2mm
0	11.78	0.82	10.96
5	12.18	0.34	11.84
15	11.84	-	11.84
30	11.84	-	11.84

Liquid level: 27% Impeller speed: 368 rpm

Wet massing time (min)	Sample weight (g)	Size class / Weight (g)	
		> 2mm	< 2mm
0	11.72	1.50	10.22
5	11.71	0.11	11.60
15	11.72	0.02	11.7
30	12.12	-	12.12

Liquid level: 30% Impeller speed: 368 rpm

Wet massing time (min)	Sample weight (g)	Size class / Weight (g)	
		> 2mm	< 2mm
0	11.37	0.88	10.49
5	11.88	0.41	11.47
15	12.54	0.01	12.53
30	12.77	-	12.77

Liquid level: 24% Impeller speed: 490 rpm

Wet massing time (min)	Sample weight (g)	Size class / Weight (g)	
		> 2mm	< 2mm
0	11.75	0.26	11.49
5	11.65	-	11.65
15	11.83	-	11.83
30	11.74	-	11.74

Liquid level: 27% Impeller speed: 490 rpm

Wet massing time (min)	Sample weight (g)	Size class / Weight (g)	
		> 2mm	< 2mm
0	12.54	0.11	12.43
5	11.64	0.01	11.63
15	11.87	-	11.87
30	13.17	-	13.17

Liquid level: 30% Impeller speed: 490 rpm

Wet massing time (min)	Sample weight (g)	Size class / Weight (g)	
		> 2mm	< 2mm
0	11.44	0.16	11.28
5	11.60	0.07	11.53
15	11.48	-	11.48
30	11.89	-	11.89

Mass percentage of granules that was larger than 2 mm

Impeller speed (rpm)	Liquid level (%)	Wet massing time (min)			
		0	5	15	30
245	**24**	21	18	6.0	-
	27	32	10	3.2	5.7
	30	27	11	4.6	0.2
368	**24**	7.0	2.8	-	-
	27	13	1.0	0.2	-
	30	7.8	3.5	0.1	-
490	**24**	2.2	-	-	-
	27	0.9	0.04	-	-
	30	1.4	0.6	-	-

B. GRANULE CIRCULARITY RAW DATA

HS (High Sensitivity) circularity is defined as the ratio of the projected area of an object to the square of the perimeter of the object (Malvern 2010).

$$HS\ Circularity = \frac{4 \times \pi \times Area}{Perimeter^2} \qquad \text{[Eqn. B.1]}$$

Effect of liquid level, impeller speed and wet massing time on granule circularity from Chapter 4: Feasibility of "Steady state" Granulation

Liquid level: 24% Impeller speed: 245 rpm

Wet massing time (min)	HS Circularity mean	HS Circularity STDV	Number of granules characterized
0	0.458	0.141	163
5	0.468	0.129	211
15	0.493	0.140	133
30	0.501	0.134	130

Liquid level: 27% Impeller speed: 245 rpm

Wet massing time (min)	HS Circularity mean	HS Circularity STDV	Number of granules characterized
0	0.499	0.141	182
5	0.487	0.130	234
15	0.523	0.116	225
30	0.523	0.131	186

Liquid level: 30% Impeller speed: 245 rpm

Wet massing time (min)	HS Circularity mean	HS Circularity STDV	Number of granules characterized
0	0.535	0.121	106
5	0.557	0.113	132
15	0.575	0.111	162
30	0.622	0.127	207

Liquid level: 24% Impeller speed: 368 rpm

Wet massing time (min)	HS Circularity mean	HS Circularity STDV	Number of granules characterized
0	0.488	0.133	140
5	0.476	0.137	230
15	0.505	0.122	150
30	0.498	0.147	166

Liquid level: 27% Impeller speed: 368 rpm

Wet massing time (min)	HS Circularity mean	HS Circularity STDV	Number of granules characterized
0	0.467	0.123	114
5	0.520	0.117	100
15	0.523	0.118	185
30	0.601	0.117	136

Liquid level: 30% Impeller speed: 368 rpm

Wet massing time (min)	HS Circularity mean	HS Circularity STDV	Number of granules characterized
0	0.505	0.104	152
5	0.522	0.117	154
15	0.630	0.130	185
30	0.662	0.128	167

Liquid level: 24% Impeller speed: 490 rpm

Wet massing time (min)	HS Circularity mean	HS Circularity STDV	Number of granules characterized
0	0.486	0.123	184
5	0.481	0.130	208
15	0.513	0.147	142
30	0.469	0.131	181

Liquid level: 27% Impeller speed: 490 rpm

Wet massing time (min)	HS Circularity mean	HS Circularity STDV	Number of granules characterized
0	0.475	0.128	252
5	0.535	0.122	202
15	0.569	0.142	188
30	0.552	0.132	177

Liquid level: 30% Impeller speed: 490 rpm

Wet massing time (min)	HS Circularity mean	HS Circularity STDV	Number of granules characterized
0	0.558	0.111	179
5	0.597	0.137	229
15	0.676	0.133	244
30	0648	0.151	189

Effect of formulation on granule circularity from Chapter 6: Effect of Varying Formulation Composition on Granule Properties and Dissolution Profile

Wet massing time: 30 min Impeller speed: 490 rpm

Lactose/MCC (wt%/wt%)	Liquid level (%)	HS Circularity mean	HS Circularity STDV	Number of granules characterized
74 / 20	**30.0**	0.648	0.151	189
69 / 25	**30.0**	0.560	0.139	166
64 / 30	**30.0**	0.513	0.157	130
59 / 35	**30.0**	0.510	0.148	147
69 / 25	**35.0**	0.727	0.109	154
64 / 30	**40.0**	0.785	0.096	111
69 / 25	**32.5**	0.708	0.125	217
64 / 30	**35.0**	0.637	0.162	212
74 / 20[1]	**30.0**	0.865	0.079	132

Note: 1. Lactose was substituted with mannitol as the soluble pharmaceutical excipient

C. GRANULE BULK DENSITIES RAW DATA

Effect of wet massing time on granule bulk density from Chapter 4: Feasibility of "Steady state" Granulation

Amount of granules: 1.00 g Liquid level: 24% Impeller speed: 245 rpm

Wet massing time (min)	Poured volume (ml)			Tapped volume (ml)		
	1	2	3	1	2	3
0	2.90	2.90	2.90	2.40	2.40	2.40
5	2.70	2.60	2.60	2.20	2.20	2.20
15	2.60	2.60	2.60	2.10	2.10	2.10
30	2.60	2.60	2.60	2.10	2.00	2.10

Amount of granules: 1.00 g Liquid level: 30% Impeller speed: 245 rpm

Wet massing time (min)	Poured volume (ml)			Tapped volume (ml)		
	1	2	3	1	2	3
0	2.80	2.80	2.80	2.40	2.40	2.40
5	2.60	2.60	2.60	2.20	2.20	2.20
15	2.20	2.20	2.20	2.00	2.00	2.00
30	2.20	2.20	2.20	2.90	2.90	2.90

Amount of granules: 1.00 g Liquid level: 24% Impeller speed: 490 rpm

Wet massing time (min)	Poured volume (ml)			Tapped volume (ml)		
	1	2	3	1	2	3
0	3.00	3.00	3.00	2.50	2.50	2.50
5	3.00	2.80	2.80	2.30	2.30	2.30
15	2.70	2.70	2.70	2.20	2.20	2.20
30	2.50	2.60	2.60	2.10	2.00	2.10

Amount of granules: 1.00 g Liquid level: 30% Impeller speed: 490 rpm

Wet massing time (min)	Poured volume (ml)			Tapped volume (ml)		
	1	2	3	1	2	3
0	2.60	2.60	2.60	2.20	2.20	2.20
5	2.30	2.30	2.30	1.90	1.90	1.90
15	2.00	2.00	2.00	1.80	1.80	1.80
30	2.00	2.00	2.00	1.70	1.70	1.70

Effect of liquid level and impeller speed on granule bulk density from Chapter 4: Feasibility of "Steady state" Granulation

Amount of granules: 2.00 g Wet massing time: 30 min
Formulation: 74 wt% lactose, 20 wt% MCC, 3 wt% HPC and 3 wt% croscarmellose sodium

Liquid level (%)	Impeller speed (rpm)	Poured volume (ml)			Tapped volume (ml)		
		1	2	3	1	2	3
24	**245**	4.85	4.90	4.80	3.90	3.80	3.80
27	**245**	4.45	4.60	4.55	3.70	3.70	3.70
30	**245**	4.20	4.15	4.15	3.60	3.60	3.60
24	**368**	4.80	4.80	4.55	3.75	3.60	3.60
27	**368**	4.45	4.30	4.30	3.40	3.40	3.40
30	**368**	3.55	3.60	3.60	3.10	3.10	3.10
24	**490**	4.75	4.70	4.55	3.80	3.80	3.70
27	**490**	4.10	4.30	4.30	3.50	3.50	3.40
30	**490**	3.45	3.60	3.40	3.00	3.00	3.00

Effect of formulation on granule bulk density from Chapter 6: Effect of Varying Formulation Composition on Granule Properties and Dissolution Profile

Amount of granules: 2.00 g Wet massing time: 30 min
Impeller speed: 490 rpm

Lactose/MCC (wt%/wt%)	Liquid level (%)	Poured volume (ml)			Tapped volume (ml)		
		1	2	3	1	2	3
74 / 20	**30.0**	3.80	3.80	3.75	3.05	3.10	3.00
69 / 25	**30.0**	4.10	4.00	4.00	3.20	3.10	3.20
64 / 30	**30.0**	4.10	4.15	4.10	3.30	3.30	3.20
59 / 35	**30.0**	4.60	4.65	4.45	3.50	3.55	3.50
69 / 25	**35.0**	3.40	3.50	3.40	3.00	3.00	2.90
64 / 30	**40.0**	3.15	3.10	3.15	2.80	2.80	2.80
69 / 25	**32.5**	3.60	3.60	3.55	3.00	3.00	3.00
64 / 30	**35.0**	3.70	3.60	3.55	3.00	2.90	2.90
74 / 20[1]	**30.0**	3.50	3.40	3.45	3.00	3.00	3.00

Note: 1. Lactose was substituted with mannitol as the soluble pharmaceutical excipient

D. DISSOLUTION TESTING RAW DATA

The assumption made to construct the calibration curve for dissolution testing was the percentage of Rhodamine B released over time was the same as that of soluble components, lactose and HPC dissolved in the dissolution medium. A stock solution of 0.04 mg Rhodamine B/ml was prepared by dissolving 73.98 g of lactose, 3 g of HPC and 20 mg of Rhodamine B in 500 ml of deionized water. The stock solution was then diluted to make six solutions of different concentrations. Four different formulations were tested by varying the composition of lactose and MCC. A new calibration curve was constructed for every dissolution testing that was carried out on a different day.

Preparation of six solutions of different concentrations using Rhodamine B stock solution (0.04 mg/ml) for the construction of calibration curve:

No.	Stock solution (ml)	Deionized water (ml)	Amount of Rhodamine B (mg)	Concentration (mg/ml)
1	30	470	1.2	0.0024
2	25	475	1.0	0.0020
3	20	480	0.8	0.0016
4	15	485	0.6	0.0012
5	10	490	0.4	0.0008
6	5	495	0.2	0.0004

Four calibration curves constructed for the four different formulations tested:

Formulation composition		**A**		**B**		**C**		**D**	
Soluble components (%)		Lactose	HPC	Lactose	HPC	Lactose	HPC	Lactose	HPC
		73.98	3	68.98	3	63.98	3	58.98	3
Rhodamine B solution		**Amount dissolved (mg)**							
No.	**%**								
1	120	4438.8	180	4138.8	180	3838.8	180	3538.8	180
2	100	3699.0	150	3449.0	150	3199.0	150	2949.0	150
3	80	2959.2	120	2759.2	120	2559.2	120	2359.2	120
4	60	2219.4	90	2069.4	90	1919.4	90	1769.4	90
5	40	1479.6	60	1379.6	60	1279.6	60	1179.6	60

A sample calculation to determine the percentage released of Rhodamine B over time is shown as below:

Time (min)	Optical density				Conc. of extracted solution (mg/ml)	Amount of RhoB extracted (mg)	Amount of RhoB in dissolution bath (mg)	Cumulative release of RhoB (mg)	% released
	1	2	3	Ave					
5					$w1$	$w1 \times 2\ ml = x1$	$w1 \times 50\ ml = y1$	$y1 = z1$	$z1/z5 \times 100\%$
10					$w2$	$w2 \times 2\ ml = x2$	$w2 \times 50\ ml = y2$	$x1 + y2 = z2$	$z2/z5 \times 100\%$
15					$w3$	$w3 \times 2\ ml = x3$	$w3 \times 50\ ml = y3$	$x1 + x2 + y3 = z3$	$z3/z5 \times 100\%$
30					$w4$	$w4 \times 2\ ml = x4$	$w4 \times 50\ ml = y4$	$x1 + x2 + x3 + y4 = z4$	$z4/z5 \times 100\%$
60					$w5$	$w5 \times 2\ ml = x5$	$w5 \times 50\ ml = y5$	$x1 + x2 + x3 + x4 + y5 = z5$	$z5/z5 \times 100\%$

Effect of operating conditions on the dissolution properties of "steady state" granules from Chapter 5: Dissolution Performance of "Steady State" Granules

A1. Calibration curve for the formulation: 74 wt% lactose, 20 wt% MCC, 3 wt% HPC and 3 wt% croscarmellose sodium

Concentration of Rhodamine B (mg/ml)	Optical density		
	1	2	3
2.4×10^{-3}	0.406	0.398	0.403
2.0×10^{-3}	0.357	0.358	0.351
1.6×10^{-3}	0.338	0.337	0.308
1.2×10^{-3}	0.272	0.252	0.274
0.8×10^{-3}	0.231	0.215	0.225
0.4×10^{-3}	0.193	0.182	0.170
0	0.138	0.143	0.131

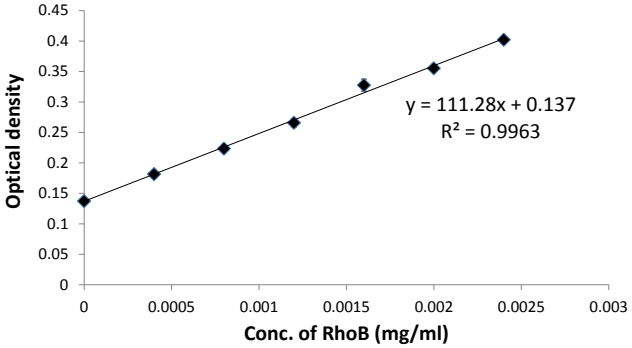

Liquid level: 24% Impeller speed: 245 rpm Wet massing time: 30 min

Dissolution Testing 1 Amount of granules: 500.2 mg

Time (min)	Optical density				Conc. of extracted solution (mg/ml)	Amount of RhoB extracted (mg)	Amount of RhoB in dissolution bath (mg)	Cumulative release of RhoB (mg)	% released
	1	2	3	Ave					
5	0.219	0.209	0.212	0.213	0.00069	0.00137	0.0343	0.0343	34.1
10	0.240	0.258	0.260	0.253	0.00104	0.00208	0.0520	0.0533	53.0
15	0.279	0.275	0.277	0.277	0.00126	0.00252	0.0629	0.0664	65.9
30	0.332	0.318	0.328	0.326	0.00170	0.00340	0.0849	0.0909	90.2
60	0.338	0.343	0.340	0.340	0.00183	0.00365	0.0914	**0.1007**	100.0

Dissolution Testing 2 Amount of granules: 500.5 mg

Time (min)	Optical density				Conc. of extracted solution (mg/ml)	Amount of RhoB extracted (mg)	Amount of RhoB in dissolution bath (mg)	Cumulative release of RhoB (mg)	% released
	1	2	3	Ave					
5	0.205	0.201	0.203	0.203	0.00059	0.00119	0.0297	0.0297	28.0
10	0.229	0.225	0.247	0.234	0.00087	0.00174	0.0434	0.0446	42.1
15	0.254	0.255	0.271	0.260	0.00111	0.00221	0.0553	0.0582	55.0
30	0.307	0.319	0.302	0.309	0.00155	0.00310	0.0774	0.0826	78.0
60	0.353	0.362	0.348	0.354	0.00195	0.00391	0.0977	**0.1059**	100.0

Dissolution Testing 3 Amount of granules: 500.1 mg

Time (min)	Optical density				Conc. of extracted solution (mg/ml)	Amount of RhoB extracted (mg)	Amount of RhoB in dissolution bath (mg)	Cumulative release of RhoB (mg)	% released
	1	2	3	Ave					
5	0.246	0.222	0.233	0.234	0.00087	0.00174	0.0434	0.0434	41.4
10	0.258	0.282	0.264	0.268	0.00118	0.00235	0.0589	0.0606	57.7
15	0.289	0.288	0.304	0.294	0.00141	0.00282	0.0704	0.0745	70.9
30	0.352	0.338	0.343	0.344	0.00186	0.00373	0.0932	0.10007	95.3
60	0.357	0.341	0.343	0.347	0.00189	0.00377	0.0944	**0.10499**	100.0

Time (min)	% released			
	1	2	3	Ave
5	34.1	28.0	41.4	34.5
10	53.0	42.1	57.7	50.9
15	65.9	55.0	70.9	63.9
30	90.2	78.0	95.3	87.8
60	100.0	100.0	100.0	100.0

Liquid level: 24% Impeller speed: 490 rpm Wet massing time: 30 min

Dissolution Testing 1 Amount of granules: 500.6 mg

Time (min)	Optical density				Conc. of extracted solution (mg/ml)	Amount of RhoB extracted (mg)	Amount of RhoB in dissolution bath (mg)	Cumulative release of RhoB (mg)	% released
	1	2	3	Ave					
5	0.283	0.262	0.252	0.266	0.00116	0.00231	0.0578	0.0578	49.4
10	0.300	0.308	0.302	0.303	0.00150	0.00299	0.0747	0.0770	65.9
15	0.346	0.344	0.336	0.342	0.00184	0.00368	0.0921	0.0974	83.3
30	0.349	0.347	0.355	0.350	0.00192	0.00383	0.0959	0.1048	89.7
60	0.371	0.385	0.350	0.369	0.00208	0.00416	0.1041	**0.1169**	100.0

Dissolution Testing 2 Amount of granules: 500.6 mg

Time (min)	Optical density				Conc. of extracted solution (mg/ml)	Amount of RhoB extracted (mg)	Amount of RhoB in dissolution bath (mg)	Cumulative release of RhoB (mg)	% released
	1	2	3	Ave					
5	0.267	0.291	0.273	0.277	0.00126	0.00252	0.0629	0.0629	55.9
10	0.336	0.328	0.333	0.332	0.00176	0.00351	0.0878	0.0903	80.2
15	0.346	0.333	0.340	0.340	0.00182	0.00364	0.0911	0.0972	86.2
30	0.337	0.348	0.332	0.339	0.00182	0.00363	0.0908	0.1004	89.2
60	0.354	0.370	0.350	0.358	0.00199	0.00397	0.0993	**0.1126**	100.0

Dissolution Testing 3 Amount of granules: 500.3 mg

Time (min)	Optical density				Conc. of extracted solution (mg/ml)	Amount of RhoB extracted (mg)	Amount of RhoB in dissolution bath (mg)	Cumulative release of RhoB (mg)	% released
	1	2	3	Ave					
5	0.242	0.236	0.234	0.237	0.00090	0.00180	0.0451	0.0451	40.5
10	0.270	0.276	0.275	0.274	0.00123	0.00246	0.0614	0.0632	56.8
15	0.306	0.300	0.303	0.303	0.00149	0.00298	0.0746	0.0788	70.8
30	0.370	0.351	0.369	0.363	0.00203	0.00407	0.1016	0.1089	97.8
60	0.362	0.356	0.361	0.360	0.00200	0.00400	0.1000	**0.1114**	100.0

Time (min)	% released			
	1	2	3	Ave
5	49.4	55.9	40.5	48.6
10	65.9	80.2	56.8	65.8
15	83.3	86.2	70.8	79.2
30	89.7	89.2	97.8	90.9
60	100.0	100.0	100.0	100

A2. Calibration curve for the formulation: 74 wt% lactose, 20 wt% MCC, 3 wt% HPC and 3 wt% croscarmellose sodium

Concentration of Rhodamine B (mg/ml)	Optical density		
	1	2	3
2.4×10^{-3}	0.454	0.453	0.436
2.0×10^{-3}	0.384	0.388	0.388
1.6×10^{-3}	0.341	0.336	0.357
1.2×10^{-3}	0.299	0.292	0.313
0.8×10^{-3}	0.254	0.261	0.252
0.4×10^{-3}	0.204	0.243	0.199
0	0.173	0.17	0.168

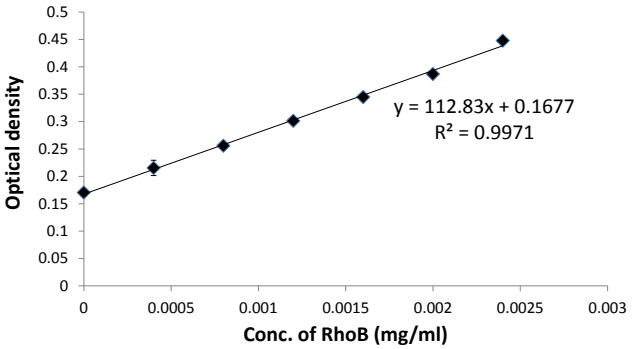

Liquid level: 30% Impeller speed: 245 rpm Wet massing time: 30 min

Dissolution Testing 1 Amount of granules: 500.5 mg

Time (min)	Optical density				Conc. of extracted solution (mg/ml)	Amount of RhoB extracted (mg)	Amount of RhoB in dissolution bath (mg)	Cumulative release of RhoB (mg)	% released
	1	2	3	Ave					
5	0.332	0.317	0.322	0.324	0.00138	0.00276	0.0691	0.0691	64.0
10	0.393	0.387	0.39	0.390	0.00197	0.00394	0.0985	0.1013	93.8
15	0.39	0.387	0.385	0.387	0.00195	0.00389	0.0973	0.1040	96.4
30	0.385	0.386	0.386	0.386	0.00193	0.00386	0.0966	0.1072	99.3
60	0.38	0.378	0.378	0.379	0.00187	0.00374	0.0935	**0.1080**	100.0

Dissolution Testing 2 Amount of granules: 500.8 mg

Time (min)	Optical density				Conc. of extracted solution (mg/ml)	Amount of RhoB extracted (mg)	Amount of RhoB in dissolution bath (mg)	Cumulative release of RhoB (mg)	% released
	1	2	3	Ave					
5	0.346	0.35	0.346	0.347	0.00159	0.00318	0.0796	0.0796	74.3
10	0.382	0.395	0.383	0.387	0.00194	0.00388	0.0970	0.1002	93.6
15	0.387	0.382	0.384	0.384	0.00192	0.00384	0.0960	0.1031	96.2
30	0.384	0.377	0.376	0.379	0.00187	0.00375	0.0936	0.1045	97.6
60	0.376	0.38	0.373	0.376	0.00185	0.00370	0.0925	**0.1071**	100.0

Dissolution Testing 3 Amount of granules: 500.4 mg

Time (min)	Optical density				Conc. of extracted solution (mg/ml)	Amount of RhoB extracted (mg)	Amount of RhoB in dissolution bath (mg)	Cumulative release of RhoB (mg)	% released
	1	2	3	Ave					
5	0.343	0.335	0.343	0.340	0.00153	0.00306	0.0765	0.0765	70.0
10	0.387	0.377	0.383	0.382	0.00190	0.00380	0.0951	0.0982	89.8
15	0.382	0.38	0.381	0.381	0.00189	0.00378	0.0945	0.1014	92.7
30	0.382	0.377	0.376	0.378	0.00187	0.00373	0.0933	0.1040	95.1
60	0.379	0.379	0.388	0.382	0.00190	0.00380	0.0950	**0.1093**	100.0

Time (min)	% released			
	1	2	3	Ave
5	64.0	74.3	70.0	69.4
10	93.8	93.6	89.8	92.4
15	96.4	96.2	92.7	95.1
30	99.3	97.6	95.1	97.3
60	100.0	100.0	100.0	100

A3. Calibration curve for the formulation: 74 wt% lactose, 20 wt% MCC, 3 wt% HPC and 3 wt% croscarmellose sodium

Concentration of Rhodamine B (mg/ml)	Optical density		
	1	2	3
2.4×10^{-3}	0.439	0.429	0.438
2.0×10^{-3}	0.380	0.407	0.404
1.6×10^{-3}	0.350	0.359	0.335
1.2×10^{-3}	0.322	0.313	0.303
0.8×10^{-3}	0.282	0.280	0.265
0.4×10^{-3}	0.234	0.222	0.220
0	0.171	0.165	0.176

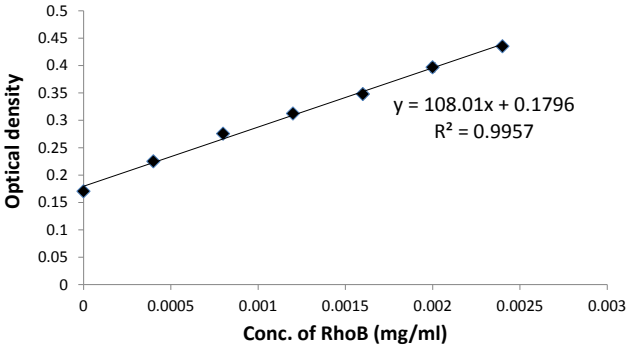

Liquid level: 30% Impeller speed: 490 rpm Wet massing time: 30 min

Dissolution Testing 1 Amount of granules: 500.4 mg

Time (min)	Optical density				Conc. of extracted solution (mg/ml)	Amount of RhoB extracted (mg)	Amount of RhoB in dissolution bath (mg)	Cumulative release of RhoB (mg)	% released
	1	2	3	Ave					
5	0.348	0.346	0.345	0.346	0.00154	0.00309	0.0772	0.0772	73.3
10	0.387	0.385	0.387	0.386	0.00191	0.00383	0.0957	0.0988	93.8
15	0.385	0.387	0.379	0.384	0.00189	0.00378	0.0945	0.1014	96.3
30	0.390	0.363	0.378	0.377	0.00183	0.00366	0.0914	0.1021	97.0
60	0.379	0.376	0.373	0.376	0.00182	0.00364	0.0909	**0.1053**	100.0

Dissolution Testing 2 Amount of granules: 500.5 mg

Time (min)	Optical density				Conc. of extracted solution (mg/ml)	Amount of RhoB extracted (mg)	Amount of RhoB in dissolution bath (mg)	Cumulative release of RhoB (mg)	% released
	1	2	3	Ave					
5	0.331	0.356	0.345	0.344	0.00152	0.00304	0.0761	0.0761	70.3
10	0.380	0.372	0.396	0.383	0.00188	0.00376	0.0940	0.0970	89.7
15	0.378	0.372	0.378	0.376	0.00182	0.00364	0.0909	0.0977	90.3
30	0.383	0.386	0.377	0.382	0.00187	0.00375	0.0937	0.1041	96.3
60	0.387	0.389	0.372	0.383	0.00188	0.00376	0.0940	**0.1082**	100.0

Dissolution Testing 3 Amount of granules: 500.4 mg

Time (min)	Optical density				Conc. of extracted solution (mg/ml)	Amount of RhoB extracted (mg)	Amount of RhoB in dissolution bath (mg)	Cumulative release of RhoB (mg)	% released
	1	2	3	Ave					
5	0.378	0.372	0.381	0.377	0.00183	0.00366	0.0914	0.0914	88.5
10	0.374	0.386	0.378	0.379	0.00185	0.00370	0.0925	0.0961	93.1
15	0.366	0.365	0.375	0.369	0.00175	0.00350	0.0875	0.0949	91.9
30	0.375	0.357	0.367	0.366	0.00173	0.00346	0.0864	0.0973	94.3
60	0.373	0.371	0.371	0.372	0.00178	0.00356	0.0889	**0.1032**	100.0

Time (min)	% released			
	1	2	3	Ave
5	73.3	70.3	88.5	77.4
10	93.8	89.7	93.1	92.2
15	96.3	90.3	91.9	92.8
30	97.0	96.3	94.3	95.8
60	100.0	100.0	100.0	100.0

Effect of formulation on dissolution performance of "steady state" granules from Chapter 6: Effect of Varying Formulation Composition on Granule Properties

B1. Calibration curve for the formulation: 69 wt% lactose, 25 wt% MCC, 3 wt% HPC and 3 wt% croscarmellose sodium

Concentration of Rhodamine B (mg/ml)	Optical density		
	1	2	3
2.4×10^{-3}	0.407	0.399	0.411
2.0×10^{-3}	0.359	0.357	0.353
1.6×10^{-3}	0.310	0.304	0.307
1.2×10^{-3}	0.282	0.261	0.278
0.8×10^{-3}	0.252	0.228	0.239
0.4×10^{-3}	0.189	0.195	0.191
0	0.150	0.133	0.151

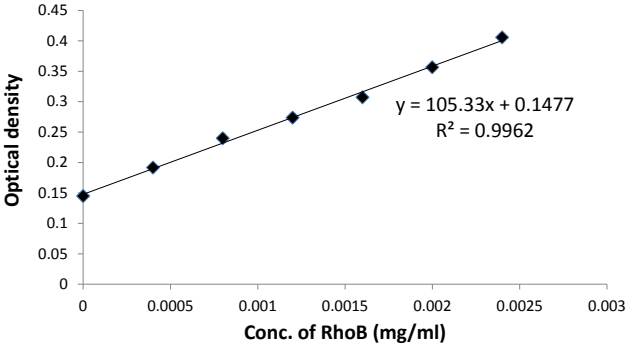

Liquid level: 30% Impeller speed: 490 rpm Wet massing time: 30 min

Dissolution Testing 1 Amount of granules: 500.4 mg

Time (min)	Optical density				Conc. of extracted solution (mg/ml)	Amount of RhoB extracted (mg)	Amount of RhoB in dissolution bath (mg)	Cumulative release of RhoB (mg)	% released
	1	2	3	Ave					
5	0.303	0.321	0.327	0.317	0.00161	0.00321	0.0804	0.0804	73.0
10	0.365	0.350	0.347	0.354	0.00196	0.00392	0.0979	0.1011	91.9
15	0.346	0.339	0.336	0.340	0.00183	0.00366	0.0914	0.0986	89.5
30	0.350	0.337	0.345	0.344	0.00186	0.00373	0.0932	0.1040	94.5
60	0.348	0.355	0.344	0.349	0.00191	0.00382	0.0956	**0.1101**	100.0

Dissolution Testing 2 Amount of granules: 500.5 mg

Time (min)	Optical density				Conc. of extracted solution (mg/ml)	Amount of RhoB extracted (mg)	Amount of RhoB in dissolution bath (mg)	Cumulative release of RhoB (mg)	% released
	1	2	3	Ave					
5	0.342	0.342	0.371	0.352	0.00194	0.00387	0.0968	0.0968	87.4
10	0.372	0.364	0.361	0.366	0.00207	0.00414	0.1035	0.1073	96.8
15	0.337	0.347	0.342	0.342	0.00184	0.00369	0.0922	0.1002	90.4
30	0.327	0.335	0.346	0.336	0.00179	0.00358	0.0894	0.1011	91.2
60	0.346	0.346	0.355	0.349	0.00191	0.00382	0.0956	**0.1108**	100.0

Dissolution Testing 3 Amount of granules: 500.4 mg

Time (min)	Optical density				Conc. of extracted solution (mg/ml)	Amount of RhoB extracted (mg)	Amount of RhoB in dissolution bath (mg)	Cumulative release of RhoB (mg)	% released
	1	2	3	Ave					
5	0.274	0.297	0.276	0.282	0.00128	0.00256	0.0639	0.0639	55.0
10	0.320	0.338	0.337	0.332	0.00175	0.00349	0.0873	0.0899	77.3
15	0.355	0.344	0.360	0.353	0.00195	0.00390	0.0975	0.1035	89.0
30	0.367	0.333	0.365	0.355	0.00197	0.00394	0.0984	0.1084	93.2
60	0.356	0.361	0.373	0.363	0.00205	0.00409	0.1023	**0.1162**	100.0

Time (min)	% released			
	1	2	3	Ave
5	73.0	87.4	55.0	71.8
10	91.9	96.8	77.3	88.7
15	89.5	90.4	89.0	89.7
30	94.5	91.2	93.2	93.0
60	100.0	100.0	100.0	100.0

Liquid level: 32.5% Impeller speed: 490 rpm Wet massing time: 30 min

Dissolution Testing 1 Amount of granules: 500.8 mg

Time (min)	Optical density				Conc. of extracted solution (mg/ml)	Amount of RhoB extracted (mg)	Amount of RhoB in dissolution bath (mg)	Cumulative release of RhoB (mg)	% released
	1	2	3	Ave					
5	0.268	0.262	0.256	0.262	0.00109	0.00217	0.0543	0.0543	50.1
10	0.310	0.311	0.308	0.310	0.00154	0.00308	0.0769	0.0791	73.0
15	0.345	0.338	0.340	0.341	0.00184	0.00367	0.0918	0.0970	89.6
30	0.357	0.342	0.350	0.350	0.00192	0.00383	0.0959	0.1048	96.8
60	0.350	0.351	0.346	0.349	0.00191	0.00382	0.0956	**0.1083**	100.0

Dissolution Testing 2 Amount of granules: 500.8 mg

Time (min)	Optical density				Conc. of extracted solution (mg/ml)	Amount of RhoB extracted (mg)	Amount of RhoB in dissolution bath (mg)	Cumulative release of RhoB (mg)	% released
	1	2	3	Ave					
5	0.303	0.309	0.305	0.306	0.00150	0.00300	0.0750	0.0750	67.2
10	0.357	0.347	0.354	0.353	0.00195	0.00390	0.0973	0.1003	89.8
15	0.345	0.340	0.339	0.341	0.00184	0.00368	0.0919	0.0988	88.5
30	0.334	0.349	0.334	0.339	0.00182	0.00363	0.0908	0.1014	90.8
60	0.346	0.355	0.358	0.353	0.00195	0.00390	0.0975	**0.1117**	100.0

Dissolution Testing 3 Amount of granules: 500.8 mg

Time (min)	Optical density				Conc. of extracted solution (mg/ml)	Amount of RhoB extracted (mg)	Amount of RhoB in dissolution bath (mg)	Cumulative release of RhoB (mg)	% released
	1	2	3	Ave					
5	0.325	0.330	0.331	0.329	0.00172	0.00344	0.0859	0.0859	79.3
10	0.356	0.356	0.353	0.355	0.00197	0.00394	0.0984	0.1018	94.0
15	0.353	0.356	0.353	0.354	0.00196	0.00391	0.0979	0.1053	97.2
30	0.349	0.332	0.348	0.343	0.00185	0.00371	0.0927	0.1040	96.0
60	0.343	0.348	0.342	0.344	0.00187	0.00373	0.0933	**0.1083**	100.0

Time (min)	% released			
	1	2	3	Ave
5	50.1	67.2	79.3	65.5
10	73.0	89.8	94.0	85.6
15	89.6	88.5	97.2	91.8
30	96.8	90.8	96.0	94.5
60	100.0	100.0	100.0	100.0

B2. Calibration curve for the formulation: 69 wt% lactose, 25 wt% MCC, 3 wt% HPC and 3 wt% croscarmellose sodium

Concentration of Rhodamine B (mg/ml)	Optical density		
	1	2	3
2.4×10^{-3}	0.429	0.431	0.433
2.0×10^{-3}	0.382	0.382	0.378
1.6×10^{-3}	0.339	0.343	0.332
1.2×10^{-3}	0.319	0.283	0.292
0.8×10^{-3}	0.250	0.242	0.246
0.4×10^{-3}	0.198	0.204	0.198
0	0.168	0.161	0.171

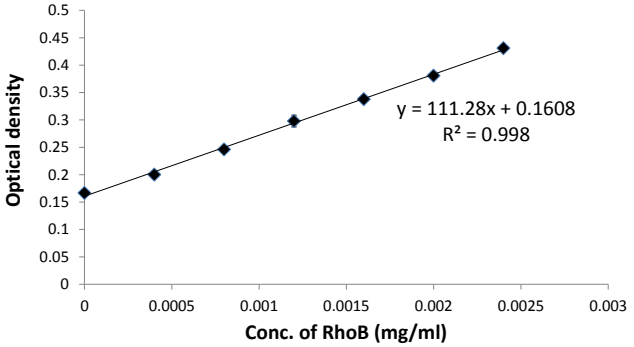

Liquid level: 35% Impeller speed: 490 rpm Wet massing time: 30 min

Dissolution Testing 1 Amount of granules: 500.3 mg

Time (min)	Optical density				Conc. of extracted solution (mg/ml)	Amount of RhoB extracted (mg)	Amount of RhoB in dissolution bath (mg)	Cumulative release of RhoB (mg)	% released
	1	2	3	Ave					
5	0.413	0.398	0.397	0.403	0.00217	0.00435	0.1087	0.1087	86.7
10	0.413	0.411	0.403	0.409	0.00223	0.00446	0.1115	0.1159	92.4
15	0.404	0.402	0.405	0.404	0.00218	0.00436	0.1091	0.1179	94.1
30	0.400	0.396	0.400	0.399	0.00214	0.00428	0.1069	0.1201	95.8
60	0.401	0.405	0.397	0.401	0.00216	0.00432	0.1079	**0.1254**	100.0

Dissolution Testing 2 Amount of granules: 500.2 mg

Time (min)	Optical density				Conc. of extracted solution (mg/ml)	Amount of RhoB extracted (mg)	Amount of RhoB in dissolution bath (mg)	Cumulative release of RhoB (mg)	% released
	1	2	3	Ave					
5	0.393	0.389	0.391	0.391	0.00207	0.00414	0.1034	0.1034	80.6
10	0.402	0.403	0.406	0.404	0.00218	0.00436	0.1091	0.1133	88.2
15	0.400	0.401	0.399	0.400	0.00215	0.00430	0.1075	0.1160	90.3
30	0.405	0.405	0.401	0.404	0.00218	0.00436	0.1091	0.1219	95.0
60	0.405	0.412	0.408	0.408	0.00222	0.00445	0.1112	**0.1284**	100.0

Dissolution Testing 3 Amount of granules: 500.6 mg

Time (min)	Optical density				Conc. of extracted solution (mg/ml)	Amount of RhoB extracted (mg)	Amount of RhoB in dissolution bath (mg)	Cumulative release of RhoB (mg)	% released
	1	2	3	Ave					
5	0.369	0.362	0.377	0.369	0.00187	0.00375	0.0937	0.0937	72.8
10	0.409	0.405	0.412	0.409	0.00222	0.00445	0.1114	0.1151	89.5
15	0.407	0.409	0.413	0.410	0.00224	0.00447	0.1118	0.1200	93.3
30	0.408	0.404	0.412	0.408	0.00222	0.00444	0.1111	0.1237	96.2
60	0.404	0.407	0.416	0.409	0.00223	0.00446	0.1115	**0.1286**	100.0

Time (min)	% released			
	1	2	3	Ave
5	86.7	80.6	72.8	80.0
10	92.4	88.2	89.5	90.0
15	94.1	90.3	93.3	92.6
30	95.8	95.0	96.2	95.6
60	100.0	100.0	100.0	100.0

C1. Calibration curve for the formulation: 64 wt% lactose, 30 wt% MCC, 3 wt% HPC and 3 wt% croscarmellose sodium

Concentration of Rhodamine B (mg/ml)	Optical density		
	1	2	3
2.4×10^{-3}	0.417	0.41	0.403
2.0×10^{-3}	0.363	0.363	0.362
1.6×10^{-3}	0.315	0.307	0.308
1.2×10^{-3}	0.285	0.260	0.273
0.8×10^{-3}	0.239	0.232	0.227
0.4×10^{-3}	0.183	0.181	0.179
0	0.138	0.130	0.143

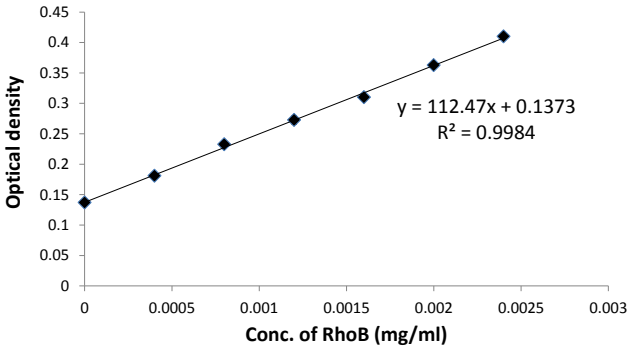

Liquid level: 30% Impeller speed: 490 rpm Wet massing time: 30 min

Dissolution Testing 1 Amount of granules: 500.2 mg

Time (min)	Optical density				Conc. of extracted solution (mg/ml)	Amount of RhoB extracted (mg)	Amount of RhoB in dissolution bath (mg)	Cumulative release of RhoB (mg)	% released
	1	2	3	Ave					
5	0.266	0.270	0.274	0.270	0.00118	0.00236	0.0590	0.0590	57.1
10	0.315	0.320	0.317	0.317	0.00160	0.00320	0.0800	0.0824	79.8
15	0.344	0.341	0.336	0.340	0.00181	0.00361	0.0903	0.0958	92.8
30	0.347	0.343	0.346	0.345	0.00185	0.00370	0.0925	0.1017	98.4
60	0.341	0.337	0.344	0.341	0.00181	0.00362	0.0904	**0.1033**	100.0

Dissolution Testing 2 Amount of granules: 500.7 mg

Time (min)	Optical density				Conc. of extracted solution (mg/ml)	Amount of RhoB extracted (mg)	Amount of RhoB in dissolution bath (mg)	Cumulative release of RhoB (mg)	% released
	1	2	3	Ave					
5	0.263	0.266	0.260	0.263	0.00112	0.00224	0.0559	0.0559	57.4
10	0.320	0.312	0.317	0.316	0.00159	0.00318	0.0796	0.0818	84.0
15	0.331	0.330	0.333	0.331	0.00173	0.00345	0.0863	0.0917	94.2
30	0.320	0.326	0.319	0.322	0.00164	0.00328	0.0820	0.0908	93.3
60	0.319	0.348	0.320	0.329	0.00170	0.00341	0.0852	**0.0974**	100.0

Dissolution Testing 3 Amount of granules: 500.4 mg

Time (min)	Optical density				Conc. of extracted solution (mg/ml)	Amount of RhoB extracted (mg)	Amount of RhoB in dissolution bath (mg)	Cumulative release of RhoB (mg)	% released
	1	2	3	Ave					
5	0.245	0.239	0.244	0.243	0.00094	0.00187	0.0468	0.0468	46.0
10	0.279	0.311	0.292	0.294	0.00139	0.00279	0.0697	0.0715	70.3
15	0.310	0.315	0.314	0.313	0.00156	0.00312	0.0781	0.0828	81.3
30	0.325	0.329	0.337	0.330	0.00172	0.00343	0.0858	0.0936	92.0
60	0.344	0.343	0.336	0.341	0.00181	0.00362	0.0906	**0.1018**	100.0

Time (min)	% released			
	1	2	3	Ave
5	57.1	57.4	46.0	53.5
10	79.8	84.0	70.3	78.0
15	92.8	94.2	81.3	89.4
30	98.4	93.3	92.0	94.6
60	100.0	100.0	100.0	100.0

Liquid level: 35% Impeller speed: 490 rpm Wet massing time: 30 min

Dissolution Testing 1 Amount of granules: 500.8 mg

Time (min)	Optical density				Conc. of extracted solution (mg/ml)	Amount of RhoB extracted (mg)	Amount of RhoB in dissolution bath (mg)	Cumulative release of RhoB (mg)	% released
	1	2	3	Ave					
5	0.254	0.252	0.261	0.256	0.00105	0.00210	0.0526	0.0526	52.3
10	0.305	0.307	0.313	0.308	0.00152	0.00304	0.0760	0.0781	77.7
15	0.334	0.327	0.333	0.331	0.00173	0.00345	0.0863	0.0914	90.8
30	0.331	0.323	0.329	0.328	0.00169	0.00339	0.0846	0.0932	92.7
60	0.331	0.332	0.347	0.337	0.00177	0.00355	0.0886	**0.1006**	100.0

Dissolution Testing 2 Amount of granules: 500.7 mg

Time (min)	Optical density				Conc. of extracted solution (mg/ml)	Amount of RhoB extracted (mg)	Amount of RhoB in dissolution bath (mg)	Cumulative release of RhoB (mg)	% released
	1	2	3	Ave					
5	0.240	0.257	0.265	0.254	0.00104	0.00208	0.0519	0.0519	47.3
10	0.287	0.301	0.317	0.302	0.00146	0.00292	0.0731	0.0751	68.6
15	0.346	0.339	0.341	0.342	0.00182	0.00364	0.0910	0.0960	87.6
30	0.357	0.344	0.364	0.355	0.00194	0.00387	0.0968	0.1054	96.2
60	0.363	0.352	0.352	0.356	0.00194	0.00388	0.0971	**0.1096**	100.0

Dissolution Testing 3 Amount of granules: 500.7 mg

Time (min)	Optical density				Conc. of extracted solution (mg/ml)	Amount of RhoB extracted (mg)	Amount of RhoB in dissolution bath (mg)	Cumulative release of RhoB (mg)	% released
	1	2	3	Ave					
5	0.243	0.259	0.262	0.255	0.00104	0.00209	0.0522	0.0522	50.7
10	0.312	0.303	0.302	0.306	0.00150	0.00299	0.0748	0.0769	74.8
15	0.323	0.336	0.336	0.332	0.00173	0.00346	0.0864	0.0915	88.9
30	0.353	0.324	0.352	0.343	0.00183	0.00366	0.0914	0.1000	97.2
60	0.348	0.339	0.337	0.341	0.00181	0.00363	0.0907	**0.1029**	100.0

Time (min)	% released			
	1	2	3	Ave
5	52.3	47.3	50.7	50.1
10	77.7	68.6	74.8	73.7
15	90.8	87.6	88.9	89.1
30	92.7	96.2	97.2	95.3
60	100.0	100.0	100.0	100.0

C2. Calibration curve for the formulation: 64 wt% lactose, 30 wt% MCC, 3 wt% HPC and 3 wt% croscarmellose sodium

Concentration of Rhodamine B (mg/ml)	Optical density		
	1	2	3
2.4×10^{-3}	0.428	0.438	0.436
2.0×10^{-3}	0.381	0.386	0.380
1.6×10^{-3}	0.340	0.342	0.342
1.2×10^{-3}	0.298	0.312	0.299
0.8×10^{-3}	0.256	0.275	0.252
0.4×10^{-3}	0.196	0.193	0.192
0	0.171	0.163	0.165

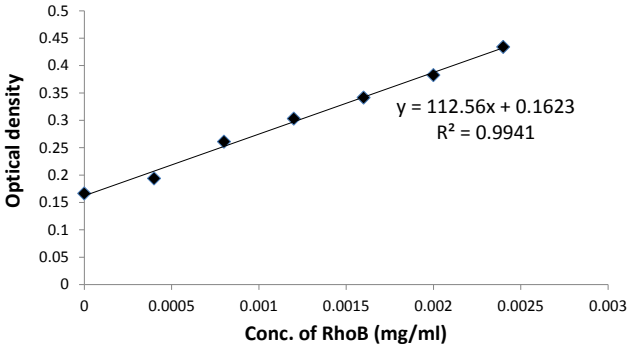

Liquid level: 40% Impeller speed: 490 rpm Wet massing time: 30 min

Dissolution Testing 1 Amount of granules: 500.7 mg

Time (min)	Optical density				Conc. of extracted solution (mg/ml)	Amount of RhoB extracted (mg)	Amount of RhoB in dissolution bath (mg)	Cumulative release of RhoB (mg)	% released
	1	2	3	Ave					
5	0.392	0.387	0.390	0.390	0.00202	0.00404	0.1010	0.1010	90.7
10	0.385	0.390	0.387	0.387	0.00200	0.00400	0.1000	0.1040	93.4
15	0.382	0.376	0.377	0.378	0.00192	0.00384	0.0960	0.1040	93.4
30	0.382	0.369	0.376	0.376	0.00190	0.00379	0.0948	0.1067	95.8
60	0.388	0.372	0.373	0.378	0.00191	0.00383	0.0957	**0.1113**	100.0

Dissolution Testing 2 Amount of granules: 500.8 mg

Time (min)	Optical density				Conc. of extracted solution (mg/ml)	Amount of RhoB extracted (mg)	Amount of RhoB in dissolution bath (mg)	Cumulative release of RhoB (mg)	% released
	1	2	3	Ave					
5	0.361	0.367	0.374	0.367	0.00182	0.00364	0.0911	0.0911	81.5
10	0.372	0.382	0.375	0.376	0.00190	0.00380	0.0951	0.0987	88.4
15	0.371	0.372	0.373	0.372	0.00186	0.00373	0.0932	0.1006	90.0
30	0.377	0.370	0.366	0.371	0.00185	0.00371	0.0927	0.1039	93.0
60	0.389	0.371	0.381	0.380	0.00194	0.00387	0.0969	**0.1117**	100.0

Dissolution Testing 3 Amount of granules: 500.8 mg

Time (min)	Optical density				Conc. of extracted solution (mg/ml)	Amount of RhoB extracted (mg)	Amount of RhoB in dissolution bath (mg)	Cumulative release of RhoB (mg)	% released
	1	2	3	Ave					
5	0.373	0.372	0.375	0.373	0.00187	0.00375	0.0937	0.0937	84.0
10	0.377	0.383	0.374	0.378	0.00192	0.00383	0.0958	0.0996	89.2
15	0.366	0.373	0.365	0.368	0.00183	0.00365	0.0914	0.0990	88.6
30	0.365	0.357	0.366	0.363	0.00178	0.00356	0.0890	0.1002	89.8
60	0.371	0.379	0.391	0.380	0.00194	0.00387	0.0969	**0.1116**	100.0

Time (min)	% released			
	1	2	3	Ave
5	90.7	81.5	84.0	85.4
10	93.4	88.4	89.2	90.3
15	93.4	90.0	88.6	90.7
30	95.8	93.0	89.8	92.8
60	100.0	100.0	100.0	100.0

D1. Calibration curve for the formulation: 59 wt% lactose, 35 wt% MCC, 3 wt% HPC and 3 wt% croscarmellose sodium

Concentration of Rhodamine B (mg/ml)	Optical density		
	1	2	3
2.4×10^{-3}	0.395	0.394	0.396
2.0×10^{-3}	0.348	0.336	0.334
1.6×10^{-3}	0.315	0.301	0.307
1.2×10^{-3}	0.266	0.266	0.296
0.8×10^{-3}	0.214	0.225	0.225
0.4×10^{-3}	0.174	0.176	0.188
0	0.158	0.146	0.135

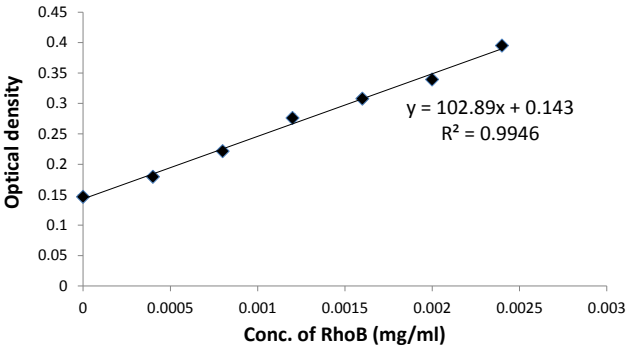

Liquid level: 30% Impeller speed: 490 rpm Wet massing time: 30 min

Dissolution Testing 1 Amount of granules: 500.5 mg

Time (min)	Optical density				Conc. of extracted solution (mg/ml)	Amount of RhoB extracted (mg)	Amount of RhoB in dissolution bath (mg)	Cumulative release of RhoB (mg)	% released
	1	2	3	Ave					
5	0.236	0.237	0.238	0.237	0.00091	0.00183	0.0457	0.0457	41.3
10	0.275	0.284	0.276	0.278	0.00132	0.00263	0.0658	0.0676	61.1
15	0.317	0.306	0.304	0.309	0.00161	0.00323	0.0807	0.0851	76.9
30	0.346	0.334	0.342	0.341	0.00192	0.00384	0.0961	0.1037	93.7
60	0.346	0.348	0.347	0.347	0.00198	0.00397	0.0991	**0.1107**	100.0

Dissolution Testing 2 Amount of granules: 500.2 mg

Time (min)	Optical density				Conc. of extracted solution (mg/ml)	Amount of RhoB extracted (mg)	Amount of RhoB in dissolution bath (mg)	Cumulative release of RhoB (mg)	% released
	1	2	3	Ave					
5	0.263	0.255	0.263	0.260	0.00114	0.00228	0.0570	0.0570	52.4
10	0.318	0.308	0.311	0.312	0.00165	0.00329	0.0823	0.0846	77.7
15	0.334	0.330	0.337	0.334	0.00185	0.00371	0.0927	0.0982	90.3
30	0.334	0.342	0.336	0.337	0.00189	0.00378	0.0944	0.1037	95.3
60	0.344	0.339	0.337	0.340	0.00191	0.00383	0.0957	**0.1088**	100.0

Dissolution Testing 3 Amount of granules: 500.6 mg

Time (min)	Optical density				Conc. of extracted solution (mg/ml)	Amount of RhoB extracted (mg)	Amount of RhoB in dissolution bath (mg)	Cumulative release of RhoB (mg)	% released
	1	2	3	Ave					
5	0.218	0.258	0.226	0.234	0.00088	0.00177	0.0442	0.0442	39.6
10	0.280	0.280	0.284	0.281	0.00134	0.00269	0.0672	0.0690	61.8
15	0.314	0.318	0.313	0.315	0.00167	0.00334	0.0836	0.0880	78.8
30	0.339	0.341	0.361	0.347	0.00198	0.00397	0.0991	0.1069	95.7
60	0.342	0.340	0.364	0.349	0.00200	0.00400	0.0999	**0.1117**	100.0

Time (min)	% released			
	1	2	3	Ave
5	41.3	52.4	39.6	44.4
10	61.1	77.7	61.8	66.9
15	76.9	90.3	78.8	82.0
30	93.7	95.3	95.7	94.9
60	100.0	100.0	100.0	100.0

E1. Calibration curve for the formulation: 74 wt% mannitol, 35 wt% MCC, 3 wt% HPC and 3 wt% croscarmellose sodium

Concentration of Rhodamine B (mg/ml)	Optical density		
	1	2	3
2.4×10^{-3}	0.443	0.443	0.447
2.0×10^{-3}	0.387	0.385	0.384
1.6×10^{-3}	0.348	0.338	0.333
1.2×10^{-3}	0.305	0.297	0.296
0.8×10^{-3}	0.266	0.241	0.255
0.4×10^{-3}	0.205	0.205	0.199
0	0.172	0.161	0.171

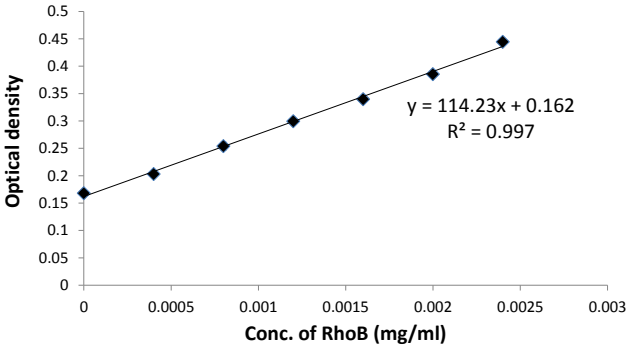

Liquid level: 30% Impeller speed: 490 rpm Wet massing time: 30 min

Dissolution Testing 1 Amount of granules: 500.5 mg

Time (min)	Optical density				Conc. of extracted solution (mg/ml)	Amount of RhoB extracted (mg)	Amount of RhoB in dissolution bath (mg)	Cumulative release of RhoB (mg)	% released
	1	2	3	Ave					
5	0.261	0.259	0.258	0.259	0.00085	0.00170	0.0426	0.0426	34.1
10	0.295	0.305	0.293	0.298	0.00119	0.00238	0.0594	0.0611	48.9
15	0.322	0.321	0.317	0.320	0.00138	0.00277	0.0692	0.0732	58.7
30	0.392	0.392	0.390	0.391	0.00201	0.00402	0.1004	0.1072	85.9
60	0.424	0.424	0.419	0.422	0.00228	0.00456	0.1140	**0.1248**	100.0

Dissolution Testing 2 Amount of granules: 500.6 mg

Time (min)	Optical density				Conc. of extracted solution (mg/ml)	Amount of RhoB extracted (mg)	Amount of RhoB in dissolution bath (mg)	Cumulative release of RhoB (mg)	% released
	1	2	3	Ave					
5	0.273	0.274	0.272	0.273	0.00097	0.00194	0.0486	0.0486	40.6
10	0.305	0.308	0.310	0.308	0.00128	0.00255	0.0638	0.0657	54.9
15	0.344	0.339	0.337	0.340	0.00156	0.00312	0.0779	0.0824	68.8
30	0.406	0.400	0.413	0.406	0.00214	0.00428	0.1069	0.1146	95.7
60	0.402	0.419	0.404	0.408	0.00216	0.00431	0.1078	**0.1197**	100.0

Dissolution Testing 3 Amount of granules: 500.0 mg

Time (min)	Optical density				Conc. of extracted solution (mg/ml)	Amount of RhoB extracted (mg)	Amount of RhoB in dissolution bath (mg)	Cumulative release of RhoB (mg)	% released
	1	2	3	Ave					
5	0.263	0.266	0.261	0.263	0.00089	0.00177	0.0444	0.0444	34.6
10	0.293	0.303	0.309	0.302	0.00122	0.00245	0.0611	0.0629	49.1
15	0.334	0.334	0.326	0.331	0.00148	0.00296	0.0741	0.0783	61.2
30	0.381	0.373	0.389	0.381	0.00192	0.00383	0.0959	0.1030	80.5
60	0.426	0.429	0.433	0.429	0.00234	0.00468	0.1170	**0.1280**	100.0

Time (min)	% released			
	1	2	3	Ave
5	34.1	40.6	34.6	36.5
10	48.9	54.9	49.1	51.0
15	58.7	68.8	61.2	62.9
30	85.9	95.7	80.5	87.4
60	100.0	100.0	100.0	100.0

The amount of RhoB released during dissolution testing was compared with the theoretical amount of RhoB used i.e. 0.02 wt% (dry basis). Approximately 500 mg of "steady state" granules was tested and the amount of RhoB entrapped was about 0.1000 mg. Both theoretical and experimental values were an average of triplicate measurements. All percentage errors were in acceptable range except for experiments M and Q, greater than 20%. One plausible explanation is the liquid distribution may be less uniform and these granules had higher dye content.

Experiment	Lactose/MCC (wt%/wt%)	Liquid level (%)	Impeller speed (rpm)	Theoretical amount of RhoB (mg)	Experimental amount of RhoB (mg)	% Error
A	**74 / 20**	**24.0**	**245**	0.1001	0.1039	3.8
C	**74 / 20**	**30.0**	**245**	0.1001	0.1081	8.0
F	**74 / 20**	**24.0**	**490**	0.1001	0.1033	13.2
D	**74 / 20**	**30.0**	**490**	0.1001	0.1056	5.5
J	**69 / 25**	**30.0**	**490**	0.1001	0.1124	12.3
K	**64 / 30**	**30.0**	**490**	0.1001	0.1008	0.7
L	**59 / 35**	**30.0**	**490**	0.1001	0.1104	10.3
M	**69 / 25**	**35.0**	**490**	0.1001	0.1275	27.4
N	**64 / 30**	**40.0**	**490**	0.1002	0.1116	11.4
O	**69 / 25**	**32.5**	**490**	0.1002	0.1094	9.3
P	**64 / 30**	**35.0**	**490**	0.1001	0.1026	2.5
Q	**74 / 20**[1]	**30.0**	**490**	0.1001	0.1242	24.1

Note: 1. Lactose was substituted with mannitol as the soluble pharmaceutical excipient

Effect of amount of lactose (cavities for the penetration of dissolution medium) on the percentage release of Rhodamine B

Mass of "steady state" granules used for dissolution testing was 0.5 g / 500 mg. Bulk densities for each ingredient were obtained from Rowe *et al.* (2006). The total volume of a granule is assumed to be the sum of individual volume by each ingredient:

$$V_{Total} = \frac{m_{lactose}}{\rho_{lactose}} + \frac{m_{MCC}}{\rho_{MCC}} + \frac{m_{HPC}}{\rho_{HPC}} + \frac{m_{CCNa}}{\rho_{CCNa}} \qquad \text{[Eqn D.1]}$$

The calculated volume percentage of lactose corresponds to the matrix porosity of granules:

$$\varepsilon = \%Vol_{lactose} = \frac{V_{lactose}}{V_{Total}} \qquad \text{[Eqn. D.2]}$$

Formulation Composition A					
Component	**Weight (%)**	**Weight (g)**	**Density (g/cm^3)**	**Volume (cm^3)**	**Volume (%)**
Lactose	74.0	0.370	0.560	0.661	**64.1**
MCC	20.0	0.100	0.320	0.313	30.3
HPC	3.0	0.015	0.500	0.030	2.9
CCNa	3.0	0.015	0.529	0.028	2.7
			Total	1.032	

Formulation Composition B					
Component	**Weight (%)**	**Weight (g)**	**Density (g/cm^3)**	**Volume (cm^3)**	**Volume (%)**
Lactose	69.0	0.345	0.560	0.616	**57.8**
MCC	25.0	0.125	0.320	0.391	36.7
HPC	3.0	0.015	0.500	0.030	2.8
CCNa	3.0	0.015	0.529	0.028	2.7
			Total	1.065	

Formulation Composition A					
Component	**Weight (%)**	**Weight (g)**	**Density (g/cm^3)**	**Volume (cm^3)**	**Volume (%)**
Lactose	64.0	0.32	0.560	0.571	**52.0**
MCC	30.0	0.150	0.320	0.469	42.7
HPC	3.0	0.015	0.500	0.030	2.7
CCNa	3.0	0.015	0.529	0.028	2.6
			Total	1.099	

Formulation Composition B					
Component	**Weight (%)**	**Weight (g)**	**Density (g/cm^3)**	**Volume (cm^3)**	**Volume (%)**
Lactose	59.0	0.295	0.560	0.527	**46.5**
MCC	35.0	0.175	0.320	0.547	48.3
HPC	3.0	0.015	0.500	0.0300	2.7
CCNa	3.0	0.015	0.529	0.0284	2.5
			Total	1.132	

List of experiments done for Figure 6.17 from Chapter 6: Effect of Varying Formulation Composition on Granule Properties and Dissolution Profile

Experiment	Lactose/MCC (wt%/wt%)	Liquid level (%)	Impeller speed (rpm)	Porosity	% Release of RhoB at 5 min DT	% Release of RhoB at 10 min DT
D	**74 / 20**	**30.0**	**490**	0.641	77.4	92.2
J	**69 / 25**	**30.0**	**490**	0.578	71.8	88.7
K	**64 / 30**	**30.0**	**490**	0.520	53.5	78.0
L	**59 / 35**	**30.0**	**490**	0.465	44.4	66.9
O	**69 / 25**	**32.5**	**490**	0.578	65.5	85.6
P	**64 / 30**	**35.0**	**490**	0.520	50.1	73.7

E. FOCUSED BEAM REFLECTANCE MEASUREMENT PLOTS

Granule size distribution profiles during dissolution testing from Chapter 5: Dissolution Performance of "Steady State" Granules

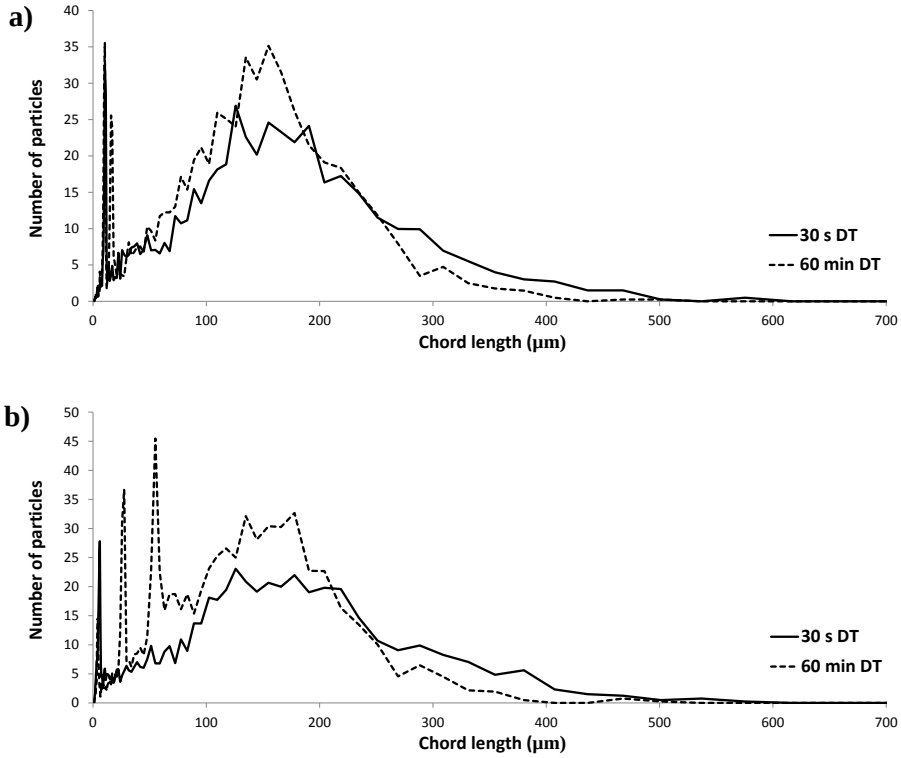

Figure E.1: Evolution of granule size distribution profiles during dissolution testing: a) Run 1 and b) Run 2 for irregular-shaped granules produced at 24% LL and 245 rpm

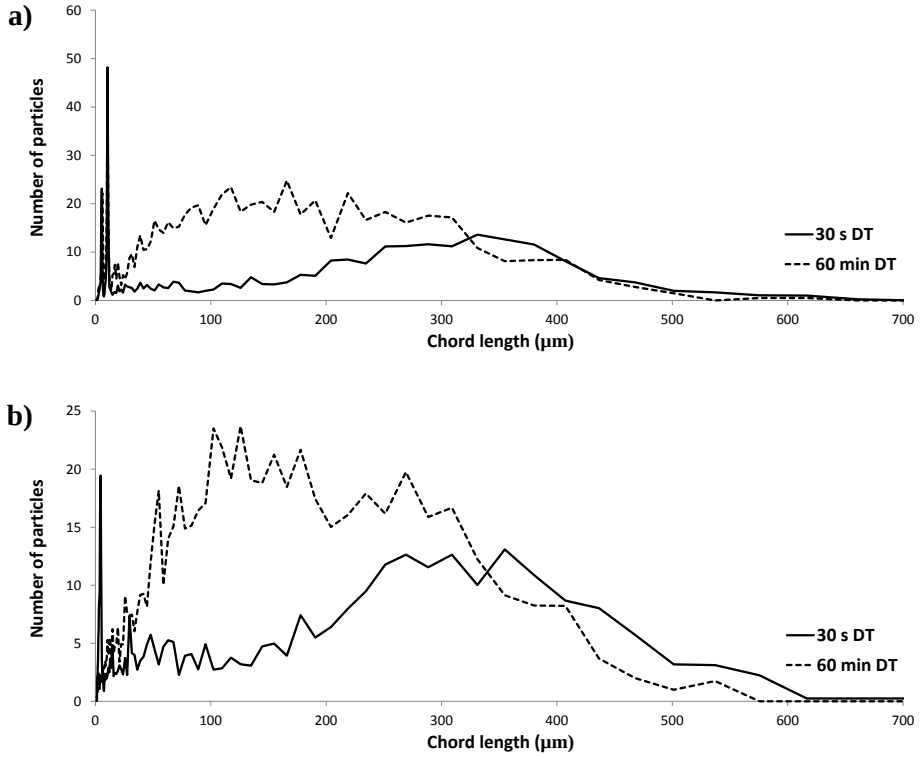

Figure E.2: Evolution of granule size distribution profiles during dissolution testing: a) Run 1 and b) Run 2 for regular, spheroidal granules produced at 30% LL and 490 rpm